

Tregilgas, L

September 2017

Doctor of Philosophy

Investigating the effects of glucose exposure on synoviocytes and chondrocytes as a model for musculoskeletal ageing

Thesis submitted in accordance with the requirements of the University of Liverpool for the degree of Doctor of Philosophy by Luke Tregilgas.

29 September 2017

Acknowledgements

Firstly I would like to thank my supervisors Dr Elizabeth Canty-Laird, Prof Peter Clegg, Dr Louise Reynard, Prof John Loughlin and Dr Simon Tew, for the wealth of support and guidance they have each provided me over the course of my studies. An extra special thanks to my primary supervisor Elizabeth, for all of her time and energy spent moulding me into a better scientist and for providing a positive role model.

A very big thank you to all of the research and support staff and students at Leahurst Campus and the William Henry Duncan Building, of whom there are too many to mention here, for their time and patience in teaching me. I am glad to call many of you my close friends.

Thank you also to Andrew Skelton of Newcastle University for his advice and training in bioinformatics; to Dr Marie Phelan of the University of Liverpool's NMR Centre for her help and training in nuclear magnetic resonance spectroscopy; and to Dr Lakis Liloglou from the University of Liverpool's Institute of Translational Medicine for his help and training in next generation sequencing.

For their love and support throughout my studies, thank you to my family and friends.

My final thanks to my wife Emma, whose unwavering belief and support has seen me through many difficult times, and without whom my thesis would never have been completed.

Abstract

Introduction: It is well established that elevated glucose exposure is a major factor in the progression of the ageing process in the vascular system. There is a growing body of evidence that suggests similar effects in the musculoskeletal system. A trend showing increasing levels of glucose consumption has been shown globally over the past 50 years, with a postulated link to a similar growth in metabolic disorders and diabetes incidence. The list of secondary pathologies associated with diabetes, characterised by chronic elevated blood glucose levels, has been extended in recent years to include musculoskeletal disorders such as joint-stiffening and osteoarthritis. The goal of this project was to characterise potential age-related effects of life-long excessive glucose consumption, with the key area of focus being the human knee-joint. The majority of this research has been carried out on key cell types native to the human knee-joint that are equally implicated in the onset and progression of joint disorders - fibroblast-like synoviocytes; and articular chondrocytes.

Results: The major glucose transporters expressed in synoviocytes and chondrocytes were shown to be those that are known to be non-insulin dependent with a high affinity for glucose, indicating the sensitivity of these cells to extracellular fluctuations in glucose concentrations. Two high-glucose concentrations were used (11mM and 30mM). Data showed an increase in glucose uptake, dose-dependently, at 16h (n = 5). Glucose uptake was reduced by 73% after 14d of 30mM glucose exposure ($P < 0.01$, n = 5). The more physiological treatment, given over a short time-period (11mM, 16 hours), showed the largest effect on synoviocyte methylation (n = 3). Interestingly, the increase in glucose uptake, relative to the 5.5mM control, did not change over time in the 11mM treatment ($P = 0.632$, n = 5), although a significant hypomethylation of CpG sites was only observed in these cells after 16 hours. Cellular adhesion markers (protocadherins) were among the most

commonly differentially-methylated genomic regions in this treatment group. The largest level of significant transcriptional changes was observed in the 11mM treatment after 14d. Microarray data implicating DNA damage was not corroborated by observed DNA strand-breaks, but a trend in the data might suggest a larger effect of the 11mM treatment (n = 3, not significant).

Conclusions: A great deal of prior research into the effects of glucose on ageing has used a concentration of 30mM as the standard high-glucose treatment. The data from the current study shows that there is a propensity for a more physiologically relevant 11mM treatment to cause DNA hypomethylation – which is consistent with ageing - in key cells implicated in musculoskeletal pathologies. Other potential downstream effects include DNA damage and cell adhesion. The effects of a more modest 11mM glucose treatment could also prove to be more profound than those of the 30mM treatment, due to a sustained high-glucose exposure. This is in contrast to the celluloprotective reduction in glucose uptake following a 30mM glucose treatment for 14 days. In addition, this work provides a significantly more detailed understanding of the effects of high-glucose exposure in cells from synovial joints.

Table of Contents

1. General Introduction.....	1
1.1 A growing interest in sugar	2
1.2 Glucose biology	5
1.2.1 Glucose metabolism.....	9
1.2.1.1 Glycolysis	10
1.2.1.2 Oxidative phosphorylation.....	13
1.2.1.3 Alternate glucose metabolic pathways	16
1.2.1.4 The polyol pathway	17
1.2.1.5 Advanced glycation end-product formation	17
1.2.1.6 Diacyl glycerol production	19
1.2.1.7 Activation of the hexosamine biosynthesis pathway.....	19
1.2.1.8 Pentose Phosphate Pathway.....	21
1.2.2 Glucose transporters.....	22
1.2.2.1 Class I GLUTs	22
1.2.2.2 Class II GLUTs	22
1.2.2.3 Class III GLUTs	23
1.3 A note on fructose: metabolism and bioavailability.....	23
1.4 History of glucose toxicity	27
1.4.1 Diabetes.....	27
1.4.2 Effects on ageing in the vascular system	28
1.4.3 AGEs in the musculoskeletal system.....	31
1.5 Chondrocyte and Synoviocyte biology and glucose	33
1.6 Epigenetics.....	37
1.6.1 Methylation.....	37
1.6.2 Metabolic memory.....	38
1.7 Ageing	38
1.7.1 Age-related musculoskeletal pathology	38
1.7.2 Ageing and epigenetics	39
1.7.3 Diet may affect your transcriptome and even your methylome	39
1.8 Summary	40
1.8.1 Diabetes.....	40
1.8.2 Ageing and musculoskeletal diseases.....	40
1.8.3 Future	40
1.9 Aim.....	41
1.10 Hypothesis.....	42

2. Materials and Methods	43
2.1 Cell Culture and Reagents.....	44
2.2 Glucose uptake.....	46
2.2.1 Hexokinase	47
2.2.2 Fluorescent glucose analogue	48
2.2.3 NMR Spectroscopy	48
2.3 RNA Extraction.....	50
2.4 Reverse Transcription.....	51
2.5 Real-Time Quantitative PCR.....	52
2.6 DNA Extraction.....	57
2.7 Microarray	58
2.7.1 Affymetrix microarrays	58
2.7.2 Illumina Human Gene HT-12 v4 Arrays.....	59
2.7.3 Illumina Human Methylation 450k Arrays	61
2.8 Pyrosequencing.....	62
2.9 Oxidative DNA Damage.....	66
2.9.1 Single cell gel electrophoresis.....	66
2.9.2 Reactive oxygen species.....	68
2.10 Cell adhesion.....	68
2.11 pH.....	69
2.12 Statistical Analysis.....	69
2.13 Manufacturer details	70
3. Glucose uptake is reduced in chondrocytes and synoviocytes following high glucose exposure	71
3.1 Introduction.....	72
3.2 Chondrocytes	73
3.2.1 Chondrocyte glucose uptake.....	73
3.2.2 Chondrocyte metabolomics.....	75
3.2.3 Chondrocyte transporter expression (Class 1 – GLUT1, 3 & 14).....	77
3.2.4 Chondrocyte glucose transporter expression (Class 2 – GLUT5, 9 & 11).....	78
3.2.5 Chondrocyte glucose transporter expression (Class 3 – GLUT6, 8, 10, 12 & 13).....	81
3.2.6 Chondrocyte cell number	83
3.2.7 Chondrocyte metabolic state.....	84
3.3 Synoviocytes	85
3.3.1 Synoviocyte glucose uptake.....	85
3.3.2 Synoviocyte metabolomics.....	85
3.3.3 Synoviocyte glucose transporter expression (Class 1 – GLUT1, 3 & 14).....	88
3.3.4 Synoviocyte glucose transporter expression (Class 2 – GLUT5, 9 & 11).....	90
3.3.5 Synoviocyte glucose transporter expression (Class 3 - GLUT6, 8, 10, 12 & 13).....	90

3.3.6 Synoviocyte cell number	94
3.3.7 Synoviocyte metabolic state.....	95
3.3.8 Synoviocyte extracellular pH	95
3.4 Discussion.....	96
3.4.1 Chondrocytes and glucose transport in the literature.....	96
3.4.2 Glucose uptake appears to be reduced after long-term 30mM but maintained in long term 11mM.....	97
3.4.3 Reduction in glucose uptake is not just a result of reduced cell number	98
3.4.4 Could the reduced uptake be due to an effect on expression of glucose transporters?.....	99
3.4.5 Effects on ATP production.....	101
3.4.6 Synoviocytes and glucose transport in the literature.....	102
3.4.7 Synoviocyte glucose consumption	102
3.4.8 Is the reduction a result of decreased synoviocyte glucose transporter expression?	104
3.4.9 Is cellularity the key?	105
3.4.10 What are the effects on synoviocyte metabolic state?	105
3.4.11 Effects on pH	105
3.5 Conclusions.....	106
4. Transient high glucose exposure may affect cell cycle processes in chondrocytes and synoviocytes, and may cause DNA damage in synoviocytes	107
4.1 Introduction.....	108
4.2 Results	109
4.2.1 Effects of transient high glucose on gene expression in synoviocytes and chondrocytes	109
4.2.1.1 Cell cycle and DNA damage are affected after transient high glucose exposure in synoviocytes.....	111
4.2.2 Cell cycle is affected in chondrocytes following transient exposure to high glucose	128
4.3 Discussion.....	134
4.3.1 Synoviocytes and high glucose exposure.....	134
4.3.1.1 Preliminary data suggests high glucose mediate DNA Damage in Synoviocytes	134
4.3.1.2 Synoviocyte cell cycle.....	135
4.3.1.3 DNA Damage and Repair Markers	136
4.3.1.4 DNA Damage	137
4.3.1.5 Oxidative damage.....	137
4.3.2 Chondrocytes and high glucose exposure.....	138
4.3.2.1 High glucose could increase chondrocyte proliferation	139
4.4 Potential limitations.....	140

5. Synoviocyte methylome may be susceptible to transient high glucose exposure141

5.1 Introduction.....	142
5.2 Synoviocyte DNA methylation.....	143
5.2.1 DNA methylation age	143
5.2.2 Glucose-mediated differential DNA methylation in Synoviocytes.....	144
5.2.3 Methylation microarray vs targeted pyrosequencing.....	150
5.2.3.1 Insulin-like growth factor 2 (IGF2)	150
5.2.3.2 Zinc Finger Protein 20 (ZNF20)	150
5.2.3.3 F-Box Protein 47 (FBXO47).....	153
5.2.3.4 Zinc Finger Imprinted 2 (ZIM2) and Paternally Expressed Imprinted Gene 2 (PEG2).....	153
5.2.3.5 Transforming Growth Factor Beta Induced (TGFBI).....	154
5.2.3.6 Polymerase associated factor (PAF1).....	156
5.2.3.7 Preferentially Expressed Antigen In Melanoma (PRAME).....	156
5.2.3.8 Myristoylated alanine-rich C-kinase substrate (MARCKS)-like 1 (MARCKSL1)	160
5.2.3.9 Poly(A)-Specific Ribonuclease (PARN).....	160
5.2.3.10 Additional downstream effects of potential hypomethylation	161
5.3 Gene expression study.....	166
5.3.1 Glucose-mediated differential gene expression.....	166
5.3.2 Potential functional relevance of gene expression changes	168
5.4 Is synoviocyte cell adhesion affected by exposure to high glucose?	171
5.5 Discussion.....	171
5.5.1 Is a change in DNA methylation profiles causal?.....	173
5.5.2 Can high glucose exposure affect ageing through differential methylation in synoviocytes?	174
5.5.3 Can high glucose exposure affect imprinting genes?	174
5.5.4 Effects of high glucose exposure on cell adhesion	175
5.5.5 Limitations inherent in human sample groups	176
5.5.6 Pyrosequencing versus DNA methylation microarray.....	176
5.5.7 Statistical power.....	177

6. Chondrocyte methylome is robust to the effects of high glucose, but cell cycle and cell adhesion may be affected.....178

6.1 Introduction.....	179
6.1.1 Chondrocytes.....	179
6.1.2 Ageing cartilage	179
6.1.3 Aims of this study.....	180
6.2 DNA Methylation.....	181

6.2.1 DNA Methylation Age	181
6.2.2 Glucose-mediated differential DNA methylation	184
6.2.2.1 Homeobox B13 (HOXB13).....	185
6.3 Gene Expression Study	185
6.3.1 Glucose-mediated differential gene expression.....	188
6.3.2 Long term (14 day) exposure to 30mM glucose	188
6.3.2.1 Whole transcriptome microarray	191
6.3.2.2 Targeted replication of whole transcriptome data.....	193
6.3.3 Long term (14 day) exposure to 11mM glucose	193
6.3.3.1 Whole transcriptome microarray	193
6.3.3.2 Functional association	197
6.3.3.3 Targeted replication of whole transcriptome data.....	199
6.4 Similarities in expression changes between chondrocytes and synoviocytes.....	199
6.5 Cell adhesion.....	202
6.6 Discussion	205
7. General Discussion	211
7.1 Glucose uptake is affected following long-term high glucose exposure of human chondrocytes and human synoviocytes	212
7.2 Transient high glucose may cause DNA damage and affect the cell cycle in human chondrocytes and human synoviocytes	214
7.3 Transient moderate high glucose has the potential to affect the methylome of human synoviocytes.....	216
7.4 The chondrocyte methylome is robust to the effects of high glucose, but long term exposure could affect the chondrocyte transcriptome	218
7.5 Conclusions.....	218
7.6 Limitations	219
7.6.1 Sample size	219
7.6.2 Transcriptomic analysis.....	220
7.6.3 Cell models	221
7.6.4 High glucose treatments.....	222
7.6.6.1 Cell adhesion assay.....	223
7.6.6.2 DNA damage assay	223
7.6.6.3 ATP assay	224
7.7 Further work	224
8. Appendices	226
8.1 Appendices.....	227
9. Bibliography.....	229
9.1 References	230

1. General Introduction

1.1 A growing interest in sugar

The latter half of the 20th century saw some of the most noteworthy advancements in collective scientific understanding on record. The burst of technological revelations across a plethora of scientific disciplines rivalled the industrial revolution. It is widely accepted that advances in the field of biomedical research over this period have provided profound improvements to life expectancy in developed countries. Together with improved infant mortality rates in developing countries (1, 2), this increased life expectancy has created a population growth trajectory that will eventually become top-heavy, with our ageing population being the most populous demographic.

This is demonstrable through trends showing the ageing population as the fastest growing demographic within developed countries (3). The resulting increased prevalence of age-related conditions is already creating a mammoth economic burden in developed countries that is only projected to rise over the coming decades (4-6). In fact, non-communicable diseases are one of the largest drains on the economies of advanced countries (4), and are increasing in prevalence within low- to middle-income countries (4). Such diseases include cardiovascular complications; diabetes; obesity; and the list has recently been amended to include musculoskeletal disorders such as osteoarthritis. The prevalence of non-communicable diseases, such as diabetes and obesity, has been steadily increasing over recent years (5); reaching epidemic proportions in many developed countries throughout the world (7). This follows a trend of changing dietary patterns, which includes increasing levels of sugar consumption year-on-year (8-10).

Advances in our understanding of genetics toward the end of the 20th century explained how our genes can affect our predisposition to a wide variety of conditions. In spite of this, it was still becoming increasingly apparent that environmental factors were also a critical source of many non-communicable diseases (11). One of the primary environmental factors identified as affecting our wellbeing was our diet (12). In the 1980s, the dietary guidelines for Americans (13) began to be published and continuously updated every 5 years. These were

curated following advice from leading contemporary nutrition scientists in America. Accounts of research conducted at this time pointed almost exclusively toward dietary saturated fats and cholesterol playing a critical role in the onset and progression of a number of highly prevalent conditions. This was driven by a great deal of scientific evidence (11) and was substantiated by prominent nutrition experts and government advisors, such as Ancel Keys. These nutritional guidelines were the first instance of a government advising its people to eat less of something rather than a little of everything, and together with the media coverage, garnered a great deal of attention from the general public. The resulting public stigma against fat-content in food led to wide-spread initiative within the food industry to reduce the fat component of our food during the manufacturing process (14). Upon the omission of fat content from food, taste suffered considerably, and customer satisfaction plummeted as a consequence (14). Until this point it was widely considered that replacing fat content with “added sugar” would not only circumvent the reported dangers of a high-fat diet, but also prove to be more popular with consumers (14). The increased prevalence of added sugar acted to mediate the public response to reduced fat-content and managed to salvage the ailing satisfaction of consumers (14). There was, however, insufficient evidence of the safety of an increase in sugar consumption to support this “added sugar” within our food during production. In fact, upon the emergence of the first national dietary guidelines and the association of dietary saturated fat with coronary heart disease incidence, a number of leading scientists from other countries spoke to the contrary (12, 15).

John Yudkin, a British nutritional expert, had long been an proponent of the toxic effects of high dietary sugar, and found correlations between the extent of sugar consumption and the incidence of coronary mortality (16); however, prominent contemporaries viewed Yudkin’s work with open scepticism (12). It has been argued that added sugar in common dietary staples could be as harmful, if not more so, than increased fat content. Dietary sugar consumption has also been linked to obesity and subsequent metabolic disorders and diabetes (17).

The problems caused by an increased exposure to dietary sugar were exacerbated by increased availability, brought about by easier manufacture and subsequent reductions in import costs; together with effective marketing campaigns, with £254 million being spent on advertising 'unhealthy' foods in 2014, one third of total food advertising (18).

Historically, throughout the evolution of our species, exposure to simple sugars is said to have been limited by a seasonal availability of fruit (16). Throughout the rest of the year, our bodies were unlikely to have experienced a high-sugar load. By contrast to the low sugar exposure, the diet of early man was likely rich in protein and saturated fats (16). The adaptation of our bodies, over millennia, to the high levels of such molecules in our diet means that high protein and high saturated fat are less likely to be considered a removal from the dietary norm. Subsequent loss of healthy functioning as a result of exposure to such substances is therefore less likely than as a result of exposure of substances to which our bodies are comparatively naïve.

The advent of agriculture increased the availability of sugar to the point where exposure was year-round. The time since, on the evolutionary timescale, accounts for a relatively short period of exposure to high sugar, compared to the majority of our period of evolution spent being exposed to high protein and fat. It is the comparatively short period of high sugar exposure that leads some to hypothesise that it is in fact this molecule that our bodies have not been able to adapt to, and thus is more likely to be the cause of pathologies than the well-ingrained dietary staples of protein and fat (16, 19).

The steady increase in dietary sugar consumption that followed the widely accepted stigma against saturated fat consumption (10) has become a critical cause for concern in recent years, drawing a high level of focus from scientific research (20). The toxic potential of sugar is becoming increasingly apparent, at a time when dietary consumption of sugar is at an all-time high (21). With the prevalence of non-communicable diseases at a similarly critical level (20), it has now become more important than ever to investigate the role that dietary sugar

consumption could play in the onset and progression of these conditions. With an ageing population that threatens to outgrow any other demographic in the near future, any associated non-communicable diseases resulting from the current state of dietary sugar intake could have lasting effects on the economy of the future (4).

The increased focus on added sugar as a potent regulator of ageing in various tissues has not escaped the attention of the media. Public awareness of the issue is increasing through the improved accessibility of information on the subject – including a widely circulated mobile application for identifying the added-sugar content within commonly consumed foods (22). The debate has even received political attention, with there being, at the time of writing, calls for taxation on added sugar in food and drink (23).

Diagnostic technologies have progressed to the point where blood-glucose meters are now a commonly purchased commodity. Investment in glucose technology has led to a recent venture into self-diagnosing contact lenses, suggested to be able to estimate blood-glucose levels from the glucose content in tears (24).

To understand any pathological effects that may be caused by an increase in dietary sugar consumption, it is first important to understand the biology of the molecule itself. The component of dietary sugar that is most highly exposed to tissues throughout the human body is glucose.

1.2 Glucose biology

D-Glucose ($C_6H_{12}O_6$) is a hexose monosaccharide - often termed a “simple sugar” – and as the primary source of energy obtained from our diet, is one of the most important dietary components to humans. As well as acting as an energy currency, glucose is also a key component of countless essential signalling and extracellular matrix molecules. The importance of the role of glucose, along with other saccharide molecules, in the formation of these key biological moieties is exemplified by the existence of a distinct discipline of study dedicated specifically to these molecules, termed “glycobiology”. Glycoproteins,

glycosaminoglycans and proteoglycans are a subsection of these molecules that play a vital role in signalling and biomechanical structure within tissues throughout the body.

Glucose is ingested primarily as part of a heterodimeric disaccharide, with the other component being fructose. These two components exist bound by a beta-glycosidic bond between the first carbon atom of glucose and the second carbon atom of fructose, in a 1:1 ratio to yield one of the most common forms of dietary sugar, sucrose.

In humans, digestion of sucrose into its constituent monomeric components occurs principally within the intestinal mucosa of the duodenum, where membrane-bound brush border hydrolases (glycocalyx) cause splitting of sucrose through the hydrolysing effect of the beta-fructosidase (sucrase), in slightly acidic conditions. The resulting metabolites, glucose and fructose are then absorbed at a similar rate by different glucose transporters within intestinal enterocytes. At the apical membrane, glucose is absorbed into enterocytes, up a concentration gradient, via facilitative diffusion through the sodium/glucose co-transporter SGLT1. Sodium is effused into capillaries through a battery of sodium potassium pumps located at the basolateral membrane of the cells. This vast transport of sodium maintains the electrochemical gradient across the epithelium, providing the energy necessary for simultaneous glucose transport up a concentration gradient. The sodium transport also provides an osmotic gradient facilitating the diffusion of water into the blood. Fructose, in contrast to glucose, is transported into enterocytes via diffusion through the fructose transporter GLUT5. Both glucose and fructose are then effused into capillaries through the glucose/fructose transporter GLUT2 (see Figure 1.1).

The sensing of nutrients and the presence of glucose by enteroendocrine cells causes a release of the incretin hormones: glucose-dependent insulinotropic peptide (GIP) released from K cells in the proximal small intestine (duodenum and jejunum); and glucagon-like

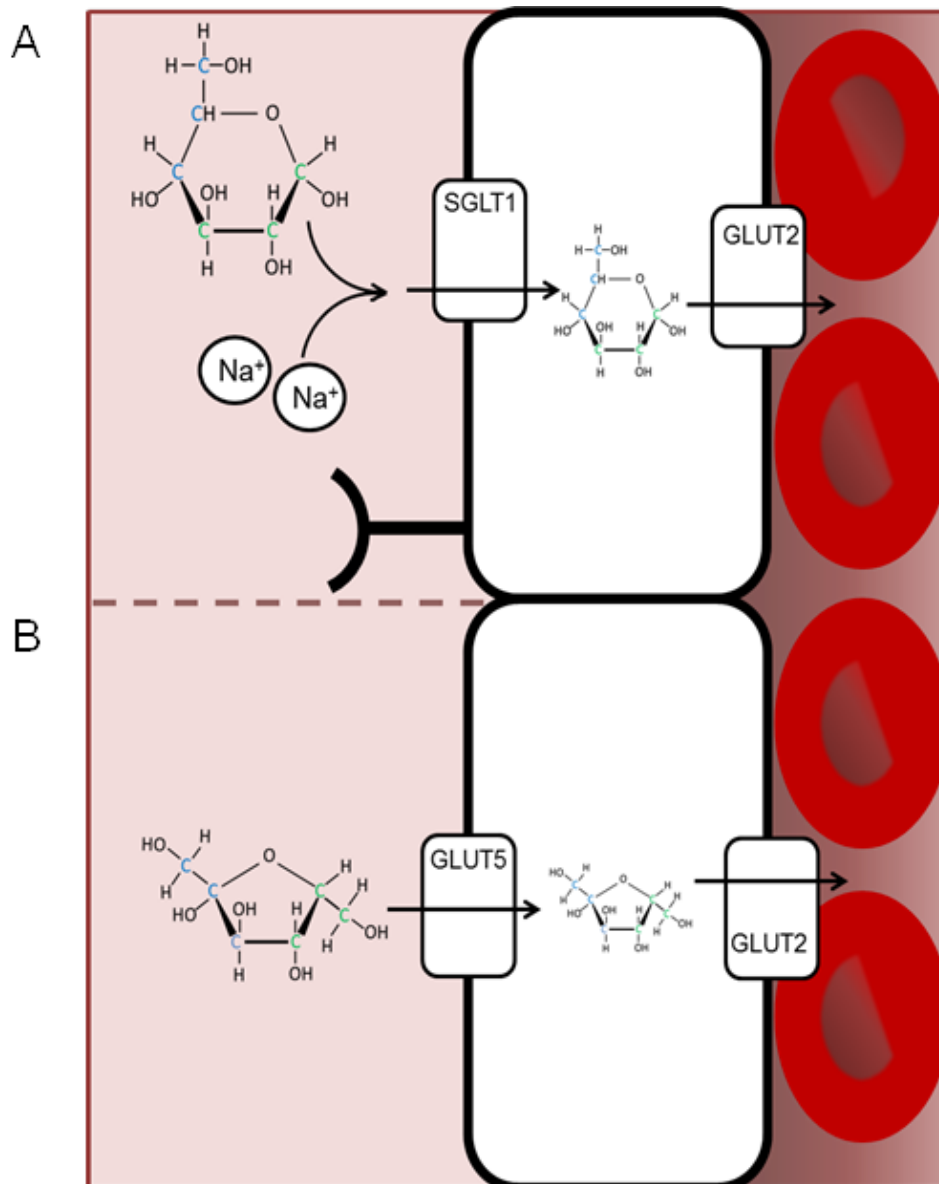


Figure 1.1. Intestinal glucose (A) absorption is carried out primarily in the duodenum following breakdown of disaccharides such as sucrose, lactose and maltose into constituent monomers by brush border hydrolases in the glycocalyx. Sodium-glucose co-transporters (SGLT1) in intestinal K cells transport one molecule of glucose for every 2 sodium ions, up a concentration gradient. Glucose is then effused down a concentration gradient through GLUT2 transporters into capillaries of the portal system. Fructose (B) absorption is carried out further down the small intestine, in the duodenum and ileum by L cells expressing the GLUT5 transporter. Like glucose, fructose is effused into the portal capillaries by GLUT2. These monomers are then transported to the liver by the hepatic portal system for first pass metabolism prior to exposure to the systemic circulation.

peptide 1 (GLP-1) released from L cells in the distal small intestine (ileum and colon). These insulinotropic peptides cause activation of dedicated receptors (GIPR & GLP-1R) on pancreatic beta cells, leading to glucose-dependent increases in cAMP and intracellular Ca^{2+} and subsequent insulin secretion. This is termed the incretin effect – the insulinaemic augmentation brought about by oral glucose administration that is contrastingly not observed following intravenous glucose administration. The presence of elevated glucose levels detected by enteroendocrine cells and subsequent release of GLP-1 also causes a dampening of glucagon release from pancreatic alpha cells and thus an inhibition of glycogenolysis and gluconeogenesis in the liver.

Upon efflux of glucose and fructose from the intestinal enterocytes, the resulting capillary network within the intestinal villi is then responsible for transporting these metabolites to the liver via the hepatic portal system. This leads to the exposure of hepatocytes to glucose and fructose before the molecules reach the systemic circulation. The high expression of hepatic GLUT2 leads to the principal removal of fructose from the blood. The majority of GLUT2 expression occurs in the hepatocytes of the liver, enterocytes of the intestine, and beta islet cells of the pancreas - where GLUT2 is postulated to have a glucose-sensing role due to its low affinity (indicated by a high K_m) for the molecule. First-pass metabolism and an early purge of fructose from the blood (25) is brought about by a number of mechanisms including fructolysis. The majority of fructose is converted to glucose and lactate in the liver (26-29). The remainder is converted to glycogen and glycerol (29). A small percentage (~1%) is converted to free fatty acids and cholesterol (29). Glucose becomes the major monosaccharide to reach the systemic circulation in significant quantity.

Following a post-prandial increase in blood-glucose level, the primary pathway for homeostatic reduction in blood-glucose begins with the detection of elevated blood-glucose by beta cells in the pancreas. This is shortly followed by insulin release. Glucose is then taken up by cells expressing the insulin-dependent facilitative glucose transporter GLUT4, such as myocytes and adipocytes. This removal of glucose from the blood acts to normalise

blood glucose levels and limits the negative effects associated with high blood glucose. Depending on sucrose content in the diet, blood glucose level is increased dramatically prior to a steady reduction over a period of hours. Typical fasting blood glucose level is around 5mM. In this instance, a fasting period is considered to be 8 hours and the normal range is typically between 70mg/dL (~3.5mM) and 130mg/dL (~7.5mM). After 8 hours fasting, if blood glucose level exceeds 130mg/dL (~7.5mM), an individual is considered to be suffering from a fasting hyperglycaemia. Similarly, after a meal, post-prandial blood glucose can exceed 200mg/dL (~11mM), but is expected to be under 180mg/dL (~10mM) after a recovery period of 2 hours. Should blood glucose levels exceed this after the 2 hour recovery period, the individual is suspected of suffering from post-prandial hyperglycaemia.

In cells expressing insulin-sensitive glucose transporter GLUT4 (primarily, adipocytes and myocytes), insulin is considered to cause translocation of vesicular glucose transporters to the cell membrane via a signal transduction mechanism, upon response of cell surface insulin receptors to extracellular insulin. The increased exposure of glucose transporters to extracellular insulin creates a rapid increase in the rate of glucose uptake. The insulin receptor GLUT4 is almost exclusively present within skeletal muscle and fat tissue. Insulin responsiveness has been suggested to be, in part, a result of a di-leucine repeat motif (LL) in the structure of GLUT4 molecules (30, 31). This same motif is found in other, less-well characterised yet more widely expressed, glucose transporters such as GLUT8 (32), and could hint at a potential role for these transporters in being responsive to extracellular fluctuations in glucose concentration.

1.2.1 Glucose metabolism

Under normal glycaemic conditions and in an aerobic environment, glucose typically undergoes glycolysis to form pyruvate and a small amount of ATP (2 molecules of ATP per molecule of glucose), followed by oxidative phosphorylation to generate a much larger amount of ATP (32 molecules of ATP per molecule of glucose).

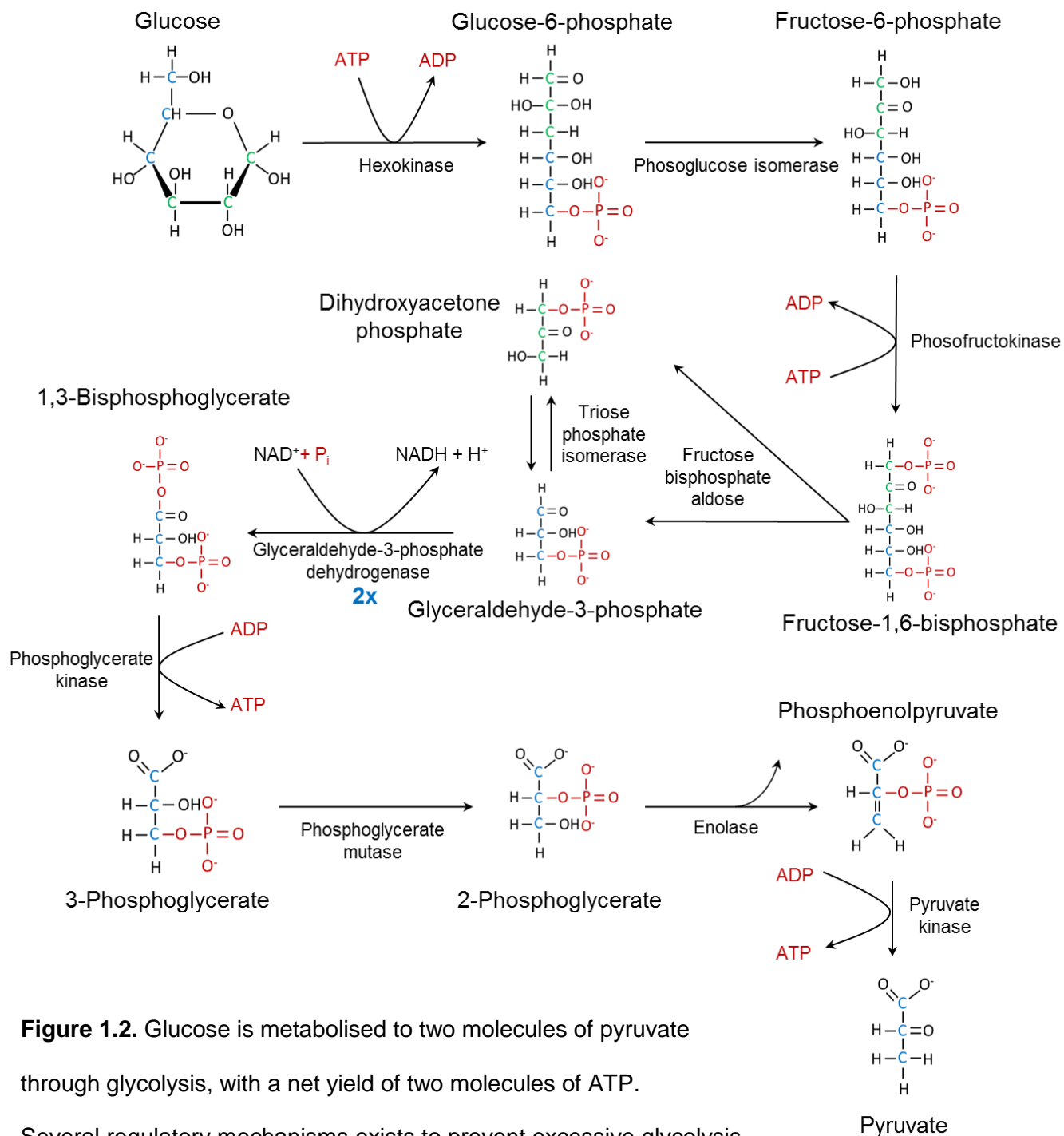
1.2.1.1 Glycolysis

Glycolysis (see Figure 1.2) begins with the phosphorylation of the hydroxyl group of the sixth carbon atom on the glucose ring by hexokinase (or glucokinase in the liver) to form glucose-6-phosphate. The terminal phosphorus atom in ATP is typically shielded from nucleophilic attack by the negative charge maintained at the periphery of the group by the surrounding electronegative oxygen atoms. This helps to prevent spontaneous hydrolysis of the phosphate groups in solution.

Kinase enzymes present positive charges within their active sites in the form of magnesium ions and positively charged amino acid side chains, in order to engage the negatively charged ATP molecule and thereby lower the activation energy barrier sufficiently to facilitate nucleophilic attack by the hydroxyl group of the glucose substrate. Hydrolysis of the ATP using water (the most common nucleophile in the cell system) is prevented since, once bound, the hexokinase enzyme envelopes both substrates ensuring that only the C₆ oxygen atom is presented to ATP for phosphorylation. Any further phosphorylation reactions follow the same mechanism and thus will not be explained in detail.

Following initial phosphorylation, glucose-6-phosphate then undergoes acid-base catalysis to form fructose-6-phosphate via the action of phosphoglucose isomerase. Amino acid residues in the active site of the enzyme are responsible for catalysing the conversion into fructose-6-phosphate by sequential protonation and deprotonation. The hydroxyl group on the 1st carbon in the fructose-6-phosphate ring is then phosphorylated to form fructose-1,6-bisphosphate through the action of phosphofructokinase.

While hexokinase is inhibited by large amounts of glucose-6-phosphate, it is phosphofructokinase that is widely accepted as the major rate limiting step of glycolysis. This step is the first irreversible commitment to the glycolytic pathway. Prior to this, glucose-6-phosphate could be converted to glucose-1-phosphate toward the production of glycogen. Alternatively, the glucose-6-phosphate could be used in the production of nucleic acid via the



pentose phosphate pathway. The conversion of glucose-6-phosphate to fructose-6-phosphate by acid-base catalysis is also reversible. Not only is phosphorylation of the fructose-6-phosphate to fructose-1, 6-bisphosphate irreversible, this product is also an exclusive component of the glycolytic pathway, hence the commitment to this fate. The activity of phosphofructokinase is regulated by the energetic state of the cell – determined by the ratio of ATP to AMP, augmented by reduced pH. The inhibitory action of a reduced pH on continued glycolytic activity acts to protect tissues from acidosis in anaerobic conditions, where enhanced glycolysis results in elevated hydrogen ions.

Fructose bisphosphate aldolase is responsible for the reversible splitting of fructose-1, 6-bisphosphate into two triose phosphate isomers, dihydroxyacetone phosphate and glyceraldehyde-3-phosphate, termed the triose phosphate mixture. These two isomers exist in equilibrium, shuttled between states by the enzyme triose phosphate isomerase. Glyceraldehyde-3-phosphate is the isomer that follows further down the glycolytic pathway, which undergoes dehydrogenation through covalent catalysis via the glyceraldehyde-3-phosphate dehydrogenase enzyme. The use of glyceraldehyde-3-phosphate in this manner causes the equilibrium of the triose phosphate mixture to shift in favour of glyceraldehyde-3-phosphate production. The splitting of a hexose molecule into two triose molecules then results in the following steps in the glycolytic pathway being carried out twice for each molecule of glucose. Phosphorylation of glyceraldehyde-3-phosphate during the conversion of NAD^+ and inorganic phosphate to NADH in this dehydrogenation reaction produces 1,3-bisphosphoglycerate. This is a key step in glycolysis, in that it requires the reduction of a molecule of NAD^+ , which is in short supply in the cytosol. The replenishment of NAD^+ stores is critical to the continued facility for glycolysis and ATP production. Depending on the oxygen availability, this replenishment can occur via two different mechanisms. In aerobic conditions, the replenishment of NAD^+ molecules comes via the oxidation of NADH by one of several available hydrogen carrier molecules, which transport the hydrogen to the respiratory chain of the mitochondria, where together with free oxygen, water is produced. In anaerobic

conditions, in order to maintain sufficient stores of NAD^+ molecules, NADH is oxidised in the conversion of pyruvate (which acts as a hydrogen acceptor) into lactate by lactate dehydrogenase.

The successive removal of phosphate groups in subsequent reactions is responsible for the replenishment of the two molecules of ATP converted into ADP in preceding reactions, together with two further molecules of ATP to bring the net ATP production of each complete glycolysis of a single glucose molecule to 2. First, through the action of phosphoglycerate kinase, 3-phosphoglycerate is produced creating the first molecule of ATP from ADP. This is then followed by isomerisation into 2-phosphoglycerate by the action of phosphoglycerate mutase. The penultimate step in the glycolytic pathway then follows, involving the condensation action of enolase to produce phosphoenolpyruvate. The final molecules of ATP (one for each of the two triose molecules to pass through this step) are produced by the dephosphorylation of phosphoenolpyruvate by the action of pyruvate kinase. The product of this reaction (besides the two ATP molecules produced), and the end product of the glycolytic pathway is pyruvate. The ATP yield from this reaction may seem considerably modest by comparison to that of oxidative phosphorylation, but the rate at which glycolysis can occur and produce ATP is over 100 times greater than its aerobic counterpart. Depending upon the oxygen availability, the fate of this molecule could be decided by two separate mechanisms. In a low oxygen environment, lactate dehydrogenase converts pyruvate into lactic acid. As a toxin this is exported into the circulation and can be cleared upon replenishment of the oxygen debt. In the presence of plentiful oxygen, aerobic respiration by oxidative phosphorylation is the favoured pathway.

1.2.1.2 Oxidative phosphorylation

Pyruvate dehydrogenase is the enzyme responsible for initiation of oxidative phosphorylation. The reaction takes place in the mitochondrion which requires transport of the pyruvate resulting from glycolysis into the mitochondrion. The porins of the mitochondrial outer membrane facilitate the free permeation of small molecules like pyruvate through the

outer membrane. Active transport is required for permeation through the inner membrane, the energy for which is provided by the cotransport of a proton. Once inside the mitochondria, the initiation of pyruvate degradation by pyruvate dehydrogenase involves a coenzyme complex made up of 3 distinct subunits each with their own coenzyme:

1. pyruvate dehydrogenase (coenzyme: thiamine pyrophosphate),
2. dihydrolipoyl transacetylase (coenzyme: lipoamide)
3. dihydrolipoyl dehydrogenase (coenzyme: flavin adenine dinucleotide)

The complex also includes a regulatory kinase and phosphatase subunits. The result of the reaction is the degradation of pyruvate and the subsequent acetylation of coenzyme A into acetyl-CoA. The enzyme pyruvate dehydrogenase is also strictly regulated by products and substrates in the reaction. Pyruvate dehydrogenase kinase and pyruvate dehydrogenase phosphatase, each a part of the enzyme complex, act to inhibit and activate the enzyme respectively, with each being subject to their own regulatory stimuli from reactants and products of the conversion of pyruvate, NAD^+ and CoA into acetyl-CoA and NADH.

The first step in the tricarboxylic acid (TCA) cycle (see Figure 1.3), a precursor to the primary ATP generation step of oxidative phosphorylation (the electron transport chain), involves the conversion of acetyl-coA into citrate via oxaloacetate. The acid-base catalysis reaction is facilitated by aspartate and histidine residues in the active site of citrate synthase which together with oxaloacetate produce citryl-coA, which is finally hydrolysed to citrate.

Following the conversion of citrate into isocitrate by the action of citrate isomerase, the isocitrate is decarboxylated and dehydrogenated to yield α -ketoglutarate by isocitrate dehydrogenase. α -ketoglutarate is then converted to succinyl-coA by α -ketoglutarate dehydrogenase. Succinyl-coA is converted into succinate by succinate thiokinase. Succinate is then converted to fumarate by succinate dehydrogenase. Fumarate is hydrated to L-malate by the action of fumarase. Finally, malate is dehydrogenated to oxaloacetate by the

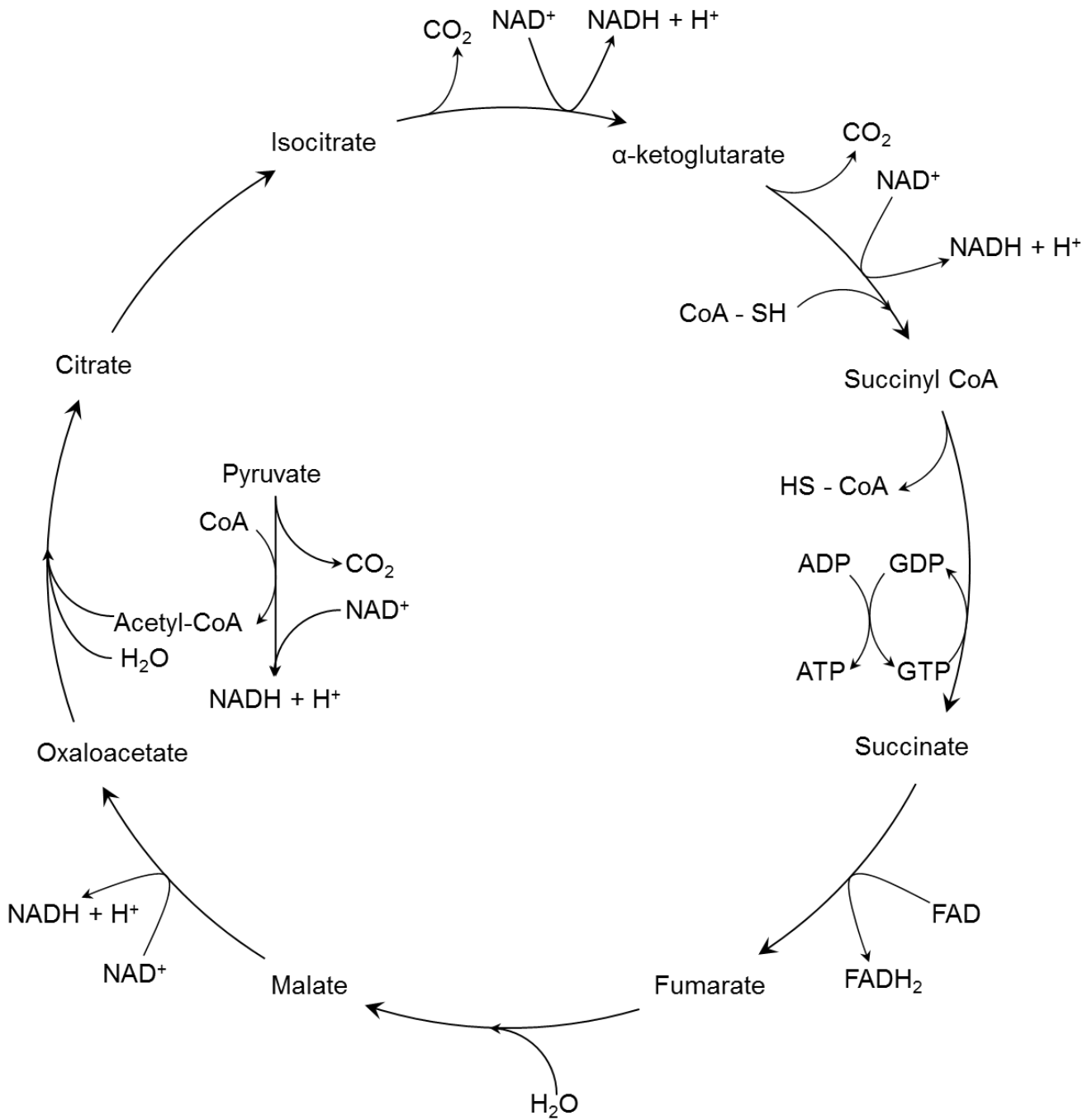


Figure 1.3. Following glycolysis, pyruvate is transported to the mitochondria and degraded, which aids in the acetylation of coenzyme A into acetyl-CoA and subsequent production of citrate, which initiates the tricarboxylic acid (TCA) cycle and kick-starts oxidative phosphorylation and production of ATP from ADP.

action of malate dehydrogenase. The cycle is completed once oxaloacetate subsequently takes part in the citrate synthase reaction which generates citrate from acetyl-coA.

Critically, NADH and FADH₂ produced during the TCA cycle continue to take part in energy generation by donating electrons (oxidation) in the electron transport chain, where successive electron transport across mitochondrial complexes I, III, IV and II, III and IV leads to proton efflux from the mitochondrial matrix. A resulting proton gradient causes proton influx into the mitochondrial matrix leading to the activation of ATP synthase and the phosphorylation of ADP using inorganic phosphate to ATP.

1.2.1.3 Alternate glucose metabolic pathways

The rate of glycolysis is regulated by multiple mechanisms, not least the availability of substrate, but in hyperglycaemic states by the increased availability of ATP and the subsequent inhibition of the key rate-limiting enzyme, phosphofructokinase. ATP binds to a specific regulatory binding site on phosphofructokinase causing a reduction in function. The availability of H⁺ and therefore pH has also been shown to limit phosphofructokinase activity and thus limit further acidosis (33). A further regulatory mechanism comes by way of the inhibition of hexokinase by its product glucose-6-phosphate. Though it is a less prominent form of glycolytic regulation, the inhibition of hexokinase is potentiated by the inhibition phosphofructokinase and subsequent increase in fructose-6-phosphate. This is brought about since a build-up of fructose-6-phosphate causes a consequent build-up of glucose-6-phosphate, both of which exist in equilibrium. One regulatory mechanism that may be more acutely tied to the levels of destructive bi-products of glucose metabolism, reactive oxygen species, is the concomitant inhibition of redox-sensitive glyceraldehyde-3-phosphate dehydrogenase (GAPDH) by activation of poly-ADP-ribose polymerase. The subsequent reduction in glycolysis by these regulatory steps means that the irreversible glycolytic intermediates are likely to follow alternative pathways. There are five such pathways that are described below.

1.2.1.4 The polyol pathway

The polyol pathway (see Figure 1.4.) is the first of five alternate metabolic pathways involving glucose that will be discussed. This pathway involves the conversion of glucose into fructose, with the poly-alcohol, sorbitol (from which the pathway derives its name) as the primary metabolic intermediate. Aldose reductase, the enzyme responsible for catalysing the conversion of glucose into sorbitol, has a low affinity for glucose (34, 35) and as such the percentage of total glucose converted via this pathway under normal glucose conditions in non-diabetics is very small. In a hyperglycaemic state, however, flux through this pathway has been shown to increase (35), although this increase could be variable depending on tissue type or species. The conversion of glucose into sorbitol is supported by the oxidation of NADPH to NADP⁺. Sorbitol is subsequently converted into fructose by the action of sorbitol dehydrogenase, using up stores of NAD⁺ as it is reduced to NADH.

1.2.1.5 Advanced glycation end-product formation

Advanced glycation end-products can form non-enzymatically in the presence of high glucose and involve the glycosylation of proteins, whether these be intracellular or extracellular. While these products can be formed in the presence of glucose, evidence suggests that AGEs form much more readily in the presence of glucose metabolic intermediates (35). This suggests that while originally postulated to be regulated by the extracellular environment (36), AGEs may be sourced either intracellularly or by the exported products of intracellular glucose metabolism.

The fragmentation of glyceraldehyde-3-phosphate and dihydroxyacetone phosphate, two molecules that can be increased intracellularly in the event of reduced glyceraldehyde-3-phosphate dehydrogenase functionality (i.e. in the presence of oxidative stress), can lead to the production of AGEs via the reactive intermediates methylglyoxal, glyoxal, 3-deoxyglucosone.

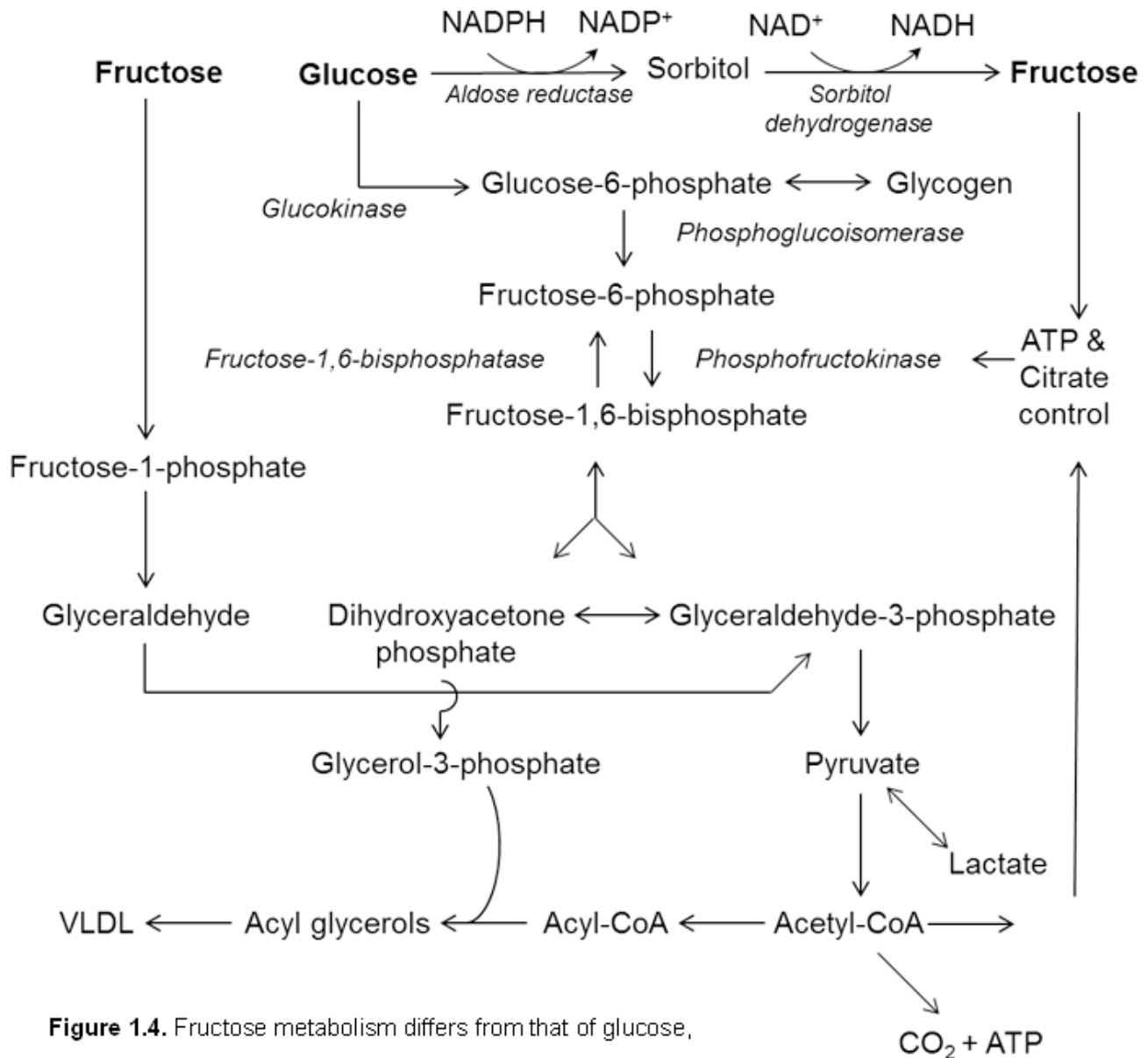


Figure 1.4. Fructose metabolism differs from that of glucose, primarily in being able to avoid the phosphofruktokinase rate-limiting bottleneck in glycolysis that prevents excessive glucose metabolism and acidosis. Fructose can be metabolised glyceraldehyde-3-phosphate from fructose-1-phosphate and glyceraldehyde. Triglyceride synthesis can also result from fructose metabolism by way of glycerol-3-phosphate. Production of diacyl glycerol from dihydroxyacetone phosphate has been suggested to be involved in protein kinase C (PKC) activation following metabolism of both glucose and fructose. Fructose metabolism can also contribute to oxidative phosphorylation and ATP production. Fructose can be derived from glucose in high glucose environments, by way of the polyol pathway, in which sorbitol is produced from glucose by aldose reductase. Sorbitol is then converted to fructose by sorbitol dehydrogenase.

These AGE precursors can cause detriment to the intracellular milieu by modifying proteins leading to reduction, alteration or loss of function. Extracellular matrix molecules can also be modified causing an altered interaction with the surrounding matrix (37) and may also interrupt cell-matrix interactions (38, 39). Matrix molecules that carry out a structural function (e.g. collagen) are typically long-lived, and the characteristic low turn-over leads to an accumulation of protein modifications. The essential role that these structural proteins play in maintaining the biomechanical integrity of their surrounding tissue means that any cumulative adjustment to function caused by AGE formation can conceivably have pathological consequences. This appears to be the case in connective tissues, with AGEs being implicated in tissue stiffening through crosslinking of extracellular matrix proteins such as collagen and elastin (40-42).

A number of studies have shown the proclivity of AGEs to increase reactive oxygen species formation, potentially through interaction with a receptor for AGEs, RAGE (43).

1.2.1.6 Diacyl glycerol production

An increase in glycolytic activity can provide an increased availability of the intermediate dihydroxyacetone phosphate, which can be converted to glycerol-3-phosphate, a precursor for diacyl glycerol (DAG) formation (see Figure 1.4). Diacyl glycerol is an activator of various protein kinase C isoforms, which have been shown to increase vascular pathologies, inflammation and reactive oxygen species production (44, 45).

1.2.1.7 Activation of the hexosamine biosynthesis pathway

The hexosamine biosynthetic pathway (HBP) is reportedly only responsible for around 1-5% of total glucose metabolism (46-48), but has been suggested to be a major factor in the aetiology and progression of diabetic insulin resistance (46, 49). The post-translational glycosylation of transcription factor proteins has been linked to altered transcriptional activity and has been associated with the secondary pathologies associated with diabetes such as

diabetic retinopathy. O-glycosylation as a result of the HBP is also more recently considered as a potential mechanism for glucose-mediated epigenetic modifications of histones (50-53).

The pathway begins with the conversion of fructose-6-phosphate and glutamine into glucosamine-6-phosphate via the rate-limiting enzyme glutamine:fructose-6-phosphate amidotransferase.

Giaccari et al (48) suggested that cells that are more likely to be exposed to the deleterious effects of the hexosamine biosynthesis pathway are insulin-sensitive cells, i.e. those expressing insulin-sensitive glucose transporter GLUT4, such as myocytes and adipocytes .

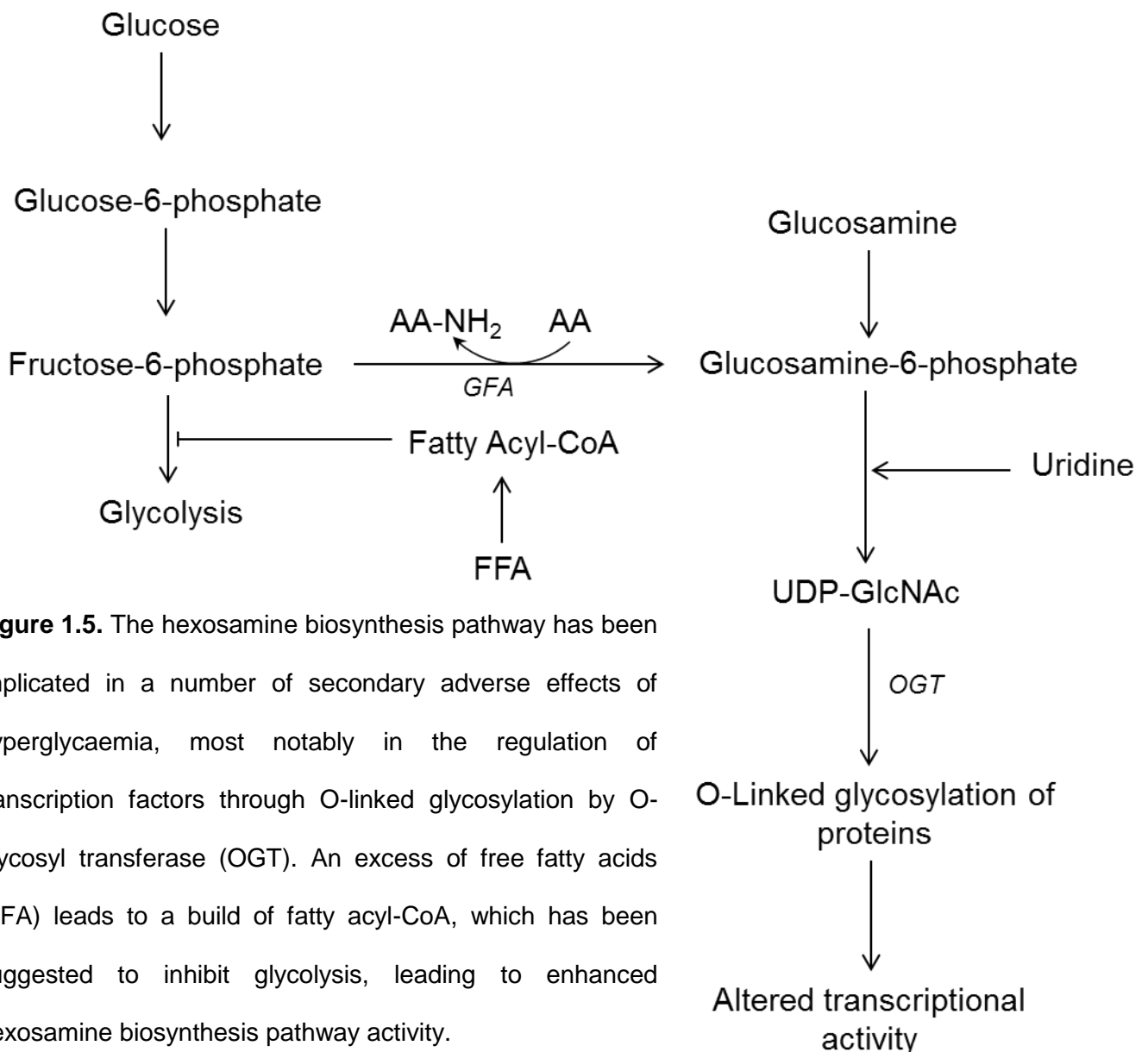


Figure 1.5. The hexosamine biosynthesis pathway has been implicated in a number of secondary adverse effects of hyperglycaemia, most notably in the regulation of transcription factors through O-linked glycosylation by O-glycosyl transferase (OGT). An excess of free fatty acids (FFA) leads to a build of fatty acyl-CoA, which has been suggested to inhibit glycolysis, leading to enhanced hexosamine biosynthesis pathway activity.

1.2.1.8 Pentose Phosphate Pathway

The pentose phosphate pathway occurs parallel to glycolysis and is initiated using a product of the early stages of glycolysis, glucose-6-phosphate. The pentose phosphate pathway is responsible for the production of a precursor for nucleic acid synthesis, ribose-5-phosphate. The pentose phosphate pathway is also important for providing, as a further product, erythrose 4-phosphate used in the synthesis of amino acids. Cell stores of NADPH are also partly replenished as a result of the pentose phosphate pathway, altering the redox state of a cell to allow for reductive biosynthesis of, for example, fatty acids.

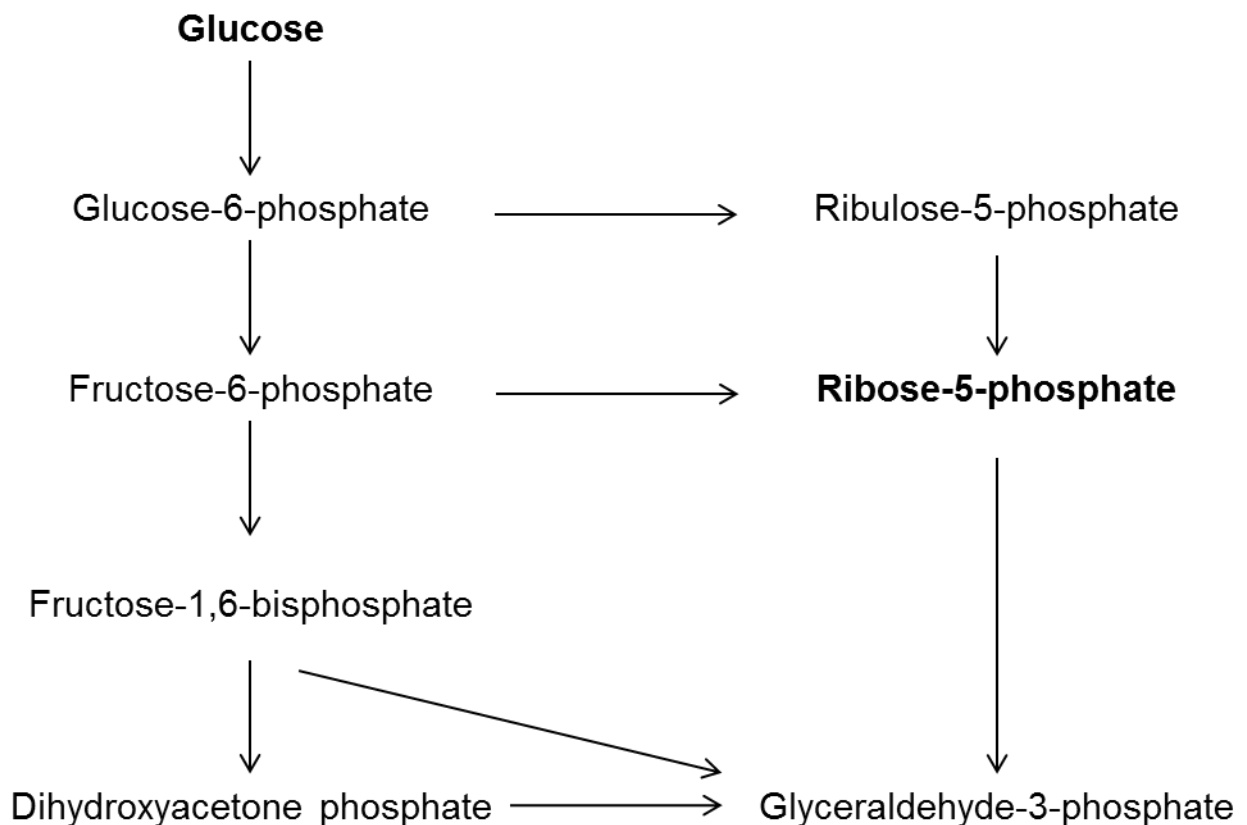


Figure 1.6. The pentose phosphate pathway provides an additional alternate glucose metabolism pathway in which ribose-5 phosphate results from fructose-6-phosphate. Glucose-6-phosphate can also alternatively result in ribose-5-phosphate by way of ribulose-5-phosphate.

Having reactions grouped into two phases, an oxidative phase followed by a non-oxidative phase, the pentose phosphate pathway begins in the former phase by replenishing cell

stores of NADPH, during the multi-stage conversion of glucose-6-phosphate to ribulose-5-phosphate.

Ribulose-5-phosphate is then used in the production of ribose-5-phosphate and erythrose-4-phosphate. Each of these products can be metabolised further to yield additional downstream components of the glycolysis pathway.

The production of NADPH from NADP⁺ is important in the reduction of glutathione via glutathione reductase, which is used in the quenching of reactive oxygen species and limiting the effects of oxidative stress on intracellular components.

1.2.2 Glucose transporters

The most common and well-defined hexose transporters are the major facilitative superfamily (MSF) of transmembrane proteins which comprises the GLUT transporters. Each of these proteins is derived from the solute carrier 2A (SLC2A) family of genes. GLUT proteins are classified into 3 main groups according to their structural composition.

1.2.2.1 Class I GLUTs

Class I comprises the 4 best characterised and most widely expressed glucose transporters, GLUTs 1 to 4, and GLUT14. GLUT1 is almost ubiquitously expressed, but shares similarities with the more tissue-specific GLUT4 in that its relatively low affinity for glucose is such that it can act as a glucose sensor. With a K_m of around 5mM, GLUT1 and GLUT4 can act as detectors of hyperglycaemia and modify glucose uptake accordingly. It is this mechanism that stimulates secretion of insulin from pancreatic beta cells, which are one of the few cell types to express GLUT4. In contrast to GLUT1, GLUT4's discreet tissue distribution limits its expression almost exclusively to myocytes, adipocytes and pancreatic beta cells.

1.2.2.2 Class II GLUTs

Class II (GLUT5, GLUT7, GLUT9 and GLUT11) contains transporters that have quite specific tissue distributions and are known to transport both glucose and fructose. With the

exception of GLUT5, each of the transporters in Class II shows a high affinity for glucose ($K_m < 1\text{mM}$), with GLUT5 having been shown to be almost exclusively a fructose transporter. The structural differences between the first two classes of GLUTs are subtle. It is such that the substrate specificity for Class II is much more pronounced, with none of these transporters being shown to transport galactose or 2-deoxy-D-glucose.

1.2.2.3 Class III GLUTs

Class III (GLUT6, GLUT8, GLUT10, GLUT12 and GLUT13) are the third and final class of MSF hexose transporters, with all but one (GLUT13) containing a di-leucine (LL) targeting motif. LL motifs have been shown to affect transit of transporter proteins between specific sites within the cell. In the case of GLUT4 - a known insulin-sensitive transporter that also contains a dileucine motif - translocation from intracellular compartments where it resides under basal conditions, to the plasma membrane has been shown to be stimulated by insulin. The presence of LL motifs on the majority of Class III glucose transporters suggests that these transporters may also have different locations based on basal and activated states. In the case of GLUT8 it has been suggested that insulin may be responsible for translocation of these transporters from their intracellular compartments to the cell membrane (54). Whether such mechanisms exist is yet to be elucidated.

Additional hexose transporter superfamilies are the sodium/solute symporter family (SSSF) and a more recently discovered group of sugar transporters, the SWEET (not an acronym) family of transporters.

1.3 A note on fructose: metabolism and bioavailability

Aside from glucose, fructose is another major component of dietary sugar, as the second component of the disaccharide, sucrose. The absorption of fructose from the gut has been reported to be similar to that of glucose (55). Upon absorption by the intestinal mucosa, fructose is transported to the liver where the majority is taken up by hepatocytes (25). Fructose then follows one of many metabolic pathways, with the majority being converted

into glucose, galactose or used for glycogen production (56, 57). A small portion (<1%) is converted to triglycerides and cholesterol, which are destined for the systemic circulation (29, 57). After travelling through the liver, the amount of remaining fructose to reach the systemic circulation, and therefore be exposed to cells in the rest of the body, is but a fraction of that originally absorbed during digestion (see section 1.2 above). Serum fructose levels do not appear to exceed micromolar levels (58), with fasting serum fructose concentration estimated to be around 10 μ M (59, 60) and post-prandial serum fructose estimated at around 200 μ M (59, 60).

Fructose has received a considerable amount of attention from researchers in recent years due to the widespread use of high-fructose corn syrup (HFCS), primarily in North America (9). The abundance of corn agriculture in North America means that HFCS is a cheaper alternative to sucrose, typically derived from sugar cane or sugar beet, for use as a sweetener in food manufacture. The “high-fructose” in high-fructose corn syrup refers to the higher fructose:glucose ratio than that found in sucrose. This ratio differs depending on the intended use for HFCS and is obtained during the manufacturing process, where a proportion of the glucose component of corn starch is converted to fructose enzymatically (8). The most common form of HFCS used as added sugar in food is HFCS-55 (8), which typically contains around 55% fructose and around 40% glucose, with the remainder being water. The increased fructose component causes HFCS to work well as a sweetener, however there has been an explosion in evidence supporting the role of fructose in the onset of a number of pathologies including obesity and insulin resistance (8, 9, 20, 61-71). This evidence has been sufficient to cause a ban on the use of the substance in the manufacture of food in most countries, but the HFCS is still widely used in North America where the abundance of corn agriculture provides a considerable financial incentive. While there are tenuous links between fructose consumption and increased circulating triglyceride (69, 72-75), this effect appears to be isolated to hepatocytes which express a large number of fructose transporters by comparison to tissues in the rest of the body (76). Due to the low

levels of fructose detected in serum when compared to glucose (59, 60, 77), the lack of systemic exposure of fructose could limit any further negative effects on other tissue systems.

After absorption in the gut, fructose metabolism differs quite markedly from that of glucose. While glycolysis is under strict regulatory control by the finite availability of the rate-limiting enzyme, phosphofructokinase, fructose is able to bypass this step (78). The conversion of fructose to fructose-1-phosphate by fructokinase (79) is followed by subsequent conversion into the two triose molecules, dihydroxyacetone phosphate and glyceraldehyde, by aldolase B (78). Each of these can then be converted to glyceraldehyde-3-phosphate, allowing fructose to enter the glycolytic pathway at a stage that avoids the regulatory action of phosphofructokinase. There are however, further regulatory mechanisms preventing acidosis through overproduction of lactate, including the exhaustion of NAD^+ from the cytosol and consequent lack of an electron acceptor in the further phosphorylation of glyceraldehyde-3-phosphate to 1,3-bisphosphoglycerate. While the remaining glyceraldehyde from fructolysis can be metabolised into glyceraldehyde-3-phosphate through the action of glyceraldehyde kinase, it can also be converted to glycerol. Glycerol can be converted to glycerol-1-phosphate and then triacylglycerol. This is the proposed mechanism implicating fructose in the onset of obesity. Aldolase B is naturally unable to handle the volume of fructokinase products under a heavy fructose load, which typically results in depleted liver ATP. This could provide further evidence in support of the hypothesis that our bodies are evolutionarily maladapted to high sugar exposure. There also exists a hereditary homozygous defect in the aldolase B gene that can result in severe fructose intolerance. The idea that, until very recently, the human body may have been relatively naïve to frequent high levels of sugar across a timescale spanning the evolution of the species from our most recent ancestor, could be supported by our apparent lack of a capacity for processing high blood-sugar levels in a manner that is conducive to the continuing health of our bodily systems. As previously discussed, high sugar exposure in humans is suggested to have

been historically limited to fruit, only available in specific seasons (16), with the year-round diet being primarily comprised of protein and fat. This could suggest that, while the human body may have faced sufficient selective pressure to adapt for correct utilisation of protein and fat throughout the evolution of the species, this may not be the case for sugar.

The conversion of glucose to fructose occurs readily in a hyperglycaemic environment. The pathway responsible for this conversion is known as the polyol pathway, with the initial enzyme being the key rate-limiter aldose reductase. This enzyme facilitates the conversion of glucose to sorbitol, which only occurs during hyperglycaemia due to the low natural affinity of aldose reductase for glucose. Sorbitol is then converted to fructose by the enzyme sorbitol dehydrogenase. The use of the glutathione reductase cofactor NADPH in this pathway suggests that the reaction could be coupled with oxidative stress. The higher cytosolic ratio of NADH/NAD⁺ is mirrored in tissue hypoxia and is responsible for inhibition of GAPDH, which has been said to lead to an accumulation of triose phosphates which are implicated in a number of deleterious pathways including the production of advanced glycation end products. The observed similarity between the hyperglycaemic state and that during tissue hypoxia has led to the term hyperglycaemia pseudohypoxia, linked specifically to the hyperglycaemia-mediated increase in intracellular fructose.

As previously discussed, serum fructose concentrations do not appear to exceed micromolar levels, which, appears low compared to serum glucose levels. The safe “window” of serum fructose may, however, be much smaller than that of glucose and as such, what are comparatively low levels may in fact have the potential to cause toxicity.

Any fructose-mediated pathology may occur due to the lack of glycaemic and insulinotropic effects of fructose. Unlike glucose, elevated levels of serum fructose do not cause an increase in serum insulin, thus leading to a prolonged “high” fructose level in the blood and increased exposure to a variety of tissues. The apparent relative lack of fructose transporter expression by the majority of cells in the body does however suggest that most tissues lack

a vulnerability to high serum fructose. This hypothesis relies on what is currently known about the tissue distribution of those members of the glucose transporter family that have an affinity for fructose (GLUT2, GLUT5, GLUT7, GLUT8, GLUT9, GLUT11, and GLUT12). Most of the 14 known glucose transporters have thus far been quite poorly characterised, and their distribution in many different cell types, is not well defined in the literature.

Fructose biology and bioavailability are hereinbefore discussed for the purpose of completeness and to address a burgeoning interest in the deleterious effects of high dietary fructose. While there is reason to suggest that high dietary fructose may play a role in a number of pathologies, fructose is not the subject of substantial focus within the present project, with the focus instead being upon glucose, to which systemic tissues are exposed to a much greater extent.

1.4 History of glucose toxicity

Sugar consumption has long been correlated with the incidence of disease, with some of the pioneering research into these correlations being carried out over three decades ago (16). Since then there have been waves of studies implicating sugar consumption in the onset and progression of non-communicable diseases such as coronary heart disease, insulin resistance, obesity and diabetes (48).

A potential reason for the susceptibility of the human body to increases in dietary sugar consumption has been suggested to be rooted in the historical dietary patterns of the species (61).

1.4.1 Diabetes

Diabetes mellitus is characterised by a pathological lack of glycaemic control, and manifests in two fundamentally different conditions. Type 1 diabetes mellitus (T1DM) comprises a mounted immune response against pancreatic beta cells. This is followed by a subsequent loss of function, characterised by a lack of an insulinotropic response to hyperglycaemia. The lack of facility for insulin secretion means that sufferers are required to provide

exogenous insulin to normalise blood glucose levels. By virtue of the need for additional insulin supplementation, this condition is often termed insulin-dependent diabetes mellitus. In contrast to this, the second form of diabetes, Type 2 diabetes mellitus (T2DM), is non-insulin dependent and has a tendency to occur with increased age, indicating that the ageing process may be involved. Symptoms can manifest as increased thirst and increased urination as an attempt to normalise blood osmolarity.

1.4.2 Effects on ageing in the vascular system

The tendency toward continuous high-glucose exposure within the systemic tissues of diabetes sufferers has been suggested to act as an accelerant of the ageing process (80). The primary tissues affected by this are those with the most immediate exposure to the fluctuations in blood-glucose levels, the vascular system. This advanced ageing process occurring within the vascular system of diabetics invariably leads to a well-studied secondary pathology associated with diabetes, which is the incidence of microangiopathies (81). These are characterised by deleterious and injurious effects on the microvasculature, which can ultimately result in tissue disruption and organ failure. Microangiopathies such as nephropathy and retinopathy result in further complications of diabetes such as renal failure and eye-sight attenuation respectively.

Studies into the mechanisms associated with the aetiology of microangiopathies have alluded to a number of potential causes, such as inflammation and oxidative damage, largely pertaining to increased glucose exposure (81).

The incidence of type-2 diabetes is reaching epidemic proportions in many developed countries (41). As the lifespan of the global population increases, this naturally increases the likelihood that type-2 diabetes will occur in individuals at some point during their lifetime. It is crucial therefore that the further potential effects on additional systems within the body are identified and that potential secondary conditions can be anticipated and prevented. The effects seen in diabetes could be an accelerated model for the effects of frequent and

prolonged high glucose insults throughout the lifetimes of healthy individuals. The results of these effects would be expected to occur later compared with those seen in diabetic individuals. With a population that has an ever increasing life expectancy however, effects of more modest high glucose exposure have a greater time in which to accumulate.

Prolonged increases in glucose exposure provide a greater availability for the increased incidence of crosslinks through glycation. The form of glycation referred to occurs non-enzymatically and therefore takes place readily when glucose is in the presence of susceptible proteins and other organic molecules. Among the first investigators of cross-linked proteins in the human extracellular matrix were Sell and Monnier, with their seminal paper from 1989 (82), which was among the first to describe a tenable link between sugars and the ageing process. Sell and Monnier identified a pentose-derived crosslink termed pentosidine, which was one of the first identified products of this glycation-induced crosslinking. Products of this form of glycation are termed advanced glycation end products (AGEs) and have since been implicated in a number of pathologies including secondary conditions associated with diabetes (83).

The process resulting in AGEs has now been fairly well characterised, with a key reaction leading to their formation being the Maillard reaction. This reaction is also sometimes referred to as the Maillard-browning reaction, due to the resultant browning of food with high protein content when heated in the presence of reducing sugars. This has since later been referred to simply as glycation, especially when referring to the slow cumulative process occurring in vivo (84). The non-enzymatic glycation occurring during the formation of AGEs occurs via glycooxidative changes (83), such as condensation of the carboxyl moiety of reducing sugars (83) to the epsilon amino group of lysine or hydroxylysine residues of proteins. Such condensation results in the formation of a Schiff base, which subsequently undergoes Amadori-rearrangement, following the Maillard-browning process, to form a stable end-product (83-86).

It has been indicated that the threat posed by non-enzymatic glycation of proteins and the formation of AGEs can be further subcategorised by source. Glucose-mediated AGE formation has been suggested to occur less readily than fructose-mediated AGE formation (87), with there also existing a stereo-spacial contrast between localisation of AGE formation arising from fructose or glucose origins. Some research suggests that the extracellular matrix possesses more glucose-mediated AGE formation than that derived from fructose (62, 87). By contrast, there would appear to be a greater propensity for fructose-mediated AGE formation intracellularly (62, 87), with fructose being considered as 8 to 10 times more reactive than glucose (88). This could be simply a result of the greater exposure of the extracellular environment to glucose over prolonged periods, with this being the primary monosaccharide present within the blood in any significant quantity. The rate of glucose metabolism within the cell, together with intracellular conversion of glucose to fructose via aldose reductase and sorbitol dehydrogenase in the polyol pathway, could be a potential route for increased incidence of fructose-mediated glycation of intracellular proteins. Although with this said, the polyol pathway is biased to occur only in hyperglycaemic conditions due to the low affinity of aldose reductase for glucose (89-91). Fructose-mediated AGE formation has also been suggested to be more likely to cause vascular complications than AGEs derived from glucose (58, 92, 93).

AGEs are also known to be formed on DNA, particularly on adenine and guanine residues. This does have the tendency to lead to base excision and repair, which advantageously results in a lack of accumulation of AGEs on DNA due to this high turnover. The DNA repair mechanisms however are not perfect and are far from being free from erroneous insertions, deletions and mutations of bases. These 'mistakes' in the DNA repair processes can therefore accumulate in the same way that AGEs can accumulate on long-lived molecules like structural proteins. An accumulation of these indels can lead to increased instability and functional aberrations within cells (94).

The mechanistic role of AGEs in vascular complications remains unclear, with several studies indicating potential mechanisms ranging from loss of biomechanical integrity of key structural tissues; imbalance of extracellular matrix turnover; increased oxidative stress due to an accumulation of reactive oxygen species; and increased inflammatory state within localised tissues.

Studies have identified dedicated receptors for AGEs, one of the most well-known being the Receptor for AGEs (RAGE). Additional AGE receptors include gallectin-3 which is expressed by key cell types within the musculoskeletal system. Activation of receptors for AGEs would appear to induce an upregulation of the receptors themselves, followed by an activation of NFκB and production of heme-oxygenase 1 (83). Studies have shown that this then has the propensity to result in increased reactive oxygen species and inflammatory cytokine production and localised tissue inflammation and destruction (84). The association between AGEs and increased oxidative stress has been suggested to have a number of aetiologies including the physical proximity of a glycated protein, acting as an oxidising source, to the cell membrane and stimulation of signal transduction pathways that increase the production of intracellular oxidants. Effects of AGE receptor activation can include TNFα and IL-1 production and uptake of AGEs into intracellular vesicles, which is seen as a potential route of AGE degradation as is seen in scavenger receptors. AGEs have also been shown to have varying effects on inflammatory cells depending upon the state in which the AGE is found. A soluble ligand (free AGE) has been shown to act to induce monocyte migration, whereas bound ligand (immobilised AGE) can, by contrast, slow down monocyte migration (95).

1.4.3 AGEs in the musculoskeletal system

Consideration of the effects of AGEs within the musculoskeletal system is important due to the nature of the proteins making up the tissues within this system. Many of these proteins, such as collagen, are long-lived proteins, suffering a very low rate of turnover. Long-lived proteins such as collagen and lens crystallins have been postulated to have a lifespan of over one hundred years (94, 96, 97). The accumulation of AGEs particularly on more long-

lived proteins has been demonstrated by a study of two key proteins present in high quantities in several key structural tissues within the musculoskeletal system, collagen and aggrecan. Pentosidine (a common AGE) has been identified in aggrecan at lower levels than in a corresponding amount of collagen. Collagen is known to have a much lower turnover rate than aggrecan and thus is more likely to demonstrate AGE accumulation. Studies have shown that AGE accumulation in skin collagens is lower than the AGE presence in cartilage collagens (82, 98), showing not only that collagens with various roles within the body are similarly affected, but also that highly vascularised tissues might even be affected less than non-vascularised tissues. While there have been some studies indicating that AGEs themselves may play a role in reducing the turnover of these proteins (43, 85, 99), one study showed that AGEs were detected in a pepsin-released collagen fraction (100).

These long-lived proteins often play a critical role structurally within the tissue, as is the case with various isoforms of collagen. Should the ability of these proteins to carry out their intended functions be compromised, for instance either due to a structural change or due to an acquired resistance to degradation (43, 85, 99) – this could cause knock-on effects from the individual affected peptide to throughout the native tissue and further to other systems. Alterations to long-lived proteins in particular, via glycation, are highly important since the modified protein will likely remain within the tissue for a long period of time.

Accumulations of multiple similar modifications, on other long-lived proteins within the same system could cause tissue-wide disturbances. Potential negative effects associated with glycation of connective-tissue proteins include stiffening and resistance to degradation (43, 85, 99). This resistance to degradation has been postulated to be a result of steric hindrance, wherein an access to the binding site of proteinases is blocked by the presence of a glycation product. Alterations to these tissues and subsequent tissue-stiffening can have effects on the ambulatory patterns of individuals, such as overcompensation during walking, further causing aberrances in other limbs (40, 86). An increased stiffness of affected tissues with age could cause tissues to lose the ability to withstand mechanical wear and tear (40,

42). The cumulative wear and tear on affected tissues over the course of a lifetime – which is an ever-increasing period of time in newer generations of people – would lead to eventual increases in susceptibility to injury and a loss of an ability of the tissue to resist against tissue fatigue damage (101, 102).

Linked directly to the musculoskeletal system, diabetes sufferers have been observed to suffer higher incidence of joint space narrowing (an imaging measure for osteoarthritis), with type-2 diabetes being a predictor for knee osteoarthritis (103, 104). Diabetics have also been observed to suffer higher incidence of bilateral osteoarthritis when undergoing joint replacement surgery, than non-diabetic patients (105). A hypothesised link between diabetes or metabolic syndrome and degenerative joint disorders like osteoarthritis is receiving a growing level of support (106-109). AGE-related fluorescence of collagens from diabetes sufferers was also observed to be higher than that in non-diabetics (110) and equivalent to collagen from donors twice their age (111). AGE-related fluorescence has also been observed to be higher in cartilage at greater stages of degradation (112).

1.5 Chondrocyte and Synoviocyte biology and glucose

Chondrocytes are the only cells resident in articular cartilage (113). This resilient cell lineage exists in harsh surroundings, comprising the chondrocyte-dependant extracellular matrix which consists primarily of collagen type II and proteoglycan (113). These two primary components are responsible for the structural and compressive properties of the articular cartilage, providing sufficient rigidity to facilitate structural support of the articulating joint in which they exist; together with an ability to accommodate compressive load-bearing forces. Healthy articular cartilage can withstand varying degrees of load-induced compression due, in part, to its highly effective water-retention properties. Collagen fibrils provide a firm mesh structure, within which proteoglycan provides a cushion against compression. The fine balance between production and break-down of at least one of these two primary components (recent research suggests that collagen type II is only slightly turned over if at all (114)) is largely governed by chondrocytes.

As noted previously, cartilage can be defined as a protective layer of connective tissue that covers bone surfaces in articulating joints, such as the human knee joint. While the key components and cell-types remain the same throughout the cartilage, there exist distinct heterogeneous zonal phenotypes within this complex structural tissue (115). These distinct zonal layers comprise entirely different respective amounts of the core components (115-118), this balance being governed by entirely distinct chondrocytic phenotypes (119). These phenotypes can differ remarkably in terms of metabolic rate and corresponding cellular proliferation rate (120-127).

There has been a large amount of research dedicated to the investigation of how chondrocytes utilise glucose (128-134). A potential reason for this is that carbohydrate is such a large component of many key structural extracellular matrix proteins produced by chondrocytes. The aberrant composition of the cartilaginous extracellular matrix surrounding chondrocytes has been identified as a primary hallmark of onset and progression of a number of musculoskeletal disorders. Thus it could be said that a full understanding of the role of glucose in the healthy functioning of these cells is of relative importance.

Research suggests that chondrocytes in general have a relatively low metabolic rate and a low rate of cellular turnover (133). Contrastingly, chondrocytes do however appear to possess a ready affinity for glucose, expressing 11 out of the 14 known MSF GLUT transporters (129). Many of these transporters are however, not glucose-specific, and are known to transport fructose and galactose among other simple sugars as detailed earlier in this chapter. It should be noted that the main glucose transporter known to be insulinotropic, GLUT4 (31), does not appear to be expressed by these cells (129). This suggests that the primary mode of glucose transport is through facilitated diffusion, and that in the absence of an insulinotropic reduction in blood glucose, these cells would be highly susceptible to persistent high glucose uptake.

Research suggests that the heterogeneous zonal phenotypes of chondrocytes exhibit the Crabtree effect (135) and limit oxygen consumption with increasing proximity to the cartilage superficial layer (133). The Crabtree effect is characterised by a reduction in oxidative phosphorylation and an increase in glycolysis in the presence of large concentrations of glucose. This is in contrast to the Warburg effect, which is observed exclusively in cancerous cells and is characterised by a favouring of an anaerobic glycolytic mode of glucose metabolism over the more efficient oxidative phosphorylation even in the presence of normal or low levels of glucose. It would appear that as chondrocytes reach further distance from the superficial layer, their rate of oxygen consumption increases and their rate of glycolysis decreases (133). This is in line with the decreasing availability of glucose the further away from the superficial layer the chondrocytes are located. This has been said to be due to the fact that the primary supply of glucose and oxygen to these cells comes from the synovial fluid (136-138). It has been proposed that superficial layer chondrocytes, which consequently exist in an environment more rich in oxygen than those situated in the deep zone, utilise glucose at a faster, less efficient rate in order to reserve oxygen for the more oxygen- and glucose-sparse deep-zone chondrocytes (133).

The joint-space is isolated from the rest of the body and as such is maintained as a bacteriostatic environment. An ultrafiltered dialysate is maintained through the employment of a highly stringent influx and efflux mechanism governed by the synovial lining that encapsulates this joint space. This synovial lining is a multicellular tissue consisting primarily of two cell types, type A synoviocytes and type B synoviocytes. Type A synoviocytes are the resident macrophages of this tissue that have been said to be responsible for the highly reactive and inflammatory nature of this tissue in terms of immune response but are also key in maintaining the joint space as an aseptic cavity. The other form of synoviocytes present within the synovial lining (type B synoviocytes) is the fibroblast-like synoviocyte lineage. These cells are responsible for synthesising several key components of the synovial fluid,

which has a role in providing lubrication to soft tissues within the joint space, and articulating cartilage-layered surfaced of the encapsulated bone-faces.

The synovial fluid has been shown to contain glucose concentrations corresponding to that of blood glucose, with multiple studies finding no significant difference between the concentration of glucose within the plasma and the concentration of glucose within the synovial fluid (133, 139). In most cases however it would appear that synovial fluid glucose concentrations differ from plasma glucose concentrations by at most 1-2mM. Fluctuations in glucose concentrations observed in the blood do appear to mirror that observed in the synovial fluid, meaning that cells within immediate interface with the joint cavity are susceptible to the same fluctuations of glucose concentration as those subjected to blood glucose fluctuations. Synovial fluid glucose concentrations have however been observed to decrease markedly below that of the blood in cases of rheumatoid arthritis and joint sepsis. In the case of rheumatoid arthritis, this has been postulated to be as a result of an engorged synovial lining and resultant increase in tissue cellularity. The resultant increased glucose demand by an increased number of cells then results in a reduced synovial fluid glucose concentration. Increased cellularity is also a cause for a reduction in synovial fluid glucose concentration in cases of joint sepsis, but by contrast to rheumatoid arthritis, the increased cellularity comes by way of infectious organisms.

In comparison to chondrocytes, the level of research carried out into the use of glucose by synoviocytes is relatively sparse. In particular there would appear to be relatively few papers discussing the transport of glucose across the cell membrane of synoviocytes by transporter proteins and therefore there is a lack of conclusive knowledge of exactly which of the 14 known GLUTs are expressed in these cells.

A core component of a great deal of the functional elements of the extracellular matrices of these tissues is glucose. It is therefore conceivable that alterations to the balance between breakdown and synthesis, caused by deviations from the healthy glucose window, could

have deleterious effects on the carefully orchestrated compositions of these critical tissues. Cartilage proteoglycans have a high turnover rate, and as such proteoglycan synthesis is thus important throughout life, not just during development.

1.6 Epigenetics

Epigenetics is the study of heritable effectors of gene expression which do not involve a direct modification of the genomic sequence. Such effectors include methylation (including hydroxymethylation), acetylation, and in some cases glycosylation, among others.

1.6.1 Methylation

A major focus of epigenetic research has been on methylation and how this can cause a downstream effect on gene expression. DNA methylation is essential for a number of key biological processes associated with development, including genomic imprinting and X-chromosome inactivation. Epigenetic methylation can occur directly on cytosine residues within the genomic code, resulting in an altered ability of transcriptional machinery to bind at said residues. In such cases, methylation of DNA can result in enhanced or reduced gene expression, particularly where said methylation changes occur around the promoter region of a particular gene. Methylation is particularly associated with repression, wherein methylation of DNA can result in gene silencing, which in some cases can alter function, potentially having a deleterious effect on the cell. DNA methylation-induced transcriptional silencing has been implicated in cancer progression, and is thought to result in the recruitment and aggregation of histone-modifying proteins which result in inactive heterochromatin.

Methylation can also occur on particular amino acid residues of proteins. This can be considered an epigenetic modification when the methylation occurs on a component of the transcriptional machinery, or on histone proteins.

Primary governance of DNA methylation typically occurs through three groups of proteins, comprising enzymes considered as “writers” and “erasers”; and domains within key chromatin modifying proteins considered as “readers”. These proteins are responsible for

adding, removing and recognising DNA methylation respectively. Examples of “writer” enzymes include DNA methyl transferases (DNMTs) and histone methyl transferases (HMTs). “Eraser” enzymes include histone demethylases. “Reader” domains include adaptor proteins from the bromodomain and extraterminal (BET) family, such as Brd2. Such domains are responsible for recognising sites of methylation and other post-translational modifications, and may be responsible for regulating gene expression through interaction with transcriptional machinery.

1.6.2 Metabolic memory

One mode in which epigenetics has been shown to be potentially affected by high glucose is in type II diabetes sufferers. Type II diabetes patients given standard therapy were observed to have enduring symptoms following cessation of treatment and restoration of normal blood glucose levels. This concept of effects persisting beyond the return of a normal physiology has been termed metabolic memory, and is one of the fundamental drivers of epigenetic research in Type II Diabetes Mellitus. While research into metabolic memory has been carried out on the vascular system (83), little is known about the effects of this phenomenon within the musculoskeletal system.

1.7 Ageing

Faced with an increasing lifespan, successive generations of people are destined to accumulate a larger amount of environmental damage over their lifetimes. These cumulative injurious insults may take a greater toll on the more long-lived tissues such as those within the musculoskeletal system. Causes of such deleterious effects could be the consistent exposure to toxic levels of substrates like glucose within the blood.

1.7.1 Age-related musculoskeletal pathology

The most prominent form of age-related musculoskeletal pathology is osteoarthritis, which has recently been recognised as an umbrella term for a plethora of disorders having mechanistically distinct aetiologies and progression characteristics. Osteoarthritis remains a primary focus of a great many research studies since, in spite of a great wealth of prior

research being carried out into both palliative and preventative measures, a defining mechanism of aetiology remains to be elucidated.

1.7.2 Ageing and epigenetics

In the modern era, key long-lived environmental factors of particular interest are those relating to epigenetic changes. Links have already been made between epigenetic abnormalities and the onset and progression of a number of age-related musculoskeletal conditions such as osteoarthritis (140-146).

1.7.3 Diet may affect your transcriptome and even your methylome

Some of the seminal research indicating an effect of diet on the methylome has been carried out in the honey bee (*Apis mellifera*) (147). Within-species polymorphism is apparent throughout the insect order Hymenoptera, and has long been known as a flaw in the philosophical works of Charles Darwin's "On the Origin of Species" (148). It has only recently been discovered that this polymorphism is governed, at least in-part, by epigenetic modifications present between different castes of insect species. The great surprise to researchers in the case of the honey bee was not only that the polymorphism that governs the formation of a "queen bee" is caused by an epigenetic modification, but that this epigenetic modification may be brought about through a change in diet. The subjection of bee larvae to what is termed "royal jelly" (147), and potentially the withholding of pollen and honey (149), would appear to be the governing factor in determining the resultant morphology and fertility of the adult queen bee.

While epigenetic modifications have indeed long been considered to be of environmental origin, this provides even further evidence that alterations in the diet can be sufficient to bring about drastic alterations to phenotype.

Studies focussing on the potential effects of diet on epigenetics are highlighting interesting findings in areas as diverse as insect biology to the effects of diet on human prostate cancer survival. In association with how high glucose and epigenetics can have disease-inducing

effects, El-Osta et al have shown a possibility for high glucose to cause epigenetic modifications to loci associated with NFκB-p65 subunit in murine aortic endothelial cells (150).

New approaches to investigating the direct cellular effects of specific treatments and conditions have expanded beyond the traditional targeted studies of a select panel of genes or proteins. In recent times, there has been an explosion of rapid improvement to gold standard technologies for studying genes and proteins to facilitate affordable exploratory studies of the entire genome, transcriptome, proteome, and more recently methylome and metabolome. These techniques have provided a solution to the traditionally reductionist, targeted approaches and have allowed for more open, hypothesis generating questions to be asked.

1.8 Summary

1.8.1 Diabetes

The burgeoning threat of a diabetes epidemic in a number of developed and developing countries has placed a pressure on researchers to characterised the secondary effects of the consequential high blood glucose experienced by sufferers of the disease. While a high proportion of this research has been carried out into the vascular system, there has been relatively little research carried out into the effects on the musculoskeletal system.

1.8.2 Ageing and musculoskeletal diseases

With many long-lived resident molecules possessing such important functionality, any cumulative musculoskeletal aberrances brought about by high glucose consumption could lead to an increased period spent unhealthy during retirement (shortened health-span), for the ageing population.

1.8.3 Future

As such a high component of the modern diet, and with the prevalence of diabetes on the increase, glucose may prove to be an important mediator of a number of primary or

secondary ailments. With lives becoming longer, environmental insults therefore have longer to accumulate, particularly in long-lived tissues. Key environmental effects in the modern era are associated with the epigenome. With recent indications that epigenetics may be affected by the diet, and that diet-induced epigenetic changes may bring about large phenotypic alterations, this is an important line of inquiry for future research. As technological advances make the study of the epigenome even easier, now is a perfect time to begin to ask these key questions.

1.9 Aim

The aim of this project is to characterise the effects of high glucose on key cell types from the human musculoskeletal system. A particular focus of this project is to investigate the transcriptomic and methylomic effects of high glucose on chondrocytes and fibroblast-like synoviocytes as a model for musculoskeletal ageing in their native tissues, articular cartilage and the synovial lining of articulating joints. The population is now living longer than ever before, with this enhanced lifespan placing a greater emphasis on the importance of the longevity of our key functional tissues. Trends over recent decades have shown an increase in global dietary sugar consumption. Glucose is the one component of dietary sugar to reach our systemic circulation in the highest abundance, and therefore receives the greatest exposure to our systemic tissues. Deviations from the optimum blood-glucose concentration therefore have the potential to place a large deleterious pressure on our systems. A better understanding of the effects of these deviations from the norm, in relation to ageing, could provide targets for further research and potential future interventions. The eventual goal of this research would be to provide a better understanding of the role that glucose plays in the disruption of key functions performed by the healthy musculoskeletal system. This could further act as a primer for future research into the effects of what is a global increase in dietary sugar consumption on a key functional system within an ageing human body.

1.10 Hypothesis

As has been discussed, research has shown that glucose causes accelerated ageing in the vascular system. It is hypothesised that long-term exposure to high blood-glucose events can have cumulative deleterious effects on the human musculoskeletal system, causing accelerated ageing of associated tissues. It is further hypothesised that one mechanistic route of such effects occurs by way of epigenetic and subsequent transcriptomic modifications associated with the cell cycle and inflammation. Such modifications could occur within key cell types responsible for homeostatic mechanisms within the musculoskeletal system - these cells comprising normal healthy human chondrocytes, and normal healthy human fibroblast-like synoviocytes. Any deleterious effects may contribute, in a cumulative fashion over the period of a life-time, to the progression of age-related degeneration of the native tissues of the effected cells, within the human musculoskeletal system.

2. Materials and Methods

2.1 Cell Culture and Reagents

Two primary human cell types were used for the entirety of the study, primary normal human articular chondrocytes (HAC) and human fibroblast-like synoviocytes (HFLS). HAC were obtained from Lonza (n = 3) & Cell Applications Inc (n = 5) and HFLS were obtained from Cell Applications Inc (n = 6). All cells were obtained from separate donors, and both cell types were cultured separately. Donor information can be seen in Table 2.1 (for “Race”, “C” denotes Caucasian, and “B” denotes “Black”). Cell doublings were kept to a minimum (passage \leq 5) where possible due to the primary nature of the cell source.

Table 2.1. Donor information

Cell Type	Sample	Age	Sex	Race
HFLS	A	40	F	C
HFLS	B	52	M	C
HFLS	C	72	F	C
HFLS	D	73	F	C
HFLS	E	41	M	C
HFLS	F	60	M	C
HFLS	G	51	F	C
HFLS	H	38	F	C
HAC	1	21	M	B
HAC	2	6	F	C
HAC	3	15	M	C
HAC	4	52	F	C
HAC	5	57	F	C
HAC	6	63	F	C
HAC	7	65	F	C
HAC	8	53	F	C

Chondrocytes were cultured in a chondrogenic medium comprising Dulbecco’s Modified Eagle Medium (GIBCO) supplemented with ascorbate-2-phosphate (98 μ M, Sigma);

dexamethasone (100nM, Sigma); ITS+3 (5mL per 500mL culture media, 1x, Sigma); penicillin-streptomycin (10.5µM, GIBCO); TGF-β-3 (211pM, Peprotech); and foetal bovine serum (10%, Sigma).

HFLS were cultured in Dulbecco's Modified Eagle Medium (GIBCO) supplemented with foetal bovine serum (10%, Sigma, batch-controlled) and penicillin-streptomycin (10.5µM, GIBCO).

The cell culture method was chosen to suit the style of the assay being carried out, and is specified in individual sections later on in this chapter. In all cases cells were initially grown in standard culture conditions described above, in a glucose concentration mimicking that of fasting blood glucose (5.5mM).

Prior to assays, cells were trypsinised using a standard protocol of addition of Trypsin (0.05%)/EDTA (0.02%) for 5 minutes at 37°C prior to agitation and resuspension in culture medium. Cells were centrifuged at 300g for 10 minutes prior to resuspension in fresh culture medium.

Three primary glucose treatments were used throughout the study: 5.5mM glucose was used to mimic fasting blood glucose; 11mM glucose was used as an upper limit to the realistic level of blood glucose that may be experienced by a non-diabetic; 30mM glucose was used as a high level of diabetic blood glucose. These three conditions were chosen following indications from high glucose studies identified in the literature (108, 130, 150-169). The high glucose culture media concentrations were achieved through the addition of 10x stock concentrations of glucose in distilled water to culture media immediately prior to treatment.

For the stock solutions, powdered glucose (Sigma) was added to distilled water in a concentration 10x that required, followed by sterile filtration (0.2µm) of the high glucose solutions. Stock solutions of high glucose in distilled water were added to culture media to produce a final concentration of 1x, which was carried out immediately prior to treatment.

This ensured that there was no opportunity for glucose-mediated cross-linking of culture media proteins, which have been shown to be potent mediators of reactive oxygen species production and inflammation (83, 84, 170-173).

Synoviocytes were cultured exclusively in monolayer culture, whereas chondrocytes were cultured in either pellet culture or monolayer culture as befit the experiment to be performed.

For monolayer culture, cells were seeded at controlled cell density and passaged using a standard trypsinisation protocol described earlier, until sufficient numbers were acquired for experiments. Cell numbers were calculated using a haemocytometer. Cell media changes were carried out three times per week until the cells were harvested for experiments.

For chondrocyte pellets, cells were grown initially in monolayer culture, with minimal passaging, using the standard trypsinisation protocol described earlier, until adequate cell numbers were obtained for the experiments. Cells were trypsinised, centrifuged, and resuspended in cell culture media, before being separated into individual microcentrifuge tubes (1.5mL) at a controlled cell density (100,000 cells per tube). Cells were centrifuged (300g, 10mins) and the resulting pellet was left in the cell culture media at the bottom of the tubes. Culture media was changed three times per week (200µL per tube) with care taken not to disturb the cell pellet.

2.2 Glucose uptake

Glucose uptake was assessed as a test of whether exposure to increased concentrations of glucose has the potential to exert an intracellular effect. Had there been an indication that there was no relationship between glucose exposure and glucose uptake, there may have been little to indicate the source of an effect of high glucose exposure.

2.2.1 Hexokinase

Glucose hexokinase tests were carried out on cell culture media using a clinical bioanalyser (Konelab), in order to quantify the level of glucose in the culture media following high glucose exposure.

Three dosages of glucose exposure were used (5.5mM, 11mM and 30mM), with high glucose treatments being used for two time periods, short term (16h) and long term (14d). Cells (HAC samples 4 to 8; HFLS samples D to H) in all treatment groups were cultured for the same length of time in order to minimise the effect of the length of time spent in culture. Cells to be treated with short-term (16h) high glucose (11mM and 30mM) were cultured in normal glucose (5.5mM) media until the end of the long-term (14d) high glucose (11mM and 30mM) treatment period. 16h prior to the end of the long-term treatment period, short-term treated cells were exposed to high glucose (11mM and 30mM). A subset of the cells was treated for the entirety of the treatment period in normal glucose (5.5mM) as a control.

Media was aspirated directly from cell culture flasks and centrifuged (1000g for 5 minutes). The supernatant was then transferred to a clean microcentrifuge tube and either stored (-80°C) or directly analysed on a clinical bioanalyser (Konelab). 300µL of media was used per assay.

For glucose uptake assessment, chondrocytes were cultured in pellet culture (100,000cells per pellet) as described earlier and synoviocytes were cultured in monolayer culture (96-well plates seeded at 100,000cells per well).

DNA extraction, described later, was used to show that the cells did not significantly differ in cell number across the course of the treatments, and as such this was not a source of compounding bias to the results of this assay.

2.2.2 Fluorescent glucose analogue

Glucose uptake in cells was also assessed through the use of a fluorescent glucose analogue, 2-(*N*-(7-Nitrobenz-2-oxa-1,3-diazol-4-yl)Amino)-2-Deoxyglucose (2-NBDG). Cells (HAC samples 5, 7 and 8; HFLS samples D, E and F) were cultured in normal glucose (5.5mM) conditions to confluence, in 6 well plates. Triplicate wells were then entered into a 14 day exposure to each high glucose treatment (11mM or 30mM), with triplicate wells remaining in normal glucose (5.5mM) until 16 hours prior to the end of the 14 day exposure period. At this point, triplicate wells were treated with each high glucose treatment (11mM or 30mM) for 16 hours and the remaining cells were maintained in normal glucose (5.5mM) as a control. After completion of treatment, cells were trypsinised using the standard protocol described earlier. Cells were resuspended in their final treatment medium and seeded in 96 well plates at controlled cell density (25,000 cells/well) and centrifuged (1000g, 5 minutes). Sufficient wells were seeded to account for negative controls for triplicates of each treatment group. The negative controls comprised wells for each treatment group which were not treated with 2-NBDG, and wells for each treatment group which were treated with a glucose uptake inhibitor cytochalasin β (50 μ M) 20 minutes prior to addition of 2-NBDG. 2-NBDG (to a final concentration of 40 μ M) was then added to a section of triplicate wells for each treatment group, along with those having been treated with cytochalasin, for 10 minutes before cells were gently washed with PBS (1x, Sigma) and fluorescence was measured on a fluorescent plate reader (GloMax, Promega).

2.2.3 NMR Spectroscopy

For extracellular and intracellular glucose measurements were carried out using NMR spectroscopy. Both cell types (HAC samples 5, 7 and 8; HFLS samples D, E and F) were cultured in monolayer culture (25cm² cell culture flasks) seeded at a controlled cell density (250,000 cells per flask). As has been described previously, three dosages of glucose exposure were used (5.5mM, 11mM and 30mM), with high glucose treatments being used for two time periods, short term (16h) and long term (14d). Cells in all treatment groups were

cultured for the same length of time in order to minimise the effect of the length of time spent in culture. Cells to be treated with short-term (16h) high glucose (11mM and 30mM) were cultured in normal glucose (5.5mM) media until the end of the long-term (14d) high glucose (11mM and 30mM) treatment period. 16h prior to the end of the long-term treatment period, short-term treated cells were exposed to high glucose (11mM and 30mM). A subsection of cells were treated for the entirety of the treatment period in normal glucose (5.5mM) as a control.

Cell culture media was aspirated and centrifuged (13,000g, 10mins, 4°C) and 900µL of the resultant supernatant was aspirated and kept on ice. The remainder of the supernatant and any remaining pellet were discarded. Sodium azide solution (NaN₃) was added to the supernatant to make a final concentration of 0.02% sodium azide. Samples were transferred to storage (-80°C) until analysed. For analysis, samples were thawed at room temperature and immediately processed. For processing, a mix of 1M sodium phosphate and 100mM trimethylsilylpropanoic acid (TSP) was added in an amount of 600µL to each 900µL sample. Samples were vortexed prior to a centrifugation step (13,000g, 5mins). 600µL of the final sample was pipetted into 5mm NMR tubes and samples were analysed using an NMR spectrometer.

Cell samples were trypsinised using a standard protocol described earlier and resuspended in ice cold phosphate buffered saline (1x, GIBCO). Cells were counted briefly (TC20 automated cytometer, BioRad) and separated at a controlled cell density into microcentrifuge tubes (1.5mL, 250,000 cells per tube). Cells were centrifuged (300g, 5mins, 4°C) before the PBS supernatant was removed. Care was taken not to disturb the pelleted cells. Cells were then immediately snap-frozen in liquid nitrogen prior to being stored (-80°C). Preparation for analysis involved addition of 1mL ice-cold solvent solution (50% acetonitrile) onto frozen cells, followed by immediate vortexing and sonication. Sonication was carried out in three sets of 30 second bursts for each sample, while the remaining samples rested on ice, in order to reduce heating of the sample that might be caused by extended sonication.

Sonicated samples were transported on ice to be centrifuged (13,000g, 10mins, 4°C) before the supernatant was removed and resulting pellets were lyophilised (overnight). Lyophilised material was processed for NMR the following day through the addition of sodium phosphate/TSP solution prior to being vortexed and 600µL of the resultant solution was added to 5mm NMR tubes for analysis in the NMR spectrometer. The NMR spectrometer was operated by Dr Marie Phelan of the NMR Centre for Structural Biology, University of Liverpool.

2.3 RNA Extraction

RNA was isolated from cells in both monolayer culture and pellet. In the case of monolayer cells (HAC samples 1 to 8; HFLS samples A to H), cell culture media was aspirated, and ice-cold tri-reagent (Sigma) was added directly to the cells. The layer of monolayer cells was agitated using the tri-reagent/cell mixture through successive pipetting before the mixture was aspirated and added to microcentrifuge tubes (1.5mL) and placed on ice. Ice-cold chloroform (200µL/1mL tri-reagent, Sigma) was added to each tube and the resultant mixture was vortexed (1 minute). The tubes were then centrifuged (15,000g, 15 minutes, 4°C) to yield a tri-phasic mixture. The aqueous phase containing RNA was then transferred to microcentrifuge tubes (1.5mL) containing isopropanol (500µL, Sigma). The microcentrifuge tubes were then incubated on ice for 1 hour with periodic vortexing. After incubation the microcentrifuge tubes were centrifuged (15,000g, 10 minutes, 4°C), and the supernatant was removed. Ice cold ethanol (75%, 500µL, Sigma), was then used as a wash step, wherein the ethanol was added, the microcentrifuge tubes were agitated to release the pellet, and subsequently centrifuged (15,000g, 10 minutes, 4°C). This wash step was repeated, and the ethanol was removed with successively smaller pipette tips. This was to ensure complete removal of the ethanol without disruption of the RNA pellet. Tubes were left open to evaporate the remaining ethanol prior to dissolving the RNA pellet in ice cold nuclease free water (Promega). The procedure was carried out as quickly as possible in

order to minimise degradation of RNA, and components and reagents were pre-cooled on ice prior to use where possible.

Cells in pellet culture followed the same protocol, with an added initial agitation of the pellet within the tri-reagent mixture to enable effective pellet breakdown and access of the tri-reagent to cellular material. A centrifugation step was used (1000g, 5 minutes, 4°C) after agitation in order to remove undissolved cell- and pellet- debris prior to addition of chloroform.

RNA quality was assured using a Nanodrop spectrometer, wherein acceptable samples were determined according to their 260/280 (>1.8) and 260/230 (>1) values. The Nanodrop 1000 spectrophotometer was also used to quantify the RNA, enabling suitable dilution prior to reverse-transcription for the production of cDNA.

2.4 Reverse Transcription

cDNA was produced from RNA using a reverse transcription reaction. RNA was used in a standard amount per reaction (1µg) enabled through the quantification of RNA samples using the Nanodrop 1000 spectrophotometer.

Each reaction included RNA (1µg) diluted to 15µL in a PCR tube (200µL) using nuclease free water (Promega) and random primers (1µL, Promega) were added.

A PCR thermal cycler (Applied Biosystems) was used to carry out the reverse transcription reaction. Upon addition of random primers, the secondary structures in the template RNA were left to denature in the thermal cycler (70°C, 5 minutes). After this initial denaturing step, the tubes were removed and placed on ice. Reaction mix was added to each tube comprising: Moloney Murine Leukemia Virus Reverse Transcriptase (M-MLV RT, 200 units, Promega); M-MLV RT reaction buffer (1x, Promega); dATP, dTTP, dCTP, and dGTP (0.5mM final concentration, Promega); and RNasin (25 units, Promega). Random primer extension was then carried out in the thermal cycler (35°C, 60 minutes), followed by denaturing (95°C, 5 minutes), annealing and extension steps (60°C, 10 minutes).

2.5 Real-Time Quantitative PCR

Real-time quantitative PCR (qPCR) was carried out on an Applied Biosystems 7300 light cycler. cDNA templates were diluted according to initial RNA amount used for the reverse transcription reaction. Dilutions were performed to yield a constant amount of cDNA template, relative to the initial RNA amount, per qPCR reaction (1 ng per 25 μ L reaction).

GoTaq DNA polymerase and master mix (Promega) were used for the qPCR reactions. Stocks of upstream and downstream primers (100 μ M, Eurogentec) were diluted and mixed to a concentration of 10 μ M and added (2.5 μ L per 25 μ L reaction). Master mix was prepared by adding CRX reference dye and the resultant mix was added to each reaction (12.5 μ L per 25 μ L reaction).

The thermal cycling protocol included an initial denaturation step (95°C, 2 minutes) followed by 40 cycles of denaturation (95°C, 30 seconds), annealing (50°C, 30 seconds), and extension (70°C, 15 seconds).

Housekeeping genes for each cell type were chosen from a panel of known housekeeping genes, and selected for lack of variability in gene expression observed across the different treatment groups using the GeNorm algorithm (174) using R (175). For qPCR analysis, following the Livak (176) method, all CT values were normalised to a housekeeping control gene (GAPDH) to give Δ CT values. Where appropriate, Δ CT values for High Glucose results were also normalised to the corresponding Normal Glucose Δ CT values to give $\Delta(\Delta$ CT). From the $\Delta(\Delta$ CT) values, fold change ($E^{-\Delta(\Delta$ CT)}) was calculated following the Pfaffl (177) method, where E is equal to the efficiency component for each individual primer used. E was calculated from separate experimental data (not shown) pertaining to CT values after serial '1 in 10' (1:9) dilutions of a single cDNA template (derived from 1 μ g of RNA). The formula used for E is $101/\text{slope}$, with slope being the gradient of the best-fit line of CT values plotted against cDNA template concentration. Data were calculated as mean \pm standard deviation. Primer sequences can be seen in Tables 2.2 to 2.5 below and were obtained from journal

articles within a relevant field, PrimerBank (178-180) or Primer-BLAST (181) as noted in Tables 2.2 to 2.5.

qPCR replicate data was subjected to either ANOVA or Kruskal-Wallis tests, after the normality of the data was tested using a Shapiro-Wilk test. Corresponding post-hoc tests were subsequently used to derive P values of pairwise comparisons, with values of $P \leq 0.05$ being considered significant.

Table 2.2. Primer list for glucose transporter genes used in qPCR.

Gene	Forward	Reverse	Source
SLC2A1	ATTGGCTCCGGTATC GTCAAC	GCTCAGATAGGACATCC AGGGTA	PrimerBank ID# 166795298c3
SLC2A2	GCCTGGTTCCTATGT ATATCGGT	GCCACAGATCATAATTG CCCAAG	PrimerBank ID# 4557850c2
SLC2A2	CTAGTCAGGTGCAT GTGCCA	AGGGTCCCAGTGACCTT ATCT	BLAST
SLC2A3	GCTGGGCATCGTTG TTGGA	GCACTTTGTAGGATAGC AGGAAG	PrimerBank ID# 221136810c1
SLC2A4	ATCCTTGGACGATTC CTCATTGG	CAGGTGAGTGGGAGCA ATCT	PrimerBank ID# 83722278c2
SLC2A4	CTTCACCTTGGTCTC GGTGT	CGTAGCTCATGGCTGGA ACT	BLAST
SLC2A5	ACGTTGCTGTGGTCT GTAACC	CATTAAGATCGCAGGCA CGATA	PrimerBank ID# 207447702c2
SLC2A6	CCGGACTACGACAC CTTCC	GGATGTGTAGACCAGGG CATA	PrimerBank ID# 223029431c1
SLC2A7	CAGTACGGCTACAA CCTCTCT	TTGCGTGTGCTCAAAG TAGG	PrimerBank ID# 134053882c1
SLC2A7	ATCCATCCAGGAGG CCATCG	TGGTCTCCGGAATAACC ACG	BLAST
SLC2A8	CCGGCATCTACAAG CCCTTC	ATAGAACATGACGGCGT TGAC	PrimerBank ID# 51870928c2
SLC2A9	CAATAGACCCAGAC ACTCTGACT	TCTTCACAATTAACGTCC CCAC	PrimerBank ID# 47933386c2
SLC2A10	CTTGCTGTATCTACG TGTCAGAG	CCAGCCAGTGCATAGTT GAGG	PrimerBank ID# 39777591c1
SLC2A11	CCCTCATCGTGTCTC TGTATCC	CGAGCAGTCTTCCCAGC AT	PrimerBank ID# 190684653c2
SLC2A12	GAGGCTGCGGCATG TTTAC	CCAAGTTCATAAACCAC CAGG	PrimerBank ID# 93277101c1
SLC2A13	CAACTCGCCGAGCT TTAATTGT	GTTGCACTGTAGTACAT GATGGT	PrimerBank ID# 203098994c3
SLC2A13	AGACTGCGGTTTCTG CTACAA	GGTTTCATTTTCACACCT GCC	BLAST
SLC2A14	CTGCTCACGAATCTC TGGTCC	GCCTAATAGCACCGGCC ATAG	PrimerBank ID# 24475843c1

Table 2.3. Primer list for gene expression array validation using qPCR.

Gene	Forward	Reverse	Source
FOS	CTGATACACTCCAAGC GGAGA	TTGGCAATCTCGGTCTG CAA	BLAST
LUM	GCAGTGTCAAGACAGT AAGGATT	ACCACCAATCAATGCCA GGA	BLAST
ITGB2	AGGAGCTGAGAGGAAC AGGA	CAGCATGTCCCTCGGTG TG	BLAST
ITGA5	CAAAGGGCCTGGAGTT GGAT	AGCCTGAAACACTCAGC CTC	BLAST
IBSP	TGGCCTGTGCTTTCTC AATGAA	TGCCCTGAACTGGAAAT CGTT	BLAST
IL1R1	GGGAGCGGCAGGAAT GTG	GCGTCTACCTGGACGGA CG	BLAST
PTGS2	CAAATTGCTGGCAGGG TTGC	AGGGCTTCAGCATAAAG CGT	BLAST
TXNIP	GAAGACCAGCCAACAG GTGA	CTGAGGAAGCTCAAAGC CGA	BLAST

Table 2.4. Primer list for methylation array validation.

Gene	Forward	Reverse	Source
MEST	AGTTGTGCTTTTAC ACGGTTTTTC	CAAGGGCAATCACCCGA TGAA	PrimerBank ID# 359806891c1
ZNF43	CTTTTCCGCGTTC TCCAAC	GTAACCAACCCACCATT TCCCAG	BLAST
TGFBR3	GGATGGCGTAGTT TTGCCG	TGCAATTTTCAAACCTGC CTCGG	BLAST
NEIL3	ACAACCGCCTCTG CATTCTC	GAAGGACAAATCTGCC ATTCAAA	BLAST
PARN	CAAGGTTCCGGCC ACTCTG	ACTGATTCCTGAAAAC CCCCA	BLAST
HOXB13	GAACAGCCAGATG TGTTGCC	CCCGCTGGAGTCTGCAA ATG	BLAST
TGFBI	TGCTCCCACAAT GAAGCCT	CCTTGGCATCTCCAAG AGT	BLAST
TFPI2	TCTGCTGCTTTTC CTGACGG	CTCCGCGTTATTTCTG TTGG	BLAST
PRAME	CGTGGCAACAAGT GACTGAG	GCTCTGAATGGAACCCC ACA	BLAST
ZIM2	CGGTTTCCTTGCT CAGGACTC	AGCAGCACTAAGGGAAC TAAGT	PrimerBank ID# 226423928c1
SALL1	GCAAGCGAAGCCT CAACATT	TTTCTGTGTCTCCATCTC GCC	BLAST
ZNF20	CACCGTGACCCGC ACTATT	CCTGAAACATCATTTC CGGCT	BLAST
PAF1	TGGTCAAACATCG GGACATGA	CTCCTGCTCCTCATCTG AGCC	BLAST
HOXC9	CTGGACCCCAGCA ACCC	CTCCTTCTCCAGTTCCA GCG	BLAST
MARCKSL1	CCAACGGCCAGGA GAATGG	ATCTGTTCCGTTACAG GGG	BLAST
PRKCZ	CGACCTTCGAGGA GCTCTGT	ACCGTGCAAGGGTCACC TTC	BLAST
FBXO47	GACCCTTGGCTCA GGCTTTC	CATGCTGATATCCTTCA CTGACAA	BLAST
CTSH	TGTCTAAGCACCG TAAGACCT	ATCTTCTCCAGTTGCT GGC	BLAST

Table 2.5. Primer list comprising tissue-associated or disease-associated genes assessed using qPCR.

Gene	Forward	Reverse	Source
COL1A1	GGA GGA GAG TCA GGA AGG	GCA ACA CAG TTA CAC AAG G	Rosa et al 2011 (134)
COL2A1	GGC AGA GGT ATA ATG ATA AGG	ATT ATG TCG TCG CAG AGG	Rosa et al 2011 (134)
ACAN	CCT GGT GTG GCT GCT GTC	CTG GCT CGG TGG TGA ACT C	Rosa et al 2011 (134)
MMP1	GACTCTCCCATCTA CTG	TTA TAG CAT CAA AGG TTA GC	Rosa et al 2011 (134)
MMP13	GTT TCC TAT CTA CAC CTA CAC	CTC GGA GAC TGG TAA TGG	Rosa et al 2011 (134)
TIMP1	TGTTGCTGTGGCTGA TAG	CTGGTATAAGGTGGTCT GG	Rosa et al 2011 (134)
TIMP2	ACGATATACAGGCA CATTATG	GGTCAGGAGTCTTAACA GG	Rosa et al 2011 (134)
TIMP3	CCTACTTCCCCATTA GCCAGTCT	ACAGGGTTTTCTCTGGT TGGTTT	BLAST
ADAMTS4	ATGGCTATGGGCAC TGTCTC	CTGGCGGTCAGCATCAT AGT	BLAST
ADAMTS5	ACAAGAGCCTGGAA GTGAGC	TGCCACATAAATCCTC CCG	BLAST
TNFA	GGCTCCAGGCGGTG CTTGTTT	AGACGGCGATGCGGCT GATG	BLAST
IL1B	AACAGGCTGCTCTG GGATTC	AGTCATCCTCATTGCCA CTGT	BLAST
RPS13	GGCTTTACCCTATCG ACGCA	GTCAGATGTCAACTTCA ACCAAGTG	BLAST
RPS18	GAAGATATGCTCATG TGGTGTTG	CTTGTAAGTGGCGTGGAT TCTG	BLAST
RPS20	AGCCAGGAGTTGAG TTGATCG	AAAGTGTACTGCTGGCC CTC	BLAST
NFKB1	CGCTTAGGAGGGAG AGCCC	TATGGGCCATCTGTTGG CAGT	BLAST
COX2	CAAATCCTTGCTGTT CCCACCCAT	GTGCACTGTGTTTGGAG TGGGTTT	BLAST
NFKBIA	GAGCTCCGAGACTT TCGAGG	CGTGTGGCCATTGTAGT TGG	BLAST

2.6 DNA Extraction

DNA extraction followed a standard protocol and was the same for both monolayer (HFLS samples D, E and F) and pellet cultured cells (HAC samples 5, 7 and 8). Monolayer cells were trypsinised using the standard protocol described earlier and centrifuged (300g, 10 minutes) in microcentrifuge tubes (1.5mL) and the supernatant was aspirated. For pellet cultured cells, the cell culture media was simply aspirated from the microcentrifuge tubes (1.5mL). Cell pellets were washed with phosphate buffered saline (PBS, 1x, Sigma), centrifuged (300g, 5 minutes) and the PBS was aspirated. A standard, premade digestion buffer (300µL) was added to the cell pellet comprising:

- 100mM NaCl (Mr=58.44, 292.2mg in 50mL)
- 10mM TrisCl, pH8 (aka Tris Base) (Mr=121.44, 60.7mg in 50mL)
- 25mM EDTA, pH8 (Mr=292.24, 365.3mg in 50mL)
- 0.5% SDS
- 0.1mg/mL Proteinase K (labile, added fresh every time)

Cell pellets were incubated in digestion buffer overnight (16 hours, 50°C) prior to being vortexed. An equal volume (300µL) of Phenol:Chloroform:IAA (pH7, Sigma) was added to each tube before each tube was then vortexed (1 minute). Tubes were then centrifuged (15,000g, 10 minutes, 4°C) yielding a biphasic mixture. The top aqueous layer was transferred to a fresh tube and ammonium acetate (5M, 300µL, Sigma) was added. Ethanol (100%, Sigma) was added to make the mixture up to 1.5mL. The tubes were then incubated overnight (-20°C). Following incubation, tubes were centrifuged (15,000g, 30 minutes, 4°C) and the supernatant was removed with successively smaller pipette tips in order to remove contaminants as completely as possible. Ethanol (75%, 1mL, Sigma) was added to the pellet as a wash step, the tube was agitated to release the pellet from the bottom and the tube was again centrifuged (15,000g, 10 minutes, 4°C). This wash step was repeated and the

supernatant was removed with successively smaller pipette tips. The tubes were left open to evaporate any remaining ethanol, and the pellet was dissolved in nuclease free water (Promega).

DNA quality was assured using a Nanodrop 1000 spectrometer, wherein the quality of samples were ascertained according to their 260/260 and 260/230 values. DNA was quantified used a Quant-iT™ PicoGreen® dsDNA Kit (Turner BioSystems).

2.7 Microarray

Total RNA and DNA samples from HAC (samples 5, 7 and 8) and HFLS (samples D, E and F) in each of the treatment conditions were isolated and purified as before, prior to transportation at -80°C. Microarrays were carried out externally at the Nottingham Arabidopsis Stock Centre (Affymetrix gene expression arrays), Centre for Genomic Research, University of Cambridge (Illumina gene expression arrays) and the Edinburgh Clinical Research Facility, University of Edinburgh (Illumina DNA methylation arrays).

2.7.1 Affymetrix microarrays

cDNA microarray was carried out externally prior to the current project, by the Nottingham Arabidopsis Stock Centre (NASC) on Affymetrix Whole Transcriptome arrays, namely 'GeneChip Human Gene ST 1.0'. The Affymetrix 'Gene ST' arrays involve cDNA synthesis from the RNA samples using T7 primers, followed by in vitro transcription to cRNA. cDNA is then synthesised from the cRNA using random primers, before the resulting cDNA is fragmented, biotin labelled and mixed for hybridisation. Hybridisation occurs at 45°C for 17hours, with rotations at 60rpm.

Samples (HAC samples 1, 2 and 3; HFLS samples A, B and C) underwent quality control, which ensured that all RNA was pure and intact (RNA integrity (RIN) scores of $10 \pm 2\%$) prior to carrying out the arrays. Quality control was carried out on a 2100 Bioanalyser (Agilent), first upon receiving the samples, and again at the cRNA stage of the process. NanoDrop technology was also used assess purity ($260/280 > 1.8$ and $260/230 > 1$). All microarrays

were carried out together in order to limit environmental variability and batch effect between arrays.

GeneChip analysis was carried out during the current project using statistical packages optimised for the interrogation of large-scale gene expression data in the R environment. Raw expression data was pre-processed for differential expression (DE) analysis using the oligo package (182). Following examination of array images for spatial artefacts, pre-processing involved log-normalisation using a combination of global background correction, loess normalisation and median polish, carried out via the Robust MultiChip Averaging (RMA) algorithm. Additional packages were used for DE analysis, with limma (183) being used for modelling the normalised expression data and carrying out statistical ranking using the empirical Bayes method. Limma uses sample size, combined with the number of expression values, to determine False Discovery Rate (FDR), satisfying the necessary statistical correction for multiple hypothesis testing. The resulting q-values (FDR-adjusted p-values) were considered significant below 25%. Modelling took into account the same-sample correlation between normal glucose (5.5mM) and high glucose (30mM, 48h) expression data, as well as 'array-weight' values applied to ensure that a minimal effect was incurred by spatial artefacts.

Pathway analysis was carried out using a combination of the SPIA and KEGGgraph packages along with Ingenuity Integrated Pathway Analysis (IPA) tool. Gene Set Enrichment Analysis was carried out using R-GSEA, the R script that allows for the GSEA program (184, 185) to be ported into the R environment.

2.7.2 Illumina Human Gene HT-12 v4 Arrays

Gene expression arrays carried out using the Illumina Human Gene HT-12 v4 arrays were performed at the Centre for Genomic Research (CGR) of the University of Cambridge. The RNA samples (from HAC samples 5, 7 and 8; and HFLS samples D, E and F) were subject to quality control analysis using an Agilent bioanalyser to obtain RNA integrity values (RIN

values). The arrays were, where possible, performed together to eliminate the likelihood of environmental factors and batch effect from affecting the data. The data was analysed in the R environment using primarily packages from the Bioconductor project (186). Cell-type specific data analysis was used to limit the effect of the expected variation between different cell types on the ability of the analysis to detect subtle, but potentially important, changes in gene expression. The primary package used for interpreting the array data and carrying out initial preprocessing was the beadarray package (187). Preprocessing of the arrays involved a multi-step process that included reading the arrays into the R environment together, to create a Bead Level Data object. The arrays were then subjected to the “median” method of background correction made available through the beadarray package. A BASH algorithm was then used to enable “neighbour”-wide probe-level weights to be taken into account when later summarizing the Bead Level Data. A HULK algorithm was subsequently used which employed a “neighbourhood matrix” to smooth variation in intensities across detected spatial artefacts. After this initial preprocessing, data was then visualised and assessed for biasing. This involved using functions selecting for the visualisation of data corresponding to predetermined control probes included in the array architecture. These control probes are used to identify issues that may have occurred during any one of the many stages of processing the arrays. At this early stage it was important to identify obvious outliers in the sample set. Outlier identification was used in order to limit the effect of outliers in skewing the summarisation and normalisation of the data. Data summarization was then carried out using standard functions of the beadarray package to create a Bead Summarisation Data object. Summarised data was subsequently normalised using a quantile normalisation function available in the beadarray package. In order to limit the effect of control probes on the eventual results, known control probes were removed from the analysis at this stage. Probe-level detection scores, obtained during the summarization of the data, were used to remove probes having a detection score below the advised threshold (0.05). Probes of suboptimal “probe quality” were also removed from the analysis (quality scores of “No match”, “Bad” or anywhere probe quality scores were unavailable). Following the above

preprocessing, the data was then modelled using the linear modelling for microarrays package, limma (183). The data was arranged so that the modelling process considered the paired nature of the samples. Differential expression analysis was carried out using dedicated functions in the limma package.

2.7.3 Illumina Human Methylation 450k Arrays

Methylation arrays were carried out using the Illumina Human Methylation 450k platform at the Edinburgh Clinical Research Facility (CRF). DNA (from HAC samples 5, 7 and 8; and HFLS samples D, E and F) was subjected to quality control using spectroscopic methods and quantified using an established picoGreen assay.

Analysis of these arrays was carried out primarily using the minfi package (188). The minfi package was used to read in the data files together. As with the previous analysis methods, cell-type specific analyses were carried out to limit the large expected variability between cell-types affecting the ability of the analysis to highlight subtle differences in methylation levels. After reading the data files, the minfi package was used to carry out a Subset-quantile Within Array Normalisation (SWAN) upon the data (189). Any probes that were associated with SNPs or control probes (as identified using functions within the minfi package) were eliminated from the analysis at this stage. Probe-level failure detection was used to remove failed probes from the analysis. Data was visualised in order to identify the presence of outliers. Data was modelled in limma, taking into account the paired nature of the sample set. Differential methylation analysis was carried out using limma, minfi and DMRcate (190). Specifically, differentially methylated CpGs were identified in a point-methylation analysis, and differentially methylated regions were identified using regional analysis of multiple differentially methylated CpGs within a threshold (500bp) with a lower percentage differential methylation cut-off of 10%. P-values were corrected for false discovery rate using the Benjamini-Hochberg method.

2.8 Pyrosequencing

Differential methylation of specific CpG sites was assessed using targeted pyrosequencing. DNA was used from the same samples submitted for differential methylation analysis using the Illumina Human Methylation 450k microarray. Data from the methylation microarray data was used to identify targets for pyrosequencing analysis. 500bp surround sequences of the top ten most significantly affected CpG sites identified within the promoter region of genes and within a CpG island or shore using methylation microarray analysis were used to design primers for pyrosequencing, which can be seen in Table 2.6 below. Primers were designed using PyroMark Assay Design 2.0 (Qiagen). DNA was bisulphite converted using EZ DNA Methylation kit (Zymo Research) and amplified using Titanium Taq DNA Polymerase (Clontech). For bisulphite conversion, DNA was incubated with an M-Dilution buffer (5 μ L into 45 μ L DNA, 37°C, 15 minutes) prior to overnight treatment with a CT conversion reagent (50°C, 16 hours). After overnight incubation, samples were left on ice for 10 minutes before following a spin column protocol wherein DNA was bound to a silicon spin column and eluted in nuclease free elution buffer after a number of wash phases. Bisulphite converted samples were amplified using a multitude of target primers. 25 μ L reaction mixes comprised 10x Titanium Taq PCR buffer (2.5 μ L), 50x dNTP mix (0.5 μ L, 10mM of each of dATP, dCTP, dTTP, and dGTP), primer mix (0.5 μ L, 3.5 μ M biotinylated, 7 μ M non-biotinylated), 50x Titanium Taq DNA polymerase (0.5 μ L), DNA template (21 μ L). PCR was carried out using a multi-temperature thermal cycler. Annealing temperature ranges (\pm 6°C) were calculated according to the melting temperature of the primers used, identified using the Applied Biosystems online primer melting temperature calculator (191). The temperature protocol used comprised 95°C for 5 minutes, followed by 40 cycles of denaturing (95°C, 30 seconds), annealing (primer $T_m \pm 6^\circ\text{C}$ at intervals of 1°C, 30 seconds) and extension (72°C, 15-30 seconds), and a final extension step (72°C, 10 minutes). Samples were transported on ice for qualitative analysis using gel electrophoresis.

For gel electrophoresis, 50x TAE buffer (BioRad) was diluted to 1x using distilled water. A 1% agarose gel was made by mixing agarose (1.5g, Sigma) with the 1x TAE buffer (150mL) in a conical flask and heating in the microwave until bubbles began to form. At this point, the mixture was swirled to partially dissolve the agarose, before being placed back into the microwave to heat. Careful attention was paid to ensure the mixture did not over-excite. At multiple points the mixture was removed from the microwave and swirled, before being placed back into the microwave. This final step was repeated until no further agarose crystals were observed. The mixture was left to cool (around 2.5 minutes to 5 minutes) in a fume hood, prior to adding ethidium bromide (10 μ L/100mL 1x TAE buffer) and swirling once more, while at all times remaining in the fume hood. The mixture was then poured into pre-sealed gel tray and comb (BioRad) and left to set in the fume hood. After setting the comb and sealant (autoclave tape) were removed and blue gel loading buffer (5x, Life Technologies) was prepared to account for the number of samples being used (9 μ L for n+1 samples to account for error) and placed on ice. The set agarose gel in the gel tray was placed into a suitable horizontal gel tank (BioRad), and the tank was filled with the pre-prepared 1x TAE buffer until the buffer level was around 0.5cm above the upper surface of the set agarose gel.

PCR product samples (1 μ L) were prepared on ice and the pre-prepared loading buffer was added (9 μ L per sample) and the product/loading buffer mixture was subsequently loaded into the wells of the gel, which was then electrophoresed (5V/cm, 90 minutes) using a PowerPac 200 power bank (BioRad). Gels were then imaged using a transilluminator (SnapGene). Gels were used to identify the optimum annealing temperature protocol used for each primer, the product of which was then used for subsequent pyrosequencing.

Pyrosequencing plate layouts were designed using PyroMark Q96 software (Qiagen) and these layouts were used to arrange PCR products from bisulphite-converted DNA from each of the treatment groups within one or more PyroMark 96-well plates (Qiagen). Pyrosequencing was carried out using a PyroMark Q96 ID pyrosequencer (Qiagen), with 96-

well plate preparation being carried out on the PyroMark Q96 Vacuum Workstation. The four troughs of the workstation were filled with pre-prepared solutions of 70% ethanol in a first trough; denaturation solution in a second trough; wash buffer in a third trough; and distilled water in a fourth and fifth trough.

Table 2.6. Primer list for pyrosequencing, with [Btn] indicating biotinylation.

Gene	CpG	Forward	Reverse	Sequencing
MARCKSL1	cg00556029	GGAATTTTAGGGGTAGGTA GAGTT	[Btn]CCTTCTCCTCCTCCA AAC	TTAGGGGTAGGT AGAGT
PARN	cg00965110	AATTTTAGGGGTAGGTAGA GTT	[Btn]CTCTCCTCCTCCAAA CC	TTAGGGGTAGGT AGAGT
FBXO47	cg04120272	[Btn]AGGGTATTATGGGAGT TGGT	CCTCCCTCATAAATATTAT AAATCT	ATCTTCCCAAAAA CCCTAAC
SALL1	cg06232807	GGATTGGAATGTTGAGGT T	[Btn]ATTCTACCCCACTAA TATTTAAACC	TGGAAATGTTGAG GTT
PRAME	cg08831999	[Btn]GGGGAGTTGTATTTTG AAGTT	CAATCCCTATTA ACTCTAA TACCC	AATACCCCCTACT AACC
PAF1	cg10070151	GATTGGTTTAATTGTTTAGG G	[Btn]CTACTAAAATACAACC ATCTTCCTC	TTGGTTTAATTGT TTAGG
ZIM2	cg15678121	AGAGTTTTTTATTTATTAAG GAAAT	[Btn]AAACAAATATACACAT CTATCTAAAT	TTATTTATTAAGG AAATT
TGFBI	cg18418457	GTTTTGTAGTTTTAAGATTA GTGAGGG	[Btn]ATCCCTTAAACCTCCT ATACTACTTC	TTAAGATTAGTGA GGGAA
ZNF20	cg22715562	GTTTTTGATTGGATAAGGTA TAA	[Btn]CTTAAAAAAAAACTAT AACTAAAACC	TTTTGATTGGATA AGGTATAA
IGF2	cg25574024	AGATGAGATTTTTGTAATGA GTAAA	[Btn]ACCCCATCTACTACT ATCCC	AGATTTTTGTAAT GAGTA

A pyrosequencing master mix was first produced to bind the PCR products, comprising proportions of streptavidin-coated Sepharose beads (3 μ L per well to be used, GE Healthcare); a binding buffer (50 μ L per well to be used, Qiagen); and distilled water (17 μ L per well to be used) – proportionally adjusted to account for pipette error. 70 μ L of master mix was added to each well of a PyroMark 96-well plate, followed by 10 μ L of each PCR product sample from each cell sample and treatment group, according to the pre-prepared plate layouts. The 96-well plates were covered using 96-well plate sealing film (Thermo Scientific), and the plates were agitated (5minutes, 1000rpm, Microplate Genie, Scientific Industries Inc.) to enhance annealing of the PCR products to the beads. A fresh PyroMark 96-well plate was prepared with each sequencing primer (40 μ L of 0.4 μ M sequencing primer diluted in distilled water) according to the pre-prepared plate layouts. After agitation the 96-well plates comprising master mix and bead-bound PCR product were unsealed and the vacuum pump on the workstation was turned on. After flushing the vacuum tool with distilled water, the tool was positioned within the wells of the 96-well plate and quickly swirled to attach the beads. If beads remained visible at the bottom of the 96-well plate wells, spare master mix (minus Sepharose beads) was used to agitate the beads, and the vacuum tool was once again used within the 96-well plate. Sequentially, the vacuum tool was then placed into the trough containing 70% ethanol (5 seconds); the trough containing denaturation solution (5 seconds); and then the trough containing wash buffer (5 seconds). In between each trough the vacuum tool was upended to ensure attachment of the beads. The vacuum pump was then switched off and the vacuum tool was aligned with the 96-well plate comprising the sequencing primers. The vacuum tool was then swirled to release the beads into the wells, and was then washed in the trough comprising distilled water (10 seconds) before having the vacuum turned on the flush the vacuum tubes with distilled water. The 96-well plate comprising bead-bound PCR-products and sequencing primers was then heated in a heat block (80°C, 5 minutes). After heating, the plate was allowed to cool to room temperature (5 minutes). A PyroMark Q96 Cartridge (Qiagen) was prepared with all nucleotides (deoxyadenosine alpha-thio triphosphate (dATP α S), deoxythymine triphosphate (dTTP),

deoxycytosine triphosphate (dCTP), and deoxyguanine triphosphate (dGTP)), enzymes (DNA polymerase, ATP sulphurylase, luciferase, and apyrase), and substrate mixtures (adenosine 5' phosphosulphate (APS), and luciferin) required for pyrosequencing (PyroMark Gold Q96 Reagent kit, Qiagen). Pyrosequencing was then carried out by the Q96 ID pyrosequencer according to the predesigned assays specific to each PCR product being assessed. Subsequent data was analysed using PyroMark Q96 software (Qiagen).

2.9 Oxidative DNA Damage

An investigation into DNA damage from a gene expression perspective was followed up with a functional assessment including a DNA damage assay following high glucose treatment. Identified as a potential cause of DNA damage from the literature, reactive oxygen species levels were also assessed following treatment with high glucose.

2.9.1 Single cell gel electrophoresis

DNA damage was assessed using the comet assay (192), which uses single cell gel electrophoresis to infer fragmentation in genomic material and consequently the levels of DNA damage. Cells (HAC samples 4, 5 and 6; HFLS samples D, E and F) were cultured to confluence in normal glucose (5.5mM), prior to being either treated with high glucose (11mM or 30mM) for 14 days, or treated with normal glucose (5.5mM) for 14 days and treated with high glucose (11mM or 30mM) 16 hours prior to cessation of the experiment. Cells were separately treated with hydrogen peroxide (H_2O_2 , 100 μ M, 4 hours prior to the end of treatment, Sigma) as a positive control. Hydrogen peroxide is a standard positive control for the comet assay, with its use being discussed by Olive *et al* (192). Cells were treated in parallel with normal glucose (5.5mM) for the entire duration of the experiment as a normal glucose control.

In preparation, the upper surface of microscope slides (Greiner) were scored, defining a rough rectangular shape around half the length of the slide and with around 1mm margin from the side edges of the slide. The edges of the rectangles were scored around three to

four times, with each line being kept as close together as possible, and were scored using a diamond-tipped pen. The aim of the scorings was to enable a layer of gel to suitably adhere to the slide, and remain adhered with mild agitation and washings throughout the comet assay protocol. The centre portions of the scored rectangles were kept clear of scoring so as not to hinder the ability to view the slides under a microscope. Scored slides were quickly dipped in normal melting point agarose solution (1%, 100°C, Sigma), up to a round half the length of the slide, and left to set as a rectangular gel layer. This step was repeated multiple times to ensure that the layer of set agarose was sufficient. Slides were then refrigerated (4°C) until need.

Following treatment, cells were trypsinised using the standard protocol described earlier. Cells were resuspended in PBS (1x, Sigma), and counted using an automated cytometer (TC20, BioRad). Low-melting point agarose solution (1%, Sigma) was pre-warmed (37°C) prior to use. Cells were diluted to give 10^5 cells/100µL PBS. 700µL pre-warmed low-melting point agarose was then added to 100µL cell suspension. Cells were immediately evenly distributed using sequential pipetting (1000µL pipette tip to minimise shearing) before the agarose/cell suspension was added to a microscope slide pre-prepared as described before. The gel was allowed to set at room temperature (around 5 minutes) before the slides were added to an alkaline cell lysis buffer comprising: 1.2M NaCl; 100mM EDTA; 0.1% SDS (sodium lauryl sarcosinate); 0.26M NaOH; pH 13. The slides were left to incubate in the lysis buffer overnight (4°C).

Following lysis, slides were rinsed in an alkaline rinsing buffer for 10 minutes at room temperature comprising: 0.03M NaOH; 2mM EDTA; pH 12.3. Slides were then randomly ordered in an electrophoresis tank and the tank was filled with the alkaline rinsing buffer described earlier. The buffer level was adjusted until the current capacity was 300mA and the cells were electrophoresed (30 minutes, 0.75V/cm). After electrophoresis, the slides were removed from the tank and left to drain. Following electrophoresis, the slides were added to a picoGreen solution (10µL/100mL, Turner Biosciences) for 45 minutes. Slides

were then placed in distilled water for 10 minutes and then left to drain. After staining, slides were stored (4°C) until imaged.

Cells were imaged using a fluorescent microscope (Nikon), and the resultant images were analysed using image analysis software specifically designed for comet assay analysis, Casplab (193). Using Casplab, images of cells were analysed to quantify the “comet tail” indicating the level of DNA damage. The metric used to quantify the level of DNA damage was the Olive Tail Moment (192).

2.9.2 Reactive oxygen species

As a potential source of DNA damage, reactive oxygen species levels were assessed following high glucose treatments.

Following glucose treatment, cells (HAC samples 5, 7 and 8; HFLS samples D, G and H) were trypsinised using the standard protocol described earlier. The cells were then seeded in 96 well plates at a controlled cell density (25,000cells/well). Dichlorofluorescein diacetate (DCFDA, 25µM, Sigma) was added to each well and cells were incubated for 45 minutes (37°C). A section of cells were treated with no DCFDA, as a negative control. A positive control was used where cells were treated with hydrogen peroxide (H₂O₂, 100µM, 4 hours, Sigma) prior to addition of DCFDA. After incubation, plates were immediately read (using filter suitable for fluorescein, 460nm/515nm) for fluorescence (GloMax, Promega).

2.10 Cell adhesion

The cell adhesion capabilities of chondrocytes and synoviocytes were tested following treatment with high glucose using a cell adhesion assay. This assay tested the ability of cells to re-adhere to cell culture plastic following a trypsinisation step previously described.

Cells (HAC samples 5, 7 and 8; HFLS samples D, G and H) were seeded in 6-well plates (Greiner) and were treated with normal glucose (5.5mM), or high glucose (11mM or 30mM) for either 14 days or 16 hours. 16 hour-treated cells were in cell culture for the same length of time as 14 day-treated cells, and were cultured in normal glucose (5.5mM) conditions until

16 hours prior to the end of the 14 day treatment. In all treatments, cell culture media was changed 3 times per week. After treatment, cells were trypsinised using the standard protocol described and were counted using an automated cytometer (TC20, BioRad). Cells were then seeded at controlled cell density (25,000 cells per well) in 96-well plates and incubated (37°C) in normal glucose (5.5mM) culture media for 24 hours. After incubation, cell culture media was aspirated and wells were washed once with PBS (1x, Sigma). Wells were then filled with cell culture media containing picoGreen (3µL/mL, Turner Biosciences) nucleic acid dye as a measure of cell number. Cells were incubated for 45 minutes before fluorescence was measured on a 96-well plate reader (Glomax, Promega).

Wells containing picoGreen solution but no cells were used as no cell controls. Fluorescence values of each plate were corrected according to the corresponding no cell controls.

2.11 pH

pH of cell culture media was assessed following the different treatment conditions. Cells (HAC samples 4, 5 and 6; HFLS samples D, E and F) in monolayer culture were grown to confluence in normal glucose (5.5mM). A subsection of cells were then entered into a 14 day exposure to high glucose (11mM or 30mM), with a subsection remaining in normal glucose (5.5mM) until 16 hours prior to the end of the 14 day exposure period. At this point, a subsection of cells were treated with high glucose (11mM or 30mM) for 16 hours and the remaining cells were maintained in normal glucose (5.5mM) as a control.

At the end of the 14 day time period, the cell culture media was removed and immediately assessed for pH levels using a pH meter (Corning).

2.12 Statistical Analysis

Statistical analysis was performed in R. In the case of microarray analysis, statistical analysis was performed within specialised packages as previously described. For all other data, replicate data was subjected to either ANOVA or Kruskal-Wallis tests, after the normality of the data was tested using a Shapiro-Wilk test. Corresponding post-hoc tests

were subsequently used to derive P values of pairwise comparisons, with values of $P \leq 0.05$ being considered significant.

2.13 Manufacturer details

A list of manufacturer details is provided in Table 2.7, for the purpose of obtaining the materials and equipment described herein.

Table 2.7 Manufacturer details

Manufacturer name	Manufacturer address
Agilent	Agilent Technologies LDA UK Limited, Life Sciences & Chemical Analysis Group, Lakeside, Cheadle Royal Business Park, Stockport, Cheshire SK8 3GR
Applied Biosystems	7 Kingsland Grange, Warrington, Woolston, WA1 4SR
BioRad	Bio-Rad Laboratories Ltd., The Junction, Station Road, Watford, Hertfordshire, WD17 1ET
Cell Applications Inc	Cell Applications, Inc., 5820 Oberlin Dr, Suite 101, San Diego, CA 92121
Clontech	2 Avenue du Président Kennedy, 78100 Saint-Germain-en-Laye, France
Corning	Elwy House, Lakeside Business Village, St David's Park, Flintshire, CH5 3XD
Eurogentec	Eurogentec Ltd., The Square, Fawley, Southampton, Hampshire SO45 1DD, UK
GIBCO	Manor Park, Tudor Rd, Cheshire, Runcorn WA7 1TA
Greiner	Unit 5/Brunel Way, Stonehouse GL10 3SX
Konelab	Manor Park, Tudor Rd, Cheshire, Runcorn WA7 1TA
Life Technologies	Manor Park, Tudor Rd, Cheshire, Runcorn WA7 1TA
Lonza	Wheldon Rd, Castleford WF10 2JT
Peprotech	29 Margravine Rd, Hammersmith, London W6 8LL
Promega	Enterprise Rd, Chilworth, Southampton SO16 7NS
Qiagen	Skelton House, Lloyd St N, Manchester M15 6SH
Sigma	Fancy Rd, Poole BH12 4QH
Turner Biosystems	Enterprise Rd, Chilworth, Southampton SO16 7NS

3. Glucose uptake is reduced in chondrocytes and synoviocytes following high glucose exposure

3.1 Introduction

Being metabolically active cells, chondrocyte and synoviocytes would be expected to absorb and utilise glucose from their environment readily in order to remain functional. There have been studies that have attempted to characterise the glucose uptake in normal functioning chondrocytes (128, 129). There has, however, been relatively little prior research into the uptake of glucose by synoviocytes exposed to normal levels of glucose. Even less is known about the effects of abnormal extracellular glucose conditions on the glucose uptake by either of these key cell types.

There has been a plethora of prior research studies investigating the effects of high glucose in a variety of cell types, for instance hepatocytes and retinal pericytes (161, 194). These studies do not attempt to characterise the relationship between extracellular and intracellular glucose concentrations in each of these cell types. Since the rate of glucose uptake is typically presumed to be proportional to the extracellular concentrations of glucose in these many cell types it would appear that it is often taken for granted that these cells take an amount of glucose proportional to their surrounding environment and therefore stand to suffer deleterious consequences throughout the period of treatment. Due to the design of the present study, comprising both short-term and long-term high glucose treatments, it was deemed advisable to understand the susceptibility of these cells to extracellular high glucose loads based upon their level of glucose uptake for the term of the treatments used.

In order to identify a likely effector of the negative effects of high glucose, it is important to understand whether the level of glucose uptake corresponds with the extracellular glucose concentration. If glucose uptake does not correspond with the extracellular glucose environment, there is the potential that the response to high glucose by these cells may be limited,. Where the uptake of glucose is robust to extracellular changes, this could suggest that the cells are not likely to suffer profound effects from a high glucose insult. This of course does not account for effects that may occur through the activation of transmembrane signalling mechanisms, such as those potentially caused by alterations to the osmolarity of

the surrounding environment or secondary effects of, for example, the formation of glycation end-products.

The notion that glucose uptake could be tied to potential downstream effects does highlight the importance of understanding how these cells may react to fluctuations in extracellular glucose, and how this could act as a precursor for further effects of a high glucose insult.

3.2 Chondrocytes

3.2.1 Chondrocyte glucose uptake

The effects of increased glucose exposure on musculoskeletal cells could become evident upon an improved understanding of how these cells utilise glucose when faced with an increased supply. There has been relatively little prior research investigating the effects of high glucose exposure on glucose uptake in musculoskeletal cells across a range of high glucose concentrations. The glucose concentrations used for this study (5mM, 11mM and 30mM) provide for a range of observed effects at physiological levels of normal and high blood glucose, and at high diabetic blood glucose levels. Chondrocytes in pellet culture were tested for glucose uptake across the range of glucose concentrations described at short term (16 hours) and long term (14 days) time points. Pellet culture was used to more closely mimic the natural environment of chondrocytes and provide a culture method that was more robust to dedifferentiation of chondrocytes known to take place in monolayer culture (195). Figure 3.01A shows that glucose uptake is increased in cells subjected to physiological levels of glucose over a short time period (11mM, 16 hours, $p < 0.001$) and a high diabetic level of glucose over a short time period (30mM, 16 hours, $p < 0.05$). After a high diabetic level of glucose over a long time period (30mM, 14 days), however, glucose uptake was significantly reduced by around 70% ($p < 0.01$). Glucose uptake in cells exposed to a physiological level of high glucose over a long time period (11mM, 14 days) was not significantly increased, although the trend in the graph would suggest a partially maintained increase in glucose uptake in the 11mM treatment over the 16 hour and 14 day periods.

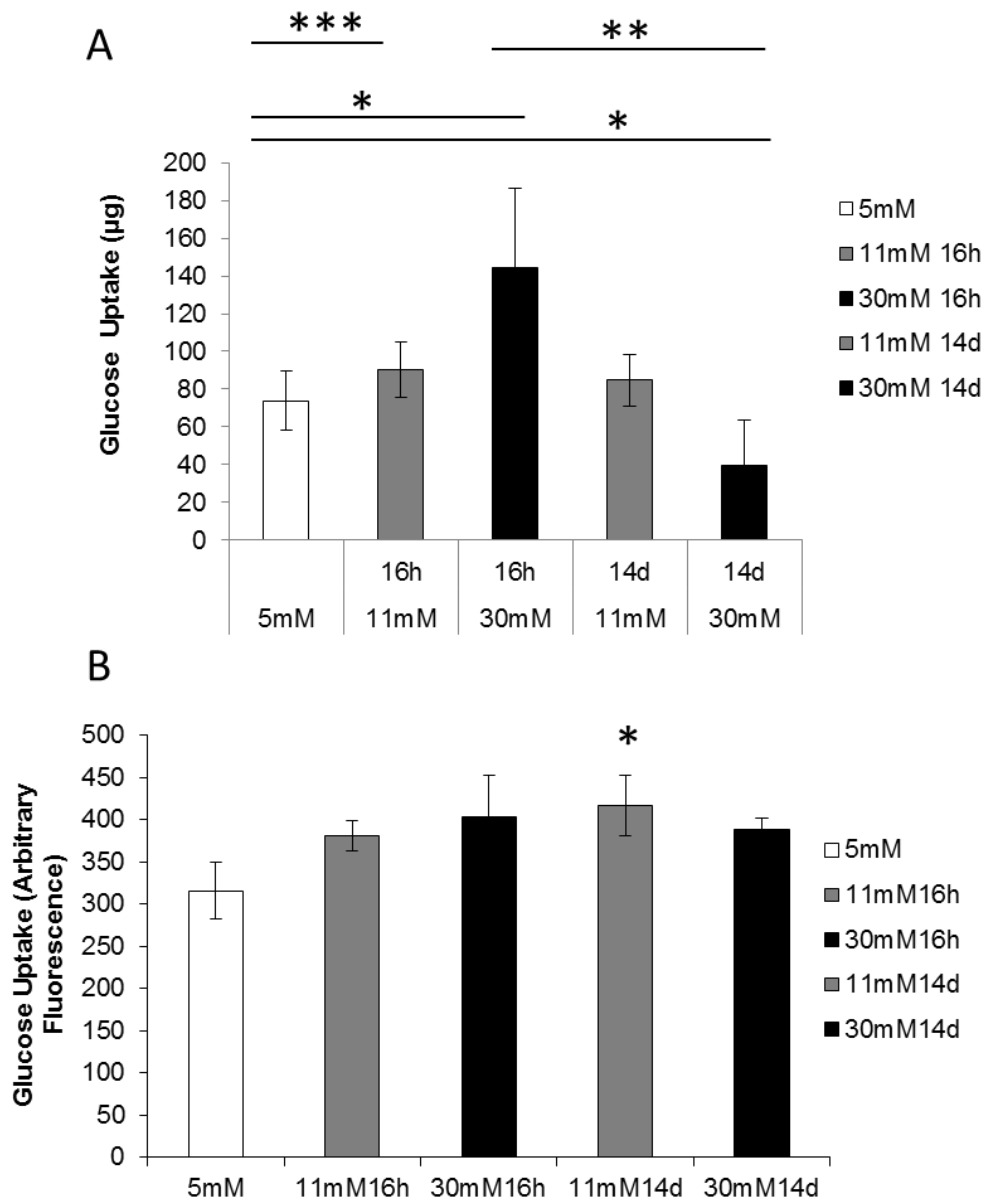


Figure 3.01. Chondrocyte glucose uptake. Cells were treated for 14d with either normal glucose (5mM) or high glucose (11mM, or 30mM). After the 14d treatments, a portion of the 5mM treated cells were treated with high glucose (11mM or 30mM) for 16h. During this period all other treatment groups had their media changed also. Glucose uptake was measured after this final 16h of glucose treatment. There was a dose-dependent increase in the amount (μg) of glucose uptake in high-glucose naïve chondrocytes (16h treated cells), but this was followed by a significant ($p < 0.01$) reduction in uptake observed in long-term (14d) 30mM treated cells (A). A 10-minute snapshot of glucose uptake *after* the final 16h of the glucose treatment is also shown (B). Data ($n = 5$) is shown as mean \pm standard deviation (*: $p < 0.05$; **: $p < 0.01$; ***: $p < 0.001$).

Chondrocytes appear to increase their glucose uptake, dose-dependently, upon subjection to a short-term (16 hours) high glucose environment (Figure 3.01A). In the long-term (14 days) however, chondrocytes appear to reduce their glucose uptake when exposed to high-diabetic concentrations of glucose (30mM), but appear to maintain their increased glucose uptake when subjected to physiological high glucose concentrations (11mM). The data in Figure 3.01A was derived from hexokinase tests (Konelab). The amount of glucose taken up from the media by the cells was determined by normalising the data to a no-cell control, converting the “consumed” concentration (mM) into a “consumed” amount (μg).

The dose-dependent increase in glucose uptake that is evident over a 16 hour time period from Figure 3.01A appears to be the result of a relatively large but transient increase in the rate of glucose uptake in these cells. This increase in the rate of glucose uptake would appear to be short lived, as can be observed in Figure 3.01B, which shows a snap-shot of glucose uptake over a short period (10 minutes) upon completion of the glucose treatments. The rate of glucose uptake over this 10 minute period is measured as an increase in fluorescence, corresponding to the magnitude of uptake of fluorescent glucose analogue, 2-(N-(7-Nitrobenz-2-oxa-1,3-diazol-4-yl)Amino)-2-Deoxyglucose (2NBDG). The rate of uptake would appear to suggest that the increased rate of glucose uptake is maintained in the physiological high glucose exposure over the long time period (11mM, 14 days, $p < 0.05$). That the trend in the data indicated by Figure 3.01A is not mirrored in that indicated by Figure 3.01B, would suggest that the increased glucose uptake from the culture media by these cells occurs early on after the change of the culture media.

3.2.2 Chondrocyte metabolomics

Glucose measurements were also taken from the extracellular and intracellular environment of chondrocytes exposed to short term (16 hours) and long term (14 days) glucose treatments (5mM, 11mM, and 30mM) using nuclear magnetic resonance spectroscopy (NMR). Figure 3.02A shows the extracellular glucose levels after the final 16 hours of the glucose treatments (immediately prior to which media was changed in all treatment groups).

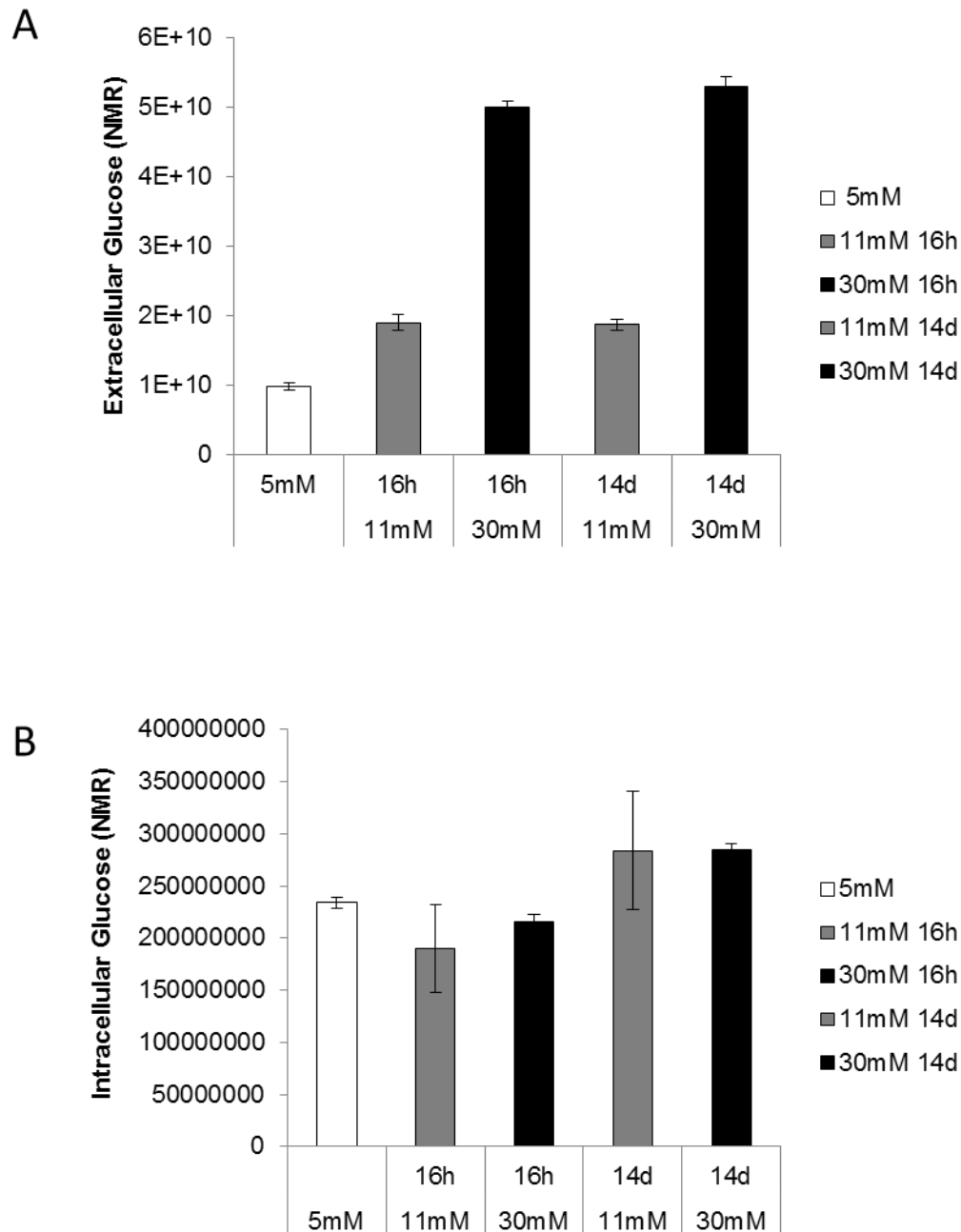


Figure 3.02. Level of glucose detected by nuclear magnetic resonance spectroscopy after 16h media changes for media of chondrocytes (A); and chondrocyte cell lysates (B). There is no time-dependent statistical difference seen in the extracellular and intracellular glucose measurements shown in A and B. Data (n = 3) is shown as mean \pm standard deviations.

In the case of the short term treatments (16 hours), this final 16 hours comprises the entire length of the high glucose treatment. In the case of the long term treatments (14 days) and

the normal glucose controls, the data representing this final 16 hours represents an effect of the long term exposure to these treatment conditions. There is no significant difference in the level of uptake from the long term high glucose treatments (11mM 16 hours and 30mM 16 hours) when compared to the corresponding short term high glucose treatments (11mM 14 days and 30mM 14 days), when considering the paired nature of the samples (Figure 3.02A). In spite of this the trend in the data would suggest a corroboration with the hexokinase test data from Figure 3.01, in that the long-term high diabetic glucose treatment (30mM, 14 days) appears to contain a greater amount of glucose remaining in the media after the term of exposure to fresh media. This may suggest less uptake of glucose in the long term treated high diabetic glucose (30mM) exposed chondrocytes. As can also be seen from Figure 3.02A, there is a lack of significant difference in the glucose present within the media between both 11mM glucose treatments. This suggests that the level of glucose uptake in these cells is maintained.

A potential reason for a reduction in glucose uptake in the long term high diabetic glucose (30mM, 14 days) exposed chondrocytes is that there is perhaps a saturation of glucose inside the cell and therefore the cells may be unable to take up any further glucose from the media. Figure 3.02B shows intracellular glucose levels in chondrocytes after the same treatments. This data suggests that there is no significant difference in the level of intracellular glucose between these treatment types at this time point. In particular, it is interesting to note that there is no significant difference between the intracellular glucose present in cells exposed to a normal glucose control (5mM) and the high diabetic glucose (30mM) conditions.

3.2.3 Chondrocyte transporter expression (Class 1 – GLUT1, 3 & 14)

From the results detecting direct glucose uptake and intracellular glucose concentrations in chondrocytes there is a potential effect of high glucose treatment on glucose uptake, with this potentially indicating an effect on glucose transporter expression. Modifications to expression levels of glucose transporters could lead to such alterations in glucose uptake.

The results from Figure 3.01 and Figure 3.02 indicate that glucose uptake after long term (14 days) high glucose (30mM) exposure is reduced, potentially suggesting a reduction in glucose transporter expression in in this treatment group.

Figure 3.03A to Figure 3.03C shows the gene expression of class I GLUTs in chondrocytes as result of exposure to physiological high blood glucose (11mM) and high diabetic blood glucose (30mM) over short term (16 hours) and long term (14 days) time periods. These treatment groups were compared to a normal blood glucose control (5mM). No detectable expression of GLUT2 (*SLC2A2*) or GLUT4 (*SLC2A4*) was observed in these cells across any of the treatment groups. Figure 3.03A shows that expression of GLUT1 (*SLC2A1*) was significantly increased as a result of exposure to high diabetic glucose levels (30mM) over short and long time periods (16 hours and 14 days respectively, $p < 0.05$). Expression of GLUT1 (*SLC2A1*) was also significantly increased after exposure to physiological levels of blood glucose over the long term (11mM, 14 days, $p < 0.05$).

Figure 3.03B shows that as with GLUT1 (*SLC2A1*), expression of GLUT3 (*SLC2A3*) was also significantly increased at both short and long term time periods (16 hours and 14 days) as a result of exposure to high diabetic glucose levels (30mM, $p < 0.05$). Gene expression of GLUT14 (*SLC2A14*) was not significantly altered as a result of high glucose exposure (Figure 3.03C). From the graphs of Figure 3.03A to Figure 3.03C, the expression of GLUT1 (*SLC2A1*) is highest amongst the class I GLUTs in chondrocytes, relative to the housekeeping gene for β -actin (*ACTB*) obtained from a selection of housekeeping genes using the GeNorm algorithm (174) applied in the R environment (175).

3.2.4 Chondrocyte glucose transporter expression (Class 2 – GLUT5, 9 & 11)

Figure 3.04 shows the expression of genes associated class II GLUTs in response to an increased exposure to extracellular glucose levels. There was no measurable expression of GLUT7 (*SLC2A7*) observed in any of the treatments groups. No significant high glucose-mediated differences in expression of genes for GLUT5 (*SLC2A5*), GLUT9 (*SLC2A9*) or

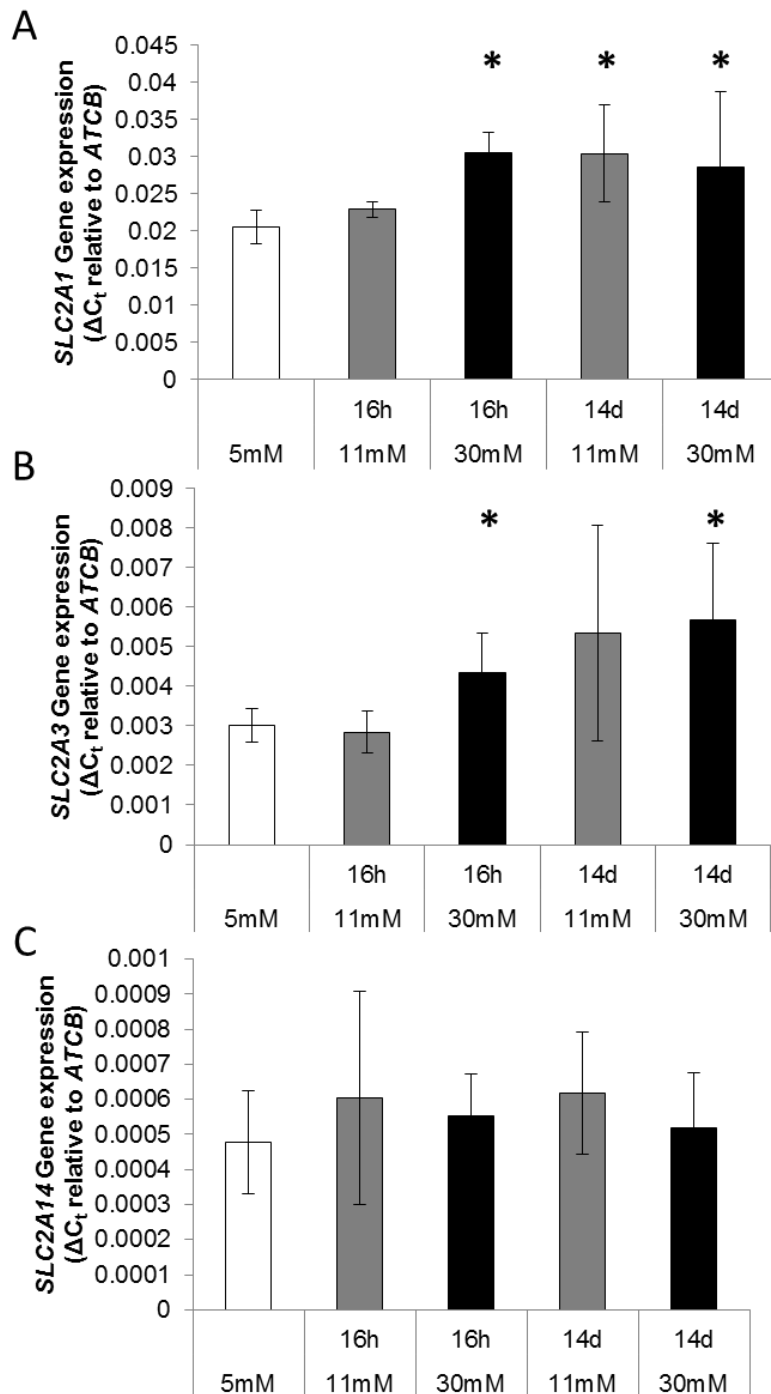


Figure 3.03. Chondrocyte gene expression of Class I glucose transporter (GLUT). A significant increase in expression of GLUT1 (*SLC2A1*) (A) and GLUT3 (*SLC2A3*) (B) was observed after treatment with 30mM glucose for 16h and 14d ($p < 0.05$). A significant increase in GLUT1 (*SLC2A1*) (A) expression was also observed after long term (14d) treatment with 11mM glucose ($p < 0.05$). No significant differences in expression were observed for GLUT14 (*SLC2A14*) (C). Data ($n = 3$) is shown as mean \pm standard deviation.

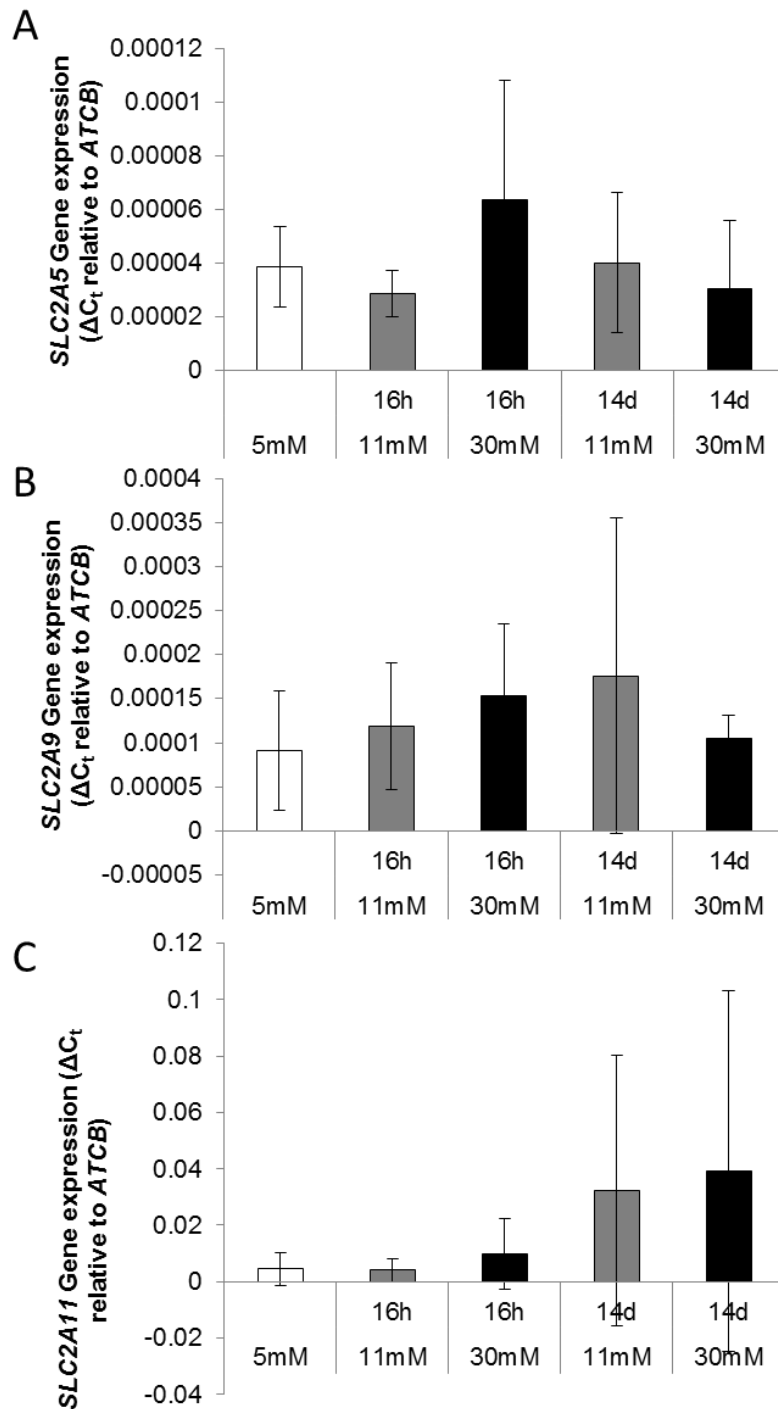


Figure 3.04. Chondrocyte expression of Class 2 glucose transporter (GLUT) genes. No significant differences were observed in chondrocyte expression of genes for GLUT5 (*SLC2A5*) (A), GLUT9 (*SLC2A9*) (B) or GLUT11 (*SLC2A11*) (C). Long term (14d) high glucose (11mM and 30mM) may appear to produce a variable response in expression of the gene for GLUT11 (*SLC2A11*) (C). Data (n = 3) is shown as mean \pm standard deviation.

GLUT11 (*SLC2A11*) were observed. The expression of GLUT11 (*SLC2A11*) can be seen in Figure 3.04C to be highly variable across the long term treatment groups.

3.2.5 Chondrocyte glucose transporter expression (Class 3 – GLUT6, 8, 10, 12 & 13)

Figure 3.05 shows the expression of the final class III of the GLUT family of glucose transporters. Like the expression of GLUT5 (*SLC2A5*) seen in Figure 3.04A, there was no significant glucose mediated effect on expression of the GLUT6 gene (*SLC2A6*).

Figure 3.05B shows that the expression of GLUT8 (*SLC2A8*) is significantly increased after short term (16 hours) treatment with high diabetic glucose concentration (30mM, $p < 0.05$). It can also be seen that the expression of GLUT8 (*SLC2A8*) is roughly doubled in both long term high glucose treatments (11mM and 30mM, $p < 0.05$).

Figure 3.05C shows that like with the expression of GLUT8 (*SLC2A8*) seen in Figure 3.05B, the expression of GLUT10 (*SLC2A10*) is also roughly doubled after long term exposure to a physiological level of blood glucose (11mM, $p < 0.05$). Expression of GLUT10 (*SLC2A10*) is also roughly doubled in the short term (16 hours) exposure to a high diabetic glucose concentration (30mM, $p < 0.05$).

Figure 3.05D shows that the expression of GLUT12 (*SLC2A12*) was not significantly affected by high glucose exposure.

In Figure 3.05E, it can be seen that the expression of GLUT13 is the largest of all of the GLUTs in chondrocytes. A statistically significant increase in expression was observed after a short term (16 hours) exposure to a high diabetic glucose concentration (30mM), although the magnitude of the increase suggests that the biological significance may not be profound.

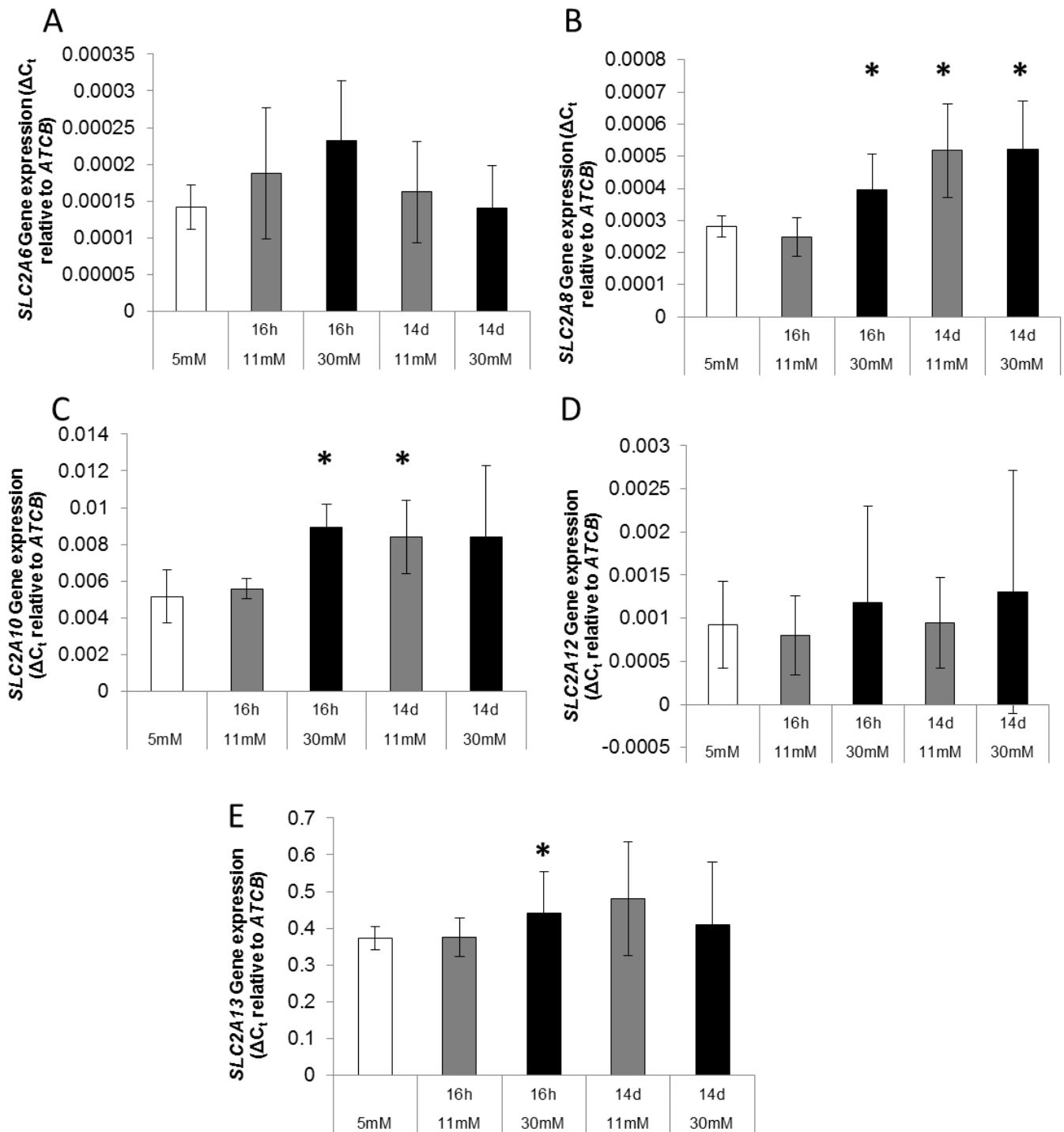


Figure 3.05. Chondrocyte Class 3 glucose transporter (GLUT) gene expression. There was no significantly different gene expression observed for GLUT6 (*SLC2A6*) (A). However, short-term (16h) high glucose (11mM and 30mM) may lead to a highly variable effect on gene expression. Gene expression of the gene for GLUT8 (*SLC2A8*) was significantly increased after short term high glucose (11mM, 16h) and long-term high glucose (11mM and 30mM, 14d) (B), $p < 0.05$. Data ($n = 3$) is shown as mean \pm standard deviation.

3.2.6 Chondrocyte cell number

It is important to note that following the treatment protocols, cell number was not affected as can be seen in Figure 3.06, which shows the amount of DNA extracted from chondrocytes (μg) as a measure of cell number. There was no significant change in the amount of extracted genomic material after the treatment protocols.

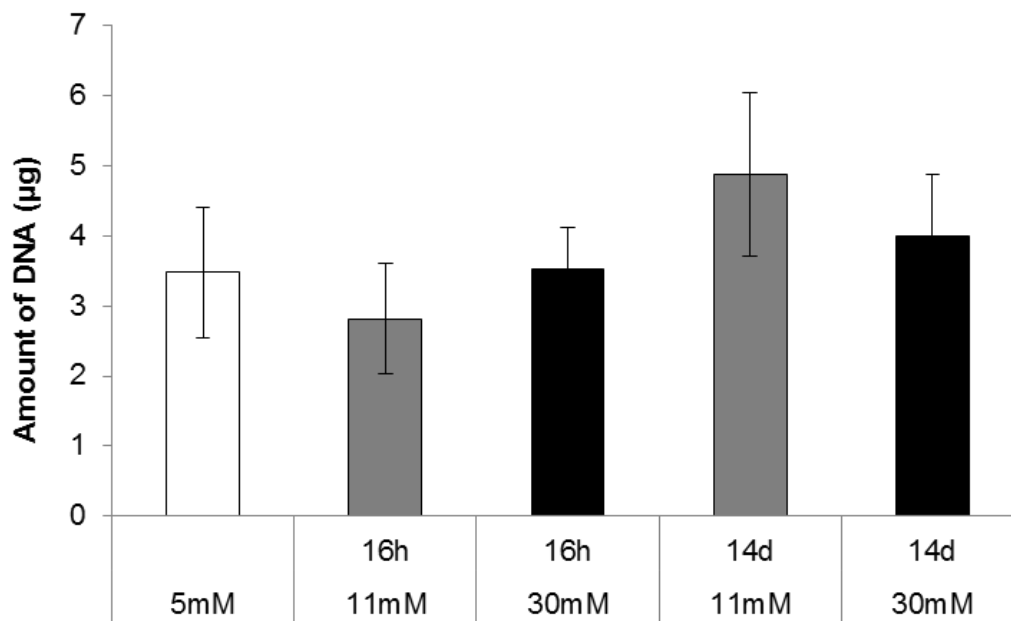


Figure 3.06. The amount of isolated DNA (μg) from chondrocytes following exposure to high glucose (11mM and 30mM) for both short term (16h) and long term (14d) treatments. At the start of the treatments the cells were seeded at controlled cell density. The amount of DNA is used as a measure of cell number after exposure to high glucose. There was no significant difference in the amount of DNA extracted between the different treatments. Data ($n = 3$) is shown as mean \pm standard deviation.

3.2.7 Chondrocyte metabolic state

Use of intracellular glucose taken up from the extracellular environment toward energy production could indicate a shift in the metabolic activity of these cells. Figure 3.07 shows the available ATP present within monolayer chondrocytes after exposure to high glucose treatments. It would appear from Figure 3.07 that there is a contrasting lack of effect of the physiological high glucose exposure (11mM) on the level of ATP production by these cells. After long-term (14 days) exposure to high diabetic glucose levels (30mM), there is a significantly greater level of ATP molecules present in these cells compared to the normal glucose (5mM) control.

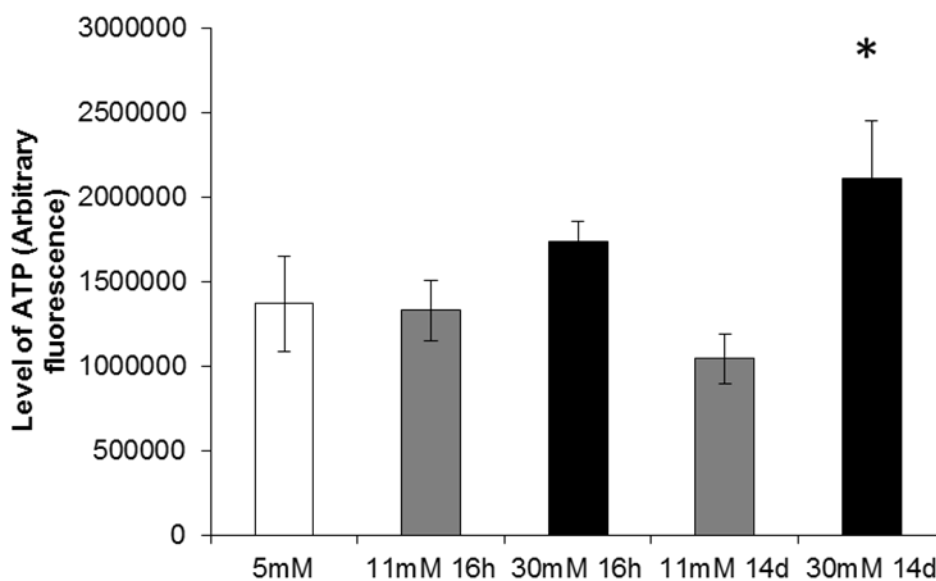


Figure 3.07. The level of ATP in chondrocytes following exposure with high glucose (11mM and 30mM) after short term (16h) and long term (14d) treatments. There was a significant difference in ATP levels after exposure to 30mM glucose for 14d when compared to the normal glucose (5mM) control ($p < 0.05$). There was no significant difference in the level of ATP in chondrocytes in any of the other treatment groups. Data ($n = 3$) is shown as mean \pm standard deviation.

3.3 Synoviocytes

3.3.1 Synoviocyte glucose uptake

Akin to the glucose uptake measured in chondrocytes, glucose uptake was also measured in synoviocytes using a hexokinase test on the high glucose media. As can be seen in Figure 3.08A, synoviocytes also increase their glucose uptake, dose-dependently, upon subjection to a short-term (16 hours) high glucose environment. Also akin to the uptake observed in chondrocytes, the synoviocytes appear to reduce their glucose uptake in the long-term when exposed to high-diabetic concentrations of glucose (30mM). The increased glucose uptake observed in the physiological high glucose treatment (11mM) over the short term (16 hours) appears to be maintained to the long term (11mM, 14 days).

The modified uptake of glucose by synoviocytes over the short-term (16 hours), evident from Figure 3.08A, appears to occur rapidly, followed by a marked reduction in glucose uptake. This can be observed from data in Figure 3.08B, which shows a snapshot of glucose uptake over a short time period (10 minutes) after the cells have been exposed to high glucose environments over the short term (16 hours) and the long term (14 days). Interestingly, the trend in the data observed in Figure 3.08B, for at least the 11mM treatments and the 30mM 16 hours treatment, almost mirrors that observed in Figure 3.08A, potentially supporting a conclusion that in these treatment groups the extent of reduction in glucose uptake over the course of the final 16 hours of treatment is a direct consequence of dose magnitude.

3.3.2 Synoviocyte metabolomics

Data from Figure 3.09A and 09B shows further glucose uptake data from synoviocytes following quantification of glucose via nuclear magnetic resonance spectroscopy (NMR). Figure 3.09A shows extracellular glucose quantified after 16 hours exposure to glucose

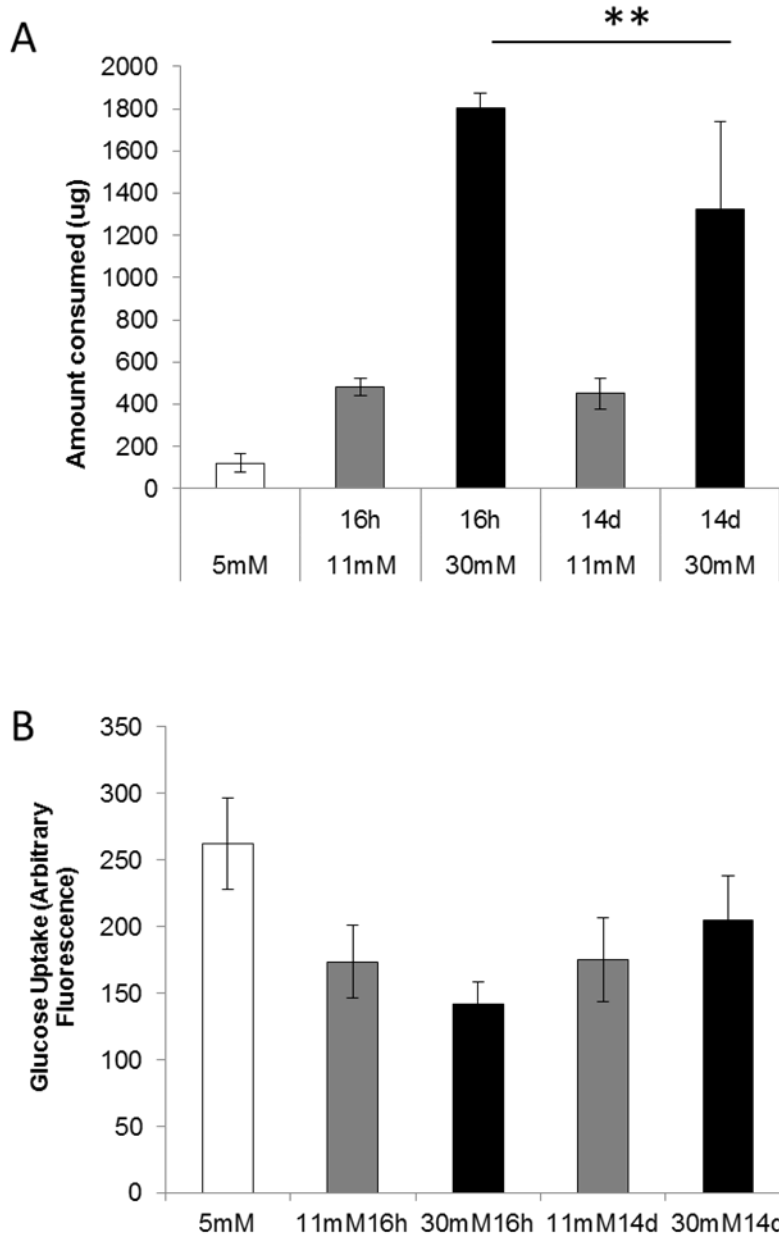


Figure 3.08. Synoviocyte glucose uptake. Cells were treated for 14d with either normal glucose (5mM) or high glucose (11mM, or 30mM). After the 14d treatments, a portion of the 5mM treated cells were treated with high glucose (11mM or 30mM) for 16h. During this period all other treatment groups had their media changed also. Glucose uptake was measured after this final 16h of glucose treatment. There was a significant decrease in the amount (μg) of glucose uptake between the short term (16h) and long term (14d) high-glucose treated synoviocytes ($p < 0.01$) (A). In a 10-minute snapshot of glucose uptake *after* the final 16h of the glucose treatment (B), the rate of glucose uptake did not mirror the large differences in glucose uptake observed over the course of the 16h treatment period in (A). Data ($n = 6$) is shown as mean \pm standard deviation.

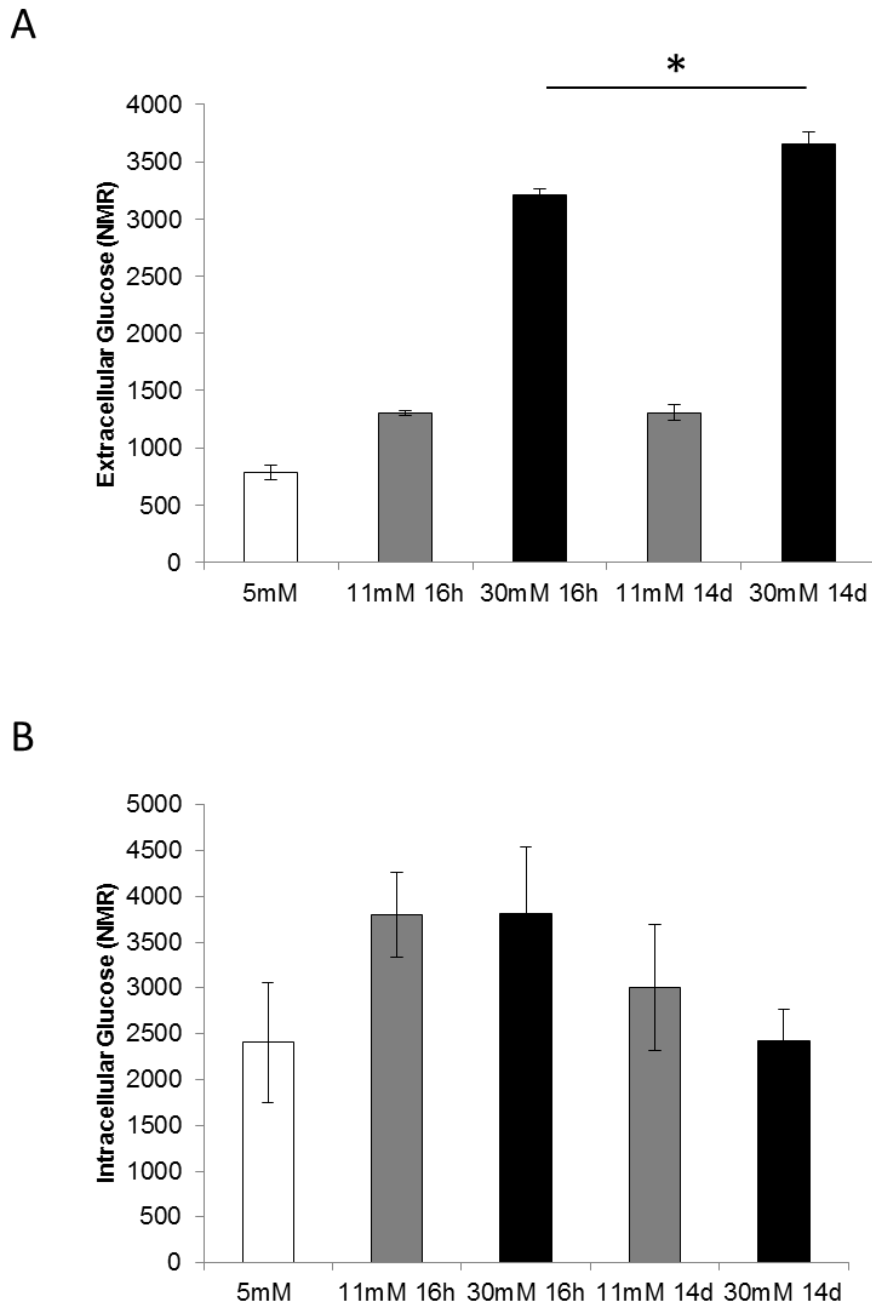


Figure 3.09. The level of glucose detected by nuclear magnetic resonance spectroscopy after 16h media changes for media of synoviocytes (A); and synoviocyte cell lysates (B). There was significantly more glucose found in the media of cells treated with long term high glucose (30mM, 14d) than with short term high glucose (30mM, 16h) ($p < 0.05$) (A). There was no statistical difference seen in the intracellular glucose measurements (B). Data ($n = 3$) is shown as mean \pm standard deviations.

treatments following 14 days of either high glucose (11mM, 30mM) in the long term treatment groups or normal glucose (5mM) in the short term treatment groups and the normal glucose controls. Figure 3.09B contrastingly shows glucose measurements taken from cell lysates following the same experiment. As can be seen from Figure 3.09A, the extracellular glucose measurements are, as expected, highest in the high diabetic glucose treatments. The extracellular glucose levels measured in the physiological high glucose treatments and the normoglycaemic control also correspond to those expected. There is however a significantly lower ($p < 0.05$) amount of glucose measured in the short term high diabetic glucose treatment compared to the long term treatment of the same concentration. This suggests uptake has been reduced after long term exposure to high glucose in synoviocytes. Interestingly, there was no significant difference observed between glucose uptake in the long term and short term physiological high glucose treatments. Figure 3.09B shows the corresponding intracellular glucose concentrations, which showed no significant effect of high glucose or period of exposure.

3.3.3 Synoviocyte glucose transporter expression (Class 1 – GLUT1, 3 & 14)

Data from Figure 3.10A to Figure 3.10C indicates the effects of high glucose exposure periods on gene expression levels of the Class I transporters from the GLUT family (GLUT1 to GLUT4 and GLUT14) in synoviocytes. Expression of GLUT2 (*SLC2A2*) and GLUT4 (*SLC2A4*) were not measurable in these cells, suggesting that GLUT2 and GLUT4 are not expressed in synoviocytes. The trend in the data from Figure 3.10A suggests that the expression of GLUT1 (*SLC2A1*) is reduced in these cells as a result of high glucose exposure. Over the short term (16 hours), both physiological high glucose (11mM) and high diabetic glucose (30mM) levels significantly reduced the level of expression of GLUT1 (*SLC2A1*) in synoviocytes compared to the normal glucose (5.5mM) control.

Figure 3.10B shows that the expression levels of GLUT3 (*SLC2A3*) were relatively unchanged in synoviocytes as a result of high glucose exposure. Neither the short term (16

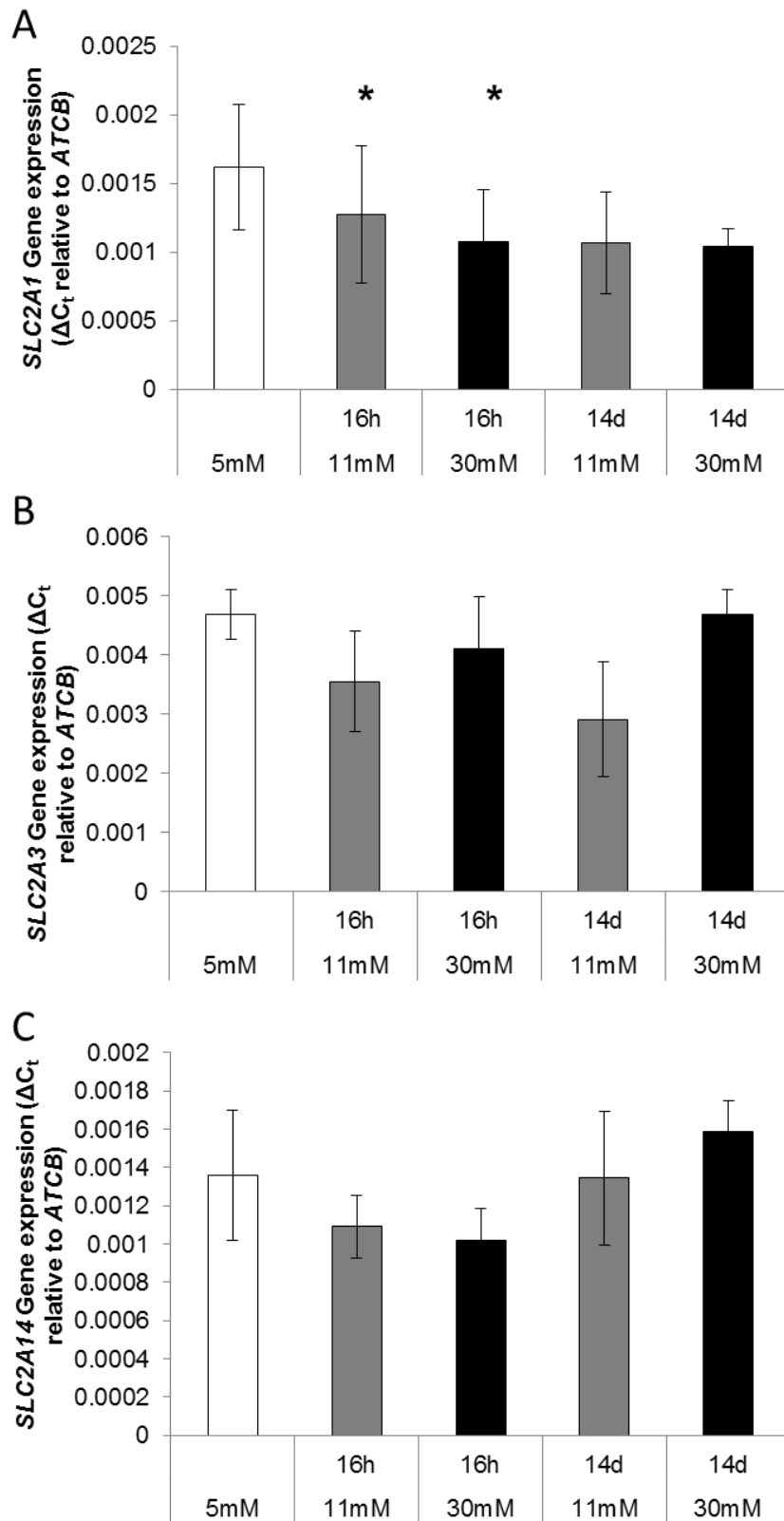


Figure 3.10. Synoviocyte gene expression of Class I glucose transporter (GLUT) genes. A significant decrease in expression of GLUT1 (SLC2A1) in the short term (16h) treatments ($p < 0.05$) was observed (A). There was no significant difference in expression of genes for GLUT3 (SLC2A3) (B) or GLUT14 (SLC2A14) (C). Data ($n = 3$) is shown as mean \pm standard deviation.

hours) nor long term (14 days) high glucose treatments (11mM and 30mM) showed any significant effects on the expression of GLUT3 in these cells.

Figure 3.10C shows that, similarly to the expression levels of GLUT3 (*SLC2A3*) shown in Figure 3.10B, the expression of GLUT14 (*SLC2A14*) in synoviocytes was not significantly affected by the exposure to high glucose levels.

3.3.4 Synoviocyte glucose transporter expression (Class 2 – GLUT5, 9 & 11)

Figure 3.11A to Figure 3.11C shows the gene expression of glucose transporters from Class II of the MSF superfamily of GLUTs, namely GLUT5 (*SLC2A5*), GLUT7 (*SLC2A7*), GLUT9 (*SLC2A9*), and GLUT11 (*SLC2A11*). Gene expression for GLUT7 (*SLC2A7*) was not measurable in these cells, suggesting that GLUT7 is not expressed in synoviocytes. As can be seen in Figure 3.11A, expression of GLUT5 (*SLC2A5*) by synoviocytes does not appear to be affected by high glucose exposure. This can also be seen with respect to GLUT9 (*SLC2A9*) in Figure 3.11B.

The trend in the data shown in Figure 3.11C suggests that the expression of GLUT11 (*SLC2A11*) is increased as a result of exposure of synoviocytes to high glucose levels. Interestingly, the only treatment group in which this exhibited effect is supported by statistical significance, however, is the short term (16 hours) physiological high glucose treatment (16 hours, $p < 0.05$).

3.3.5 Synoviocyte glucose transporter expression (Class 3 - GLUT6, 8, 10, 12 & 13)

Figure 3.12A to Figure 3.12E shows gene expression data identifying the effects of high glucose treatments on expression of genes relating to Class III of the MSF of glucose transporters. This class is composed of GLUT6 (*SLC2A6*), GLUT8 (*SLC2A8*), GLUT10 (*SLC2A10*), GLUT12 (*SLC2A12*) and GLUT13 (*SLC2A13*). As can be seen from the data in Figure 3.12A to Figure 3.12E, Class III of the GLUTs is the best represented in terms of gene expression in synoviocytes, with expression of genes for all of the transporters in this class being detectable by quantitative PCR.

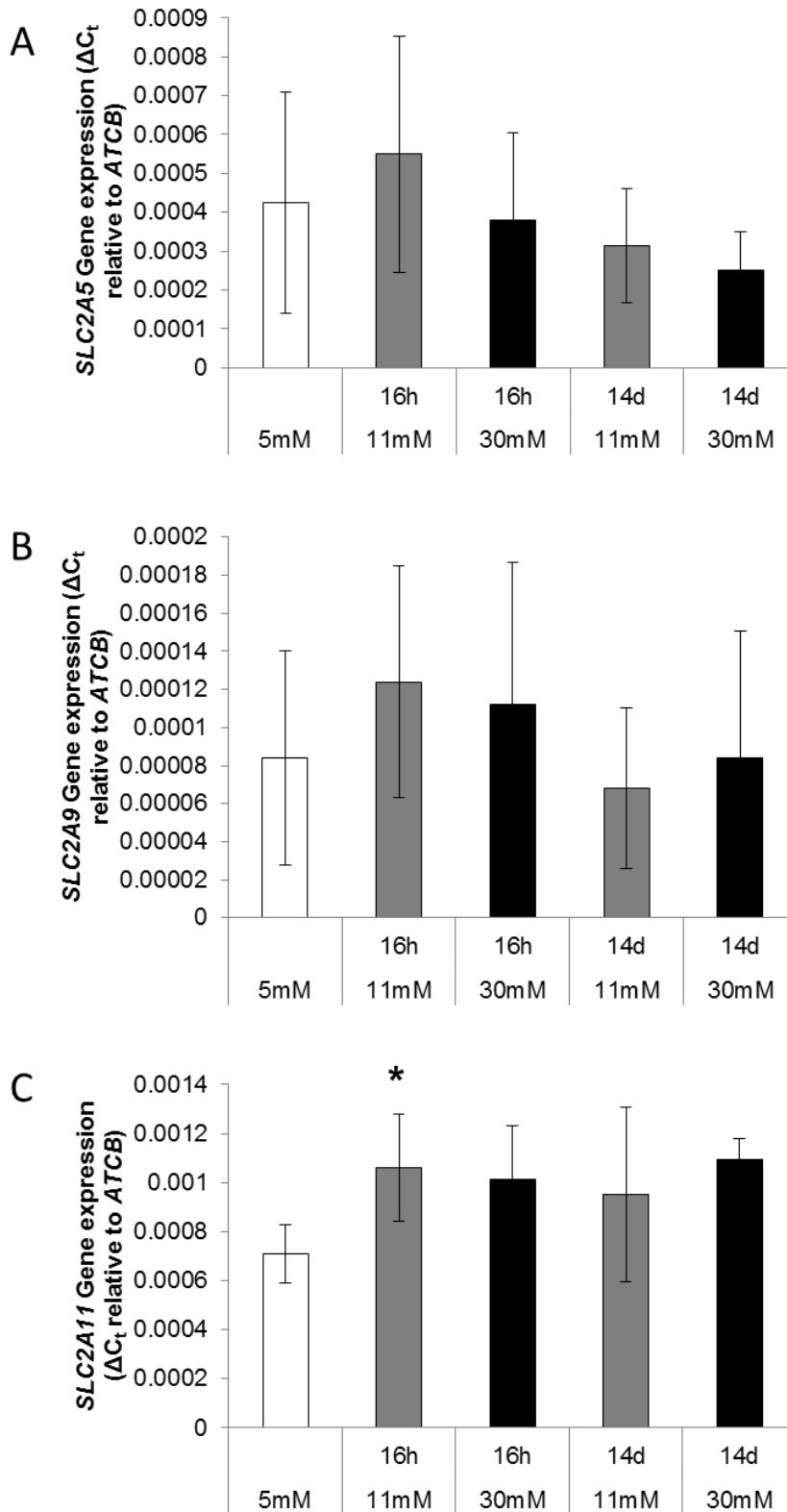


Figure 3.11. Synoviocyte expression of Class 2 glucose transporter (GLUT) genes. No significant differences were observed in synoviocyte expression of genes for GLUT5 (*SLC2A5*) (A) and GLUT9 (*SLC2A9*) (B). For GLUT11 (*SLC2A11*) (C) however, there was a significant increase in expression after short term (16h) treatment with 11mM glucose. Data (n = 3) is shown as mean \pm standard deviation.

Figure 3.12A shows a significant marked reduction in the gene expression of GLUT6 (*SLC2A6*) after long-term high glucose treatments (11mM and 30mM, $p < 0.05$). This effect appears to be limited to a long-term change due to the lack of a similarly statistically significant effect observed after the short term (16 hours) treatments at these high glucose concentrations.

Interestingly, Figure 3.12B shows similar effects of the high glucose treatments, although this time the effect is also observed at the short term (16 hours) timepoint. The effect of high glucose treatments in reducing the expression levels of the gene associated with GLUT8 (*SLC2A8*) appears to be similar regardless of dose, but the trend in the long-term (14 days) treatments interestingly mimics that observed in Figure 3.12A. This suggests that there is a more profound effect in reducing the gene expression of GLUT6 (*SLC2A6*) and GLUT8 (*SLC2A8*) in the more physiologically relevant high glucose treatment (11mM) than in that more befitting of a high diabetic blood glucose level (30mM).

Expression of GLUT10 (*SLC2A10*) shown in Figure 3.12C suggests that high glucose has no significant effect on GLUT10 (*SLC2A10*) in synoviocytes. The trend in the data does, however, suggest that a short-term (16 hours) dose-dependent increase in expression is returned to normal after long-term exposure (14 days).

Figure 3.12D shows a similar trend that also lacks the support of statistical significance, but suggests that a short term (16 hours) augmentation of gene expression of GLUT12 (*SLC2A12*) is followed by a long term (14 days) return to baseline expression.

As was shown in chondrocytes, Figure 3.12E suggests that GLUT13 (*SLC2A13*) is the most abundantly expressed glucose transporter from the MSF superfamily in synoviocytes. Figure 3.12E does, however, also show that, also as with chondrocytes, there is little effect of high glucose exposure on the gene expression of GLUT13 (*SLC2A13*) in synoviocytes.

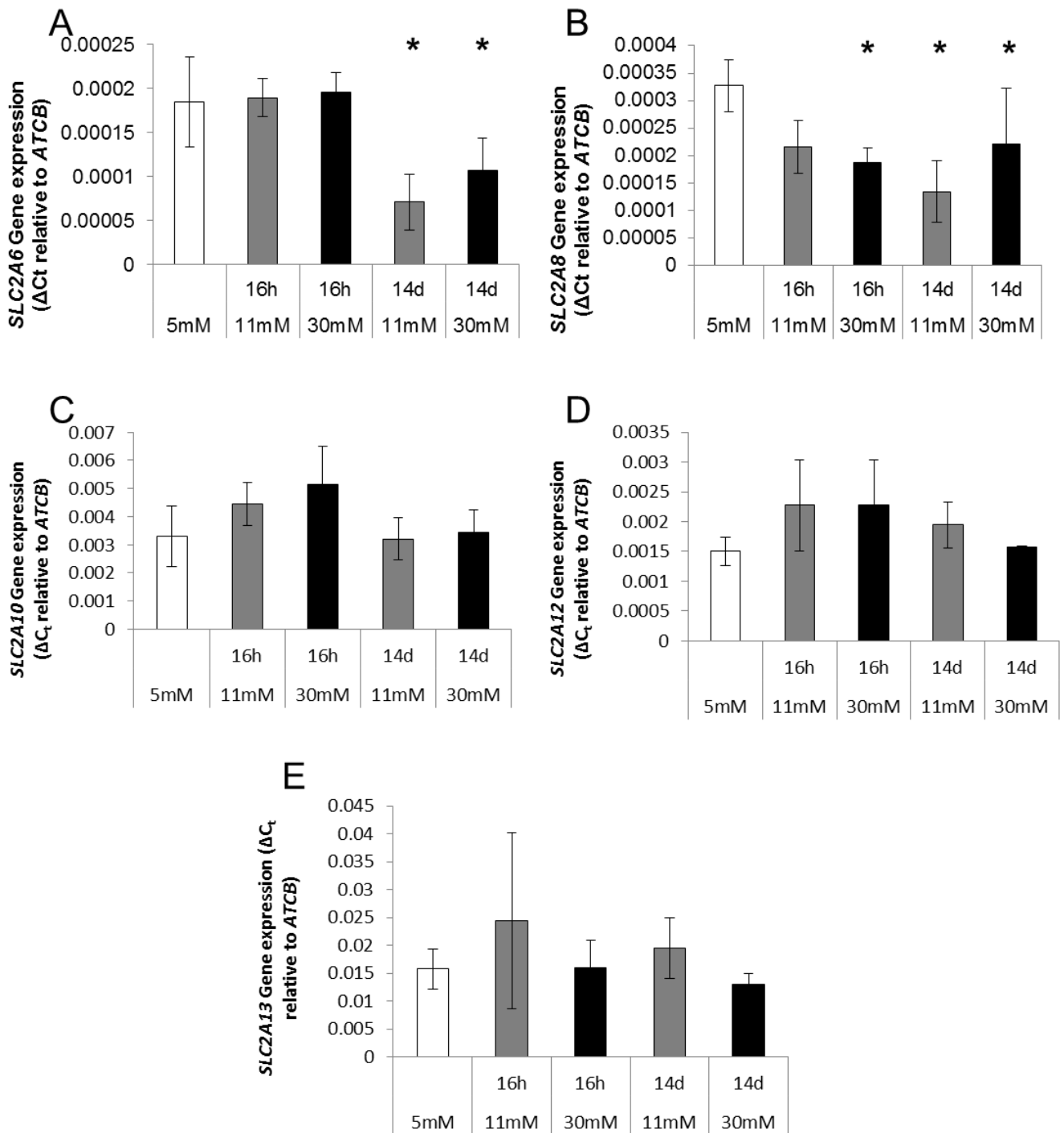


Figure 3.12. Synoviocyte Class 3 glucose transporter (GLUT) gene expression. There was a significant decrease in gene expression of GLUT6 (*SLC2A6*) after the long term (14d) treatments ($p < 0.05$) (A). However, short-term (16h) high glucose (11mM and 30mM) showed no significant difference (A). Expression of the gene for GLUT8 (*SLC2A8*) was significantly decreased ($p < 0.05$) in all but the short term (16h) 11mM treatment (B). No significant difference was seen in the gene expression of GLUT10 (*SLC2A10*) (C) or GLUT12 (*SLC2A12*) (D). Expression of GLUT13 (*SLC2A13*) across all treatment groups was shown to be highly variable (E), and no significant difference was seen in this expression relative to the normal glucose (5mM) control. Data ($n = 3$) is shown as mean \pm standard deviation.

3.3.6 Synoviocyte cell number

Following exposure to high glucose treatments in both the short term and the long term, dose-dependent effects on cell number would cause difficulties in interpreting results obtained from experiments involving these cells. It is of importance to clarify, as is shown in the data from Figure 3.13, that the cell number after these high glucose treatments was not significantly altered. There were no statistically significant differences in the amount of DNA (μg) obtained from DNA extractions in each of these treatment groups.

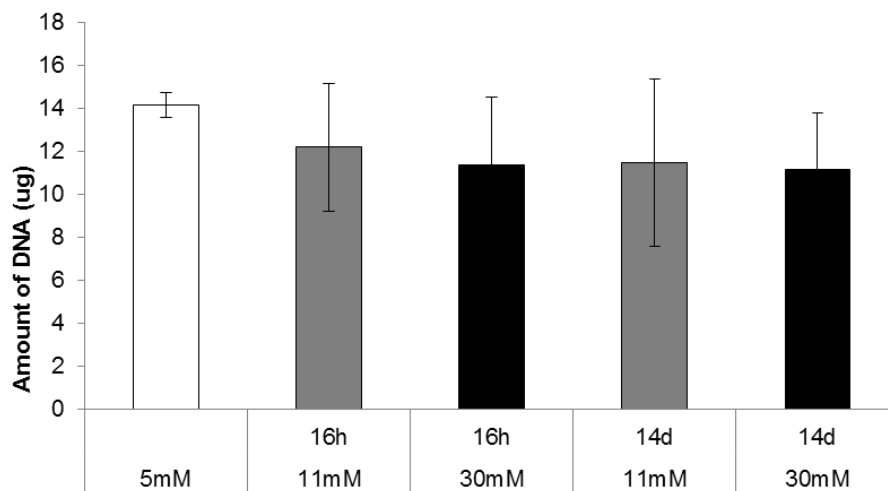


Figure 3.13. The amount of isolated DNA (μg) from synoviocytes following exposure to high glucose (11mM and 30mM) for both short term (16h) and long term (14d) treatments. At the start of the treatments the cells were seeded at controlled cell density. The amount of DNA was used as a measure of cell number after exposure to high glucose. There was no significant difference in the amount of DNA extracted between the different treatments. Data ($n = 3$) is shown as mean \pm standard deviation.

3.3.7 Synoviocyte metabolic state

Synoviocyte metabolic activity alterations as a result of high glucose exposure can be interpreted from Figure 3.14, which shows the levels of ATP present within these cells after high glucose treatments. It can be seen from Figure 3.14 that the level of ATP within synoviocytes is significantly increased after short term (16 hours) physiological high glucose levels (11mM, $p < 0.05$) and also after long term (14 days) high diabetic glucose levels (30mM, $p < 0.05$). The trend in the data from Figure 3.14 could further indicate that exposure to short term (16 hours) high diabetic glucose levels (30mM) and long term (14 days) exposure to physiological high glucose levels (11mM) also exert an effect of increasing the available ATP within synoviocytes when compared to a normal glucose control (5mM).

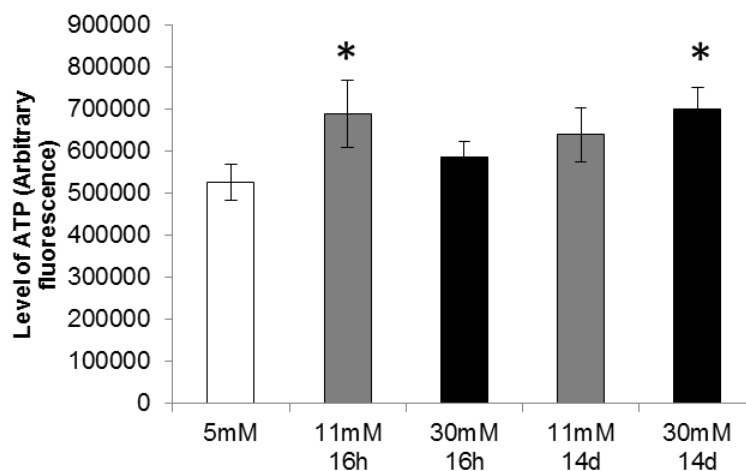


Figure 3.14. The level of ATP in synoviocytes following exposure with high glucose (11mM and 30mM) after short term (16h) and long term (14d) treatments. There was a significant difference in ATP levels after exposure to 11mM glucose for 16h and 30mM glucose for 14d when compared to the normal glucose (5mM) control ($p < 0.05$). There was no significant difference in the level of ATP in synoviocytes in any of the other treatment groups. Data ($n = 3$) is shown as mean \pm standard deviation.

3.3.8 Synoviocyte extracellular pH

Modifications to metabolic activity could result in changes to pH of the surrounding culture media, particularly where significant adjustments to ATP levels have been experienced.

Figure 3.15 shows the extracellular pH of synoviocytes after exposure to high glucose treatments. As can be seen from Figure 3.15, no significant changes in extracellular pH occurred as a result of high glucose exposure.

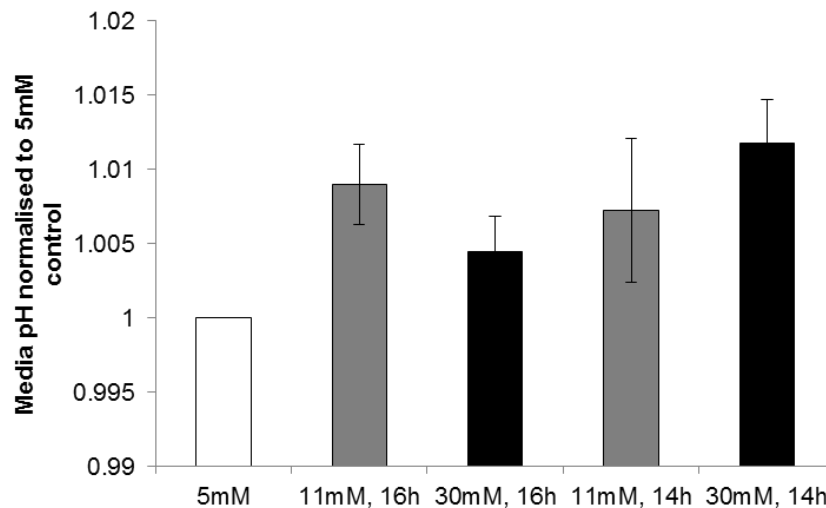


Figure 3.15. The pH level in the culture media of synoviocytes following exposure with high glucose (11mM and 30mM) after short term (16h) and long term (14d) treatments normalised to the pH observed in the cell culture media of a 5mM normal glucose control. There was no significant difference in pH level after exposure to high glucose (11mM or 30mM) when compared to the normal glucose (5mM) control. Data (n = 3) is shown as mean ± standard deviation.

3.4 Discussion

3.4.1 Chondrocytes and glucose transport in the literature

Chondrocytes exist in an avascular environment, obtaining most, if not all, of their glucose supplementation from the synovial fluid (136-138). Synovial fluid glucose measurements suggest that the glucose concentration in the synovial fluid may be lower than that of the surrounding peripheral blood (137). Research has shown that chondrocytes appear to express an array of the known glucose transporters (128, 129) and may therefore be well adapted to an environment in which the availability of glucose often scarce.

The expression of glucose transporters by chondrocytes would suggest that these cells express transporters that are not reliant upon insulin to promote their translocation to the cell membrane and enhanced activity. The majority of the transporters expressed by chondrocytes are non-insulinotropic (128, 129). It could therefore be suggested that chondrocytes themselves would be vulnerable to fluctuations within the extracellular availability of glucose, such that increases in the prolonged increases in extracellular availability cause an enhanced uptake of glucose by these cells. While knowledge of the expression of glucose transporters in these cells is supported by some key studies (128, 129), relatively little has been published previously about the effect of varying exposures to high glucose conditions on the response exhibited by chondrocytes to these changes in their environment.

3.4.2 Glucose uptake appears to be reduced after long-term 30mM but maintained in long term 11mM

Figure 3.01A (which is also supported by data from Figure 3.02A) shows that chondrocytes appear to undergo a dose-dependent increase in their uptake of glucose over the short term, but in fact reduce their rate of glucose uptake in the long term, when exposed to extremely high levels of glucose. It is interesting to note that Figure 3.01A also seems to suggest that the level of glucose uptake in cells exposed to a physiological high glucose level (11mM) appear to maintain their dose-dependent increase in glucose uptake over the long term, also supported by data from Figure 3.01B.

A consequential reduction in glucose uptake following a rise in intracellular glucose could be plausibly explained as a negative-feedback regulation mechanism. This does, however, not appear to be the case. It would appear that measured intracellular glucose levels indicate that glucose is actively metabolised by these cells upon uptake into the cell (Figure 3.02B). It could be suggested that an increased metabolic rate results from exposure to high glucose and that as such there is an inverse relationship between metabolic rate and dose of high glucose exposure (Figure 3.02B). This is not however supported by statistically significant

changes in intracellular glucose measured after short term high glucose exposure (11mM 16 hours and 30mM 16 hours) when compared with that after a normal glucose control (5mM, Figure 3.02B).

3.4.3 Reduction in glucose uptake is not just a result of reduced cell number

Previously reported studies on high glucose in varying cell types suggests that high glucose is responsible for increased inflammation (161, 170, 196, 197) and has been linked to increases in both apoptosis (152, 162, 167, 198) and necrosis (199, 200). There are a number of potential mechanisms for this, with previous studies suggesting effects of high glucose on increased advanced glycation end products (170), reactive oxygen species (161), and DNA damage (161, 194). Based on these reports it could be concluded that the reason for the reduced uptake of glucose observed in Figure 3.03A and Figure 3.02A is that the cell number in these experiments has been reduced due to the above reasons. The time point used in the long term study (14 days) leaves a great deal of time for the effects reported in the literature to take effect, with the treatment conditions being the same in most cases (30mM). Figure 3.02B does however suggest that there is a greater amount of intracellular glucose measurable in the long-term high glucose treatments (11mM and 30mM, 14 days) when compared to the normal glucose control. While this data could suggest that there are merely fewer cells with a larger amount of intracellular glucose, data from Figure 3.06 would suggest that there are in fact no differences in cell number between the various treatments. Figure 3.06 shows no significant difference in the measurable genomic material between these treatments suggesting that there is no effect of the high glucose treatments on the number of cells.

There are potential limitations to the assumption that extracted DNA is a direct indicator of cell number, although this is often used as a fairly robust measurand indicating cellularity (201). Some DNA extraction methodologies may contain steps that act to normalise the DNA extracted across samples, inadvertently incurring an element of bias to the results. Spin column protocols, for instance, may possess the limitation that there is an upper limit to the

amount of DNA capable of adhering to the silica membrane within the column, together with an upper limit on the ratio of eluted : un-eluted DNA from the column. The presently used method of DNA extraction, lacking in spin columns, does not suffer this potential limitation however.

3.4.4 Could the reduced uptake be due to an effect on expression of glucose transporters?

It does not appear therefore, that a high intracellular glucose concentration is the cause for the reduction in glucose uptake in the high diabetic glucose exposed cells over long term. It has also been shown that this reduction in glucose uptake is not caused by the reduction in cell number that would be expected based on literature findings. A potential further mechanism for this could be that the reduction in glucose uptake is the result of a reduction the gene expression of key glucose transporter proteins.

Mobasherri et al (129) found that chondrocytes express 11 of the 14 known members of the GLUT (MSF) family of glucose transporters. These transporters were shown to be GLUT1, GLUT3, GLUT5, GLUT6, GLUT8, GLUT9, GLUT10, GLUT11, GLUT12, GLUT13 and GLUT14. This correlates with the findings shown in Figure 3.03 to Figure 3.05, which show that chondrocytes do express a measurable amount of the genes responsible for the synthesis of these proteins. Of the genes that are not expressed in chondrocytes, one is GLUT4, responsible for the insulinotropic increase in glucose uptake as a result of a high glycaemic load. This protein has been found almost exclusively in myocytes and adipocytes (202, 203), with expression also being observed in the beta islet cells of the pancreas (204). The lack of this transporter in chondrocytes suggests that glucose uptake in these cells is not responsive to the effects of insulin. Of the other glucose transporter genes not expressed in chondrocytes, another is GLUT2. Most of the known expression of this transporter takes place is in gut enterocytes and hepatocytes. As a transporter of both glucose and fructose, this transporter is responsible for large scale uptake of fructose from the small intestine and also for the vast majority of glucose and fructose uptake from the blood in hepatocytes in

first pass metabolism before exposure to the systemic circulation. The specific localisation of GLUT2, and its role within these tissues, perhaps provides explanation as to why there is little expression detected in chondrocytes. The final transporter without any identifiable gene expression in chondrocytes is GLUT7. Little is known about this transporter, being the final of the GLUT transporters to be characterised in humans. Cheeseman et al provide a summary of the known research on GLUT7, identifying this as a protein largely expressed in the small intestine and colon (205). This specific localisation of GLUT7, and the lack of expression in chondrocytes, suggests that this protein plays a niche role that is not a part of the normal functioning of the musculoskeletal system.

The expectation would be that the expression of glucose transporters would be reduced as a result of high-glucose exposure, based upon what is known about negative-feedback regulation together with the data obtained in Figure 3.03A and Figure 3.02A. Contrary to these expectations however, there was no detected reduction in glucose transporter gene expression in these cells as a result of any of the high glucose treatments. In fact, Figure 3.03A, Figure 3.03B and Figure 3.05B respectively suggest that expression of GLUT1 (*SLC2A1*), GLUT3 (*SLC2A3*) and GLUT8 (*SLC2A8*) is significantly increased as a result of long-term high diabetic glucose exposure (30mM, 14 days, $P < 0.05$). Of these, GLUT1 (*SLC2A1*) appears to be the gene with the highest expression in chondrocytes, but GLUT3 (*SLC2A3*) appears to be the highest affected by the treatments (approx. 100% increase, $p < 0.05$). In all three transporters, the significant increase in gene expression is seen as early as 16 hours after treatment (30mM, 16 hours treatment). At this early time-point there is also a significant increase in GLUT10 (*SLC2A10*) expression in these cells as shown in Figure 3.05.

Chondrocytes have been suggested to have a zone-dependent glucose usage pattern based upon their localisation within the heterogeneous zones of articular cartilage (133). An environment that is naturally sparse of glucose appears to have led to a favour for glycolytic metabolism in superficial layer chondrocytes (133), potentially in order to provide for access

of the deep-zone chondrocytes to oxygen for more efficient ATP production. This, together with the apparent ready availability of glucose transporters in chondrocytes suggests an adaptation toward high glucose affinity. While adaptively advantageous in normal glucose conditions, this may have deleterious consequences in a high glucose environment. It would appear that the sensing of high glucose appears to increase the gene expression of glucose transporters in these cells as shown in Figure 3.03A, Figure 3.03B, Figure 3.05B, and Figure 3.05C and may therefore leave the cells vulnerable to the resultant effects of high glucose exposure.

The likelihood that the detected long-term reduction in glucose uptake upon exposure to high diabetic glucose concentrations is a result of an alteration to the expression of genes responsible for the synthesis of key glucose transporter proteins cannot be ruled out. It was, however, therefore necessary to confirm that this reduction in glucose uptake was not merely the result of a reduction in cell number. There are a number of reasons why this outcome could be plausible, not least the large body of literature that suggests that high glucose exposure has an effect on the viability of cells (152, 161, 167, 168, 170, 194, 196, 198, 206). This does, however, not appear to be case as according to the data provided in Figure 3.06, which shows that the genomic material extracted from these treatment groups is not affected by treatment group. Provided that this genomic material remains a reliable predictor of cell number, it can therefore be concluded from this data that cell number was not significantly affected by the exposure of various concentrations of glucose in these treatment groups.

3.4.5 Effects on ATP production

Data from Figure 3.03A and Figure 3.02A, in their comparison with data from Figure 3.02B, indicate a disparity in the levels of glucose metabolism following high glucose exposure. Figure 3.07 shows a similar disparity in the levels of ATP within these cells. Figure 3.07 would suggest that the two high glucose concentrations used have opposite effects on ATP generation over long term treatment. This data suggests that there is a significant increase in

ATP following long-term high diabetic glucose exposure (30mM, 14 days, $p < 0.05$). This could suggest a shift in metabolic activity in these cells, potentially signifying a phenotypic alteration in these cells as a result of high glucose exposure. Previous studies have highlighted a particular vulnerability of chondrocytes to dedifferentiation upon removal from native cartilage conditions (207). It is possible that there is a glucose-mediated phenotypic shift in these cells potentially evidenced by the data in Figure 3.07.

3.4.6 Synoviocytes and glucose transport in the literature

Glucose transport in synoviocytes, in relative contradistinction to chondrocytes, does not appear to have been investigated to any substantial degree in the literature. It is fast becoming the established consensus that musculoskeletal disorders are one of a number of secondary effects of diabetes (41, 103, 106, 208-210), and there have even been studies investigating the link between rheumatoid arthritis and glucose metabolism (197). As a compositional regulator of the chondroprotective synovial fluid, and an established effector in the onset and progression of various forms of arthritis, synoviocytes present a highly relevant cell type for studying proposed effects of high glucose exposure on the musculoskeletal system.

3.4.7 Synoviocyte glucose consumption

As was shown to be the case in chondrocytes in Figure 3.03A, synoviocytes exhibit a marked reduction in consumption of glucose from cell culture media (Figure 3.09a). This similarly suggests that synoviocytes, like chondrocytes, may present with a reduction in glucose uptake over long term high glucose exposure. Unlike chondrocytes, however, there might be an increase in intracellular glucose (not significant) after the short term treatments, followed by a dose-dependent reduction to baseline in the long-term treatment (Figure 3.09B). This supports the data seen in Figure 3.09A and provides evidence to suggest that the reduction in glucose uptake in the long-term high diabetic glucose treatment (30mM, 14 days) witnessed in Figure 3.08A is not a result of increased intracellular glucose (and a consequent inhibition of glucose uptake in a negative feedback manner). Critically, it is

interesting to note that while a complete reduction to baseline is observable in Figure 3.09B after the 30mM 14 days treatment, the more physiological treatment of 11mM 14 days does not suffer such a profound reduction to baseline. This could suggest that the cells are subjected to a higher intracellular glucose concentration for longer when they are exposed to more modest increases in glucose exposure. The uptake in glucose seen from the data in Figure 3.08A and Figure 3.09A would appear to be the result of a rapid increase in the rate of glucose uptake based on the information from Figure 3.08B. This would suggest that the rate of glucose uptake in the short term (16 hours) high glucose treatments is dose-dependently reduced. This initial reduction in the rate of glucose uptake may be the result of a naivety to such high glucose concentrations and is followed, in the case of 11mM treated cells, by maintenance of this response of a reduction in the rate glucose uptake. In the 30mM treated cells, however, there does appear to be less of a reduction in the rate of glucose uptake in the long term (14 days) treated cells. While the reduction in the rate of glucose uptake is still below baseline in these cells, the long term (14 days) glucose uptake over 10 minutes in the long-term (14 days) treated cells is higher than that of the short term (16 hours) treated cells.

The apparent hints at an effect of high glucose on the rate of glucose uptake taken from the data in Figure 3.08B, taken together with the apparent lower amount of intracellular glucose metabolism seen in Figure 3.09B compared with Figure 3.02B could suggest that synoviocytes, unlike chondrocytes, possess a response mechanism to the exposure of high glucose conditions which may be celluloprotective. This may be borne out of the more frequent exposure of synoviocytes to abundant glucose due to the high vascularity of their native tissue. From this data it may be possible to postulate that synoviocytes possess both a long-term and a short term correctional response to high glucose exposure that might enable them to withstand the effects of rapid glucose metabolism and resultant increases in oxidative DNA damage suggested in the literature (161). The reduced glucose metabolism however, and resultant increase in intracellular glucose could leave surplus glucose

molecules for non-enzymatic glycation together with pathways such as hexosamine biosynthesis pathway (47).

3.4.8 Is the reduction a result of decreased synoviocyte glucose transporter expression?

While in chondrocytes, glucose transporter expression would appear to be increased for a number of key transporter genes, this is not the case for synoviocytes. In fact, for genes being transcribed for GLUT6 (*SLC2A6*) and GLUT8 (*SLC2A8*), the level of transcription is drastically reduced after exposure to modest 11mM glucose exposure for 14 days. In the case of GLUT6 (*SLC2A6*), the transporter is also reduced in expression after 14 days exposure to the more extreme 30mM glucose. In the case of GLUT8 (*SLC2A8*), early reduction in transcription is experienced, with a significant reduction observed after 16 hours exposure to both 11mM and 30mM glucose. These reductions could suggest that synoviocytes have a different response mechanism to high glucose exposure compared to chondrocytes. This could potentially be explained by the natural environment in which these cells exist. There is a high level of vascularity in the native tissue of these cells and therefore there is a reduced level of naivety to plentiful glucose. As such there may exist less of a selective pressure for cells with a high affinity for glucose.

This reduction in glucose transporter expression could hint at a potential reason for the observed reduction in glucose uptake in synoviocytes after long term exposure to 30mM glucose. If true this could suggest that synoviocytes are perhaps more well adapted to fluctuating extracellular glucose levels. The observation of a more profound effect in the 11mM exposed cells, however, does not corroborate this viewpoint.

Studies investigating glucose exposure in synoviocyte are relatively few, especially those investigating the usage of glucose by these cells when exposed to high glucose levels. There are however, emergent links between glucose exposure and the onset and progression of diseases associated with synoviocytes (197).

3.4.9 Is cellularity the key?

As with chondrocytes, it does not appear from data in Figure 3.12 that there is high glucose-dependent reduction in synoviocyte cell number to attribute to the reduction in glucose uptake observed in Figure 3.08A and Figure 3.09A.

3.4.10 What are the effects on synoviocyte metabolic state?

As with chondrocytes, there would appear to be a metabolic shift in synoviocytes after long term high diabetic glucose exposure (30mM, 14 days, $p < 0.05$). Interestingly, a similar effect is observed in the short term modest high glucose exposure (11mM, 16 hours, $p < 0.05$). This could suggest that modest glucose insults, that are more likely to affect cells in vivo, have similar effects to those observed in cells exposed to long-term diabetic high glucose insult (30mM, 14 days).

3.4.11 Effects on pH

A primary concern for high glucose studies, particularly in cell culture experiments would be that an increased glucose exposure could induce a metabolic shift in favour of glycolysis. This has been shown to occur in a number of cell types investigated in the prior literature (133). An increase in glycolytic rate could increase the level of lactate produced by these cells and therefore create an acidic cell culture environment, leading to the question of whether any effects observed were merely a cause of reduced pH. As can be seen from Figure 3.15, synoviocyte extracellular pH was not significantly affected as a result of high glucose exposure. This is the case regardless of the dose of glucose used, or the time period in which glucose exposure took place. The trend in the data from Figure 3.15 might suggest an increase in pH as a result of high glucose exposure; however, as can be observed from the data, the changes experienced would be unlikely to have an effect that bears any biological significance.

3.5 Conclusions

While glucose uptake does appear to be reduced in both cell types after long term exposure to extreme glucose levels , the mechanisms of reduced uptake appears to differ. While the mechanism for synoviocytes may be a reduced glucose transporter expression, this cannot be definitively concluded without further study. Chondrocytes would appear to contrastingly experience a reduction in glucose uptake via a different mechanism. While this has shown not to be the result of a reduced cell number, or a reduction in glucose transporter expression, the mechanism for this reduced uptake would appear to remain unclear.

There are obvious limitations to studying gene expression data alone in that the levels of resultant RNA have not been proven to positively correlate with corresponding observations on proteins (211). In order to add weight to observed changes in glucose transporter expression it may be a beneficial focus of further study to carry out an investigation of the glucose transporter proteins expressed in these cells after high glucose exposure.

It would appear that while glucose uptake in both cell types appears to be reduced after long term extreme glucose exposure, a more physiological high glucose exposure does not appear to induce the same effect. In fact, it would appear that the glucose uptake in a more physiological high glucose exposure remains increased, and thus a lack of what may be a celluloprotective reduction in glucose uptake observed in more extreme doses, could pose a greater risk to these cells.

4. Transient high glucose exposure may affect cell cycle processes in chondrocytes and synoviocytes, and may cause DNA damage in synoviocytes

4.1 Introduction

From the results shown in Chapter 3, high glucose exposure may cause an altered glucose uptake in chondrocytes and synoviocytes. It was shown that while the cause of this reduction in glucose uptake remains unclear for each cell type, this effect occurs a relatively short period of time after high glucose exposure. In long-term high glucose treated cells, it would appear that the cells are sensitised to a high glucose insult and that this reduction in glucose uptake is either permanently in effect or is placed into effect much quicker than anticipated as evidenced by Figure 3.01a and Figure 3.08a.

Data from previous studies suggests that there are a plethora of deleterious effects that may be attributed to high glucose exposure in a variety of cell types (*48, 130, 152, 161, 164, 167, 169, 194, 212*). These effects range from oxidative DNA damage and inflammation to necrosis and apoptosis. In most studies, these effects are observed after only short term treatments. One epigenetic study suggests that these effects may persist after the exposure to high glucose has been removed (*150*). This study shows that effects such as increased inflammation could be the result of a long term epigenetic change after only a transient exposure to high glucose (30mM). This epigenetic change is shown to be associated with the NFκB –p65 gene promoter region.

Data from these studies suggest that while there may indeed be long-term effects attributable to high glucose exposure, these effects may actually be the cumulative result of short periods of high glucose exposure (*150*). It should be noted that very few, if any, studies exist that have investigated such effects in both chondrocytes and synoviocytes.

In an environment such as the knee joint, which needs to orchestrate the harmonious functionality of a number of critical biomechanical tissues in order to operate optimally, there exist a number of structural molecules that undergo low turnover. As such these molecules are long-lived, and therefore are more highly susceptible to any time-dependent accumulation of insults. This is particularly the case if the cells responsible for the production

and potential upkeep (although recent evidence suggests collagen in particular is inert (114)) of these crucial molecules exhibit a vulnerability to long-term cumulative damage after only transient exposure to toxic levels of commonly occurring substances.

4.2 Results

4.2.1 Effects of transient high glucose on gene expression in synoviocytes and chondrocytes

Gene expression microarray experiments were carried out in a previous study (213) using RNA from chondrocytes and synoviocytes. The microarray technology used in the previous study was Affymetrix Human Gene ST arrays. These arrays were used to carry out a whole transcriptome assessment of gene expression changes detectable after a relatively short term, 48 hour exposure to high glucose (30mM) in both chondrocytes and synoviocytes. The data from these microarray experiments was re-analysed during this project and as such the results of the analysis are described below. The data was reanalysed in the present project due to the release of more robust preprocessing and normalisation tools available in the R programming environment.

As can be seen in Figure 4.01, transient exposure to high glucose (30mM) appears to have had a larger effect on synoviocytes than on chondrocytes, with 83 synoviocyte genes being identified as significantly differentially expressed in comparison to 47 genes in chondrocytes. These values were obtained following differential expression analysis carried out in the R environment (182-185). The threshold selected to identify significant differential expression in these experiments was a \log_2 fold change of 0.5, which roughly corresponds to a 140% increase in gene expression, and a Benjamini-Hochberg false discovery rate (q-value) of 25%.

Interestingly, there were 4 genes that were significantly differentially expressed in both chondrocytes and synoviocytes, these being:

- small nucleolar RNA, H/ACA box 14A (SNORA14A);

- Kinesin Family Member 18A (KIF18A);
- Marker Of Proliferation Ki-67 (MKI67); and
- TTK Protein Kinase (TTK).

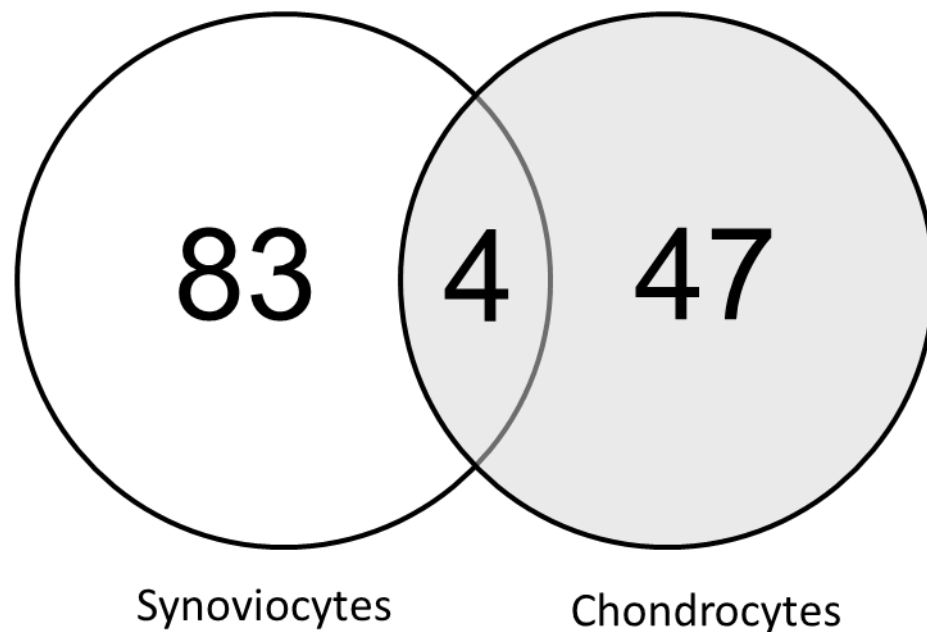


Figure. 4.01. The effects of a transient exposure (48 hours) of human chondrocytes (n = 3) and synoviocytes (n = 3) to high glucose (30mM) on whole transcriptome was assessed using microarrays. A gene was considered significantly differentially expressed if having a \log_2 fold change of greater than 0.5 (actual change of around 40%), with a false discovery rate of less than 15%. A larger effect was seen in synoviocytes (83 genes affected) than in chondrocytes (47 genes affected). A low level of cross-over was observed with 4 genes being differentially expressed in both cell types.

Three of the above genes, KIF18A, MKI67, and TTK have known roles within cell mitosis and cell proliferation.

4.2.1.1 Cell cycle and DNA damage are affected after transient high glucose exposure in synoviocytes

As described above, microarray experiments assessed the effect of 30mM glucose exposure on synoviocytes against a 5mM glucose control. The overall microarray gene expression data distributions in both synoviocytes can be seen from the volcano plot of Figure 4.02. In the volcano plot, each data point corresponds to a single differentially expressed gene after exposure of synoviocytes to 30mM glucose for 48 hours, relative to the normal glucose (5.5mM) control. \log_2 fold-change in individual gene expression can be seen on the horizontal axis. The vertical axis represents the significance of the individual gene expression changes ($-\log_{10}$ p-value). As can be seen from Figure 4.02, the fold-change expression does not exceed a \log_2 fold-change of 1.5 (roughly a real fold-change of 3). This suggests that the gene expression changes experienced in these cells as a result of high glucose exposure are modest. There are, however a number of significant gene expression changes as denoted by the grey area, which represents the boundary above which $p < 0.05$.

Following preprocessing, normalisation and modelling of the microarray data, a principal component analysis was carried out in order to attempt to identify a primary driver of variability in the data distributions. A principal component analysis (PCA) plot can be seen in Figure 4.03 A, which shows that, in synoviocytes, the data distributions from each of the individual treatments do not group on the first principal component axis (the horizontal axis) according to treatment group. If the samples were grouped according to treatment, the three data files obtained from the synoviocytes treated with 30mM glucose for 48 hours would

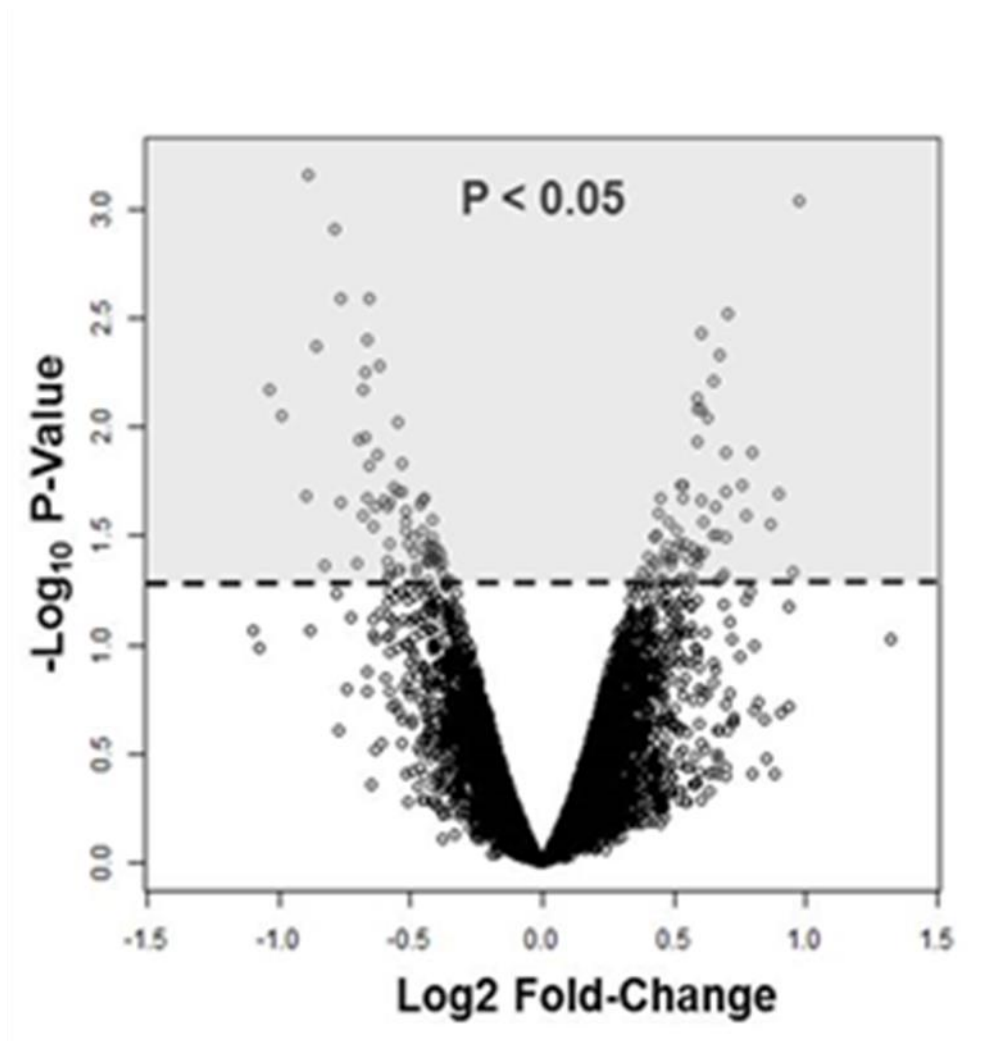


Figure. 4.02. Transient high glucose exposure (30mM for 48 hours) of synoviocytes yielded modest effects on gene expression. The above volcano plot shows significance ($-\log_{10}$ p-value) plotted against effect magnitude (\log_2 fold change). Each point on the chart represents a single gene expression change. The effects of transient high glucose exposure on global gene expression in synoviocytes was relatively low with the \log_2 fold change values not exceeding 1.5 (around 300% change). There are, however a number of gene expression changes with a p-value of 0.05 or lower (highlighted by the shaded portion).

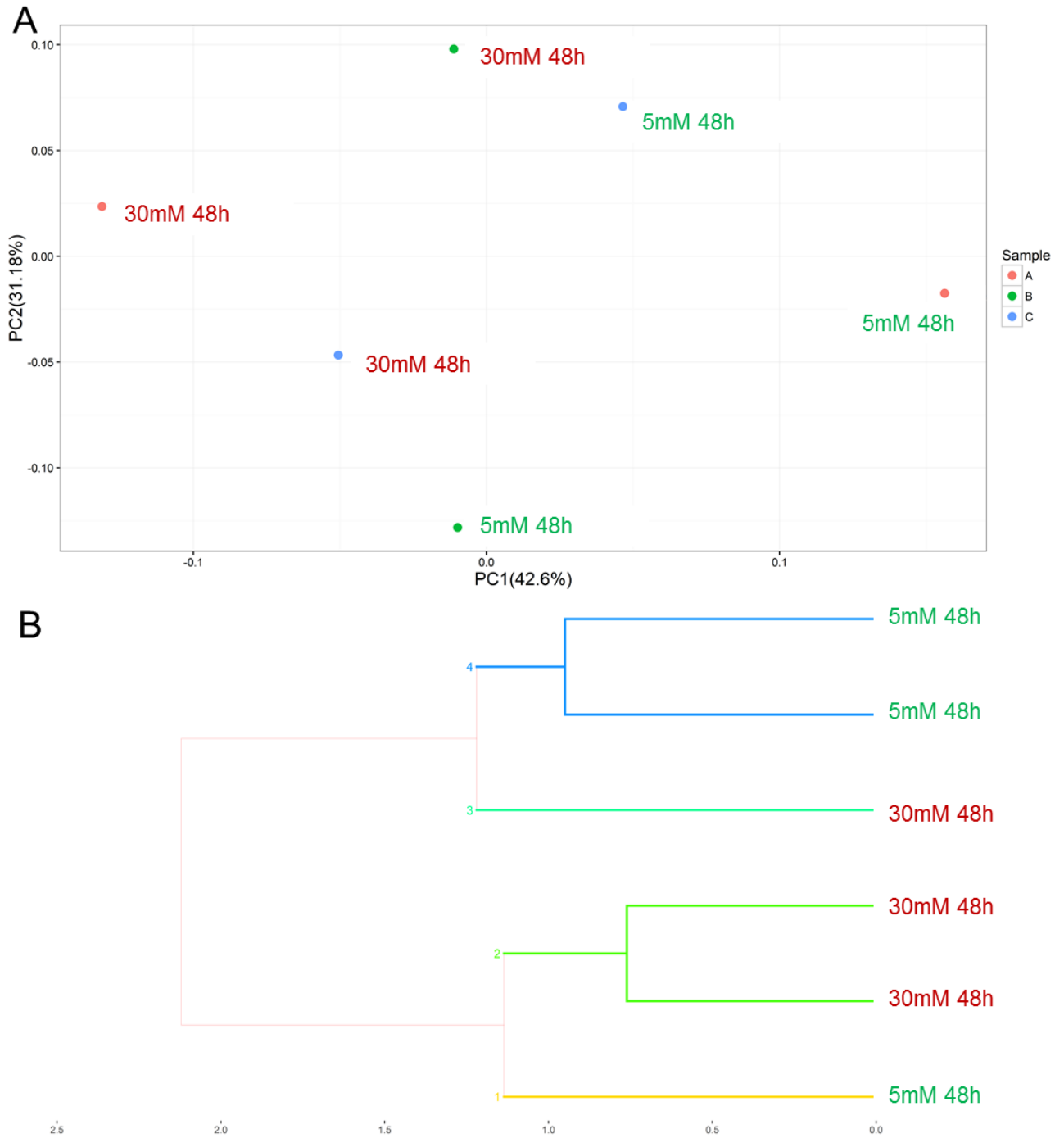


Figure 4.03. Following principal component analysis (A), a potential grouping effect of the 48 hour exposure of cells to 30mM glucose was identified, with some similar within-sample separation being seen on the 1st principal component axis (PC1) between the high glucose treated cells and the normal glucose control. The clustering analysis dendrogram of B, however, suggests that only two of the three synoviocytes cell samples grouped according to treatment type.

group separately to the three data files obtained from the synoviocytes maintained in the normal glucose control (5.5mM).

The grouping observed in the principal component analysis is corroborated using a cluster analysis algorithm, from which the data can be seen in the dendrogram of Figure 4.03 B. Here it can be seen that while for two of the three synoviocyte samples there is clustering according to treatment, this is not the case for the third sample.

The significantly differentially expressed genes following transient (48 hour) high glucose (30mM) exposure in synoviocytes can be seen in Table. 4.01a (Benjamini-Hochberg false discovery rate (q-value) < 5%) and Table. 4.01b (Benjamini-Hochberg false discovery rate (q-value) >5% and < 25%). As was seen in the Venn diagram of Figure 4.01, there were 83 synoviocyte genes that were significantly differentially expressed using false discovery rate (q-value) threshold of 5%.

One of these genes identified within the false discovery rate threshold of less than 5% was the gene for Hyaluronic Acid Synthase 2 (HAS2, \log_2 fold change = 0.75, q-value = 0.0007). This gene encodes a protein that has specific relevance to the phenotypic functioning of synoviocytes within their native tissue, the synovial lining of the joint cavity. Synoviocytes are known to produce hyaluronic acid using hyaluronic acid synthases.

An additional gene that is significantly upregulated in synoviocytes in response to transient (48 hour) high glucose (30mM) exposure is Mesenchyme Homeobox 2 (MEOX2, \log_2 fold change = 0.86, q-value = 0.02). This gene has been identified as having a key role in cell cycle arrest, and cell senescence (214-216), functional consequences that have previously been attributed to high glucose exposure (165, 217).

Table. 4.01. Differentially expressed genes following exposure of synoviocytes (n = 3) to 30mM glucose for 48 hours, having a log₂ fold change of greater than 0.5, and a false discovery rate of less than 5% (A) and less than 15% (B).

A

Gene	Log ₂ Fold Change	FDR
LOC100288884	-0.56077	0.000962
MOSPD1	-0.51498	0.001572
CCKAR	0.610667	0.002228
RNU6-14P	0.524619	0.002682
TMEM144	-0.62259	0.003037
SNORA70B	0.540979	0.005642
GDF15	-0.51418	0.006821
HAS2	0.749877	0.006834
RNU5D-1	0.542321	0.00722
RARRES3	-0.76141	0.008337
FAM64A	0.542853	0.009288
GALNT12	-0.55443	0.009947
ANP32A-IT1	0.646297	0.012397
LBP	-1.06972	0.012934
DPY19L2P1	0.557325	0.015045
KIAA0226L	-0.64118	0.015681
SNORA14A	0.540361	0.016302
LINC01140	-0.56	0.017466
RNF144A	-0.56127	0.018229
G0S2	-0.52726	0.019274
MEOX2	0.860991	0.019364
SLC14A1	0.577734	0.019939
PTGER2	0.5443	0.020962
EVI2B	-0.9287	0.02164
RELN	0.517521	0.02527
TNFAIP6	-0.65486	0.027013
KIF18A	0.549347	0.027078
NCAPH	0.515135	0.029081
HIST1H2BM	0.527204	0.029413
CASC5	0.66752	0.029997
SULT1C2	-0.65496	0.030787
ESCO2	0.551212	0.033105
HIST1H3B	0.626302	0.034384
ABCB5	-0.62071	0.03501
STON2	-0.54718	0.036968
THBS1	0.602507	0.039678
SCD	-0.50293	0.040352
PRC1	0.55193	0.040596
MME	-0.63414	0.041186
MKI67	0.576737	0.041495
BUB1	0.654573	0.043323
FST	0.550236	0.04382
FGF9	0.546805	0.047459
BUB1B	0.547173	0.049418

B

Gene	Log ₂ Fold Change	FDR
FAM111B	0.570618	0.050333
AQP1	0.588786	0.050529
SLC40A1	-0.5443	0.051412
KYNU	-0.5685	0.054021
SERPINE1	0.786313	0.055114
CKAP2L	0.581129	0.057315
DLGAP5	0.643455	0.058235
SCUBE3	0.852185	0.058826
APOBEC3B	0.508682	0.059734
INA	0.708745	0.059774
ANLN	0.539448	0.059949
CRISPLD2	-0.59001	0.060811
KIF20A	0.600379	0.060847
HIST1H3F	0.507634	0.061699
CD36	-0.62254	0.064377
DIAPH3	0.530021	0.065089
DTL	0.616486	0.065618
ASPM	0.53967	0.067217
DSG2	-0.58783	0.071244
TOP2A	0.532835	0.07261
NUF2	0.537794	0.073989
FAM20A	-0.5312	0.074956
PODXL	0.598583	0.07817
SHCBP1	0.52591	0.07842
PPARGC1A	-0.60636	0.07972
PBK	0.541741	0.082445
COLEC12	-0.70889	0.082773
EYS	0.656581	0.084452
TPX2	0.601708	0.088913
MYBL1	0.524014	0.098528
TTK	0.529614	0.104969
PPM1L	-0.53655	0.107677
FMO2	-0.54427	0.112855
EVI2A	-0.6809	0.116657
PSAT1	0.545558	0.12031
FYB	-0.66713	0.124648
SEMA7A	0.555708	0.128396
HSPB7	0.575883	0.130945
RRM2	0.529069	0.133182

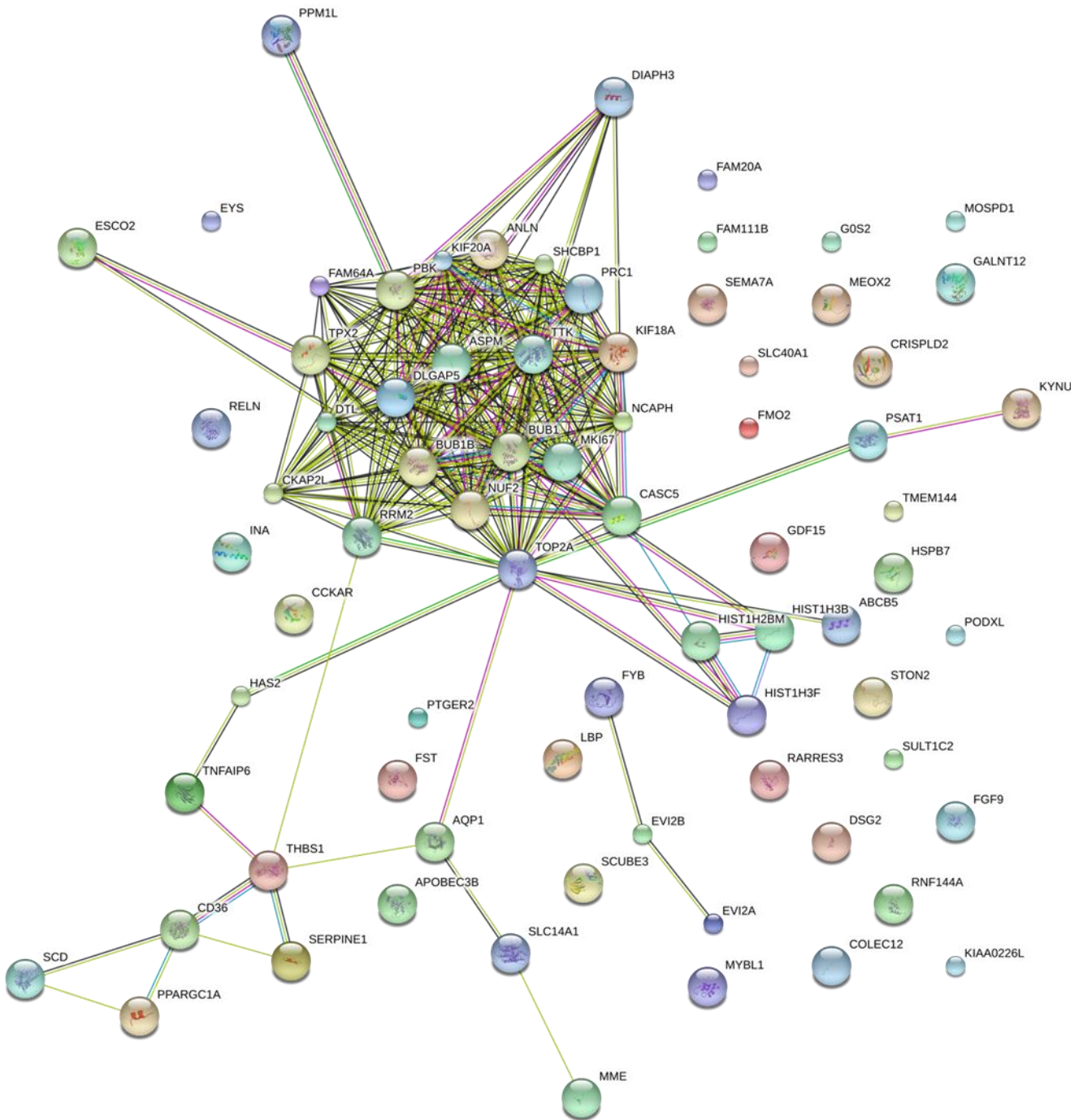


Figure. 4.04. Following identification of high glucose-mediated differentially expressed genes in synoviocytes, an assessment of protein interactions associated with the identified gene set was carried out. As can be seen in the above interaction map (STRING), a single, heavily enriched cluster of related proteins was identified.

Table 4.02. Functional analysis shows significantly enriched (false discovery rate less than 5%) gene ontology (GO) terms associated with biological processes (A). Significantly enriched GO terms associated with cellular components were also identified (B). GO terms associated with cell division and mitosis were highly enriched by the gene set obtained from the differential expression analysis and as is suggested by the protein interaction map of Figure. 4.04.

A

GO Term	Description	Count	FDR
GO:0000278	mitotic cell cycle	17	1.43E-05
GO:0000280	nuclear division	13	1.43E-05
GO:1903047	mitotic cell cycle process	16	1.43E-05
GO:0022402	cell cycle process	18	2.14E-05
GO:0007059	chromosome segregation	9	4.99E-05
GO:0007067	mitotic nuclear division	11	5.71E-05
GO:0007049	cell cycle	19	9.65E-05
GO:0051301	cell division	12	0.000124
GO:0051716	cellular response to stimulus	38	0.00445
GO:1902589	single-organism organelle organization	20	0.0056
GO:0050896	response to stimulus	41	0.00683
GO:0071173	spindle assembly checkpoint	4	0.00754
GO:0030071	regulation of mitotic metaphase/anaphase transition	4	0.0191
GO:1902170	cellular response to reactive nitrogen species	3	0.0191
GO:0048513	organ development	22	0.0266
GO:0002244	hematopoietic progenitor cell differentiation	5	0.0334
	negative regulation of proteasomal ubiquitin-dependent protein		
GO:0032435	catabolic process	4	0.0392
GO:0030194	positive regulation of blood coagulation	3	0.0439
GO:0070295	renal water absorption	2	0.0439
GO:0098813	nuclear chromosome segregation	5	0.0439
GO:0007010	cytoskeleton organization	11	0.0491

B

GO Term	Description	Count	FDR
GO.0005819	spindle	9	0.00096
GO.0000793	condensed chromosome	6	0.0341
GO.0000922	spindle pole	5	0.04

An attempt at providing a functional characterisation of the effects of high glucose on gene expression in synoviocytes involved an input of the significantly differentially expressed genes into an online tool used for predicting protein interactions (STRINGdb, (218)). A diagrammatic representation of this assessment of the predicted protein interactions potentially resulting from the differential gene expression observed in the microarray data is shown in Figure 4.04. As can be seen, there are a number of predicted interactions, providing evidence toward a downstream function being affected by the transient exposure of synoviocytes to 30mM glucose. The presence of a large clustering of interacting of interacting proteins, the gene expressions of which were all significantly affected by high glucose exposure, could provide strong evidence toward an effect of high glucose on downstream functioning in these cells.

Gene ontology analysis was used to identify the most significantly enriched gene ontology terms associated with known biological functions (Table 4.02a) and cellular components (Table 4.02b). The most significantly enriched gene sets (false discovery rate < 5%), using the differentially expressed genes from Figure 4.04, were overwhelmingly those involving the cell cycle, proliferation, cell division or mitosis. In particular, the gene ontology term, “mitotic cell cycle” (GO 0000278) includes a total of 17 genes which overlap with the current data set, and was enriched to a high degree of significance ($q\text{-value} = 1.43 \times 10^{-5}$). The proteins derived from this gene set can be seen highlighted in the protein interaction map of Figure 4.05, which shows that the proteins associated with these genes make up the large majority of the primary cluster of the protein interaction map of Figure 4.04.

Preliminary analysis of data from the aforementioned microarrays, carried out during a previous project and on which some of the experiments for the current project were based, also highlighted pathways associated with DNA damage and repair. In particular, the functional analysis of the data suggested that while DNA damage and repair markers were identified as upregulated, cell cycle checkpoint markers were, in contrast, downregulated.

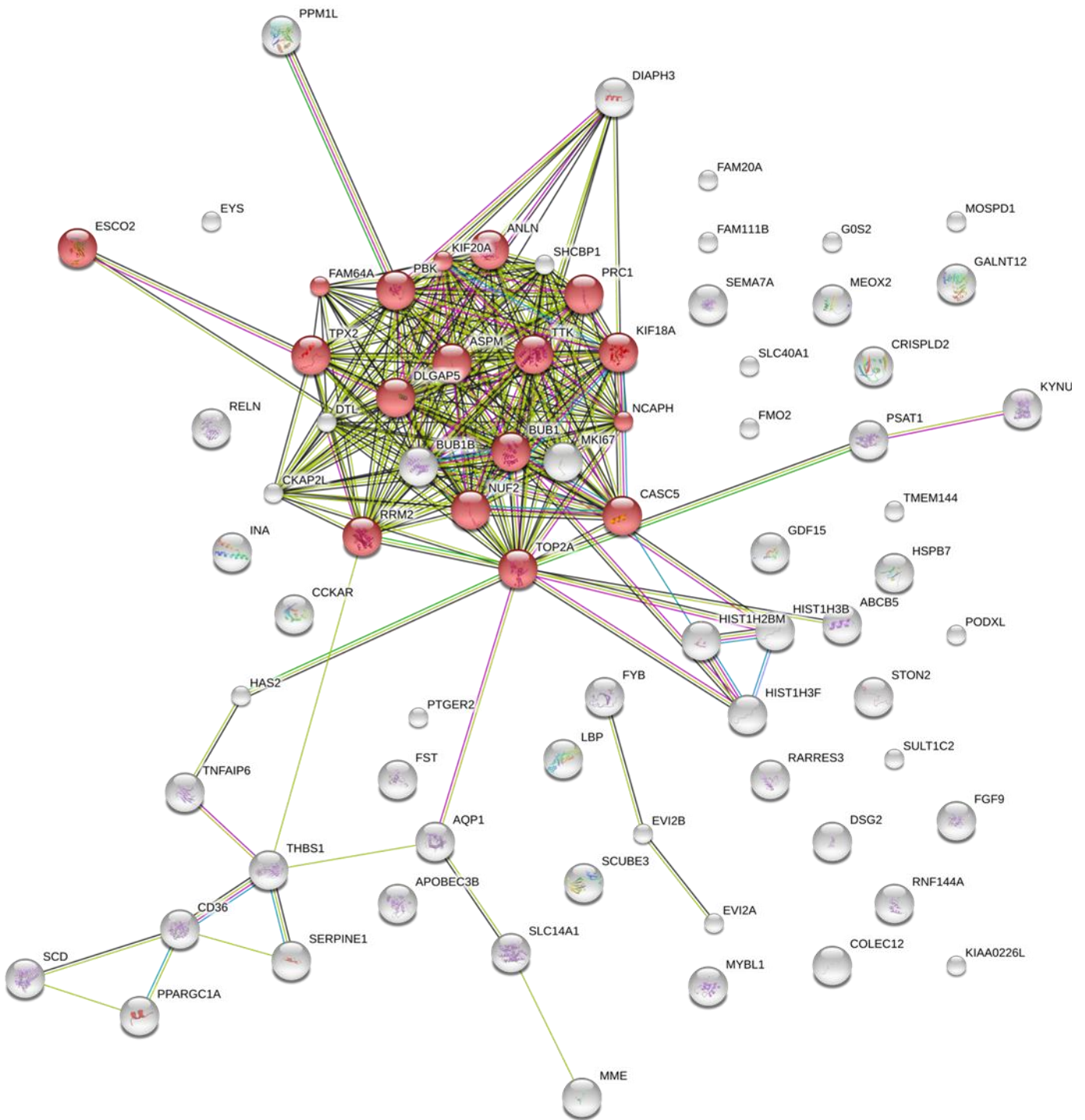


Figure. 4.05. Following a functional annotation of the high-glucose mediated differentially expressed gene set in synoviocytes in Tables. 4.02. **A** and **B**, proteins shown in the interaction map of Figure. 4.04 associated with the GO term “mitotic cell cycle” (GO:0000278, FDR = 1.43×10^{-5}) are overlapped in the above interaction map. As can be seen from the above interaction map, the single cluster of highly associated proteins suggests an effect on the gene expression of genes associated with mitosis and the cell cycle.

Representative figures from this analysis can be seen in Figure 8.01 and Figure 8.02 of the Appendices. Figure 8.01 shows the effects of 48 hour exposure of synoviocytes to 30mM glucose on the ATM signalling pathway, a pathway which was significantly enriched during the analysis ($p\text{-value} = 1.18 \times 10^{-5}$). Expression values are colour-coded, using green and red for decreased and increased expression respectively. The increasing intensity of the colours depicts the extent of the expression changes in response to high glucose. The colour coding in each pathway shown represents the \log_2 fold-change expression data in synoviocytes, in response to high-glucose. DNA damage response indicator ATM is up-regulated in response to high glucose, along with DNA repair markers such as BRCA1. The protective cell-cycle arrest mechanism normally occurring via p53/p21 appears to be inhibited, with increased expression of cyclin B/CDK1 complex.

High glucose-mediated DNA damage and a downstream repair response is supported by Figure 8.02 which shows largely an upregulation of genes associated with BRCA1-mediated DNA repair in response to DNA modification (not significantly enriched). These figures were obtained using the Ingenuity Integrated Pathway Analysis (IPA) tool.

Previously published evidence suggests that high-glucose could potentially play a role in increased inflammation (219) together with dysfunctional extracellular matrix catabolic and anabolic pathways (134, 164). These pathways are associated with the effects observed in degenerative musculoskeletal conditions and as such present a plausible scenario depicting high glucose dependence in the aetiology or progression of musculoskeletal disorders. A predetermined gene-list was used in a targeted approach to assess any potential gene expression effects of transient high glucose exposure in chondrocytes and synoviocytes.

Based on what would appear to be a corroboration of conclusions of prior studies indicating a high-glucose mediated DNA damage effect(152, 161, 168, 194), it was therefore desirable to investigate this further using a targeted approach, including data from functional assays to support the aforementioned results.

During the current project, a targeted investigation into the effects of high glucose exposure on DNA damage and repair markers was carried out using qPCR. In particular, expression of the DNA damage and repair markers, ATR, ATM and BRCA1, highlighted as upregulated in the preliminary analysis of the microarray data were assessed in synoviocytes. A focus of the targeted gene expression study was to replicate the findings of the microarray data, using synoviocytes obtained from the same donors as used previously. A further focus of the targeted assessment was to identify the time at which DNA damage and a subsequent repair response was initiated, using a range of time points (1 hour, 6 hours, 16 hours and 48 hours). One final focus of the targeted assessment was to provide a more physiological level of high glucose (11mM) for comparison to the standard high glucose concentration (30mM) used within the literature, and used for the microarray study.

The qPCR data, which can be seen in Figure 4.06, did not identify any significant differential expression in the genes for the three markers used. As can be seen from Figure 4.06 A, there was a significant differential expression of the ATR gene between the cells treated with 11mM and 30mM glucose for 1 hour. It is interesting to see that these two high glucose treatments appear to have had a contrasting effect on gene expression of ATR. It can also be seen from Figure 4.06 B and Figure 4.06 C that 30mM glucose exposure for 1 hour caused a large amount of variability in the gene expression of the different cell samples. This early effect would, however, appear to be reduced back to a baseline level at the 6 hour or 16 hour time point in all three genes investigated. In Figure 4.06, the 5mM (untreated) control is shown plotted next to the 1 hour-treated cells. This is for visual comparison of the gene expression in the untreated control against the treatment groups. During the experiment, the cells were in cell culture for the same length of time, glucose treatments being staggered so that RNA could be harvested from all cells from the different treatment groups at the same time to avoid time-dependent effects of cell culture on the results.

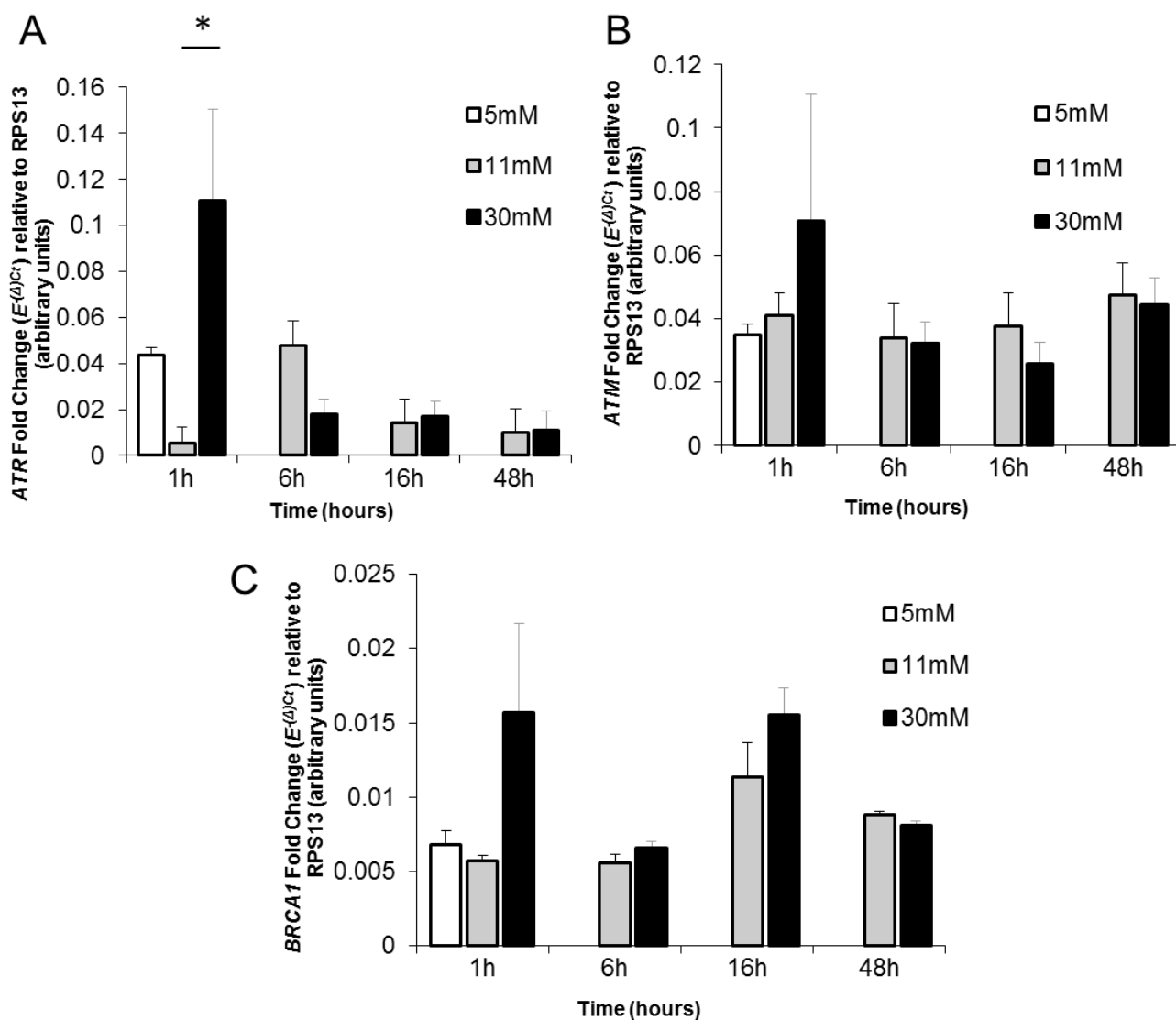


Figure 4.06. qPCR analysis of the time-dependent effects of two high glucose treatments (11mM and 30mM) across 4 time-points (1h, 6h, 16h and 48h) in human synoviocytes (n=3). Data suggests an early effect (1h) in all three markers, with ATR (in **A**) showing a significantly opposite effect ($p < 0.05$) between the two high-glucose treatments (11mM and 30mM). Although the data in **A** would initially appear to validate the microarray data with an increased expression in response to 30mM glucose (1h), there would appear to be a somewhat gradual reduction to baseline by 48h (the time-point used for the earlier microarray study). Neither the gene expression of ATM (in **B**) or BRCA1 (in **C**) was identified as significantly affected as a result of high glucose treatment in this validation study. Data is shown as mean \pm standard deviation.

DNA damage was assessed using single cell gel electrophoresis. Cells exposed to transient (16 hours) and long term (14 days) high glucose (11mM and 30mM) were lysed in gel and their nuclei electrophoresed, stained and the resultant comet-like image analysed using dedicated software (CASPlab).

While markers of DNA damage were identified in the microarray data following exposure of synoviocytes to 30mM glucose for 48 hours, as is shown in Figure 4.07, it was in fact the lower level of high glucose exposure (11mM) that experienced the largest noticeable effect on measurable DNA damage by single cell gel electrophoresis. Figure 4.07 shows data from synoviocytes, wherein the vertical axis denotes the average “Olive tail moment”, a compound metric comprising the length and density of the comet “tails” of each electrophoresed cell nucleus. As discussed, this data might suggest that there is potentially more of an effect on DNA damage observed in the 11mM treated cells at both the short term (16 hour) and the long term (14 day) time-points (not significant). Since this does not appear, from data in Figure 4.06 A-C, to be followed by a corresponding increased expression of genes associated with the DNA damage and repair response, this may present an interesting finding. Positive control samples treated with hydrogen peroxide prior to the end of high-glucose treatment showed considerable levels of DNA damage as expected.

Potential sources of DNA damage were investigated, including inflammation, and reactive oxygen species. Expression of genes associated with inflammation (IL1R1 and PTGS2) was assessed by qPCR, following treatment of cells using the same treatment protocol as was used for the single cell gel electrophoresis assessment of DNA damage described earlier. As can be seen in Figure 4.08, gene expression of IL1R1 and PTGS2 was not found to be affected by high glucose treatment, with treatment group being identified as not presenting as a significant source of variability in the data set ($p > 0.05$). Gene expression of MMP3 was also assessed in relation to any potential matrix catabolic effects of high glucose exposure in these cells. No significant effects on MMP3 expression were observed.

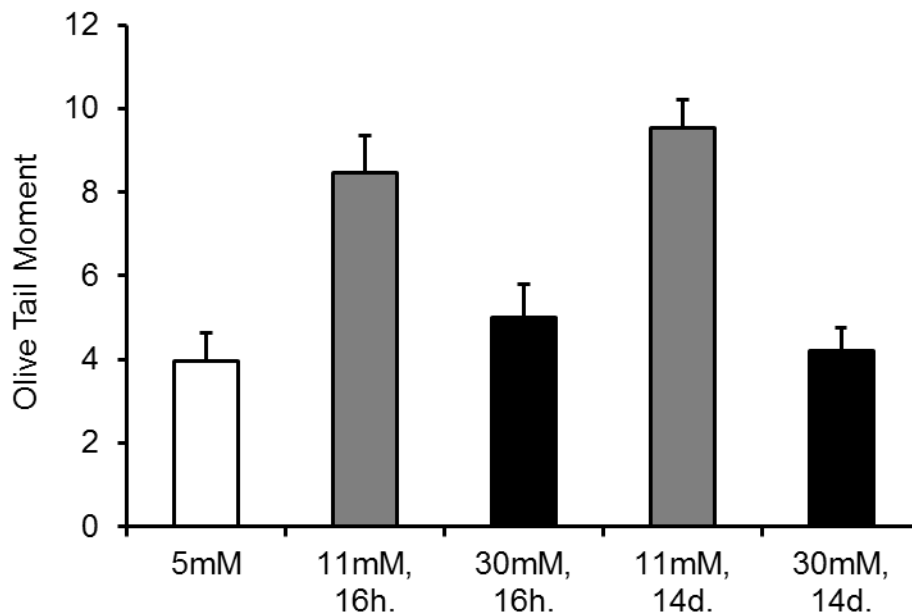


Figure 4.07. The extent of high glucose-induced DNA strand breaks were assessed using single-cell gel electrophoresis (comet assay). Briefly, synoviocytes (n=3) were treated using various glucose concentrations (5mM, 11mM and 30mM for both 16 hours and 14 days) prior to being suspended in 1% low melting point agarose gel and lysed. The remaining chromatin was then electrophoresed, with shorter, more severely damaged strands moving further through the agarose gel. The DNA was then stained using peqGREEN (Peqlab), prior to being imaged using a fluorescent microscope. Software (CASPLAB) was then used to analyse the images for the percentage of DNA contained in the tail of the comet, as a product of the tail length (measurement referred to as Olive Tail Moment). The general trend suggests larger effects of modest high glucose (11mM) on DNA damage after 16 hours when compared to normal glucose control (5mM) (not significant). Little effect is seen after 30mM glucose treatment. Data is shown as mean \pm standard deviation.

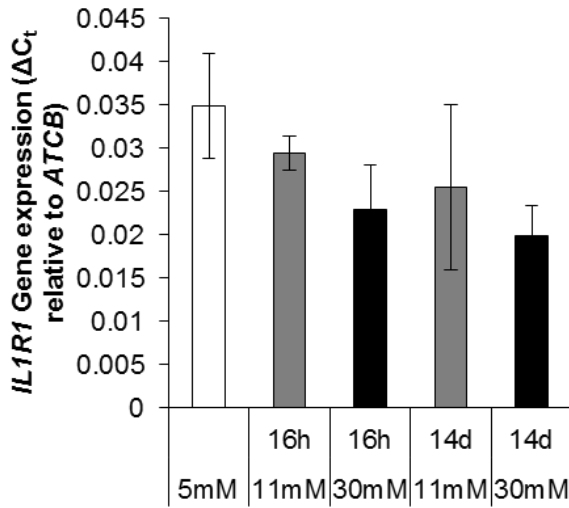
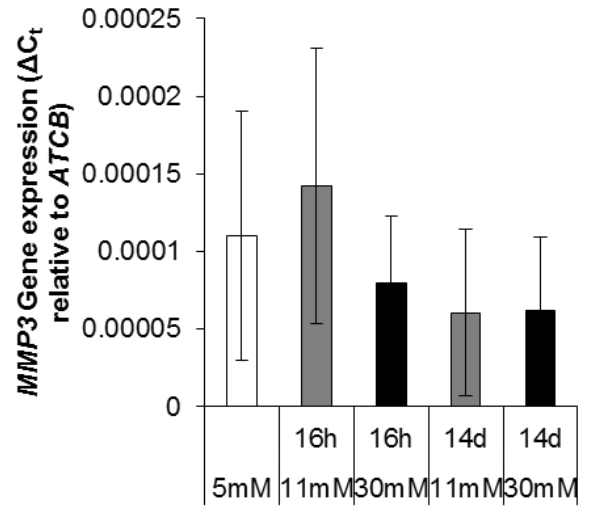
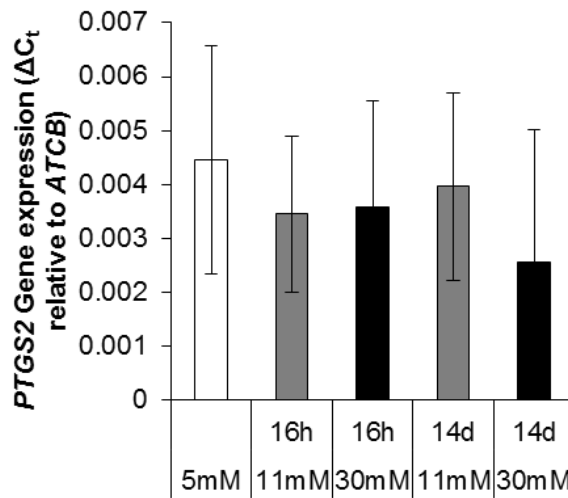
A**B****C**

Figure 4.08. Markers of inflammation and matrix catabolism were assessed using qPCR, in order to link the potential effects of high glucose on DNA damage to known pathways associated with musculoskeletal pathology. No significant differential expression was identified for IL1R1 (**A**), MMP3 (**B**) or PTGS2 (**C**). Data is shown as mean \pm standard deviation.

It was important thus to determine whether, as has been reported in previous studies (161), this potential increase in DNA damage is the result of an increase in reactive oxygen species, which could potentially be a bi-product of an altered glucose metabolism observed in Chapter 3.

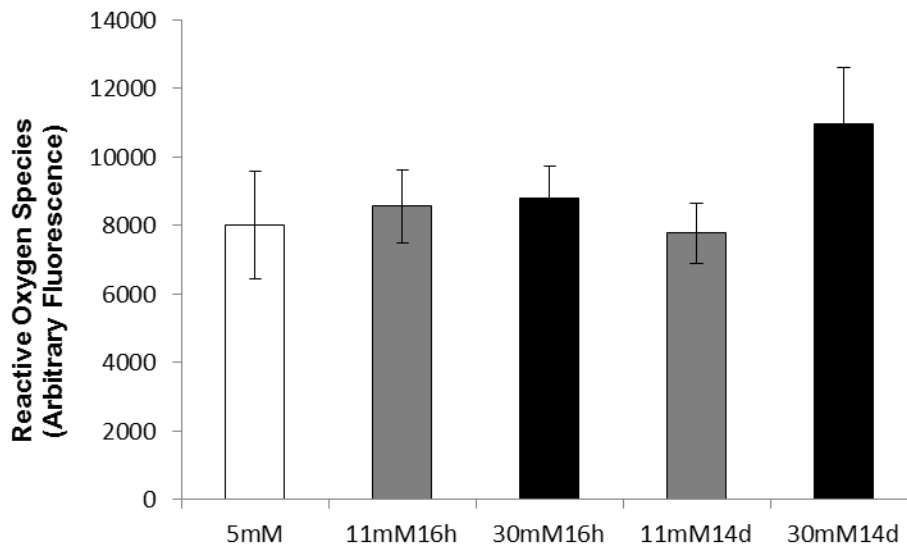


Figure 4.09. As a potential cause of DNA damage, reactive oxygen species were assessed following exposure of synoviocytes (n = 3) to high glucose (11mM and 30mM for 16h and 48h) compared with a normal glucose (5.5mM) control. Dichlorofluorescein diacetate was used as a reactive oxygen species dye, with resulting fluorescence used to indicate the amount of intracellular reactive oxygen species. There was no significant effect of high glucose exposure on reactive oxygen species production in synoviocytes. Data is shown as mean \pm standard deviation.

Reactive oxygen species were assessed in synoviocytes following long term (14 day) and short term (16h) exposure of high glucose (11mM and 30mM) using a reactive oxygen species dye (dichlorofluorescein-diacetate, DCFDA). Figure 4.09 shows the level of reactive oxygen species measurable within synoviocytes according to a fluorescence measurement.

This data suggests that the level of reactive oxygen species in these cells is not significantly affected by high glucose treatments either at short term (16 hour) or long term (14 day).

Due to an indication that cell cycle is affected in synoviocytes following high glucose treatment (30mM glucose exposure for 72 hours), following the microarray experiments, it was decided to assess the effects of high glucose exposure on cell proliferation. Cells seeded at controlled cell density (10^5 cells per well of a six well plate) were treated with six high glucose doses ranging from 5mM to 30mM, for 72 hours prior to trypsinisation and counting. The resulting cell counts for each sample were normalised to the normal glucose control (5mM) and the resultant relative cell numbers can be seen in Figure 4.10. As can be seen, there was a significant increase in cell number following treatment of cells with 15mM and 25mM glucose for the duration of the experiment (72 hours). There was not a significant correlation between dosage of glucose and cell number. At the upper extreme of the glucose

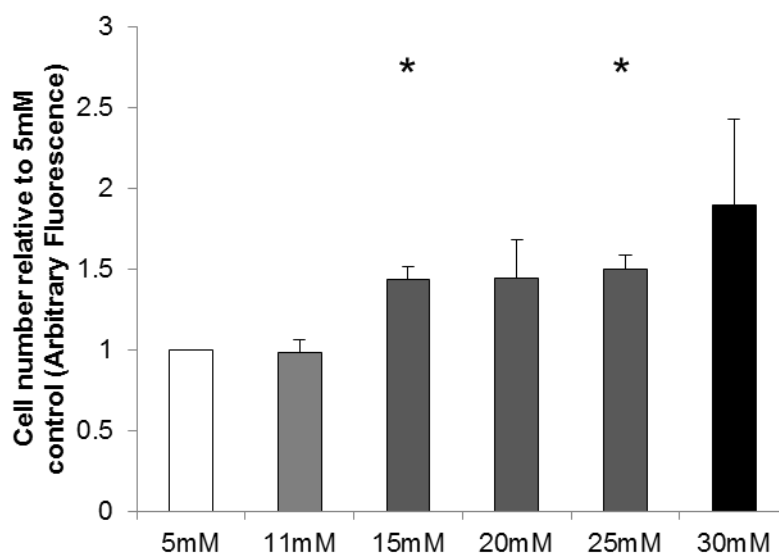


Figure 4.10. Synoviocyte proliferation assay data showed significant effects of high glucose exposure (15mM and 25mM) on synoviocyte proliferation, with each treatment showing roughly a 50% increase in cell number compared with a normal glucose (5.5mM) control ($p < 0.05$). Data is shown as mean \pm standard deviation.

dosage (30mM), the variability in the sample group was increased.

4.2.2 Cell cycle is affected in chondrocytes following transient exposure to high glucose

As was the case in synoviocytes, the effects of a transient (48 hour) exposure of chondrocytes to high glucose (30mM) on gene expression were assessed using microarrays. The effects were modest as can be seen from the volcano plot of Figure 4.11. As with the volcano plot of Figure 4.02, the volcano plot of Figure 4.11 shows the extent of the expression change in the form of a \log_2 fold-change on the horizontal axis, plotted against the significance of the expression change in the form of a $-\log_{10}$ p-value on the vertical axis. The data points on the volcano plot represent a single transcript cluster measured on the microarray. The \log_2 fold-change values were rarely measured above 1 (actual fold change of 2).

Following preprocessing, normalisation and modelling of the microarray data, a principal component analysis of the datasets revealed that the samples were divided on the first principal component axis (horizontal axis) according to treatment group as can be seen in Figure 4.12 A. This was confirmed during a subsequent cluster analysis carried out using R, and is represented on the dendrogram of Figure 4.12 B which shows two distinct clusters of treatment groups. As can be seen in Figure 4.01, in spite of the clustering of chondrocyte differential gene expression data according to treatment group, which was not seen in corresponding data obtained from synoviocytes, there were fewer differentially expressed genes identified in chondrocytes compared with synoviocytes. 47 significantly differentially expressed genes were identified in chondrocytes after exposure of cells to high glucose (30mM) for 48 hours (see Figure 4.01). Once again, the threshold for significance used was a \log_2 fold-change of 0.5 (actual percentage change of around 140%), and a false discovery rate of less than 25%. The differentially expressed genes can be seen in Tables 4.03 A and

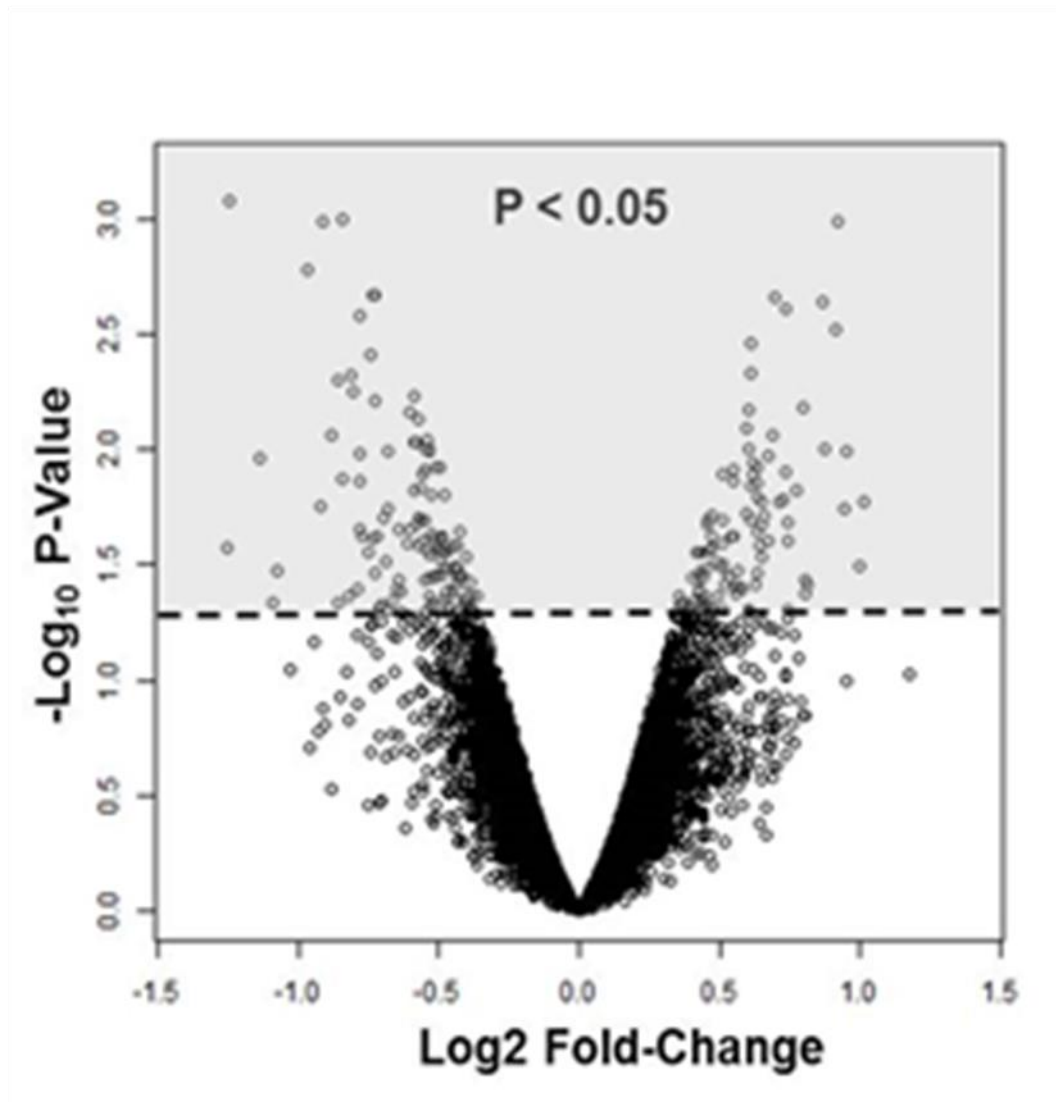


Figure. 4.11. Transient high glucose exposure (30mM for 48 hours) of chondrocytes yielded modest effects on gene expression as can be seen from the above volcano plot, which shows significance ($-\log_{10}$ p-value) plotted against effect magnitude (\log_2 fold change). Each point on the chart represents a single gene expression change. The effects of transient high glucose exposure on global gene expression in synoviocytes was relatively low with the \log_2 fold change values not exceeding 1.5 (around 300% change). There are, however a number of gene expression changes with a p-value of 0.05 or lower (highlighted by the shaded portion).

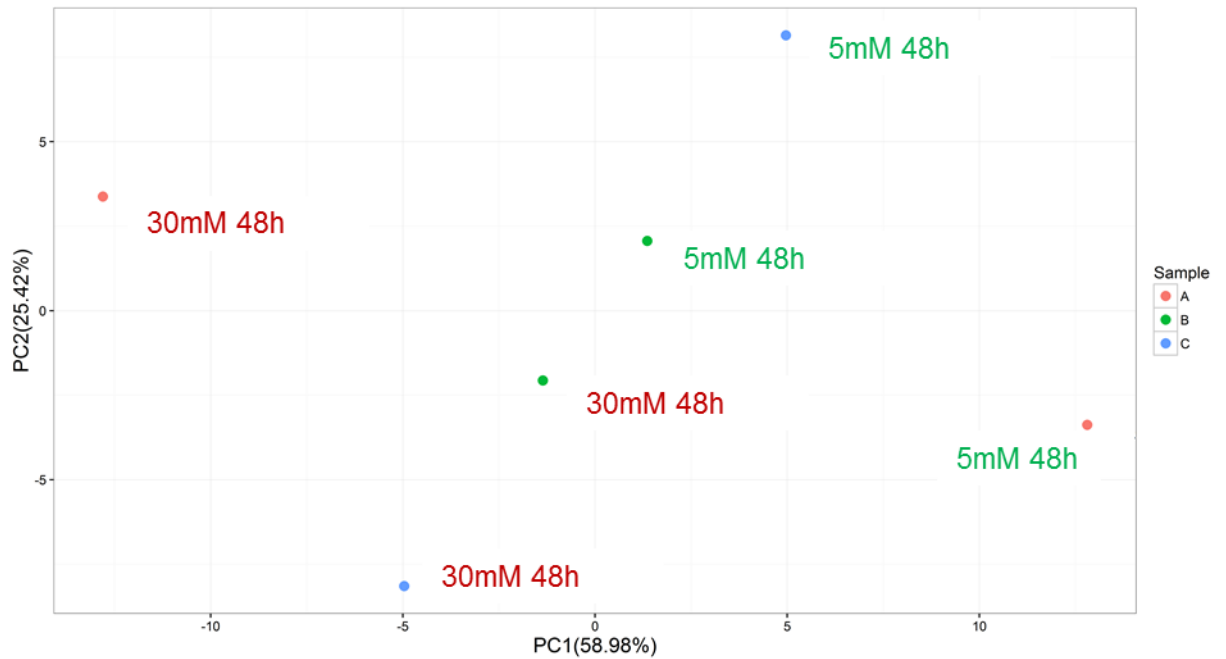
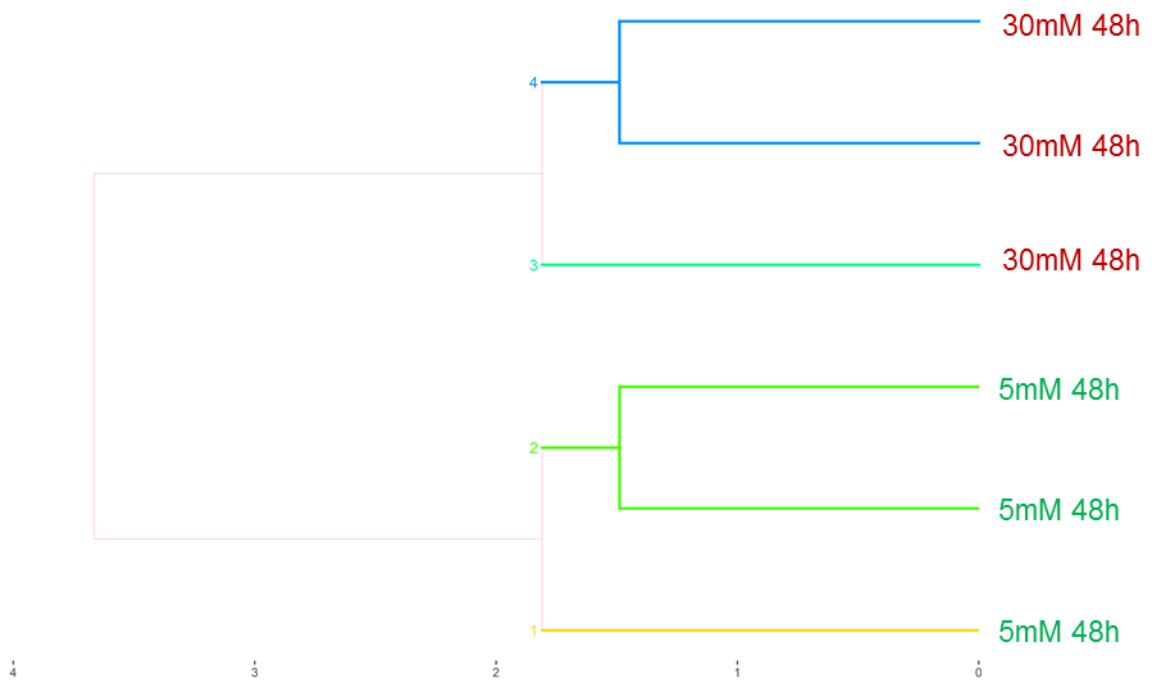
A**B**

Figure. 4.12. A principal component analysis suggested a potential grouping effect of the 48 hour exposure of cells to 30mM glucose, with some similar within-sample separation being seen on the 1st principal component axis (PC1) between the high glucose treated cells and the normal glucose control (A). A clustering analysis also suggested that the three chondrocyte cell samples grouped according to treatment type (B).

Table. 4.03. Differentially expressed genes following exposure of chondrocytes (n = 3) to 30mM glucose for 48 hours, having a log₂ fold change of greater than 0.5, and a false discovery rate of less than 5% (A) and less than 15% (B).

A

Gene	Log ₂ Fold Change	FDR
CDR1	-0.86468	0.030323
SNORD113-3	0.777238	0.030323

B

Gene	Log ₂ Fold Change	FDR
CENPE	0.571631	0.050422
ND6	-0.66469	0.050422
TTN	0.662029	0.050422
CENPK	0.561253	0.050422
MTX2	0.857898	0.050422
MIR186	0.527061	0.050422
SMC2	0.583283	0.050422
CENPI	0.537395	0.050422
MKI67	0.523622	0.050422
KIF20B	0.544546	0.050422
SNORA14A	2.643999	0.052707
CEP55	0.517644	0.062542
CDK1	0.565804	0.062542
SNORD114-2	0.547876	0.062542
BLID	0.644427	0.062542
DEPDC1	0.522286	0.072262
TAS2R50	0.553812	0.072262
SNORD104	-0.53317	0.072262
ECI2	0.600983	0.072262
SGOL1	0.519587	0.072262
ZNF487	0.548287	0.072262
RNY1	0.820054	0.072262
C3	-0.64459	0.072262
DPPA3P2	0.705282	0.072262
SERPING1	-0.51319	0.072262
TTK	0.529933	0.072262
USP8	0.682639	0.072262
MIR100	0.755536	0.072262
FLVCR1-AS1	-0.53933	0.081822
KIF18A	0.63399	0.083129
RPS5	-0.5795	0.083482
SNORA14B	0.517875	0.083482
SNORA65	-0.71798	0.083482
OR5M3	-0.52094	0.083482
PTX3	-0.52484	0.087918
TXLNGY	0.534343	0.088994
TMEM263	0.531283	0.090661
ARPP19	0.557494	0.096652
IFI44L	0.560251	0.105274
LINC00917	-0.56697	0.106295
RBM8A	-0.51955	0.111063
SCARNA9L	0.672685	0.123512
ADAM20P1	-0.51258	0.129391
SNRPG	0.910979	0.131052
EPCAM	0.573053	0.140852

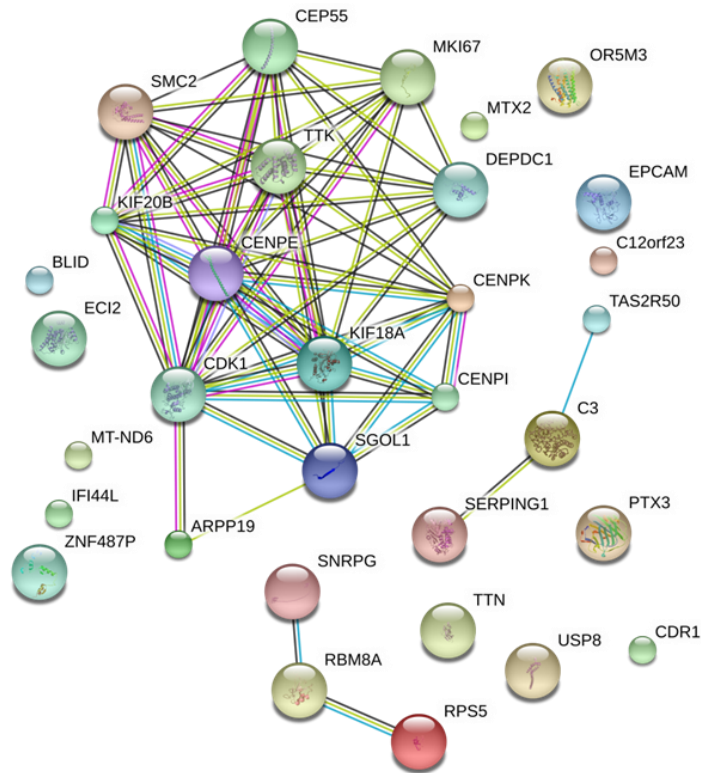
4.03 B, which show the differentially expressed genes with false discovery rates of less than 5% and less than 25% respectively.

SNORA14A and SNORA14B are both significantly upregulated, with SNORA14A being the most profoundly upregulated gene identified in the data set (\log_2 fold change of 2.64; actual fold change of 6; FDR = 5.2%). A map of predicted protein interactions developed using STRING (see Figure 4.13a) highlighted a single large cluster of genes.

Functional annotation using STRING revealed that, as with synoviocytes, among the most significantly enriched gene ontology terms relating to biological processes were those associated with the mitotic cell cycle (FDR = 8.55E-06, see Figure 4.13 B). Mitotic spindle (FDR = 0.005, see Figure 4.13 C) was unsurprisingly among the most highly enriched gene ontology terms associated with cellular components.

In spite of the evidence from the transcriptome assessment using microarrays, a functional validation failed to identify a role for high glucose exposure on cell proliferation rate. Chondrocytes seeded at controlled cell density (10^5 cells per well of a 6 well plate) were treated with varying doses of high glucose ranging from a normal glucose control (5.5mM) up to the literature standard experimental high glucose treatment (30mM) for 72 hours. Following treatment, the chondrocytes were trypsinised and counted. The resulting count data can be seen in Figure 4.14. Only marginal significance ($p = 0.054$) was identified in the doubling of chondrocyte cell number following exposure to 15mM glucose for 72 hours.

A



B

pathway ID	pathway description	count in gene set	false discovery rate
GO:0000278	mitotic cell cycle	12	8.55E-06
GO:0007067	mitotic nuclear division	9	8.55E-06
GO:0000280	nuclear division	9	3.85E-05
GO:1903047	mitotic cell cycle process	10	0.00016
GO:0051301	cell division	8	0.00077
GO:0007049	cell cycle	11	0.0026
GO:0000070	mitotic sister chromatid segregation	4	0.00767
GO:0007059	chromosome segregation	5	0.0121
GO:0022402	cell cycle process	9	0.014
GO:0006996	organelle organization	14	0.0149
GO:0098813	nuclear chromosome segregation	4	0.0343
GO:0007264	small GTPase mediated signal transduction	7	0.0401
GO:0034508	centromere complex assembly	3	0.0464

C

pathway ID	pathway description	count in gene set	false discovery rate
GO:0005819	spindle	6	0.00532
GO:0000793	condensed chromosome	5	0.00559
GO:0000776	kinetochore	4	0.0159
GO:0030496	midbody	4	0.0161
GO:0000775	chromosome, centromeric region	4	0.0366

Figure. 4.13. A single, heavily enriched cluster of related proteins was identified in a protein interaction analysis of genes from Table 4.03 (A). Subsequent functional analysis (B) shows significantly enriched (false discovery rate less than 5%) gene ontology (GO) terms associated with biological processes. Significantly enriched GO terms associated with cellular components were also identified (C). GO terms associated with cell division and mitosis were highly enriched by the gene set obtained from the differential expression analysis and as is suggested by the protein interaction map of A.

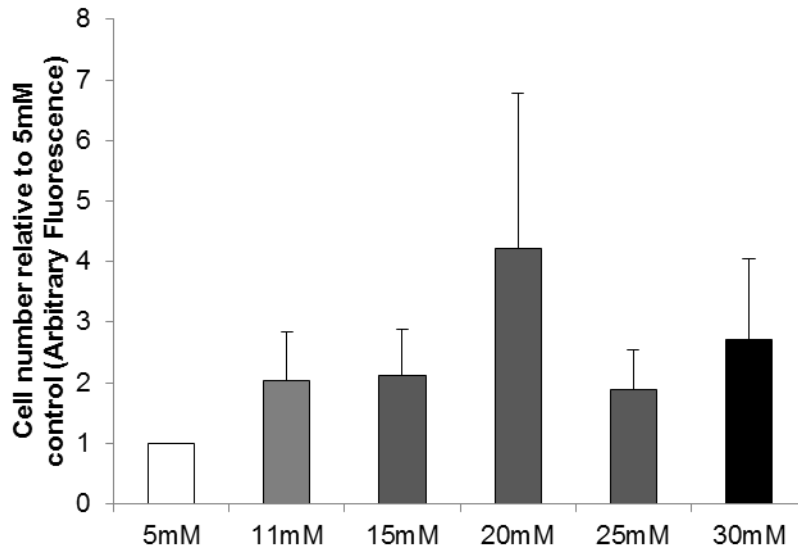


Figure 4.14. Chondrocyte proliferation assay data did not show any significant effects ($p < 0.05$) of high glucose exposure on chondrocyte proliferation. 15mM glucose exposure roughly doubled chondrocyte cell number, which showed marginal statistical significance ($p = 0.054$). Data is shown as mean \pm standard deviation.

4.3 Discussion

4.3.1 Synoviocytes and high glucose exposure

4.3.1.1 Preliminary data suggests high glucose mediate DNA Damage in Synoviocytes

The microarray data, which was obtained during experiments carried out from a previous project, would suggest that there was a significant effect of a relatively transient (48 hour) high glucose treatment (30mM) on the expression of key markers for DNA damage and the DNA repair response in synoviocytes according to a subsequent whole transcriptome analysis carried out during that project (see data from Figure 8.01; and Figure 8.02). While this may act to corroborate data that has been seen in previous studies (152, 161, 212), this data has been difficult to replicate using more targeted approaches such as qPCR and functional assays as can be seen from Figure 4.06 A - C.

The indication from Figure 4.06 A that expression of the ATR gene is significantly increased in synoviocytes after 1 hour treatment with 30mM glucose would be in line with a number of previous studies indicating that high glucose in this dose range causes DNA damage (152, 161, 162, 168, 212). These studies did, however, carry out high glucose treatments for longer than 1 hour (between 6 hours and 14 days).

This data suggests that the difference in glucose exposure was not the primary driver of variability in the data sets. Since this data was obtained from synoviocytes derived from human cartilage, it would typically be expected that, in a small size sample group such as this (n = 3), the data distributions would overwhelmingly cluster according to individual donor. This is due to the enormous inter individual variability expected being human transcriptome samples, which would be less of an issue for cells derived from genetically controlled sample groups such as those derived from inbred animal organisms. That these data distributions did not cluster according to individual donor suggests that additional factors may have been involved in causing variability between the different transcriptomes of these cell samples. While it is evident from the data shown in Figure 4.03 A and Figure 4.03 B that this additional factor was not exclusively driven by the different glucose treatments, it is possible that the treatments may have contributed to a portion of the clustering shown.

4.3.1.2 Synoviocyte cell cycle

The proteins of a large portion of the differentially expressed genes in synoviocytes were involved in the same interaction network, as can be seen in Figure 4.04. This has resulted in a highly significant enrichment of a number of gene ontology terms, most of which involve the cell cycle and mitosis as can be seen from Figure 4.05.

MEOX2 is closely associated with the progression of the cell cycle. In particular, MEOX2 is shown to interact-with CDKN1A (aka p21) and CDKN2A (aka p16), inhibitors of cyclin-dependant kinases, and has been shown to cause cell-cycle arrest through activation of these inhibitors (216) and forced expression of MEOX2 (214). In fact, MEOX2-knockdown

experiments showed that cells evaded the TGF- β mediated inhibition of cell proliferation (215), suggesting that MEOX2 is a major inhibitory factor in cell-cycle progression. A significant up-regulation in this gene (\log_2 fold change = 0.86, FDR = 0.019) might lead to an assumption that cell proliferation would be reduced, which is not the case in synoviocytes in response to high glucose as can be seen from results of the proliferation assay in Figure 4.10.

4.3.1.3 DNA Damage and Repair Markers

In synoviocytes, data from the previous study indicated that glucose appears to affect the BRCA1-mediated DNA damage response, with an apparent upregulation of genes associated within this pathway (Figure 8.02). This suggests some form of glucose-mediated DNA disruption, whether through double-strand breaks (DSBs), the presence of single-stranded DNA, or chromatin modification via acetylation or methylation. There seems to be increased expression of the checkpoint regulating kinases, ATR and ATM, with an up-regulation of genes associated with the downstream BRCA1-mediated DNA repair mechanism. There is yet insufficient experimental evidence to confidently conclude activation of this pathway, with further qPCR failing to validate expression levels of the associated genes in a targeted approach (Figure 4.06 A - C). Enhanced proliferation in synoviocytes persists in high glucose, although the BRCA1-mediated response may still occur according to gene expression microarray data, suggesting some underlying form of DNA-disruption. In the event of DNA-repair mechanism activation, the progression of the cell-cycle would typically be inhibited via various cell-cycle arrest proteins (often p53/p21-mediated) (220). This is in direct contradiction to the proliferation assay results (Figure 4.10), which suggested that the cells may have been proliferating. This indicates that while glucose may be responsible for causing DNA disruption and thus activating the resultant DNA repair mechanism, the consequent cell-cycle arrest appears to be prevented, allowing for progression of DNA-damaged (therefore potentially apoptotic) cells through the cell cycle. This conclusion is further supported by the decreased expression of p53/p21 (Figure 8.01)

along with the increased expression of the cyclin/cyclin-dependant kinase complexes (Figure 8.01).

4.3.1.4 DNA Damage

A direct functional analysis showed that DNA damage may not be significantly affected in synoviocytes following high glucose treatment (Figure 4.07). The data would suggest that there may be an effect on DNA damage observed in the 11mM treated cells at both the short term (16 hours) and the long term (14 days) time-points (not significant). Since this does not appear, from data in Figure 4.06 A - C, to be followed by a corresponding increased expression of genes associated with the DNA damage and repair response, if this can be supported by future data, then this may present an interesting finding. According to Figure 4.08 A - C, it also does not appear that, if DNA damage is caused by high glucose exposure, genes involved in inflammation and matrix catabolism are significantly affected.

It was important thus to determine whether, as has been reported in previous studies (152, 161, 162, 168), this potential increase in DNA damage is the result of an increase in reactive oxygen species, which could be a bi-product of an altered glucose metabolism observed in Chapter 3.

4.3.1.5 Oxidative damage

Figure 4.09 shows the level of reactive oxygen species measurable within synoviocytes using the reactive oxygen species dye Dichlorofluorescein diacetate (DCFDA). From this data it cannot be concluded that the level of reactive oxygen species in these cells is affected by high glucose treatments either at short term (16 hours) or long term (14 days). The data may suggest that there is a slight increase in the level of reactive oxygen species after 14 day exposure to 30mM glucose in these cells, but there is no statistical significance to support this conclusion.

Effects of high glucose on gene expression related to joint environment was observed in the significantly (FDR = 0.007) increased expression of the gene associated with hyaluronic acid synthase 2 (*HAS2*) as a result of high glucose exposure in synoviocytes. Hyaluronic acid is a key component of synovial fluid, the composition of which is tightly controlled by synoviocytes. The synthesis of hyaluronic acid is initiated by hyaluronic acid synthases, which come in three integral membrane bound isoforms, hyaluronic acid synthase 1, 2 and 3(221). The glucose-mediated upregulation of *HAS2* could suggest a role for glucose in altering the composition of the synovial fluid and potentially the incorporation of key synovial fluid constituents into cartilage. An altering of the synovial fluid and/or the cartilage composition in this way could have downstream effects on the healthy functioning of an articulating joint.

Hyaluronic acid, which as discussed is synthesised by hyaluronic acid synthases, has been implicated in mitosis and cell-cycle progression in its interaction with hyaluronan receptors CD44 (222) and RHAMM (223). Expression of CD44 and RHAMM is said to be repressed by p53 (224). It is interesting that prior analysis seen in Figure 8.01 suggests a high glucose-mediated down-regulation of p53, which could act to support *HAS2*-dependent effect of high glucose on proliferation of synoviocytes.

4.3.2 Chondrocytes and high glucose exposure

Effects of high glucose exposure on chondrocytes were similarly modest (see Figure 4.11) but had more of a grouping effect (Figure 4.12 A and Figure 4.12 B) than that seen in synoviocytes (Figure 4.03 A and Figure 4.03 B). This could suggest that while the effects of high glucose on chondrocytes produced results of less overall significance (see the differential expression Tables 4.03 A and 4.03 B), there may be a more reproducible effect according to dose of glucose exposure. This is supported in the fact that even though the number of significantly differentially expressed genes (according to an FDR threshold of 15%) was lower than that seen in synoviocytes, there are very highly significantly enriched gene ontology terms associated with the cell cycle (see Figure 4.13 B). While this is the

same as that seen in synoviocytes, only four overlapping genes were identified between the two cell types (see Figure 4.01). The proteins of three of these four genes can be seen to be involved in the cell cycle process or very closely associated with this process (Figure 4.05). *SNORA14A* codes for a small nucleolar RNA and as such does not appear on the protein interaction maps of Figure 4.04, Figure 4.05 and Figure 4.13 A. *SNORA14A* codes for a small nucleolar RNA (snoRNA). snoRNAs have recently been investigated in relation to chondrocyte differentiation, and a number of snoRNAs were identified as differentially expressed in serum of old versus young mice and in experimentally induced osteoarthritic mice versus control mice (225).

4.3.2.1 High glucose could increase chondrocyte proliferation

Cell proliferation in chondrocytes was not shown to be significantly affected (using a rigid $p < 0.05$ cut-off) using the same proliferation assay protocol used for synoviocytes (see Figure 4.14), although the relative rate of proliferation of chondrocytes in their native tissue by comparison to synoviocytes could suggest that this protocol, while successful in identifying a significant difference in proliferation in synoviocytes, may not be directly applicable to chondrocytes. 15mM glucose in chondrocytes showed roughly double the number of cells compared to a normal glucose (5.5mM) control, with marginal statistical significance ($p = 0.054$). This, together with the trend in the data showing a unanimously greater mean cell number in the high glucose treated cells, could be sufficient to suggest that high glucose may increase proliferation in chondrocytes.

Chondrocytes have been shown to experience low turnover rate in their native tissue, depending on proximity to the superficial layer. An effect of high glucose on mitosis could suggest a high glucose mediated departure from a chondrogenic phenotype. Contrastingly, any reduction in mitosis could result in a reduced cellularity in the tissue over time, resulting in a reduced capacity for tissue maintenance and repair. In either case, the observed high glucose mediated effect on mitosis could have deleterious effects on the healthy functioning of chondrocytes and the surrounding cartilaginous matrix.

4.4 Potential limitations

The cells used in this study are of primary human origin, to maximise relevance of conclusions the human musculoskeletal system. The use of human-derived samples however did present a number of limitations. While every effort was made to ensure that the sample population was as homogeneous as possible (including age, race and gender considerations), there was inevitably a large effect of natural human variability within the sample population, potentially driven as much by genetic factors as by environmental factors (such as history of high glucose exposure). This has made the identification of effects that remain congruous throughout the sample group difficult and as such a large majority of the changes identified in the data are not significant. Practicality placed limits on the overall sample size, and this may have caused the inevitable between-sample variability to have a large effect on the statistical significance of the data. Whereas, finances and time permitting, a larger sample group may have acted to reduce the effect of this variability on the overall statistical significance of the results.

5. Synoviocyte methylome may be susceptible to transient high glucose exposure

5.1 Introduction

There have been a number of proposed mechanisms for how glucose may play a role in ageing, which include a well-established link between glucose exposure and reactive oxygen species production. Data such as this supports an already well-accepted theory of ageing involving the cumulative effects of oxidative damage. Additional data suggests an increase in protein cross-linking resulting in the ageing of tissue, as a result of glucose exposure. While cross-links have the potential to support the previously discussed theory of reactive oxygen species-mediated ageing of tissues, cross-linked tissue can also provide an alternate source of ageing. Cross-linking has the potential to cause a biomechanical instability in tissues, such as tissue stiffening (40). Cumulative events can lead to significant reduction in mobility, which can have a secondary effect in accelerating age-related degeneration.

While there is evidence to support a number of these established theories on the effects of glucose in ageing, there has been relatively little study into the effects of glucose on DNA methylation. The effects of high glucose treatments on DNA methylation were assessed using the Infinium HumanMethylation450k BeadChip microarray (Illumina), with significantly differentially methylated CpG sites being assessed using targeted pyrosequencing. Subsequent gene expression and functional analysis was carried out to highlight further potential effects of high glucose, which may be occurring downstream of DNA methylation changes.

DNA methylation has been suggested to be indicative of age (226). A number of studies have shown that the genome-wide levels of DNA methylation at dense clusters of CpG loci (CpG islands) are directly proportional to chronological age (226-229). This has led some to hypothesise that DNA methylation levels can be used as a predictor of chronological age. A large number of methylomic datasets, 82 in total, have been compiled and used to train an algorithm to predict actual age using only the methylome of an individual. This has been used to create a publicly accessible tool (226), wherein in whole methylome datasets are input and predictions are made as to the chronological age of each sample. This tool uses

information specifically from Illumina microarrays (n = 7844). Variability according to DNA source is taken into consideration and the tool uses data from around 51 different tissues to also predict the source of the methylation data. The incorporated algorithm identified 353 'clock' CpG sites that together form an 'epigenetic clock' that is a biomarker of age in different cell types, different genders and different ethnicities. Several studies have used this clock to identify accelerated ageing of a number of tissues in diseased states (230-233) such as cartilage in osteoarthritis (234). This tool was used to assess the effects of glucose on the "DNAm-age" of samples, wherein the methylomes of samples treated with high glucose were assessed in comparison to a control, in order to indicate a potential source of accelerated ageing as a result of exposure to high glucose treatments.

5.2 Synoviocyte DNA methylation

Healthy human synoviocytes (n = 3) were treated with high glucose (11mM or 30mM) for either a short period (16 hours) or a long period (14 days) alongside normal glucose (5.5mM) controls. The effects of the high glucose treatments were then assessed in relation to the methylation of cytosine residues on the DNA of the chondrocytes in each treatment group. This was carried out using Illumina Human Methylation 450k arrays. Differentially methylated cytosine residues were characterised according to the promoter regions, and associated genes, they were located within. Functional analysis was carried on these genes, which was used to infer a functional relevance to the differential methylation observed. DNA methylation age was predicted from array data using a DNA methylation age calculator (226). DNA methylation was also assessed through targeted pyrosequencing (Q96 Qiagen Pyrosequencer).

5.2.1 DNA methylation age

As can be seen from Figure 5.01, no significant difference was seen in DNA methylation age as a result of high glucose treatments. Average predicted ages from all samples are shown

against the average chronological ages of the samples (dotted line). As can be seen from Figure 5.01A, the DNA methylation age calculator is an accurate predictor of chronological age for the normal glucose control, with average methylation age being within 5.875 years of average chronological age. By comparison, the high glucose treatments appear to induce inter-individual variability on methylation age and therefore the predicted chronological age, with an increase in the variability of predicted age in the case of the 11mM treated cells. Individual treatment group was not a significant source of variability in the predicted age data ($p = 0.233$). Dosage, however did prove to be a significant predictor of variability ($p = 0.048$), with 11mM treatments being significantly different to the normal glucose control ($p = 0.046$). Time-period was not a significant source of variability. Interestingly, the higher dosage of glucose (30mM) did not significantly affect the methylation age of the samples. The data is shown in Figure 5.01B normalised to the normal glucose control to indicate the extent of the difference between the predicted ages for the high glucose treated samples. As can be seen more clearly in Figure 5.01B, the high glucose treatments appear to increase the methylation ages of the samples across the board, with the 11mM treatments having the most profound effect.

5.2.2 Glucose-mediated differential DNA methylation in Synoviocytes

The effect of high glucose treatment on the DNA methylome of synoviocytes is summarised in Table 5.01, which lists the number of significantly differentially methylated CpG

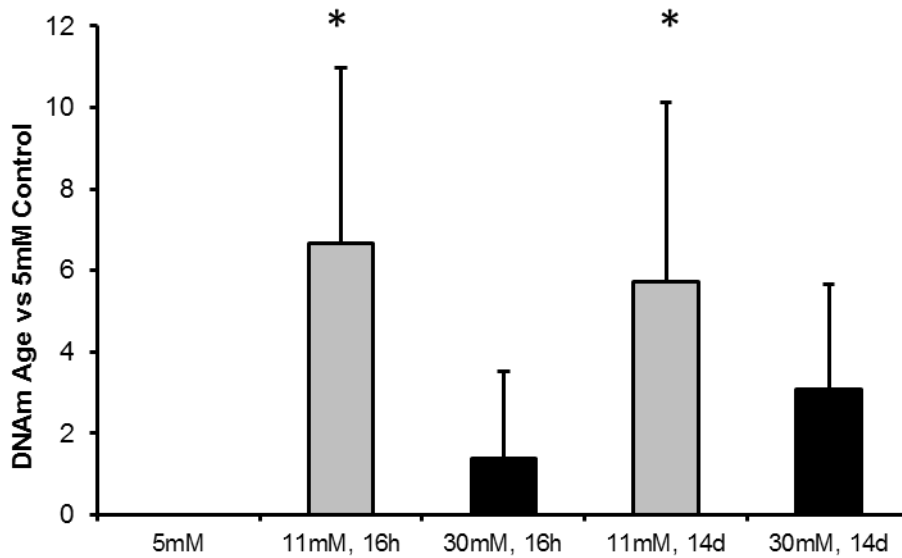
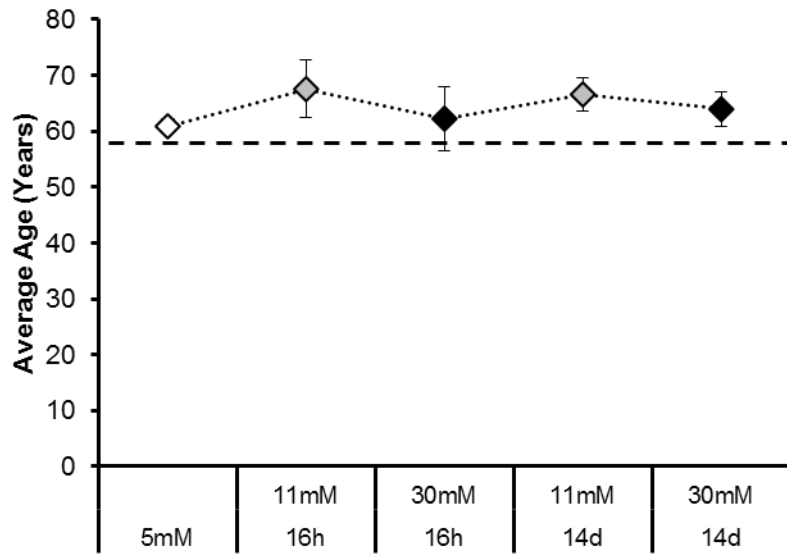


Figure 5.01. Average DNA methylation age of high-glucose treated synoviocytes (A). No significant effect of treatment group on DNA methylation age was observed. The average DNA methylation age for the normal glucose control (5.5mM) was subtracted from the other treatment groups to show the deviation from the control (B). Individual post hoc comparisons showed a significant effect of the 11mM glucose on the DNA methylation age was observed (B, *, $p = 0.046$). Data ($n = 3$) is shown as mean \pm SD.

sites (FDR corrected p value < 0.05, percentage methylation change threshold of 10%) between high glucose and 5mM glucose control. As can be seen, the 11mM 16 hours treatment is the only treatment protocol to significantly affect the DNA methylation of synoviocytes.

Table 5.01. Number of significantly differentially methylated CpG loci and significantly differentially expressed genes in synoviocytes following exposure to high glucose

	11mM 16h	30mM 16h	11mM 14d	30mM 14d
Methylation	394	0	0	0
Gene Expression	0	19	120	153

Figure 5.02 shows a word-cloud of the most frequently associated genes to differentially methylated CpG sites corrected for representation on the microarray. This data suggests that among the most affected genes are those involved in cell adhesion (PCDHGA1-3).

Table 5.02 shows the most significantly affected CpG sites from the comparison of the 11mM 16 hours treated cells with the normal glucose control, shown in the order of decreasing significance (according to their FDR corrected p values). All of the most significantly affected CpG sites are hypomethylated in the 11mM 16 hours treated cells, suggesting that this treatment causes a reduction in methylation at specific sites of the genome. The relation of the affected CpG site to a CpG island is also shown, with some studies suggesting that the presence of changes within a highly dense CpG island are more likely to be seen in the ageing phenotype (229). The direct comparison between the 11mM 16 hours treatment group and the normal glucose control can be seen from Figure 5.03.



Figure 5.02. Most frequently occurring gene annotations for significantly differentially methylated CpG sites following 11mM 16 hours glucose treatment, taken from the methylation array data. The most frequently occurring differentially methylated CpG site annotations were for protocadherin transcripts (PCDHGA1, PCDHGA2, PCDHGA3). The data was assessed for the level of representation of such gene annotations, to ensure that the protocadherin genes seen were not simply more well represented on the arrays.

Table 5.02. Differential DNA methylation data – most significantly affected CpG sites

CpG	Gene	% Change	Relation to CpG Island
cg10767216	<i>MEST</i>	-11%	N Shore
cg09003373	<i>MEST</i>	-10%	Island
cg27589003	<i>MEST</i>	-13%	Island
cg13791131	<i>IGF2</i>	-15%	Island
cg25574024	<i>IGF2</i>	-16%	Island
cg06232807	<i>SALL1</i>	-13%	Island
cg07634179	<i>HOXC9</i>	-19%	N Shore
cg12071536	<i>HOXC9</i>	-12%	Island
cg07557690	<i>TGFBR3</i>	-16%	S Shore
cg22715562	<i>ZNF20</i>	-14%	S Shore
cg10600889	<i>FBXO47</i>	-14%	Open Sea
cg04120272	<i>FBXO47</i>	-12%	Open Sea
cg15678121	<i>ZIM2</i>	-14%	S Shore
cg18418457	<i>TGFBI</i>	-13%	N Shore
cg10070151	<i>PAF1</i>	-15%	Island
cg08831999	<i>PRAME</i>	-13%	Island
cg13858139	<i>ZNF43</i>	-13%	S Shore
cg10683527	<i>NEIL3</i>	-13%	N Shore
cg18269141	<i>PRKCZ</i>	-13%	Island
cg26739865	<i>TFPI2</i>	-10%	Island
cg00556029	<i>MARCKSL1</i>	-16%	Island
cg00965110	<i>PARN</i>	-13%	S Shore

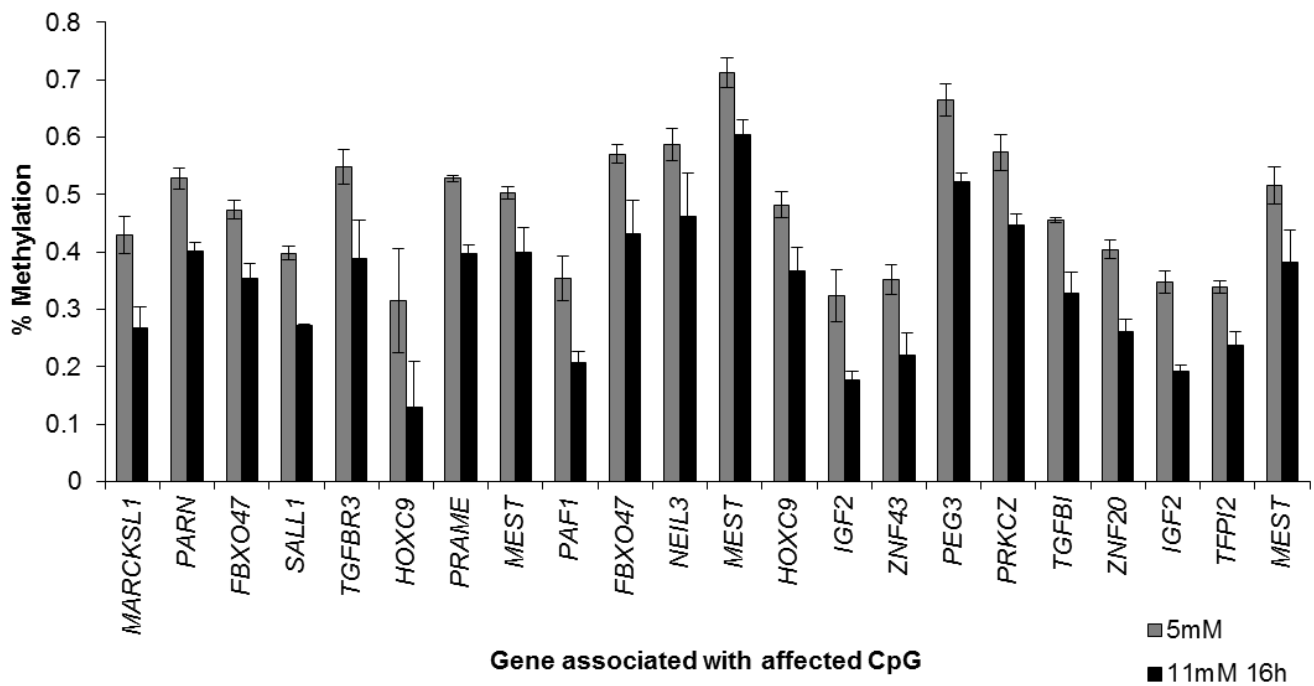


Figure 5.03. % methylation values obtained from the methylation microarray data, for CpG sites significantly differentially methylated following 11mM glucose exposure for 16 hours (Table 5.02). Data (n = 3) is shown as mean \pm SD. All comparisons with the corresponding 5mM control are significant (false discovery rate < 5%).

As can be seen from Table 5.02 and Figure 5.03, there are a number of CpG sites significantly affected by the 11mM 16 hours treatment that share association with a common gene. Of these, mesoderm specific transcript (MEST) is most frequently significantly hypomethylated. Insulin-like growth factor 2 (IGF2), homeobox C9 (HOXC9) and F-box protein 47 (FBXO47) have two associated CpG sites that are significantly hypomethylated.

DNA methylation at a number of the sites identified from the methylation array data shown in Table 5.02 and Figure 5.03 were chosen for targeted pyrosequencing, for which the same DNA was used as was used for the methylation arrays, and qPCR, for which the same RNA was used as was used for the gene expression microarrays. Figure 5.04 to Figure 5.12 show data for genes chosen for targeted pyrosequencing and qPCR. Data from Figure 5.13 and Figure 5.14 show data for genes that were chosen for qPCR only.

5.2.3 Methylation microarray vs targeted pyrosequencing

Significant differential methylation was observed in the methylation array data between the 11mM 16 hours treatment group and the normal glucose control group at all the selected CpG sites shown in Figure 5.04 to Figure 5.12. It can be seen however from Figure 5.04 to Figure 5.12, there was no significant difference in methylation observed by pyrosequencing assessment of the same CpG sites as those identified from the methylation array study. Together, this indicates that the methylation differences detected by the array were not validated when methylation of the same samples/different samples were assessed using a different technique.

5.2.3.1 *Insulin-like growth factor 2 (IGF2)*

cg25574024 is associated with Insulin-like growth factor 2 (IGF2) transcript. Interestingly, as was the case for ZIM2/PEG3, IGF2 is an imprinted gene. Differential methylation was identified by methylation microarray at cg25574024 (Figure 5.04A), but was not observed during a follow-up validation step (Figure 5.04D). Large amounts of between-sample variability were observed in both percentage methylation obtained from pyrosequencing (Figure 5.04D) and in subsequent gene expression assessment (Figure 5.04E).

5.2.3.2 *Zinc Finger Protein 20 (ZNF20)*

Data from Figure 5.05 also shows that no significant differential methylation was identified in the case of cg22715562 after pyrosequencing (Figure 5.05D), unlike that seen in the methylation array data (Figure 5.05A). cg22715562 is associated with the promoter region of

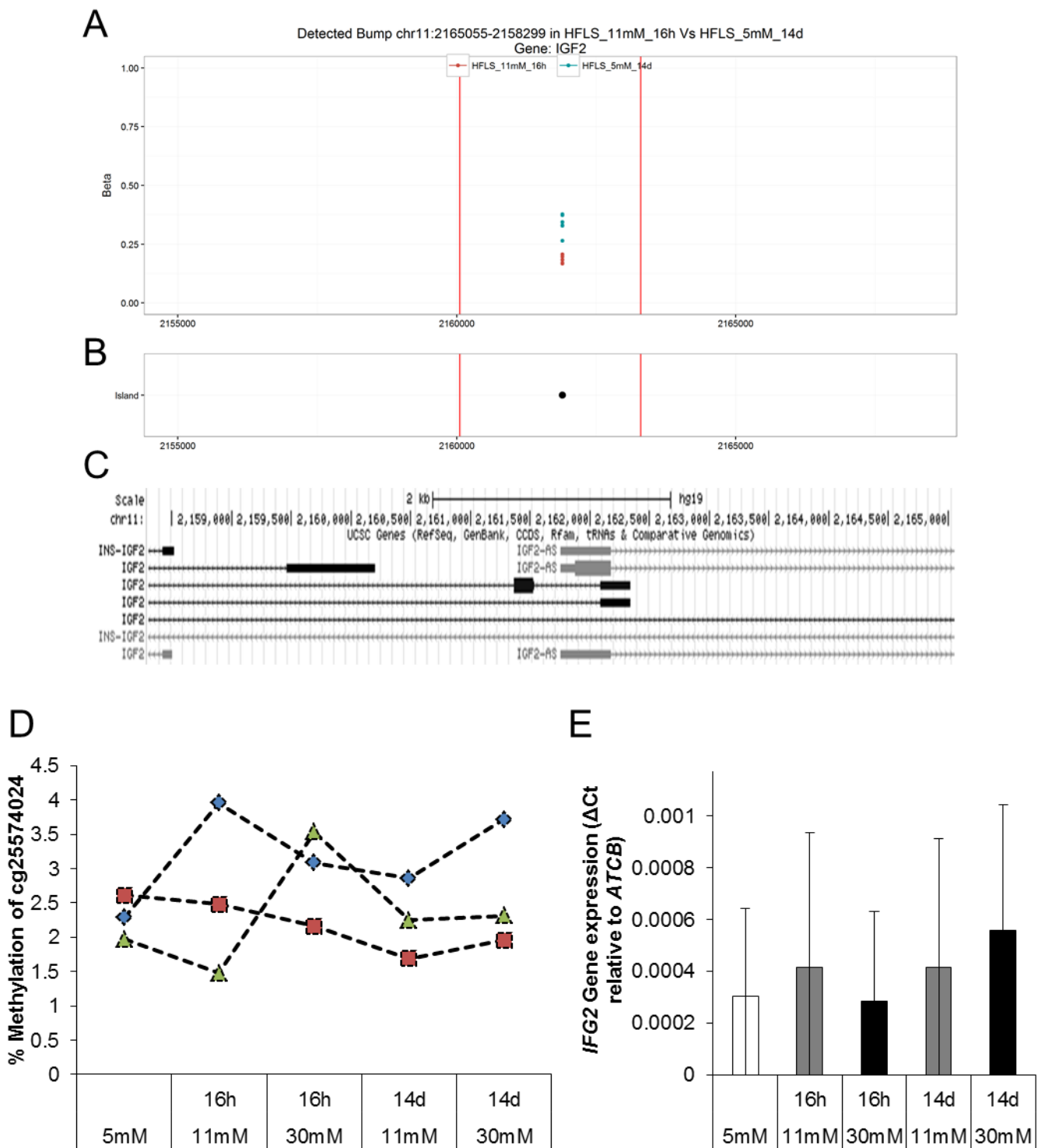


Figure 5.04. % methylation values obtained per sample for cg25574024 (A) significantly differentially methylated following 11mM, 16 hour glucose exposure. Location data shows that this CpG is located within a CpG island (B). Location of *IGF2* transcripts overlapping the CpG site were confirmed using Genome Browser (<http://genome.ucsc.edu>) (C). Pyrosequencing (C) failed to corroborate the array data, and qPCR showed no significant downstream effects on gene expression of associated *IGF2* gene - data (n = 3) is shown as mean \pm SD.

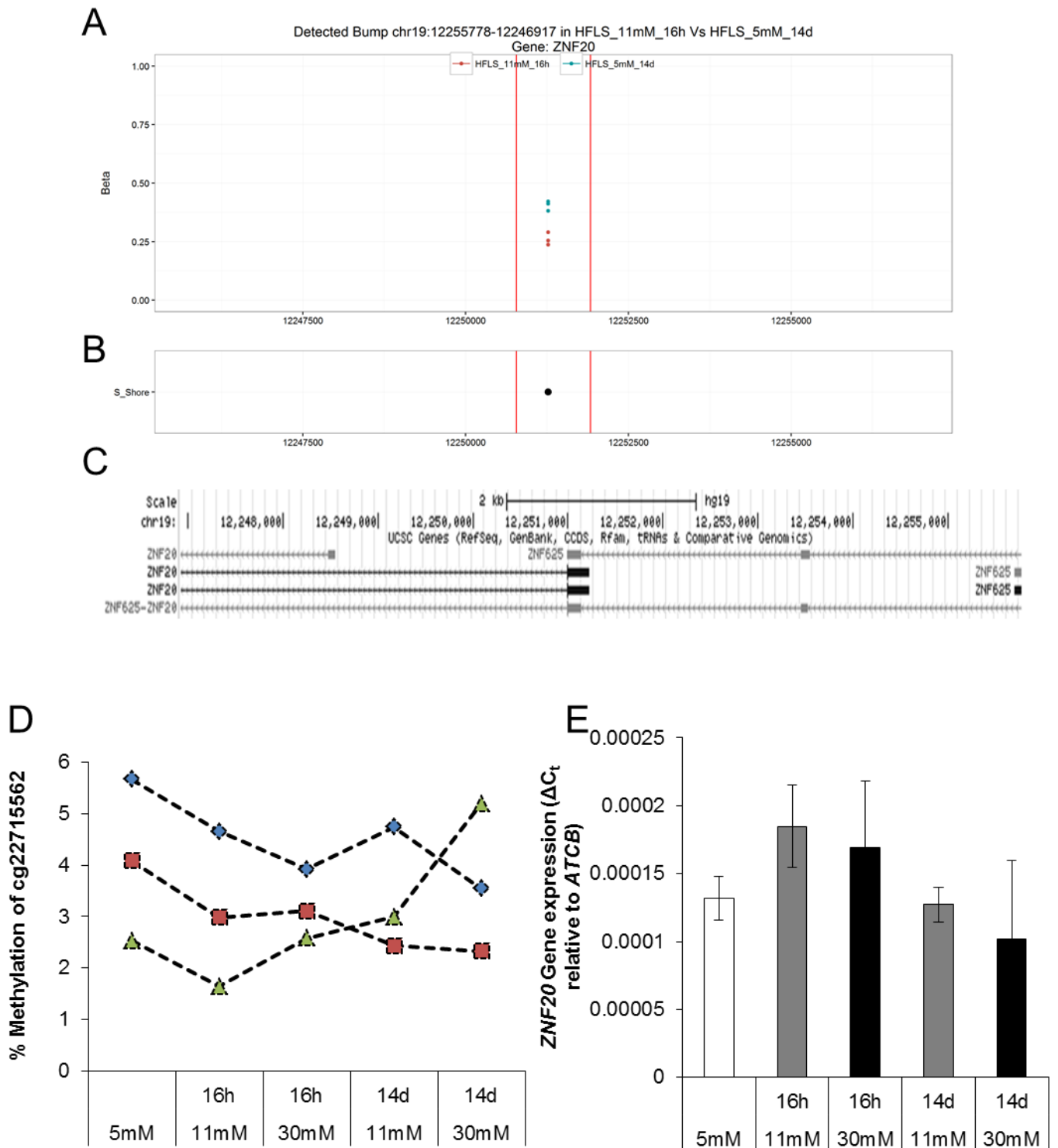


Figure 5.05. % methylation values obtained per sample for cg22715562 (A) significantly differentially methylated following 11mM, 16 hour glucose exposure. Location data shows that this CpG is located within an S-Shore region (B). Location of *ZNF20* transcripts overlapping the CpG site were confirmed using Genome Browser (<http://genome.ucsc.edu>) (C). Pyrosequencing (C) failed to corroborate the array data, and qPCR showed no significant downstream effects on gene expression of associated *ZNF20* gene - data (n = 3) is shown as mean \pm SD.

Zinc Finger Protein 20 (ZNF20) transcript. There was no significant difference in methylation observed after pyrosequencing (Figure 5.05D). High variability in the levels of methylation was observed after the 30mM 14 days treatment. Very low levels of gene expression for ZNF20 were identified in synoviocytes, with no significant differences.

5.2.3.3 F-Box Protein 47 (FBXO47)

cg04120272 is associated with the promoter region of F-Box Protein 47 (FBXO47) transcript. cg04120272 was shown to a site that was significantly differentially methylated as a result of exposure to high glucose (11mM glucose for 16 hours) using methylation microarray (Figure 5.06A). Contrastingly, subsequently obtained pyrosequencing data suggests that DNA methylation at this site is in fact not altered by high glucose exposure, with no significant difference being identified (Figure 5.06D). There was also no identified significant difference in gene expressed observed as can be seen from Figure 5.06E.

5.2.3.4 Zinc Finger Imprinted 2 (ZIM2) and Paternally Expressed Imprinted Gene 2 (PEG2)

Figure 5.07 shows data for CpG site cg1567812, which is associated with a common promoter region of both Zinc Finger Imprinted 2 (ZIM2) and Paternally Expressed Imprinted Gene 2 (PEG2), which are both imprinted genes. The methylation array data (Figure 5.07A) identifies two similarly significantly affected CpG sites within close proximity. In spite of this, however, pyrosequencing identified no significant differences in methylation at the targeted site (Figure 5.07D). Gene expression in ZIM2 was identified to be highly variable across all treatment groups.

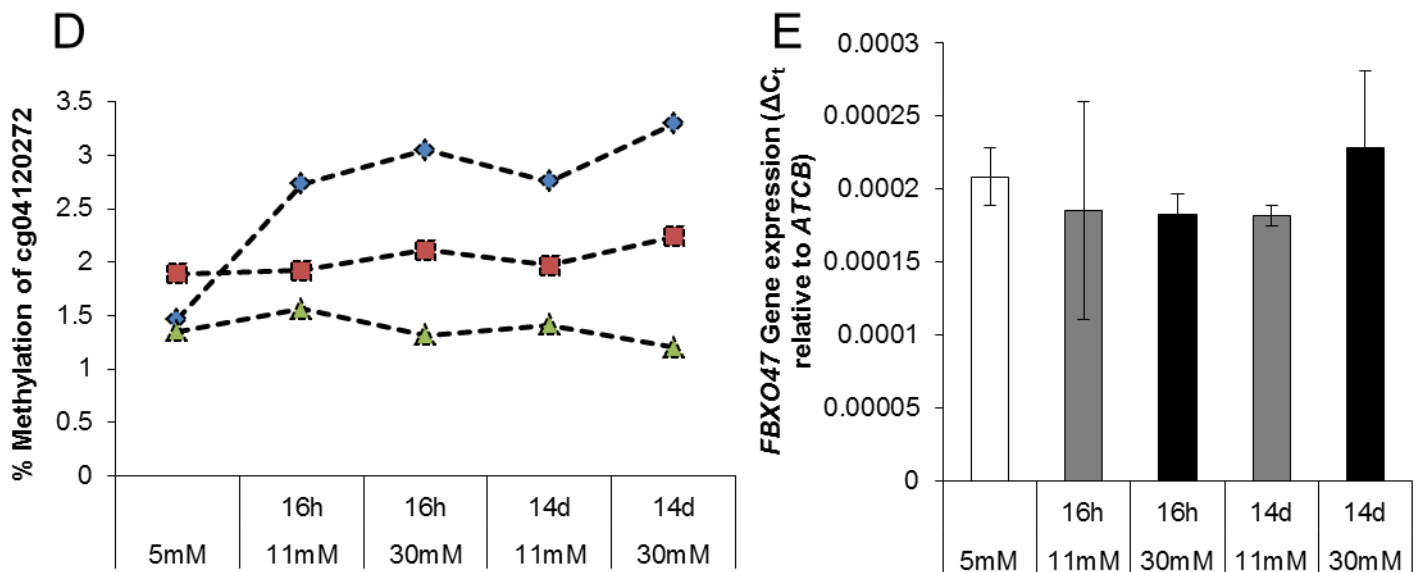
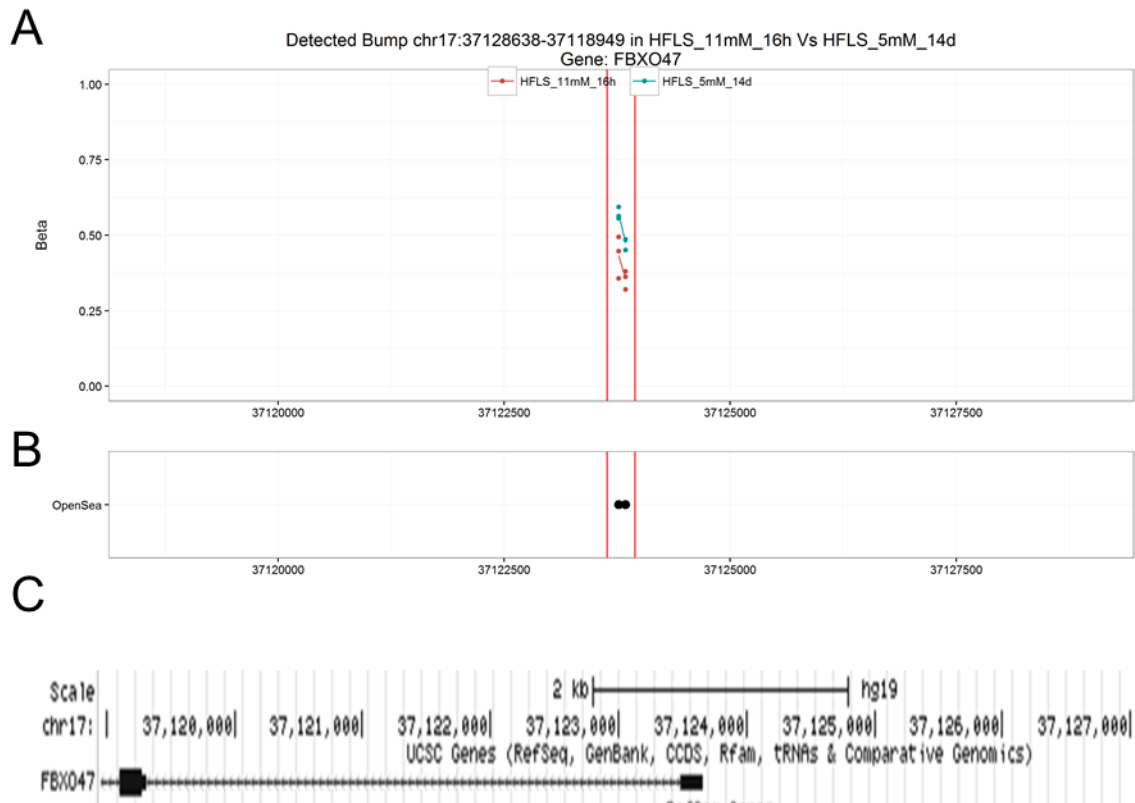


Figure 5.06. % methylation values obtained per sample for cg04120272 (A) significantly differentially methylated following 11mM, 16 hour glucose exposure. Location data shows that this CpG is located within an open sea region (B). Location of *FBXO47* transcripts overlapping the CpG site were confirmed using Genome Browser (<http://genome.ucsc.edu>) (C). Pyrosequencing (C) failed to corroborate the array data, and qPCR showed no significant downstream effects on gene expression of associated *FBXO47* gene - data (n = 3) is shown as mean ± SD.

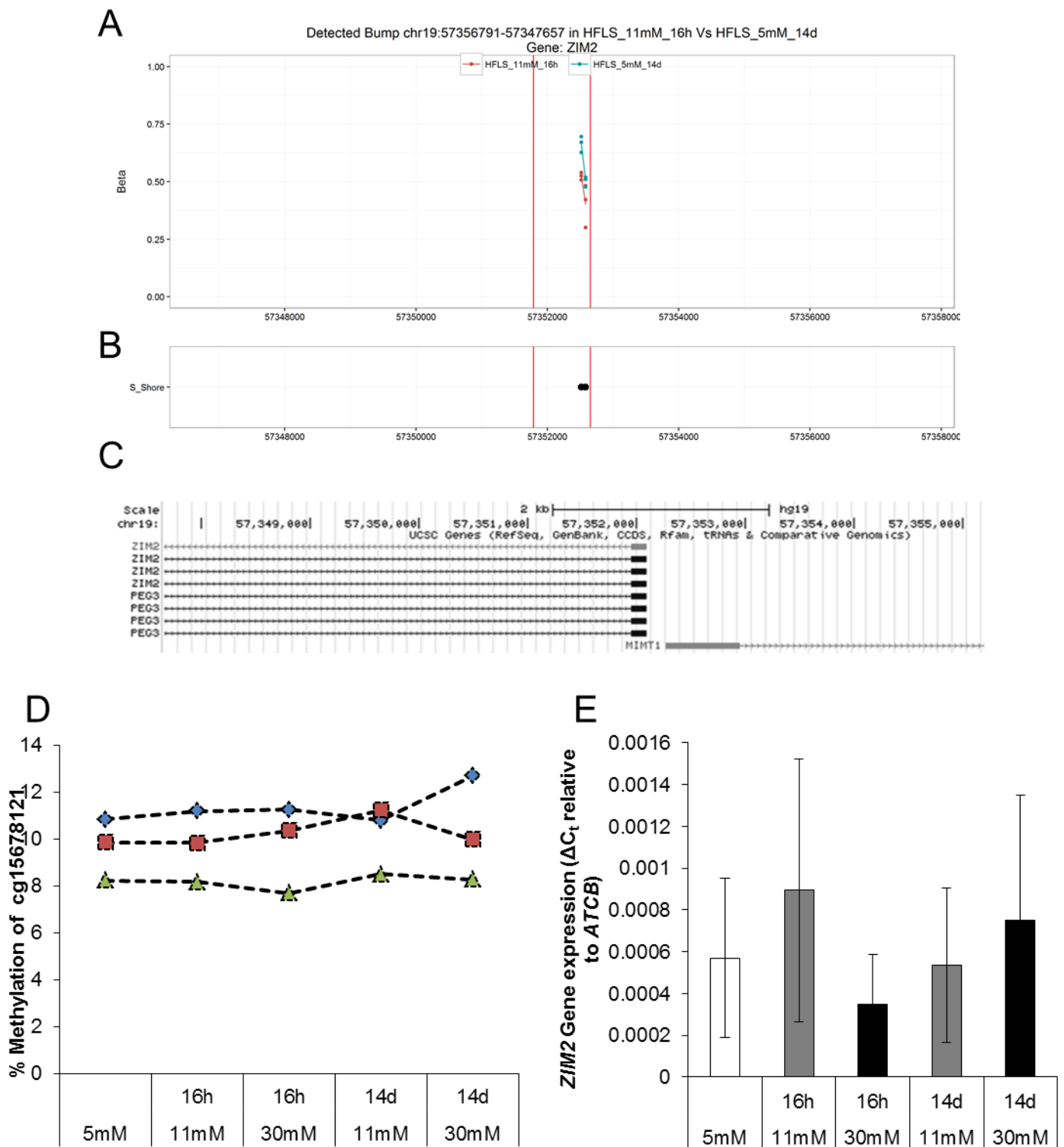


Figure 5.07. % methylation values obtained per sample for cg15678121 (A) significantly differentially methylated following 11mM, 16 hour glucose exposure. Location data shows that this CpG is located within an S-Shore region (B). Location of *ZIM2* transcripts overlapping the CpG site were confirmed using Genome Browser (<http://genome.ucsc.edu>) (C). Pyrosequencing (C) failed to corroborate the array data, and qPCR showed no significant downstream effects on gene expression of associated *ZIM2* gene - data (n = 3) is shown as mean \pm SD.

5.2.3.5 Transforming Growth Factor Beta Induced (TGFB1)

Data from Figure 5.08 shows that, as mentioned earlier, while significant differential methylation was observed in cg18418457, a site associated with the promoter region of a Transforming Growth Factor Beta Induced (TGFB1) transcript, in the methylation array data (Figure 5.08A), there was no significant differential methylation observed in the follow-up pyrosequencing experiment (Figure 5.08D). The individual percentage methylation values for cg18418457 in each of sample can be seen in Figure 5.08A, along with the relationship of this CpG site to the nearest CpG island in Figure 5.08B. Figure 5.08D shows the percentage methylation differences observed in the pyrosequencing data, corrected within-sample to the values obtained for the normal glucose control treated cells in each corresponding sample. High variability was observed in both the percentage methylation information obtained from pyrosequencing (Figure 5.08D), and also in the level of gene expression observed across the different treatment groups (Figure 5.08E).

5.2.3.6 Polymerase associated factor (PAF1)

Figure 5.09A shows that cg10070151 is significantly differentially methylated in synoviocytes in response to 11mM 16 hours glucose exposure. This data is not corroborated with follow-up pyrosequencing assessment however (Figure 5.09D). Both of the 11mM treatments induced a great deal of variability in the level of DNA methylation as can be seen from Figure 5.09D. Gene expression of PAF1 was shown not to be affected by high glucose exposure (Figure 5.09E).

5.2.3.7 Preferentially Expressed Antigen In Melanoma (PRAME)

DNA methylation data for cg08831999, a CpG site associated with the promoter region of Preferentially Expressed Antigen In Melanoma (PRAME) transcript is shown in Figure 5.10A

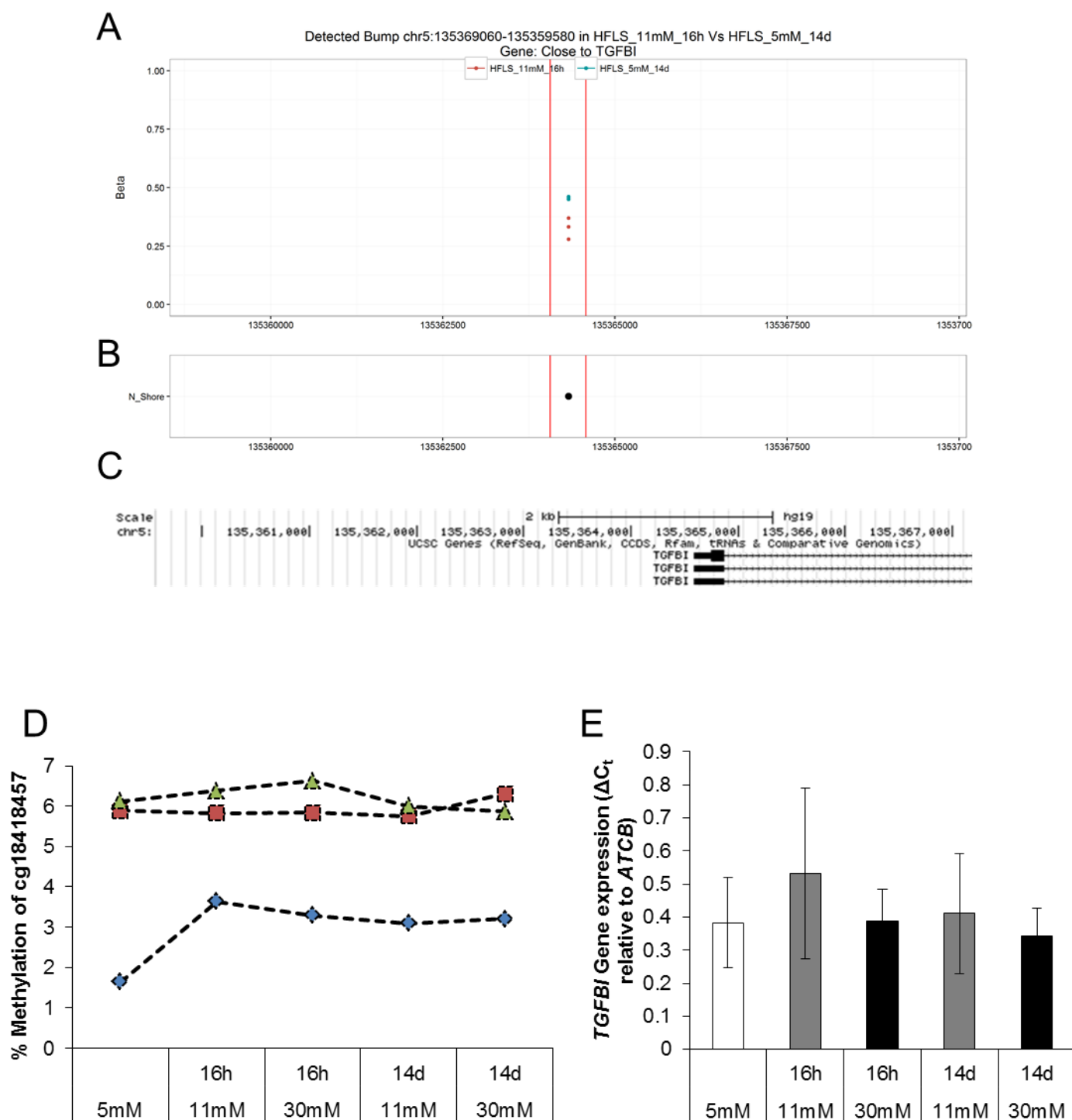


Figure 5.08. % methylation values obtained per sample for cg18418457 (A) significantly differentially methylated following 11mM, 16 hour glucose exposure. Location data shows that this CpG is located within an N-Shore region (B). Location of *TGFBI* transcripts overlapping the CpG site were confirmed using Genome Browser (<http://genome.ucsc.edu>) (C). Pyrosequencing (C) failed to corroborate the array data, and qPCR showed no significant downstream effects on gene expression of associated *TGFBI* gene - data (n = 3) is shown as mean \pm SD.

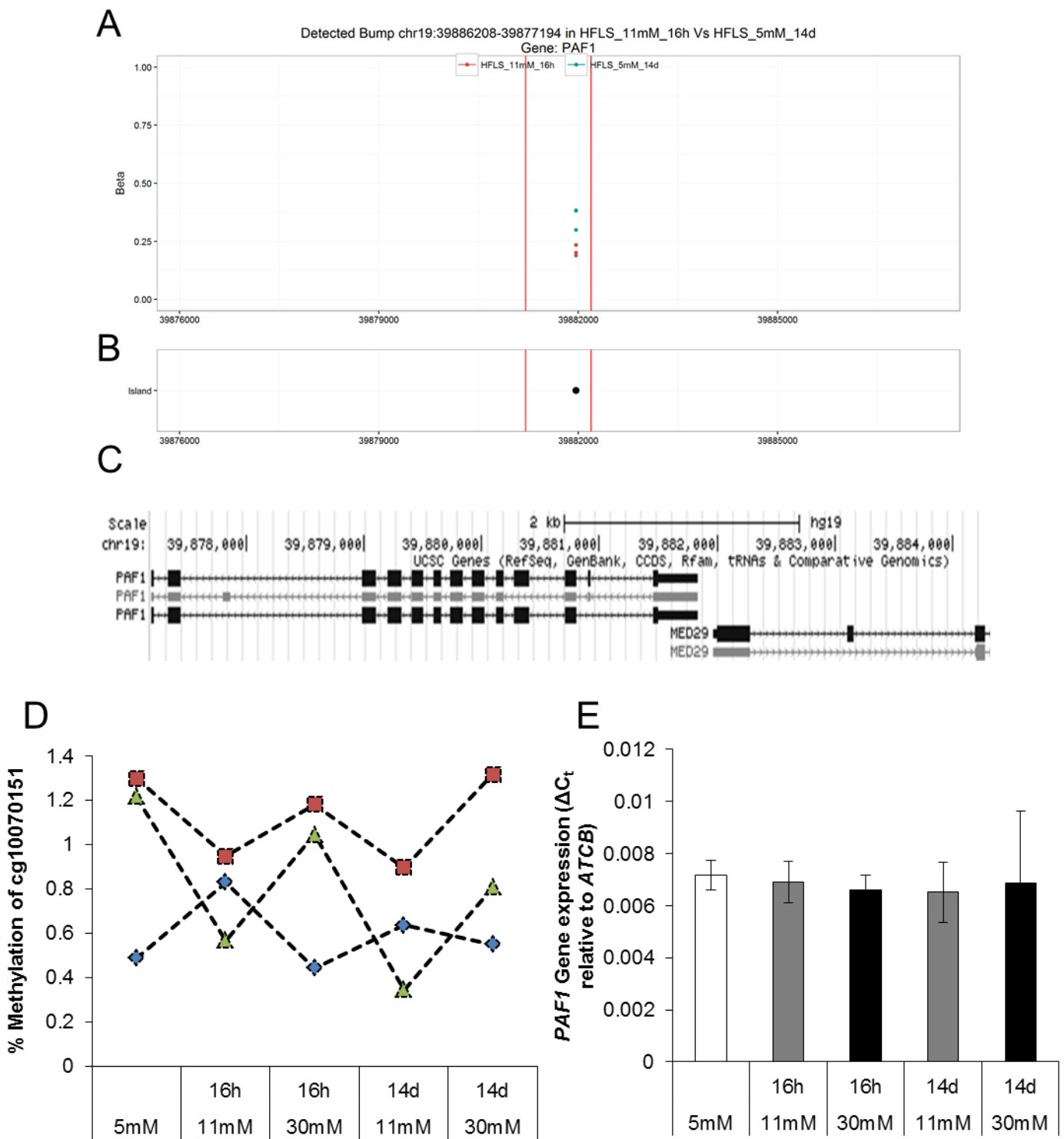


Figure 5.09. % methylation values obtained per sample for cg10070151 (A) significantly differentially methylated following 11mM, 16 hour glucose exposure. Location data shows that this CpG is located within a CpG island (B). Location of *PAF1* transcripts overlapping the CpG site were confirmed using Genome Browser (<http://genome.ucsc.edu>) (C). Pyrosequencing (C) failed to corroborate the array data, and qPCR showed no significant downstream effects on gene expression of associated *PAF1* gene - data (n = 3) is shown as mean \pm SD.

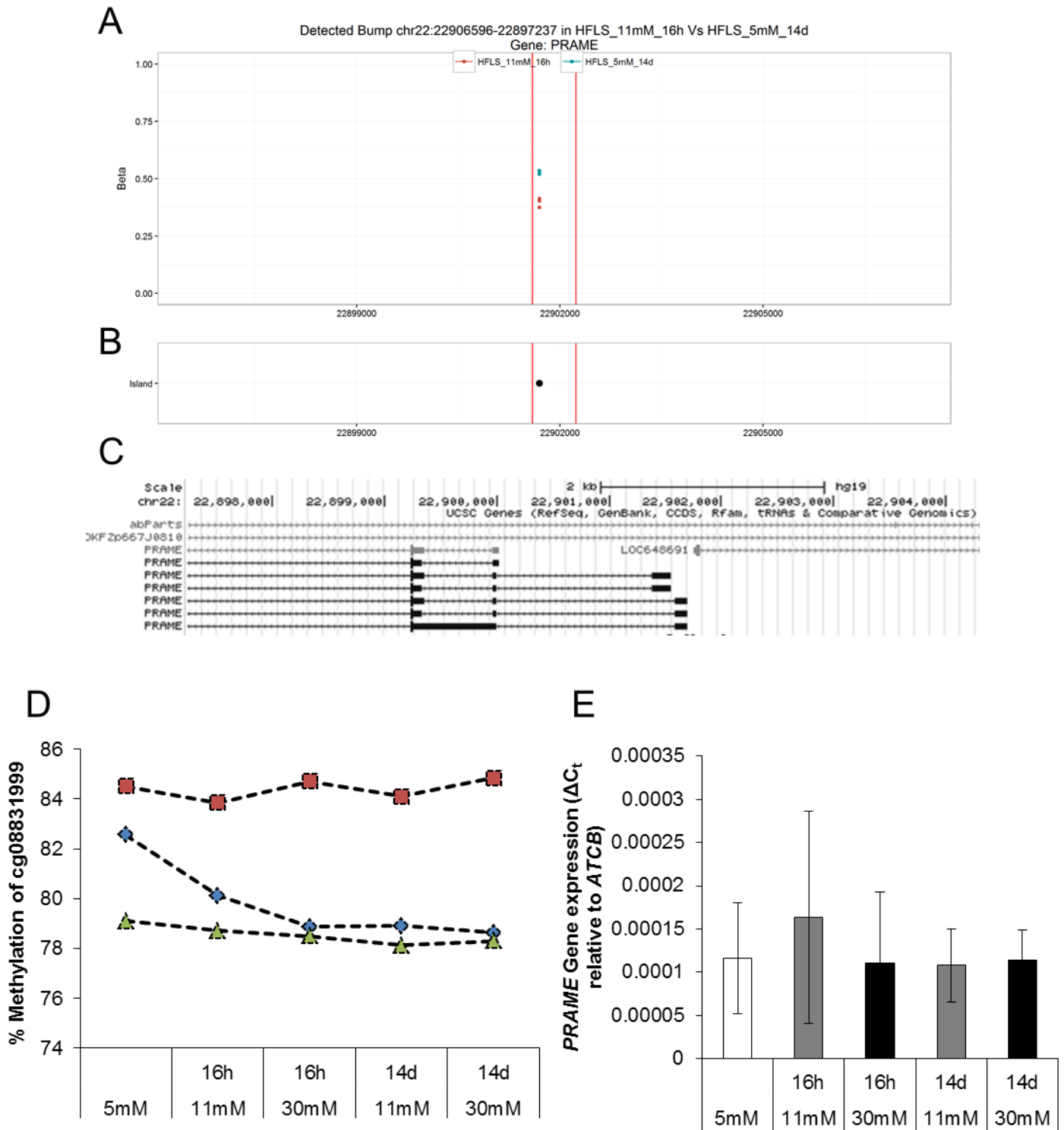


Figure 5.10. % methylation values obtained per sample for cg08831999 (A) significantly differentially methylated following 11mM, 16 hour glucose exposure. Location data shows that this CpG is located within a CpG island (B). Location of *PRAME* transcripts overlapping the CpG site were confirmed using Genome Browser (<http://genome.ucsc.edu>) (C). Pyrosequencing (C) failed to corroborate the array data, and qPCR showed no significant downstream effects on gene expression of associated *PRAME* gene - data (n = 3) is shown as mean ± SD.

(methylation microarray) and Figure 5.10D (pyrosequencing). Once again there were no significant differences identified in the methylation status of this CpG site in pyrosequencing experiments. Downstream effects on gene expression are shown to be minimal (Figure 5.10E), with there being a large amount of variability observed in the gene expression of this gene.

5.2.3.8 Myristoylated alanine-rich C-kinase substrate (MARCKS)-like 1 (MARCKSL1)

cg00556029 is associated with the promoter region of Myristoylated alanine-rich C-kinase substrate (MARCKS)-like 1 (MARCKSL1) transcript. As was the case with all CpG sites assessed through pyrosequencing, while initial microarray data identified the cg00556029 site as significantly differentially methylated (Figure 5.11A), subsequent pyrosequencing assessment was unable to identify any significant differences (Figure 5.11D). Gene expression of MARCKSL1 was shown to be significantly affected by exposure to glucose, with the treatment groups proving to be a significant source of variability in the data distributions ($p = 0.05$). It would appear from Figure 5.11E that short term high glucose (11mM and 30mM) exposure may have the effect of increasing MARCKSL1 gene expression. Only 16 hour exposure to 11mM glucose, however, caused a significant change in gene expression following post-hoc pairwise comparisons ($p < 0.05$).

5.2.3.9 Poly(A)-Specific Ribonuclease (PARN)

cg00965110 is a CpG site associated with Poly(A)-Specific Ribonuclease (PARN) transcript and is shown in Figure 5.12A to be differentially methylated. Data from targeted pyrosequencing (Figure 5.12D) does not appear to corroborate this however, with there being no identified differences in gene expression (Figure 5.12E).

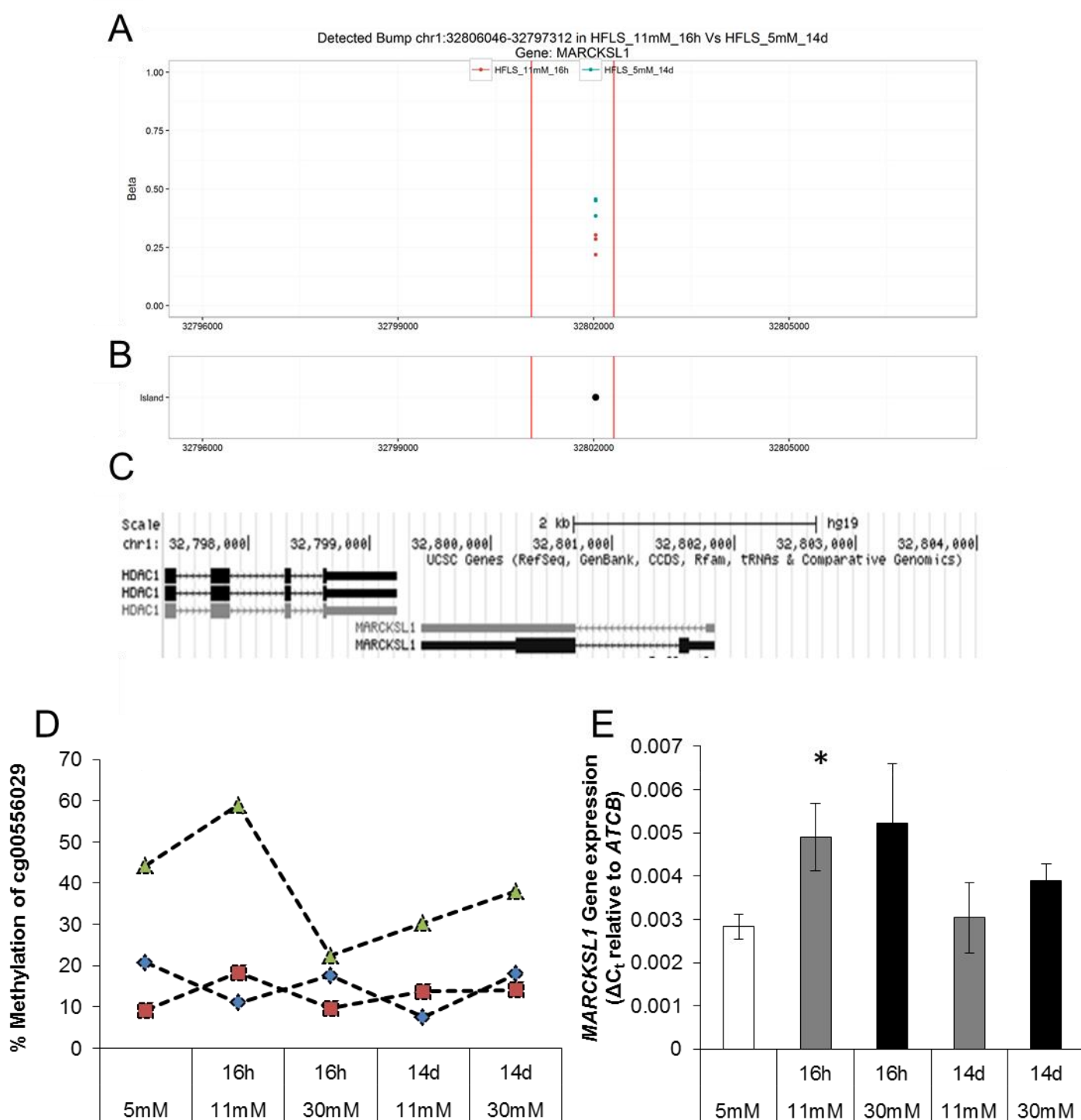


Figure 5.11. % methylation values obtained per sample for cg00556029 (A) significantly differentially methylated following 11mM, 16 hour glucose exposure. Location data shows that this CpG is located within a CpG island (B). Location of *MARCKSL1* transcripts overlapping the CpG site were confirmed using Genome Browser (<http://genome.ucsc.edu>) (C). Pyrosequencing (C) failed to corroborate the array data, but qPCR showed a significant effect of treatment group on variability in downstream gene expression of associated *MARCKSL1* gene ($p = 0.05$) - data ($n = 3$) is shown as mean \pm SD.

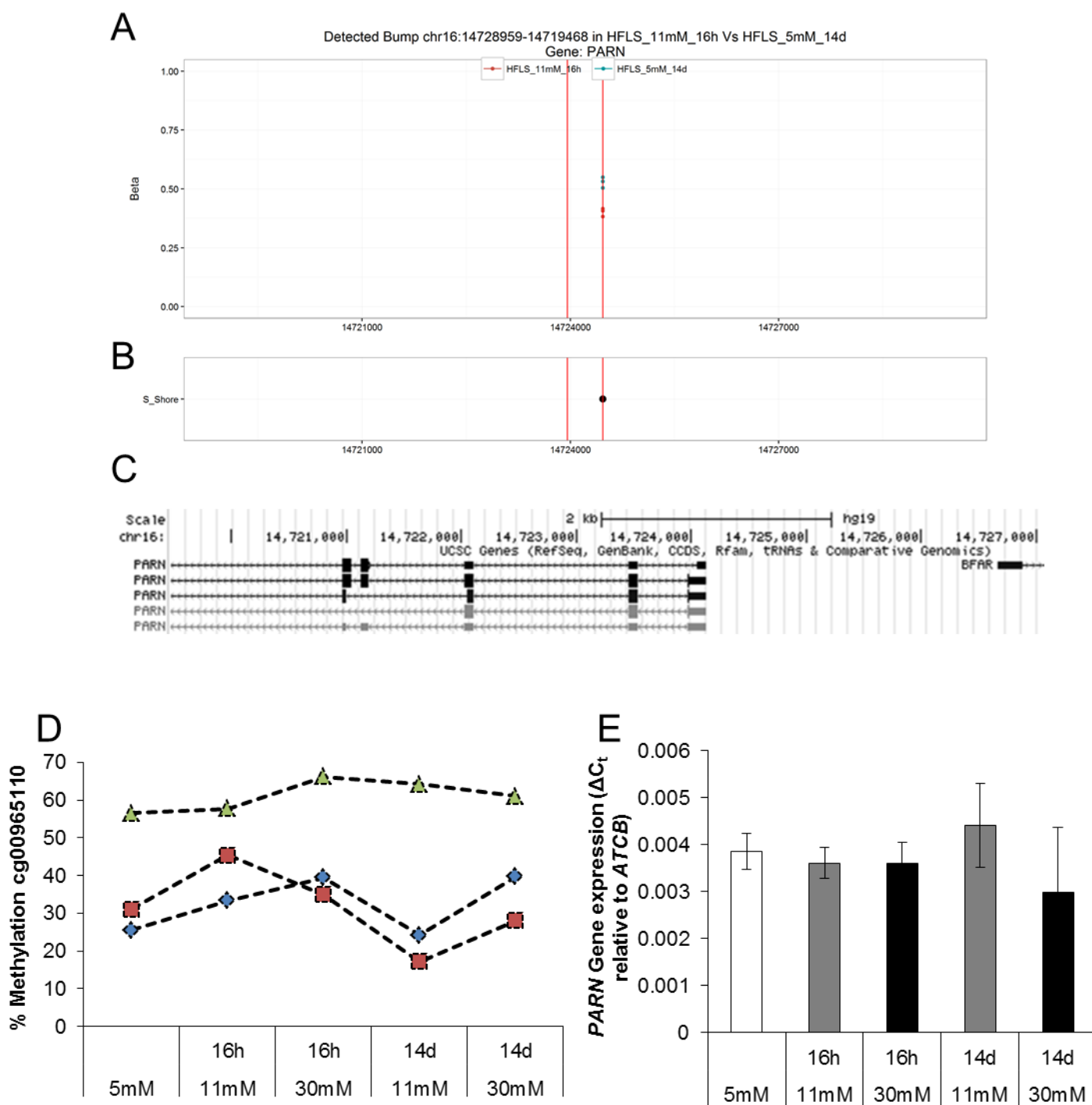


Figure 5.12. % methylation values obtained per sample for cg00965110 (A) significantly differentially methylated following 11mM, 16 hour glucose exposure. Location data shows that this CpG is located within an S-Shore region (B). Location of *PARN* transcripts overlapping the CpG site were confirmed using Genome Browser (<http://genome.ucsc.edu>) (C). Pyrosequencing (C) failed to corroborate the array data, and qPCR showed no significant downstream effects on gene expression of associated *PARN* gene - data (n = 3) is shown as mean \pm SD.

5.2.3.10 Additional downstream effects of potential hypomethylation

A number of other gene expression measurements were made for genes relating to identified differentially methylated CpGs from the methylation array data, for which a pyrosequencing assessment was not performed. As can be seen from Figure 5.13A-C, there were no significant differences in gene expression identified in genes for Zinc Finger Protein 43 (ZNF43), Transforming Growth Factor β Receptor 3 (TGFB3) or Tissue Factor Pathway Inhibitor 2 (TFPI2). For Spalt Like Transcription Factor 1 (SALL1), treatment group was identified as a significant source of the variation ($p = 0.02$) as can be seen in Figure 5.13d, with there being a significant post hoc pairwise increase in expression observed after exposure to 30mM for 14 days. Interestingly, the trend in the data would suggest that there is a near-significant time dependent increase ($p = 0.07$) in expression of SALL1 after treatment with 30mM.

In Figure 5.14A it can be seen that gene expression for Protein Kinase C Zeta (PRKCZ) is not significantly affected after treatment with high glucose. It would appear from Figure 5.14A that the long term treatments reduce variability observed in the sample group, potentially indicating a non-significant glucose-dependent inhibition of expression after long term treatment. There would appear from Figure 5.14B that the gene expression of Nei Like DNA Glycosylase 3 (NEIL3) is not significantly affected by glucose exposure. Treatment group is a near significant source of variability ($p = 0.06$).

Gene expression of Mesoderm Specific Transcript (MEST) was significantly decreased as a result of long term (14 days) treatment with high glucose (30mM) as can be seen Figure 5.14C. MEST is an imprinted gene like ZIM2/PEG3 and IGF2, with hypomethylation potentially being linked to a reactivation of these genes. The significant reduction in MEST gene expression observed after the 30mM 14 days treatment could suggest an interesting response to the hypomethylation of the promoter region of this gene.

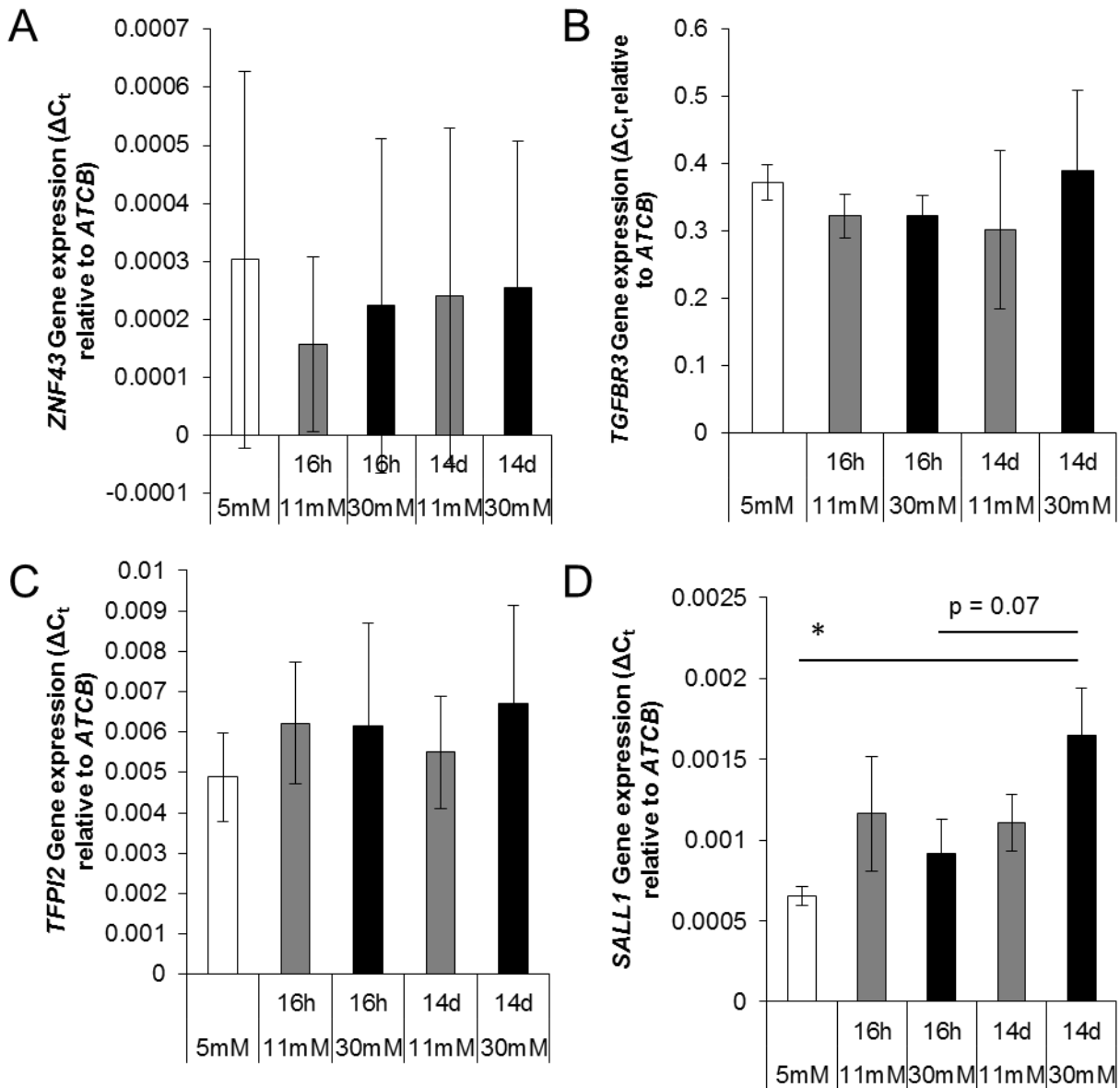


Figure 5.13. Additional qPCR assessment of potential downstream effects on gene expression following identification of differential methylation. No significant downstream gene expression differences were observed in *ZNF43* (A), *TGFBR3* (B) and *TFPI2* (C). A significant effect of long-term (14 days) 30mM glucose exposure was seen in *SALL1* gene expression (D), with an almost significant time-dependent effect also observed between the 30mM treatments ($p = 0.07$). Data ($n = 3$) is shown as mean \pm SD.

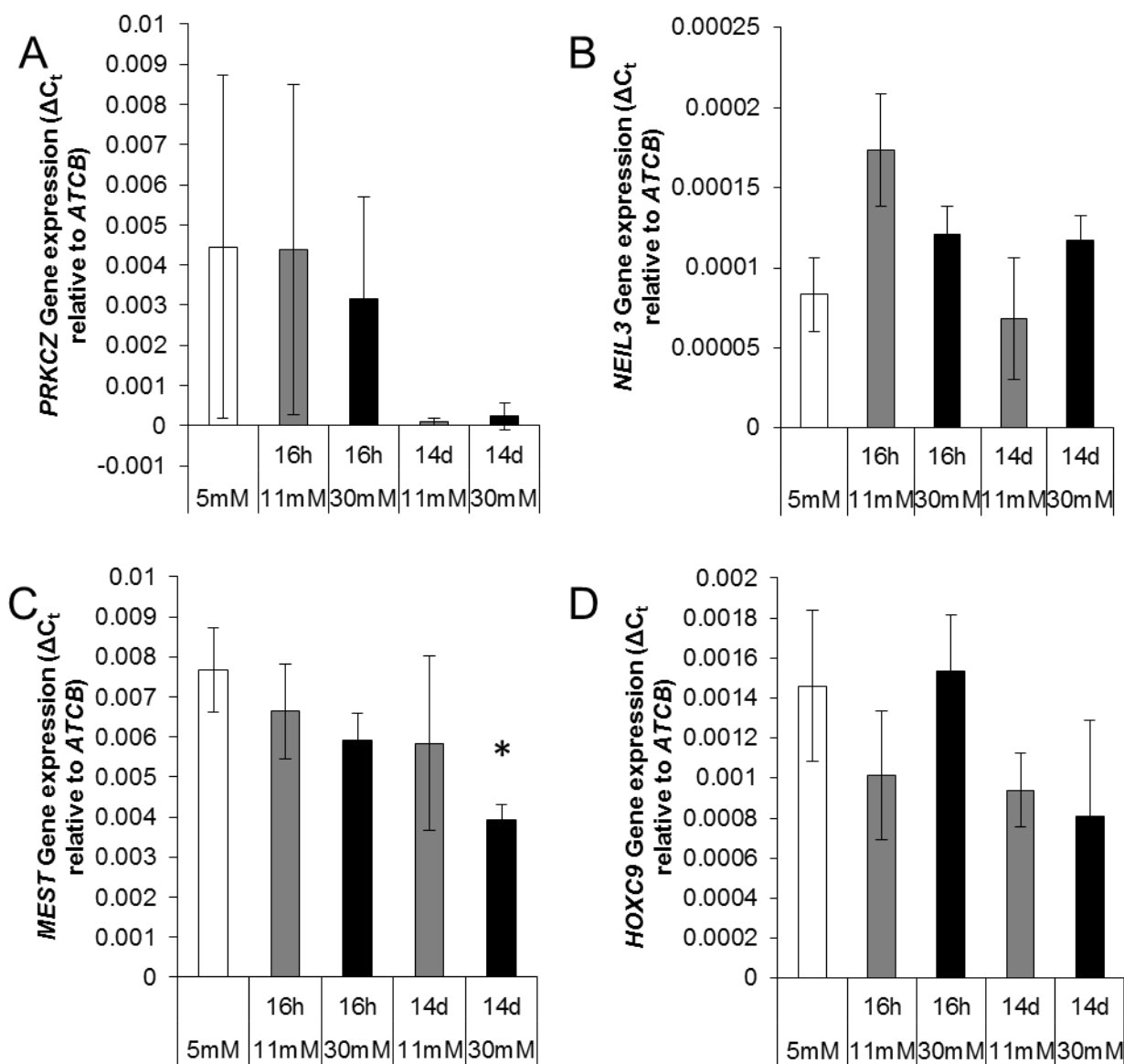


Figure 5.14. Additional qPCR assessment of potential downstream effects on gene expression following identification of differential methylation. No significant downstream gene expression differences were observed in PRKCZ (A) and HOXC9 (D). A near-significant effect of treatment group on variability was seen in *NEIL3* expression (B, $p = 0.06$). A significant effect of long-term (14 days) 30mM glucose exposure was seen in *MEST* gene expression (C). Data ($n = 3$) is shown as mean \pm SD.

Homeobox C9 (HOXC9) does not appear to be significantly affected as a result of high glucose treatment as can be seen in Figure 5.14D.

5.3 Gene expression study

A gene expression analysis of the effects of high glucose treatments on synoviocytes was carried out using gene expression microarrays (Illumina HT12V4) and follow-up qPCR (n = 3).

5.3.1 Glucose-mediated differential gene expression

Gene expression analysis of synoviocytes revealed that, as was found previously and detailed in Chapter 4, high glucose produces relatively modest effects on gene expression. Table 5.01 shows the number of differentially expressed genes in each treatment group relative to the 5.5mM normal glucose control. False discovery rate correction through Benjamini-Hochberg proved to have a large detrimental effect on corrected p values, with only a very small number of probes surviving a false-discovery rate correction with a corrected p value (q value) < 0.05. This was most likely affected by the identification of an outlier in the sample group during the preprocessing stage of the microarray data, which was removed prior to further processing and differential expression analysis. A more lenient q-value cut-off of 0.25 was used to identify what were perhaps more subtle changes in gene expression, but which may have been better representative of more wide reaching systems-level changes in gene expression in order to make best use of the huge coverage of the array technology. As can be seen from Table 5.01, the long term (14 days) high glucose (30mM) treatment yielded the greatest number of genes (156) within the proposed threshold significance range. $-\text{Log}_2$ of all of the corrected differentially expressed q-values in the pairwise comparison between the 30mM 14 days treatment and the 5.5mM control can be seen in Figure 5.15A. As can be seen from this graph the changes identified in this, the

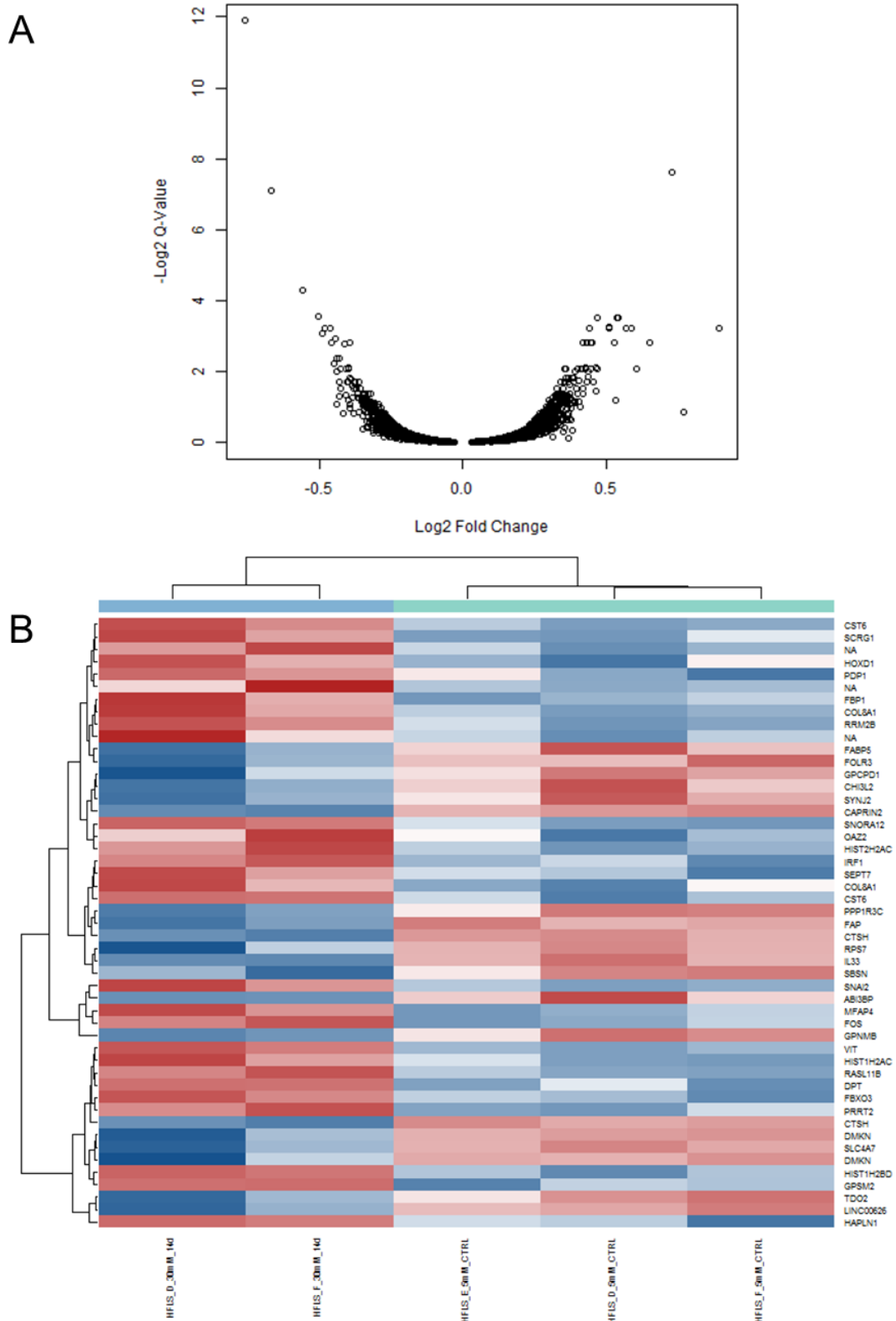


Figure 5.15. Following gene expression microarray analysis, $-\log_2$ Q-values (FDR corrected p values) for all differentially expressed genes were plotted against \log_2 fold change of expression (A) to show significance of expression change against extent of expression change. The most significant differentially expressed genes were then plotted as a heatmap (B) showing that the samples group according to treatment.

highest dosage treatment, were still relatively modest, with few changes exceeding a \log_2 fold change of ± 0.5 (actual gene expression change of around $\pm 50\%$).

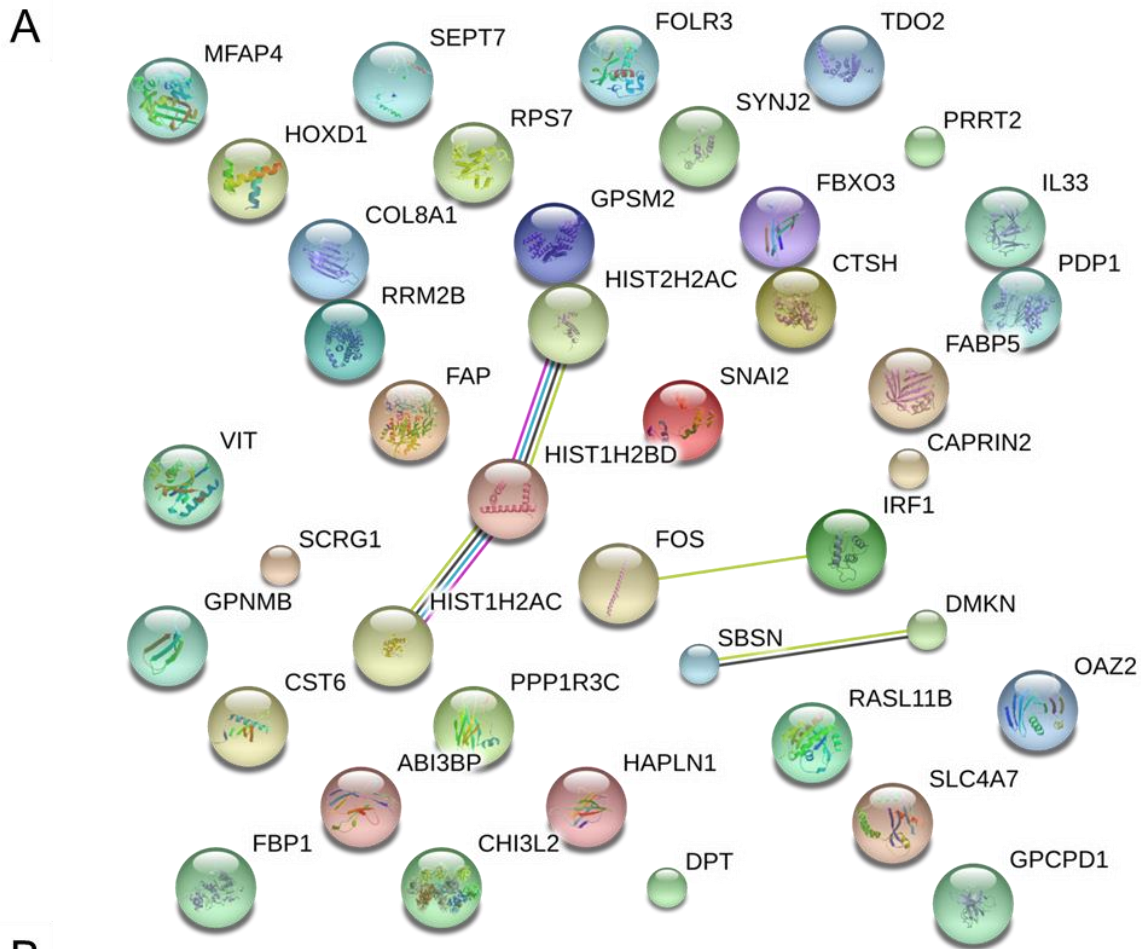
A heatmap of top 50 most differentially expressed gene expression probes is shown in Figure 5.15B. There is a mixture of increased and decreased gene expression as a response to long term high glucose treatment. The differences driven by the dosage of glucose used is sufficient to group the gene expression data according to treatment.

5.3.2 Potential functional relevance of gene expression changes

The top 50 most significantly affected probes were assessed for functional relevance (STRING) (218) and the expected protein interactions can be seen in Figure 5.16A. The number of interactions expected between the proteins of each of these genes was fairly minimal. The best-supported interactions identified were those associated with histone proteins (HIST1H2AC, HIST1H2BD, HIST2H2AC).

Interestingly, as can be seen from Figure 5.16B, the most significantly affected biological functions identified during gene ontology analysis (DAVID) (235, 236) were associated with cell adhesion (GO0010811; GO0007155), extracellular matrix organisation (GO0030198), and cell cycle (GO0008285).

Of the genes most significantly differentially expressed, genes for Cathepsin H (CTSH) and Fos Proto-Oncogene, AP-1 Transcription Factor Subunit (FOS) were chosen for further analysis through targeted qPCR. Interestingly, each of these genes was also identified as significantly differentially expressed in chondrocytes. As can be seen in Figure 5.17A, gene expression for CTSH was shown to significantly reduced in the long-term treatments (11mM and 30mM for 14 days), when compared to the corresponding short term treatments.



B

Term	Count	P.Value	Genes
GO:0010811~positive regulation of cell-substrate adhesion	3	0.00333	COL8A1, VIT, ABI3BP
GO:0007155~cell adhesion	6	0.003562	HAPLN1, FAP, GPNMB, MFAP4, COL8A1, DPT
GO:0030198~extracellular matrix organization	4	0.009786	HAPLN1, COL8A1, VIT, ABI3BP
GO:0008285~negative regulation of cell proliferation	4	0.059841	HIST1H2AC, IRF1, GPNMB, DPT
GO:0030335~positive regulation of cell migration	3	0.064924	GPNMB, SNAI2, CTSH
GO:0006342~chromatin silencing	2	0.097046	HIST1H2AC, HIST2H2AC

Figure 5.16. Expected protein interactions were identified for the list of significant differentially expressed genes using STRING (A). As was the case with the 14 day 30mM glucose treatment, it would appear that there is a highly enriched interaction network associated with ribosomal proteins (A). There was an interesting grouped interaction between histone proteins, and PRELP-LUM (A). Significantly enriched gene ontology terms associated with the gene set were also investigated (B, C and D).

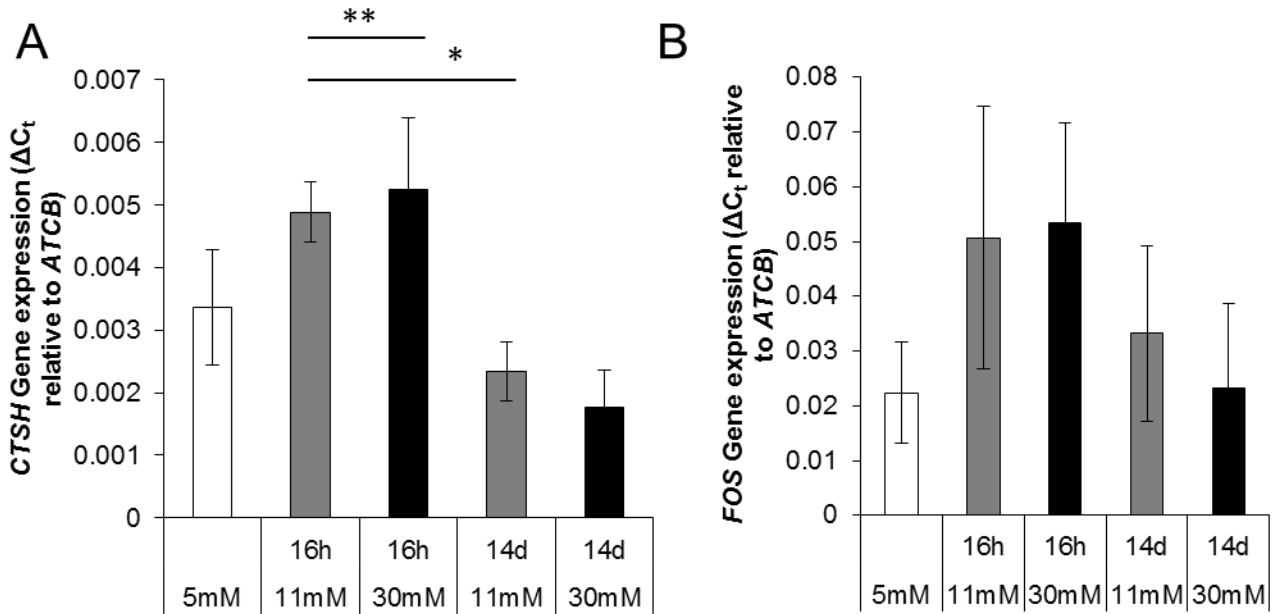


Figure 5.17. A crossover of effects of high glucose on gene expression between different cell types was assessed using targeted qPCR experiments. Both *CTSH* and *FOS* were identified as significantly differentially expressed in the synoviocyte gene expression microarray data. *CTSH* (A) showed significant time dependent decrease in expression following 11mM glucose (**, $p < 0.01$) and a significant dose-dependent increase in expression over the 16 hour treatments (*, $p < 0.05$). There was no significant effect of high glucose on *FOS* (B) expression by contrast. Data ($n = 3$) is shown as mean \pm SD.

Treatment group was shown as a significant source of variability in the data distributions ($p = 0.004$) and as can be seen from Figure 5.17A, it would appear that short term glucose treatments (11mM and 30mM for 16h) may cause a dose-dependent increase in expression of *CTSH*, followed by a dose-dependent reduction after 14 days. Figure 5.17B shows that there was no significant difference in gene expression identified for *FOS*, wherein treatment group was not identified as a significant source of variation in gene expression. As can be seen from Figure 5.17B, there was a large amount of inter-individual variability observed in *FOS* gene expression data.

5.4 Is synoviocyte cell adhesion affected by exposure to high glucose?

An indication from methylation array data (Figure 5.02) and gene expression array data (Figure 5.16B) that cell adhesion may be affected was unofficially corroborated by anecdotal observations that cells cultured in high glucose were more sensitive to trypsin. Observations were made during the study that indicated that adhesion of long-term high glucose treated cells to cell culture plastic was more easily disrupted than for cells treated with normal glucose or short term high glucose treated cells.

However, it would appear from data shown in Figure 5.18A and Figure 5.18B that cell adhesion is in fact not affected by high glucose treatment. No significant difference in the number of cells remaining adhered to cell culture plastic was observed after cells were first treated with high glucose before being trypsinised and allowed to re-adhere for 24 hours.

5.5 Discussion

Synoviocytes exist in a highly vascularised layer of synovium which acts to filter blood constituents to provide a nutritious synovial fluid and bacteriostatic joint environment for optimum joint functioning. The exposure of synoviocytes to glucose is therefore dependent upon the fluctuations of glucose concentration experienced within the blood. While in healthy adults, blood glucose concentration rarely exceeds 7mM, it has been shown that extremes of blood glucose concentration can reach as high as 11mM in healthy adults. As a potential primer for further study in this area, the choice of 11mM was made to assess the potential effects observed at the extremes of the healthy blood glucose concentration range. As such the 11mM treatment is considered to be the more closely physiologically relevant, to high glucose levels experienced in the blood of normal healthy adults, of the two high glucose treatments used.

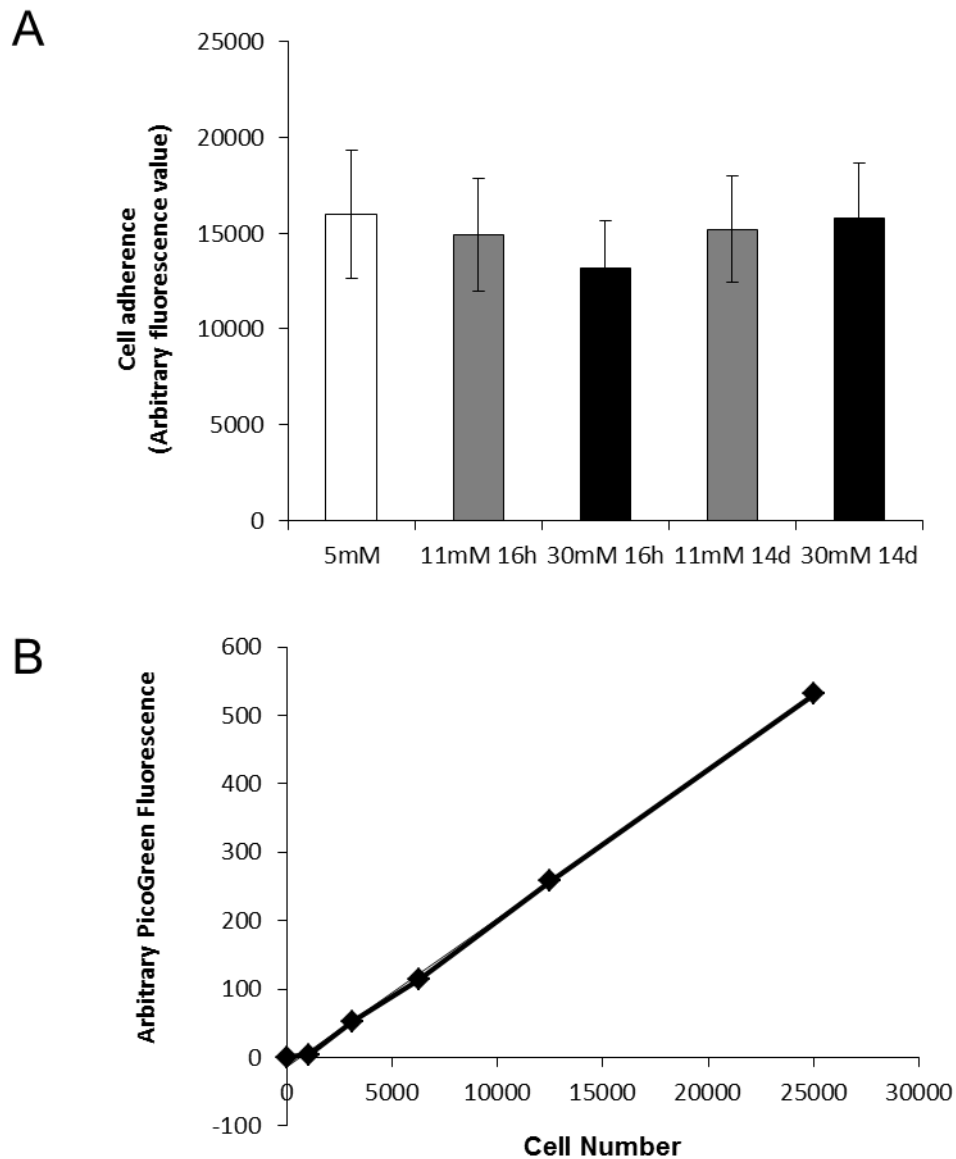


Figure 5.18. The effects of high glucose exposure on cell adhesion in synoviocytes. This was driven by an identification of differential expression of cell adhesion associated genes (Figure 5.02 and Figure 5.16), and supported by observations that cells exposed to long-term high glucose were more susceptible to the effects of trypsin (anecdotal). In contrast to early observations, a cell adhesion assay found no significant effect of high glucose on cell adhesion in synoviocytes (A, $p > 0.05$). picoGreen was a strong indicator of cell number (B). A represents the number of cells remaining adhered after overnight re-adhesion following trypsinisation after exposure to high glucose. Data ($n = 3$) is shown as mean \pm SD.

5.5.1 Is a change in DNA methylation profiles causal?

While DNA methylation has been shown to be indicative of age, there is a question of causality that has yet to be answered. There remains uncertainty as to whether advanced age leads to corresponding effects on DNA methylation, whether DNA methylation causes effects in ageing, or indeed whether there is an interaction between these two factors.

Early in this chapter it was discussed whether a tool such as the DNA methylation age calculator (226) could indicate effects of glucose on ageing. The question in this instance makes an assumption that the differences in DNA methylation profiles observed have downstream effects on function. In this instance, this assumption is tested using gene expression arrays and functional assays, with each subsequent step being informed by the previous experiments.

In Figure 5.01 it is shown that a DNA methylation age calculator makes the prediction based on 82 prior datasets that samples exposed to an intermediary high glucose level (11mM) exhibit DNA methylation profiles indicative of a more advanced age than those exposed to normal glucose levels (5.5mM), or very high glucose levels (30mM). In the first instance this data suggests that a physiological high glucose level (11mM) is sufficient to cause a greater level of DNA methylation changes associated with ageing, than other doses. This change is not significant with the current sample group (n=3).

A global hypomethylation, like the large levels of hypomethylation observed following the 11mM 16 hours treatment of synoviocytes, has been suggested to occur in ageing, but certain promoter specific hypermethylation sites are also said to be characteristic of an ageing methylome (237). It is particularly interesting that this treatment group would be considered to have the least profound effect due to 11mM being the lower of the two high glucose treatments, together with 16 hours being the shorter of the two treatment periods. That the 11mM 16 hours treatment produced the most profound effect suggests that high

blood glucose in the physiological range may have the potential to affect the methylome of synoviocytes.

5.5.2 Can high glucose exposure affect ageing through differential methylation in synoviocytes?

While little of the DNA methylation array data obtained from the Illumina 450k arrays was able to be validated through pyrosequencing, it was interesting to note that one of the genes highlighted as potentially affected has an association with the glucose treatments, IGF2. IGF2 has also been linked to ageing (238). With literature support, this gene appeared to be a suitable candidate for further analysis. As can be seen from Figure 5.04D however, the differential methylation observed at this CpG site in the methylation array data was not observed using targeted pyrosequencing. Further gene expression analysis failed to identify any downstream effects of a potential hypomethylation in CpGs associated with the promoter region of this gene. As ageing is a lifelong process, it may be possible for successive modest effects on DNA methylation associated with this gene to accumulate over time. No studies have indicated that methylation may play a role in this gene's associated with ageing, but this remains a possible route for further study.

5.5.3 Can high glucose exposure affect imprinting genes?

CpG methylation is essential in the inactivation (gene silencing) of genes located in the X chromosome, and therefore the establishment and maintenance of the mono-allelic expression of imprinted genes (239). Reactivation of some of these imprinted genes has been reported to be associated with longevity and ageing (240-242).

Three of the sites identified as significantly affected in the array data are have been shown to be paternally imprinted genes (IGF2, MEST and ZIM2/PEG3) (243-246). In the case of IGF2, the loss of imprinted status has been associated with a number of pathologies (244), and the roles of imprinting in ZIM2/PEG3 and MEST have been investigate with respect to type 1 diabetes (246).

A high glucose-mediated effect of reactivation of key imprinted genes through hypomethylation could provide a link between high glucose exposure and ageing, among other potential conditions.

5.5.4 Effects of high glucose exposure on cell adhesion

Matrix degradation and cell adhesion have relevance in degenerative musculoskeletal conditions associated with ageing (247). Studies have previously alluded to potential effects of glucose on cell adhesion in the vascular system (248). These effects have been relatively poorly studied in the musculoskeletal system.

As can be seen from Figure 5.18, it would appear that cell adhesion is not affected in synoviocytes exposed to high glucose. This assay tested the ability of cells exposed to varying concentrations of glucose to re-adhere to cell culture plastic following trypsinisation. While this was used as a measure of the effects of high glucose on cell adhesion, this may not be an optimal measure of these effects. It was difficult to identify an optimal measure of cell adhesion after treatment with high glucose. It was initially proposed that the effect of trypsin be measured directly by treating cells with trypsin for a predetermined time period prior to counting the number of cells that were released from the culture plastic. There are, however a number of limitations to this method, not least that there can be no guarantee that cell number would not be affected during the extensive treatment periods. In this instance the potential effects of cell number could act to compound an eventual measurement of cell number. Additional re-adhesion time periods were used, with 24 hours providing the most reproducible measure. A concern was that 24 hours would be sufficient time for all cells to re-adhere. As can be seen from the vertical axis of Figure 5.18A, however, this is shown not to be the case. Cells were reseeded at 25,000 cells per well. In each treatment group there would appear to be roughly 60% re-adhesion. Future study would be required in order to

confirm the most optimal method for assessing cell adhesion capability following high glucose exposure.

5.5.5 Limitations inherent in human sample groups

The large amount of variability observed in many of the experiments could potentially be attributed to the large amount of expected between-sample variability inherent in data from human cells. While every effort was made to limit the between-sample variability by race-matching (Caucasian), and roughly age-matching the samples (58 ± 13 years), a natural amount of human variability is still to be expected. In a sample group comprising $n = 3$, this variability could have a limiting effect on the level of significance observed in the data.

5.5.6 Pyrosequencing versus DNA methylation microarray

As has been discussed, none of the pyrosequencing assays managed to clarify or support the findings of the methylation microarray data. There are a number of steps during the pyrosequencing protocol presenting a likelihood of affecting downstream steps. Processing of the DNA following receipt of the microarray results involved an interim period wherein the DNA was stored at -80°C . DNA methylation, being a covalent modification of cytosine residues, is relatively stable and would be expected to have robustness against freeze-thaw cycles. There has been relatively little published in this regard, but one study indicated that repeated freeze-thawing induced progressive random alterations in CpG methylation detected using Illumina BeadChip technology similar to that used in this study (Illumina Infinium HumanMethylation27 arrays) (249). The bisulphite conversion of DNA carried out using EZ DNA Methylation kit (Zymo) is routinely used among other lab members with no indication of unsuitability for the present applications. The kit itself is considered to involve a 99% conversion rate. Pyrosequencing assays were designed comprising primers having optimal predicted melting temperature and secondary structure characteristics, and were designed to identify the target CpG site differentially methylated in the microarray data, along with other CpG sites in the vicinity of the target. A number of probes on the Illumina Infinium HumanMethylation450k arrays have been suggested to cross-react with additional regions

within the genome (250) and as such could indicate incorrect differential methylation levels relating to the CpG sites found to be differentially methylated during this study. Future work would require additional pyrosequencing assays per CpG site in order to better describe the methylation landscape surrounding the target CpG site.

5.5.7 Statistical power

Sample size for the current study was restricted for feasibility, although a power calculation is often used to estimate the optimum sample size for maximising statistical power. An example sample size calculation was performed using the sizepower package in Bioconductor (186) for exemplification purposes only, using data obtained from the gene expression microarray study in synoviocytes (Table 5.01).

The sizepower package uses the below formula for estimating sample sizes:

$$n = \left(\frac{z_a + z_b}{|\mu_1| / \sigma_d} \right)^2$$

Where n is the sample size for each group. If we take α_0 to be the probability of a type I error for any single gene among the genes on the array that are not differentially expressed (G_0), a is $1 - \alpha_0/2$. b is the desired power of the test, z_a and z_b are the lower a and b percentiles of the standard normal distribution, and σ_d is the standard deviation of the difference in expression between treatment and control samples. $|\mu_1|$ denotes the expression difference between the treatment and control groups.

Using the data from the present study it can be ascertained that:

$$n = \left(\frac{1.79}{0.566} \right)^2$$

Using the above formula, the desired sample size, to achieve optimum statistical power, is 10.

6. Chondrocyte methylome is robust to the effects of high glucose, but cell cycle and cell adhesion may be affected

6.1 Introduction

6.1.1 Chondrocytes

As the only cell type native to the cartilage of articulating joints, chondrocytes play an integral role in the maintenance of their surrounding tissue, which protects the underlying bone against a highly diverse array of loading cycles and stochastic loading events over the course of a lifetime. Inability to sustain the finely attuned buffering properties of the cartilage matrix has been a failing in chondrocytes which appears to occur increasingly with age.

6.1.2 Ageing cartilage

Age-related decline in cartilage composition has been shown to be an important factor in the aetiology and progression of degenerative diseases such as the perennial age-associated joint “condition”, osteoarthritis; now considered to represent an array of pathologies with a number of different aetiologies but exhibiting similar symptomatic manifestations. While age would appear to be a clear causal factor, the mechanism of onset for what has become a complex class of diseases has proven to be multifaceted and remains elusive.

A number of studies indicated that the age-associated reduction in the buffering capacity of cartilage is the result of a cumulative effect of injurious events sustained over the course of a lifetime (251-253). Chondrocytes are known for having a low cell turnover coupled with a slow rate of extracellular matrix repair (254), which could be due to their nutrient sparse, avascular environment; necessitating the uptake of required nutrient molecules by matrix perfusion from synovial fluid and vascularised subchondral bone. The slow recovery time of cartilage has been suggested to allow the effects of deleterious events to accumulate (255), with such injurious events including loading-related injury among others.

More recently, other mechanisms have been described for the aetiology of cartilage degeneration, which have included cell-based mechanisms such as premature chondrocyte senescence and a reduction in chondrocytic phenotype with age: potentially brought about by low-level systemic inflammation increasing with age (253). There have also been

extracellular matrix-based mechanisms suggested, which have included persistent or permanent alterations to the cartilage tissue, such as the crosslinking of key structural proteins and the effects of this on protein turnover and matrix repair (40).

Most recently, transcriptomic assessment has yielded many positive insights into age-related chondrogenic decline, but this has still failed to provide definitive answers to the issue of causality. DNA methylation studies may bring us closer to an answer in this regard, with studies slowly generating a portfolio of hallmark genes for which distinct methylation profiles have been observed in cells from osteoarthritic tissue compared to those from healthy tissue.

Studies have linked diabetes and joint disorders such as osteoarthritis, primarily investigating the role that dysinsulinaemia plays in the maintenance of connective tissue extracellular matrix (196). The use of glucose by chondrocytes has been fairly well characterised, with chondrocytes exhibiting a readiness for glucose import (129). While studies have assessed the effects high glucose on targeted gene transcription, there have been relatively few to no studies indicating a role for excessive glucose consumption in affecting whole transcriptome and methylome profiles of chondrocytes. There has, in particular, been no assessment into the different effects of short-term and long-term exposure to high glucose in chondrocytes, with a view to isolating changes that may have a cumulative effect on chondrogenicity with ageing.

6.1.3 Aims of this study

This study assesses the effects of short term and long term high glucose exposure on healthy human chondrocytes, with a view to identifying potential changes that could accumulate with successive high glucose exposure over the term of a lifetime.

Healthy human chondrocytes (n = 3) were treated with high glucose (11mM or 30mM) for either a short time period (16 hours) or a long time period (14 days) alongside normal glucose (5.5mM) controls. The effects of the high glucose treatments were then assessed in

relation to the methylation of cytosine residues on the DNA of the chondrocytes in each treatment group. This was carried out using Illumina Human Methylation 450k arrays. Differentially methylated cytosine residues were characterised according to the promoter regions, and associated genes, they were located within. Functional associations were assessed for these genes, which was used to infer a functional relevance to the differential methylation observed.

6.2 DNA Methylation

DNA methylation microarray data analysis required an initial data normalisation, visualisation and preprocessing step to identify any outliers, the results from which can be seen in the principal component analysis plot of Figure 6.01A and the dendrogram of Figure 6.01B. No outliers were identified and following normalisation, the DNA methylation microarray data from Illumina Human Methylation 450k arrays showed that samples plotted on the first principal component (PC1) did not group according to treatment protocol as can be seen from the plot in Figure 6.01A. This lack of grouping for treatment type is supported by the dendrogram of Figure 6.01B. From these data visualisations, it would appear that treatment group was not the primary factor driving variability in the data.

As this data was from obtained from chondrocytes derived from human articular cartilage, a large portion of the variability was likely driven by the natural expected inter-individual methylomic differences between donors. The relatively short high glucose exposures did not therefore result in significant widespread differential methylation. This can be seen in Figure 6.02, which shows that the extent by which DNA methylation age differs between samples is modest.

6.2.1 DNA Methylation Age

As has been previously described in Chapter 5.1, DNA methylation age was assessed using a publicly available DNA methylation age calculator (226, 256). Pre-processed and normalised

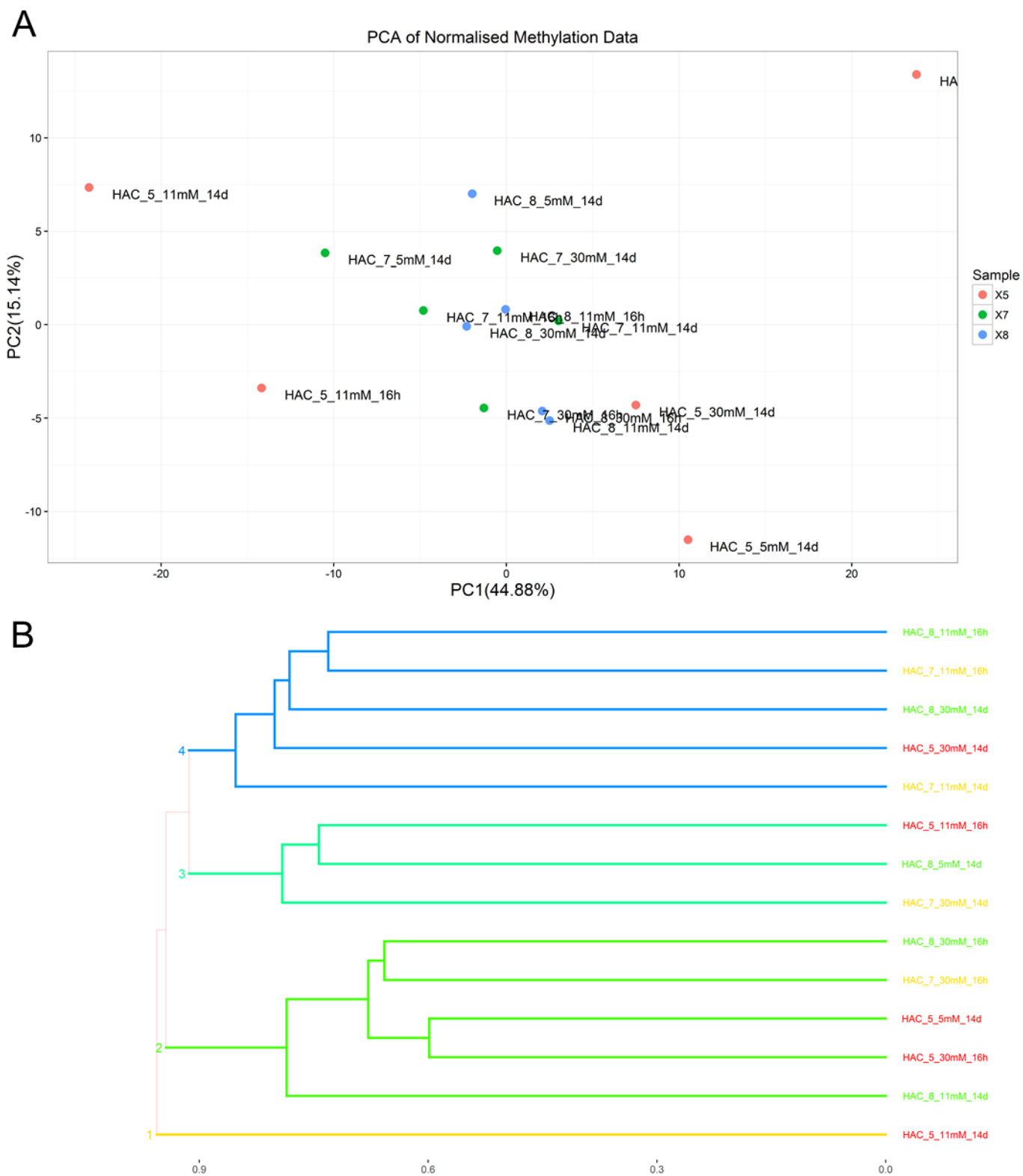


Figure 6.01. Principal component analysis (PCA) of DNA methylation data (A) showed that, while samples did not group according to individual sample donor, they also did not group according to treatment, suggesting that treatment group was not the only source of variability in this dataset. Cluster analysis corroborated the PCA data (B). Data (n = 3) is show colour-coded to sample donor.

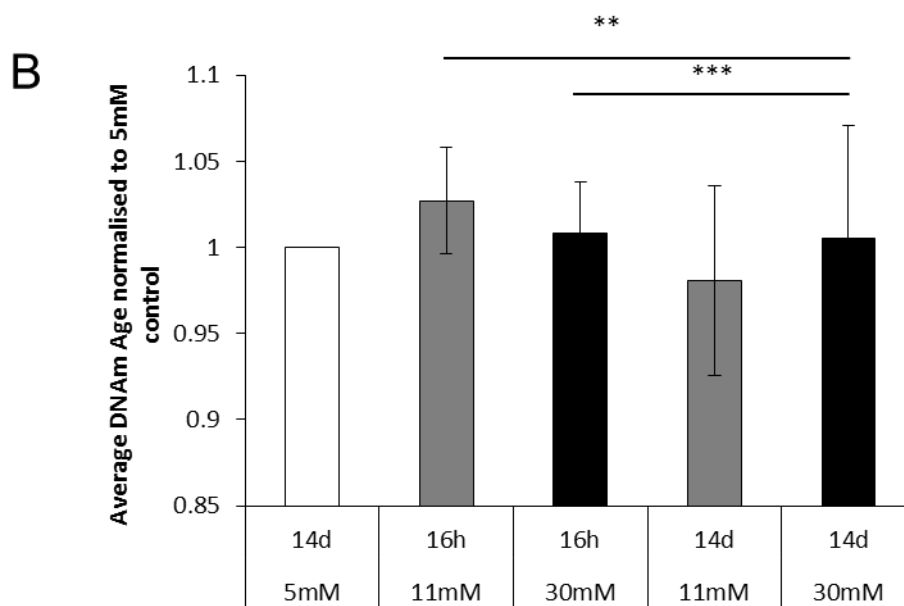
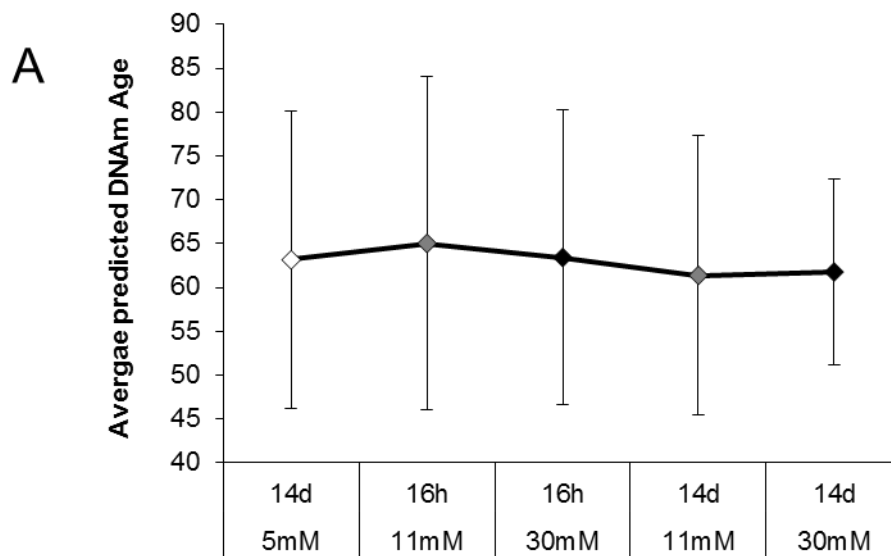


Figure 6.02. DNA methylation age of high-glucose treated chondrocytes. There was a large inter-individual variability in the data (A). This was mitigated through the normalisation of each sample to the respective internal control (5.5mM) (B). A highly significant effect of treatment group on the predicted DNA methylation age of the samples was observed (B, $p = 0.0058$). Individual post hoc comparisons showed that there was a significant time-dependent effect of the 14 day 30mM exposure on DNA methylation age when compared to the short term (16h) 11mM (**, $p = 0.01$) and 30mM (***, $p = 0.004$) treated cells. Data ($n = 3$) is shown as mean \pm SD.

DNA methylation array beta values for each sample were input into the online tool and the predicted DNA methylation ages for each chondrocyte sample obtained from the tool were assessed for the extent of deviation from an average of the actual chronological ages of the chondrocyte sample donors. This data is shown in Figure 6.02A, in which it can be seen that there was no significant difference in the predicted methylation ages generated by the DNA methylation age calculator. However, data normalised to the normal glucose (5.5mM) control in Figure 6.02B showed that treatment group was a significant cause of variability in the data set ($p = 0.0058$), with significant reductions being observed in post-hoc pairwise comparisons being between the short term treatments (11mM 16h, 30mM 16h) and the 30mM 14d treatment. While these comparisons were statistically significant, the biological significance of the reductions in predicted methylation age observed over time from the short term treatments to the long term high glucose (30mM) treatment may be an issue of debate.

6.2.2 Glucose-mediated differential DNA methylation

As can be seen from Table 6.01, there were minimal effects of high glucose treatments on DNA methylation in chondrocytes. Only one significant differentially methylated site was identified in response to high glucose treatments when compared to a normal glucose control. cg23470128 is associated with the Homeobox B13 (*HOXB13*) gene and would appear to be significantly hypomethylated in response to all of the high glucose treatments as can be seen in Figure 6.03A.

Table 6.01. Number of significantly differentially methylated CpG loci and significantly differentially expressed genes in chondrocytes following exposure to high glucose.

	11mM 16h	30mM 16h	11mM 14d	30mM 14d
Methylation	1	1	1	1
Gene Expression	0	0	18	52

6.2.2.1 Homeobox B13 (HOXB13)

The significant hypomethylation shown in Figure 6.03A would appear not to affect downstream *HOXB13* gene expression in chondrocytes. Gene expression measurement of *HOXC9* was carried out using qPCR, based upon RNA derived from the same chondrocyte samples, and gene expression was determined relative to gene expression of β -actin (*ACTB*). As can be seen from the gene expression data shown in Figure 6.03B, no significant difference in *HOXC9* gene expression was observed after any of the high glucose treatments when compared to the normal glucose control. Glucose dosage and treatment period were both shown to have non-significant effects on the variability in the dataset. High variability in gene expression was observed after short term (16 hour) treatments and the normal glucose control. Variability would appear to be reduced in the longer term (14 day) treatments.

6.3 Gene Expression Study

Whole transcriptome gene expression was assessed in chondrocytes (n = 3) using the Illumina Human Transcriptome HT12 v4 microarray. Similar to the DNA methylation array analysis, initial preprocessing, normalisation and visualisation was carried out in order to identify outliers and primary drivers of variability in the gene expression data. It was noted that, for two of the three donors, the long term (14 day) high glucose treated chondrocytes were distinct from the other treatment groups for these same donors on the first principal component axis of the PCA plot (Figure 6.04A). This can be seen more clearly in the dendrogram shown in Figure 6.04B, which shows the long term high glucose treated chondrocytes of two of the three donors grouped together with the short term high glucose treated chondrocytes of the third donor.

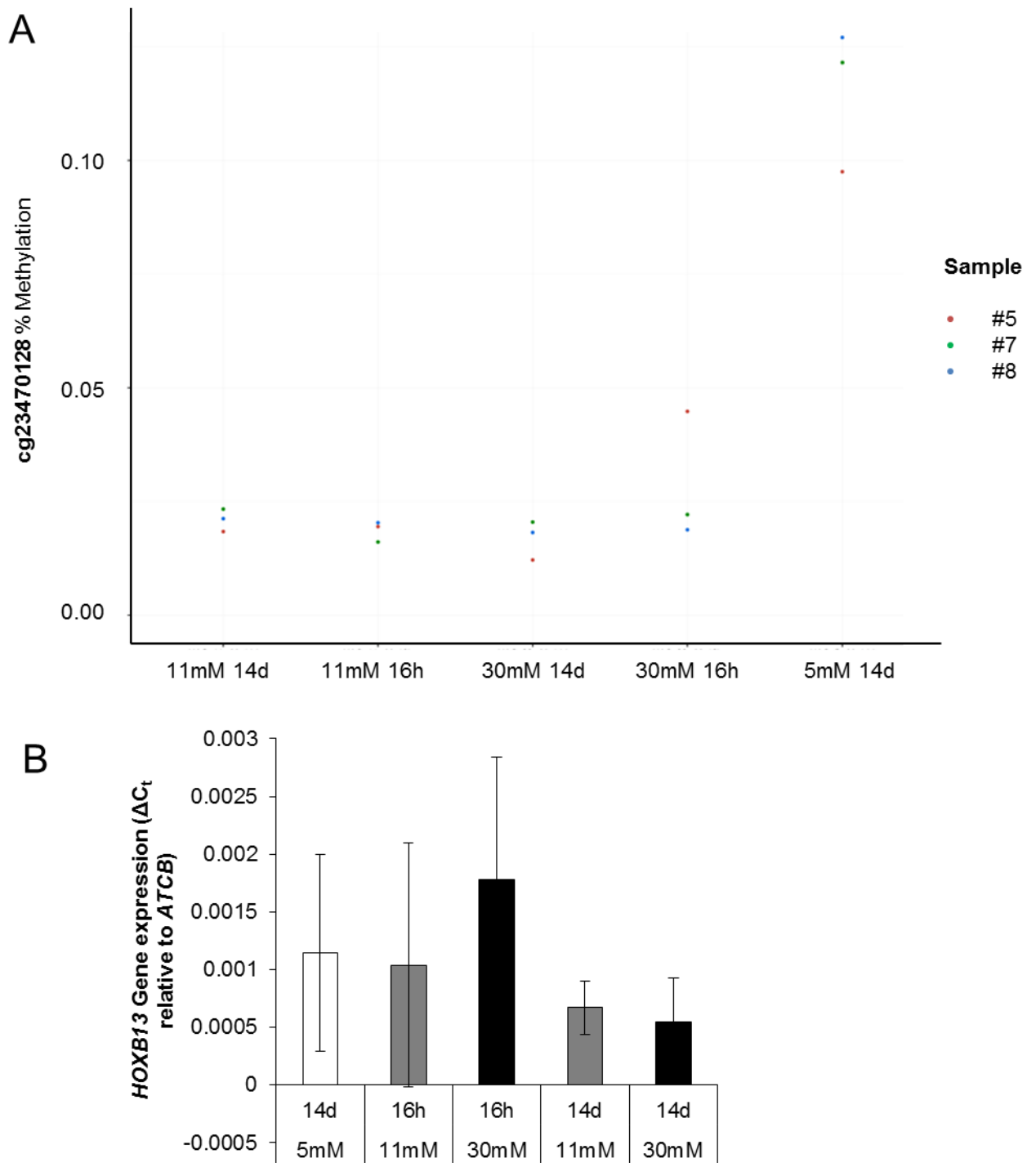


Figure 6.03. There was only one CpG locus (cg23470128) that was significantly differentially methylated (HOXB13, hypomethylated) as a result of the high glucose treatments (A). The high glucose had similar effects across all three samples in each treatment group (A). The differential methylation identified (A) does not appear to have a downstream effect on gene expression in the time periods investigated (B). Data (n = 3) in B is shown as mean \pm SD.

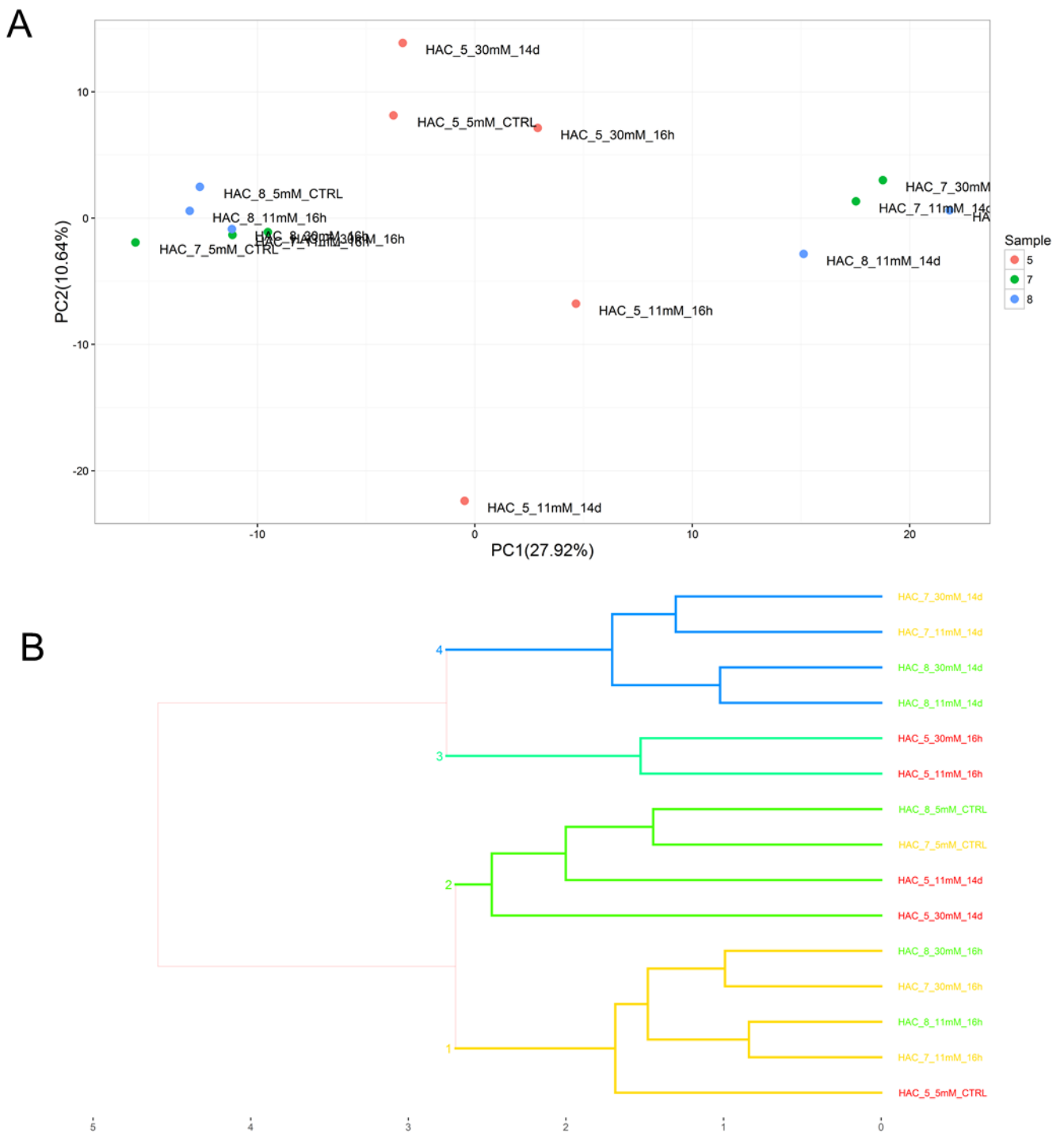


Figure 6.04. Principal component analysis (PCA) of gene expression microarray data showed that the long term (14 day) high glucose (11mM and 30mM) treatment groups clustered together away from the rest of the treatment groups on the primary principal component axis in two of the three samples (A). This is supported by cluster recognition carried out on the normalised dataset (B). Data (n = 3) is shown colour-coded according to sample donor.

6.3.1 Glucose-mediated differential gene expression

As can be seen from Table 6.01, the long term high glucose treatments had the largest significant effect on gene expression, with 18 and 52 significant differentially expressed genes identified for 11mM 14 day and 30mM 14 day treatments respectively.

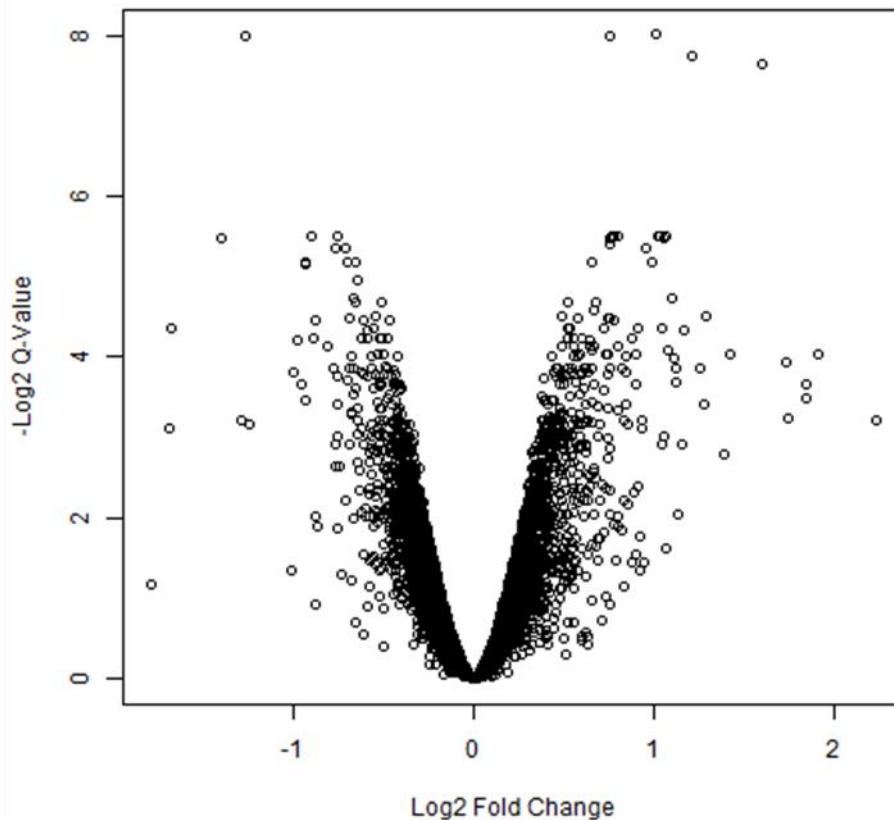


Figure 6.05. The largest effect on gene expression was seen after the exposure of chondrocytes to 30mM glucose for 14 days. This plot represents the significance of the effect of a 14 day 30mM glucose exposure on chondrocytes against the extent of the effects. The effects were relatively modest, with the \log_2 fold change rarely exceeding 2 (actual fold change of 4).

6.3.2 Long term (14 day) exposure to 30mM glucose

The largest of the effects on gene expression was observed after exposure of chondrocytes to 30mM glucose for 14 days. This treatment group had 52 significant differentially

expressed genes (FDR-corrected p value < 0.05, log₂ fold-change > 0.5). Figure 6.05 shows a volcano plot depicting each transcript on the gene expression array represented by a log₂ FDR-corrected p-value (log₂ q-value). These log₂ q-values are plotted on the vertical against log₂ fold-change on the horizontal axis. Figure 6.05 shows how the level of differential expression observed after exposure of chondrocytes to 30mM glucose for 14 days was relatively modest, with most genes having a log₂ fold-change less than ±2 (actual fold-change less than ±4). The heat map shown in Figure 6.06, which represents row-wise z-

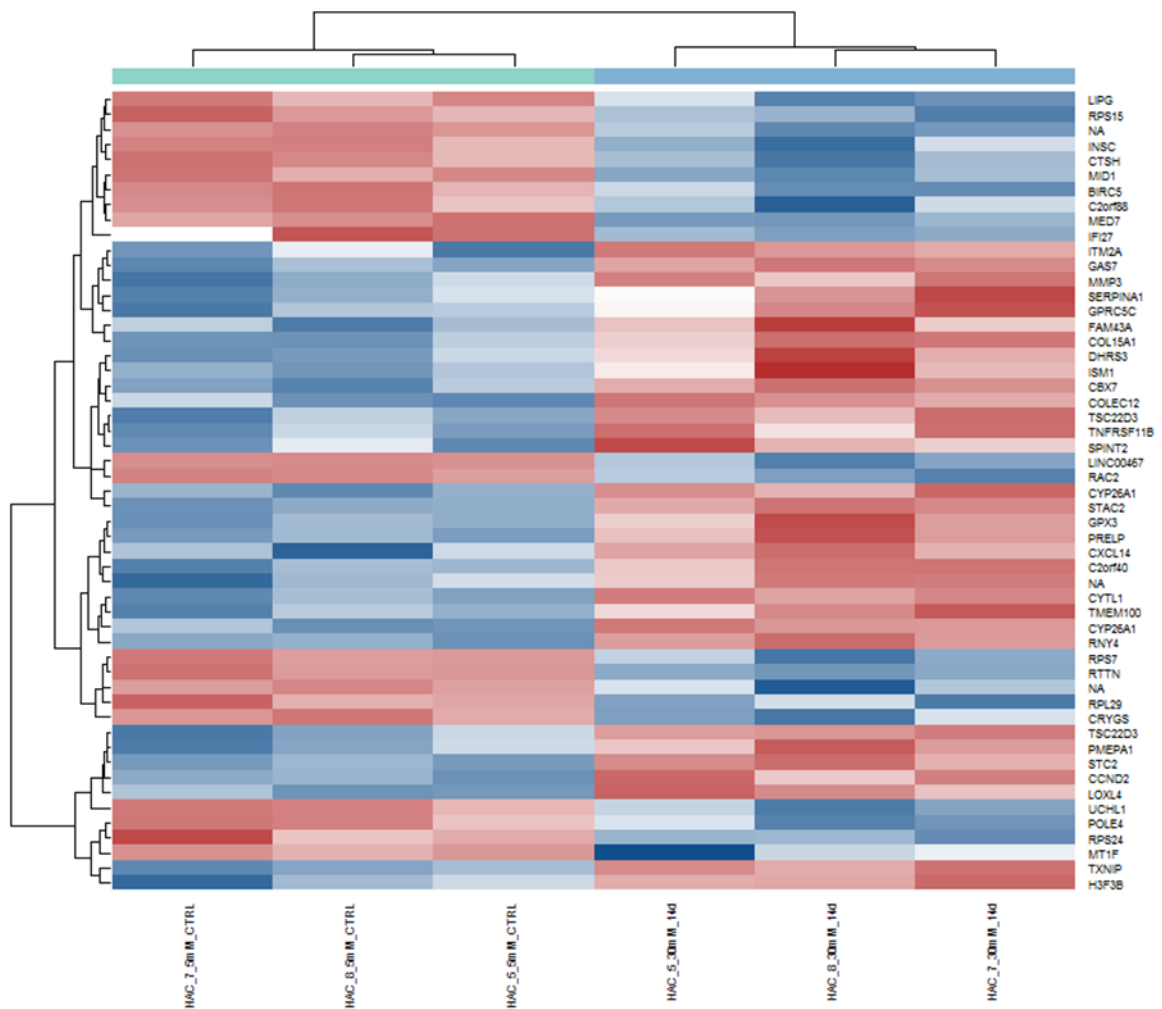


Figure 6.06. The heatmap shows the significant differentially expressed genes identified as a result of treatment of chondrocytes with 30mM glucose for 14 days (FDR-corrected p-value < 0.05, log₂ fold change > 0.5). As can be seen, the data group according to treatment protocol.

Table 6.02. The significant differentially expressed genes in chondrocytes as a result of 30mM glucose exposure for 14 days.

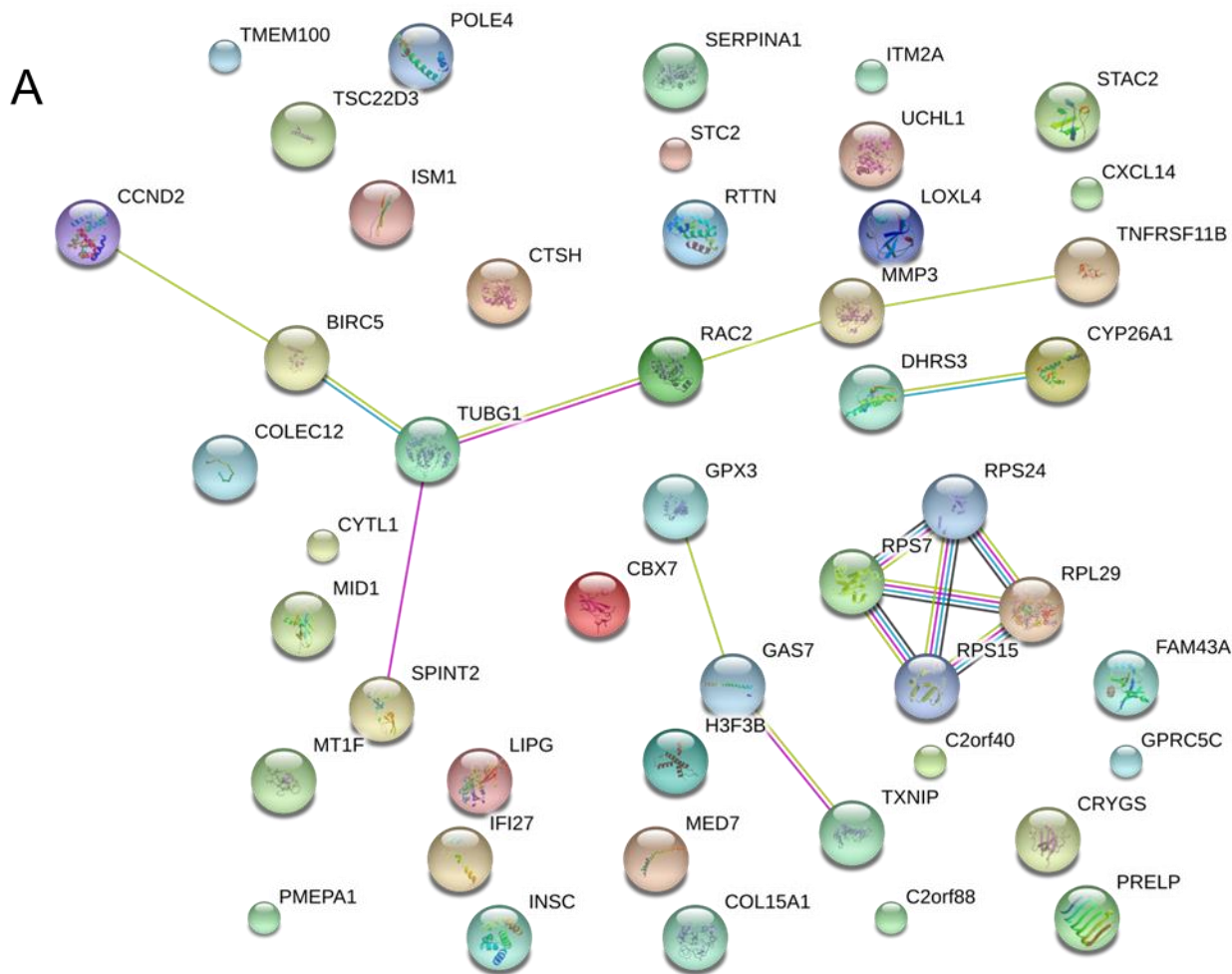
Symbol	Log₂ Fold Change	FDR
CYP26A1	1.009988	0.003935
STAC2	0.757433	0.003977
CTSH	-1.26445	0.003977
MMP3	1.210943	0.00472
C2orf40	1.604468	0.005103
CYP26A1	0.776452	0.022378
TSC22D3	0.785361	0.022378
LINC00467	-0.75195	0.022378
TXNIP	1.031053	0.022378
FAM43A	1.072145	0.022378
TMEM100	1.037504	0.022378
CYTL1	0.80714	0.022378
CRYGS	-1.40716	0.022481
PRELP	0.75678	0.022481
DHRS3	1.054595	0.022733
GAS7	0.762573	0.023773
COL15A1	0.959183	0.024909
BIRC5	-0.77076	0.024909
RTTN	-0.71511	0.025003
CXCL14	0.987792	0.027598
INSC	-0.93059	0.027598
UCHL1	-0.65051	0.027598
TSC22D3	0.655032	0.027598
RAC2	-0.69922	0.027598
RPL29	-0.64155	0.032688
MID1	-0.66942	0.038213
LOXL4	1.107513	0.038213
CCND2	0.52544	0.039383
C2orf88	-0.6531	0.039383
PMEPA1	0.686069	0.039383
RPS15	-0.51533	0.039383
STC2	0.671905	0.042
RNY4	0.486079	0.044364
SERPINA1	1.288831	0.044723
RPS7	-0.54871	0.044723
CBX7	0.584842	0.044723
LIPG	-0.69276	0.044723
TNFRSF11B	0.756924	0.044723
ITM2A	0.748455	0.044723
MED7	-0.47057	0.04613
MT1F	-0.88342	0.04613
RPS24	-0.60576	0.04613
GPRC5C	0.786509	0.04613
IFI27	-1.67614	0.049314
SPINT2	0.722525	0.049314
H3F3B	0.540086	0.049314
COLEC12	0.521823	0.049314
ISM1	1.048856	0.049314
POLE4	-0.5541	0.049368
GPX3	0.912349	0.049368

scores for each of the 52 genes that were significantly differentially expressed, shows that in chondrocytes exposed to 30mM glucose for 14 days, the gene expression z-scores group according to treatment.

6.3.2.1 Whole transcriptome microarray

Table 6.02 shows the \log_2 fold changes and FDR-corrected p values for each of the significantly differentially expressed genes, resulting from exposure of chondrocytes to 30mM glucose for 14 days. *CTSH* expression, a gene which encodes for Cathepsin H, was significantly decreased (\log_2 Fold Change = -1.3, FDR corrected p value = 0.004) in cells exposed to 30mM glucose for 14 days. A similar reduction was observed for synoviocytes as detailed in Chapter 5. Additionally, genes associated with the musculoskeletal system were significantly increased as a result of long-term high glucose exposure. Such genes include those encoding for matrix metalloproteinase 3 (*MMP3*), and collagen 15A1 (*COL15A1*). *TXNIP*, a gene encoding for Thioredoxin-interacting Protein, was also significantly increased as a result of long-term high glucose exposure.

The estimated protein interactions of the significantly differentially expressed genes can be seen in Figure 6.07A (STRING). As can be seen from the interaction network, the cluster with the most highly supported interactions is that between *RPS7*, *RPS15*, *RPS24* and *RPL29*. All four of these genes encode ribosomal proteins, split between the 40S and 60S subunit. Expression of all four of these genes has been reduced in these chondrocytes as a result of long-term high glucose exposure. The fact that these four genes provide high support for a single cellular component and biological function, means that the most frequently obtained pathway IDs and gene ontology terms obtained from freely available gene ontology tools were associated with the ribosome, protein synthesis and translation. Figures 6.07B and C contain example tables, produced using the online functional analysis tool, DAVID (256), which illustrate this.



B

pathway ID	Pathway Description	Gene Count	FDR
GO:0005615	extracellular space	12	0.0188
GO:0022626	cytosolic ribosome	4	0.0353
GO:0022627	cytosolic small ribosomal subunit	3	0.0353

C

Term	Count	%	P Value
GO:0042274~ribosomal small subunit biogenesis	3	6.122449	7.51E-04
GO:0006614~SRP-dependent cotranslational protein targeting to membrane	4	8.163265	0.001782675
GO:0019083~viral transcription	4	8.163265	0.00293583
GO:0000184~nuclear-transcribed mRNA catabolic process, nonsense-mediated decay	4	8.163265	0.003483542
GO:0006413~translational initiation	4	8.163265	0.005165961
GO:0007566~embryo implantation	3	6.122449	0.005168055
GO:0000226~microtubule cytoskeleton organization	3	6.122449	0.014233445
GO:0006364~rRNA processing	4	8.163265	0.017325365
GO:0048387~negative regulation of retinoic acid receptor signaling pathway	2	4.081633	0.025321063
GO:0006412~translation	4	8.163265	0.026792551
GO:0071773~cellular response to BMP stimulus	2	4.081633	0.07409849
GO:0048839~inner ear development	2	4.081633	0.09990116

Figure 6.07. Expected protein interactions identified for the list of significant differentially expressed genes were obtained from STRING (A). It would appear that there is a highly enriched interaction network associated with ribosomal proteins. Significantly enriched gene ontology terms associated with the gene set were also investigated (B and C).

6.3.2.2 Targeted replication of whole transcriptome data

Replication experiments were carried out using qPCR, with gene expression being measured relative to expression of the β -Actin gene (*ACTB*). The expression of cathepsin H (*CTSH*) was not significantly affected by high glucose treatment although variability in its expression appeared to increase with increasing dose of glucose over the short term 16 hour treatments (Figure 6.12A). Variability in the expression of *CTSH* across the different cell samples was reduced by the long term treatments of glucose (14 days).

Matrix metalloproteinase 3 (*MMP3*) gene expression was also assessed in replication experiments (Figure 6.12E), and while no treatment-dependent significant differential expression was observed, the general trend would suggest a dose- and time-dependent increase in *MMP3* gene expression in chondrocytes.

Expression of genes relevant to connective tissue, such as those for collagen type XV, alpha 1 (*COL15A1*), prolargin (*PRELP*) and lumican (*LUM*), were also assessed in replication experiments using qPCR, after each was identified as significantly upregulated in response to high glucose treatment (Figure 6.12B, C and D respectively). No significant differences were observed.

6.3.3 Long term (14 day) exposure to 11mM glucose

6.3.3.1 Whole transcriptome microarray

The second largest effect on gene expression as a result of treatment of chondrocytes with high glucose was observed in chondrocytes treated with 11mM glucose for 14 days (Table 6.01). As was the case with the long term 30mM treated cells, the long term 11mM treated chondrocytes exhibited a transcriptomic profile that was distinct by principal component analysis from the normal glucose control (5.5mM) in two of the three cell samples used in the experiment (Figure 6.04A). This is further supported when the data is used to plot a dendrogram (Figure 6.04B), which shows the distinct grouping of the long term 30mM treated cells from two of the cell donors. The increase in glucose treatment in these cells

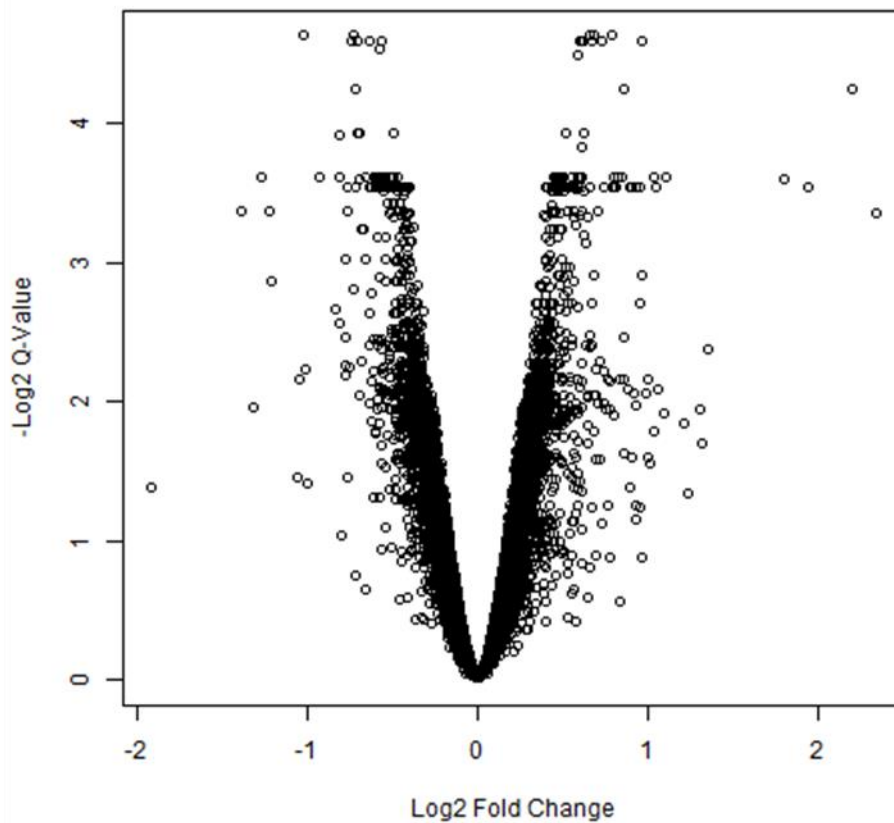


Figure 6.08. The second largest effect on gene expression was seen after the exposure of chondrocytes to 11mM glucose for 14 days. This plot represents the significance of the effect of a 14 day 11mM glucose exposure on chondrocytes against the extent of the effects. The effects were relatively modest, with the \log_2 fold change rarely exceeding 2 (actual fold change of 4).

could be considered relatively modest compared to the more commonly used, and less physiologically relevant, 30mM treatment. The effect of this fairly modest 11mM glucose treatment appears to be one of the primary drivers of variability in the transcriptomic profiles of the chondrocytes from these two donors according to the data from Figure 6.04A and Figure 6.04B. The fact that the high level of expected inter-individual differences between donors is not the primary effector on the variability in the transcriptomic profiles is interesting.

The significance of each gene expression change is plotted against the extent of the expression change in Figure 6.08. This shows the distribution of \log_2 false-discovery rate adjusted p values (\log_2 q values) plotted against the \log_2 fold change values and illustrates how the expression changes induced by 11mM glucose exposure are modest, with only 2 genes exceeding a \log_2 fold change of 2.

Table 6.03. The significant differentially expressed genes in chondrocytes as a result of 11mM glucose exposure for 14 days.

Symbol	Log ₂ Fold Change	FDR
<i>RPS27</i>	0.656085	0.040256
<i>HIST1H2BD</i>	-0.7248	0.040256
<i>CYP26A1</i>	0.78435	0.040256
<i>LUM</i>	0.676283	0.040256
<i>CTSH</i>	-1.0286	0.040256
<i>RPL7</i>	0.617131	0.041125
<i>RPS8</i>	0.603092	0.041125
<i>CD248</i>	-0.73734	0.041125
<i>DSG2</i>	0.96908	0.041125
<i>PRELP</i>	0.724803	0.041125
<i>LDLR</i>	-0.63756	0.041125
<i>H3F3B</i>	0.606968	0.041125
<i>GFRA1</i>	-0.70133	0.041125
<i>HIST1H2BK</i>	-0.70897	0.041125
<i>UGP2</i>	0.67505	0.041125
<i>TROAP</i>	-0.57968	0.042935
<i>ATF4</i>	0.582906	0.044104

The analysis identified 18 genes that were significantly differentially expressed following 11mM treatment of chondrocytes for 14 days (Table 6.03 and Figure 6.09). *CTSH*, the gene encoding for cathepsin H was again found to be down-regulated as a result of high glucose treatment. An additional gene differentially expressed in *LUM*, which codes for the extracellular matrix protein lumican. As was the case in the 30mM 14 day treatment, genes

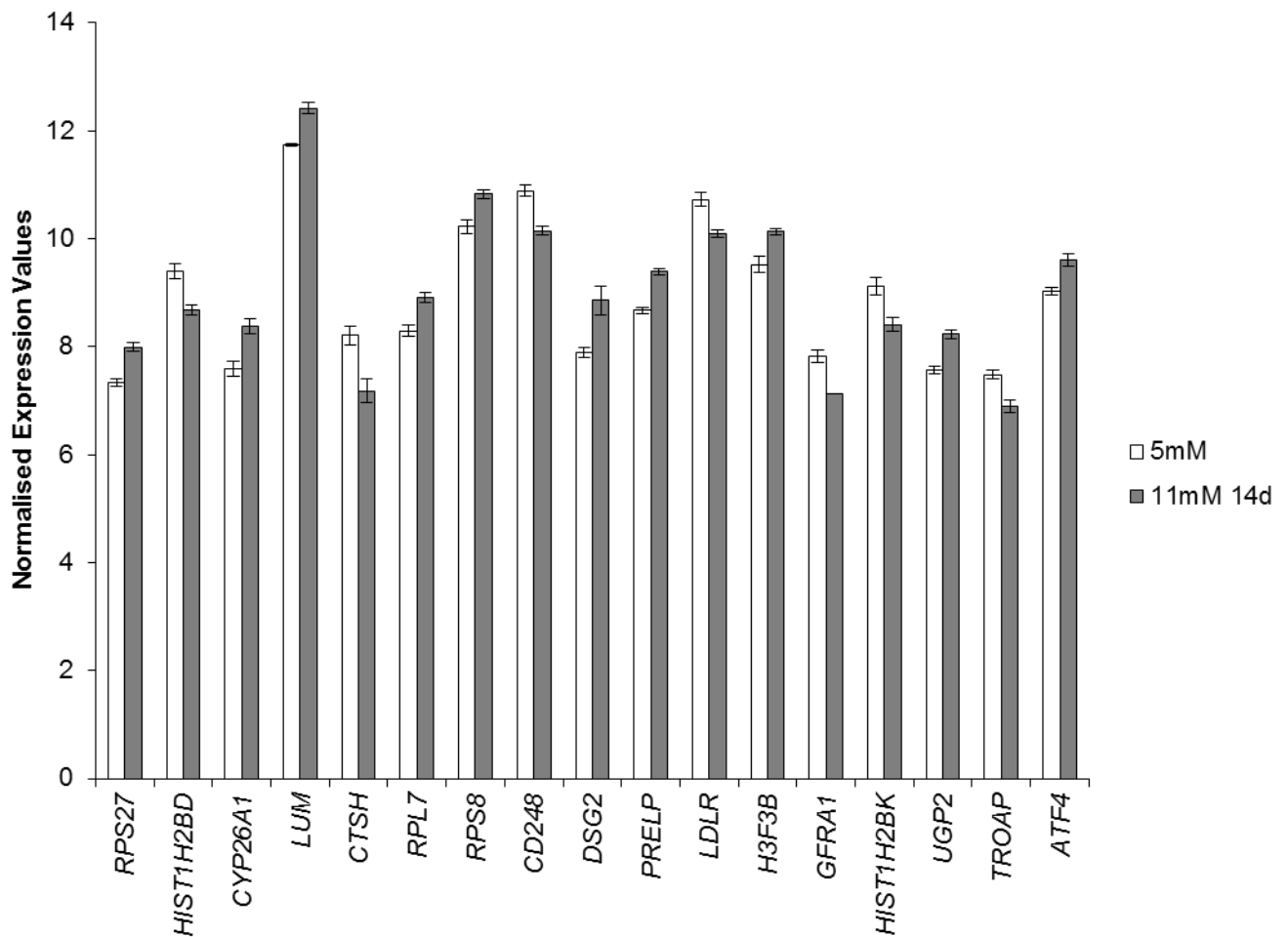


Figure 6.09. Normalised expression values obtained from the gene expression microarray data, for genes significantly differentially expressed following 11mM glucose exposure for 14 days (Table 6.03). Data (n = 3) is shown as mean \pm SD. All comparisons with the corresponding 5mM control are significant (false discovery rate < 5%).

coding for ribosomal proteins were significantly affected, although this time the genes affected were *RPS27*, *RPL7* and *RPS8*. The heat map in Figure 6.10 represents row-wise z scores for the gene expression values of each gene across all samples from 14 day 11mM treated cells and the normal glucose control treated cells. As can be seen from the heatmap, the expression values are grouped by the two different glucose treatments.

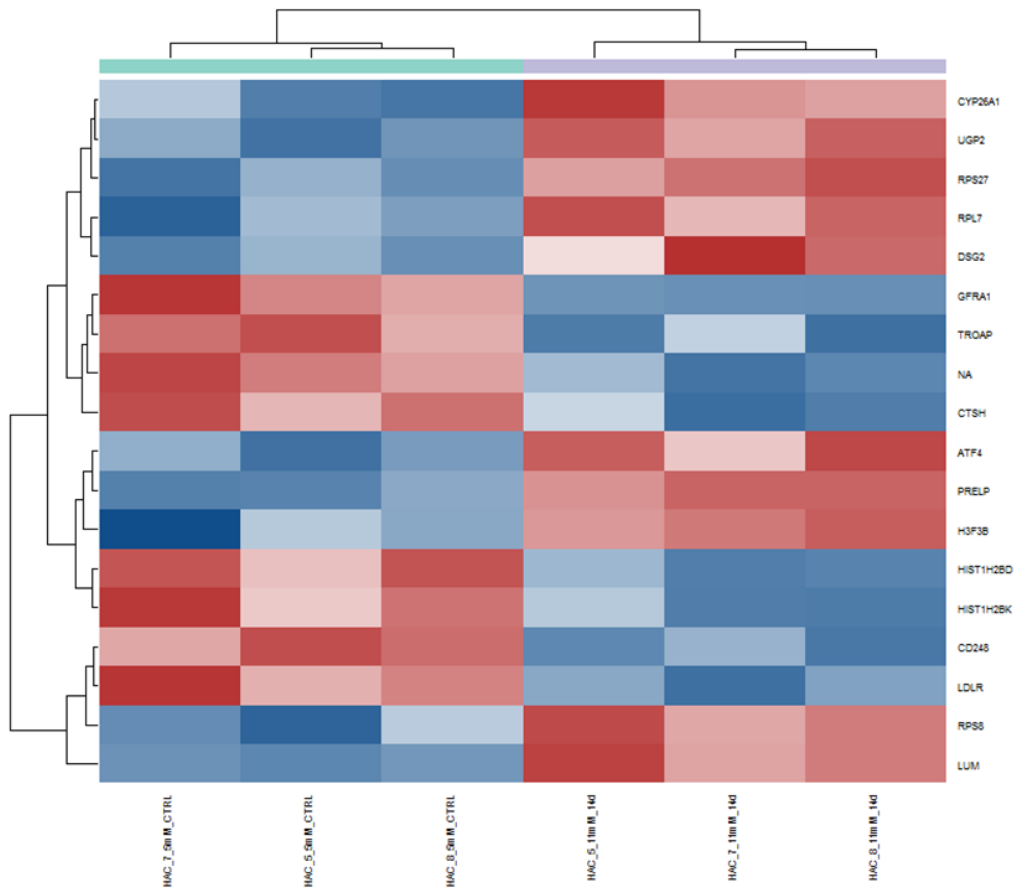
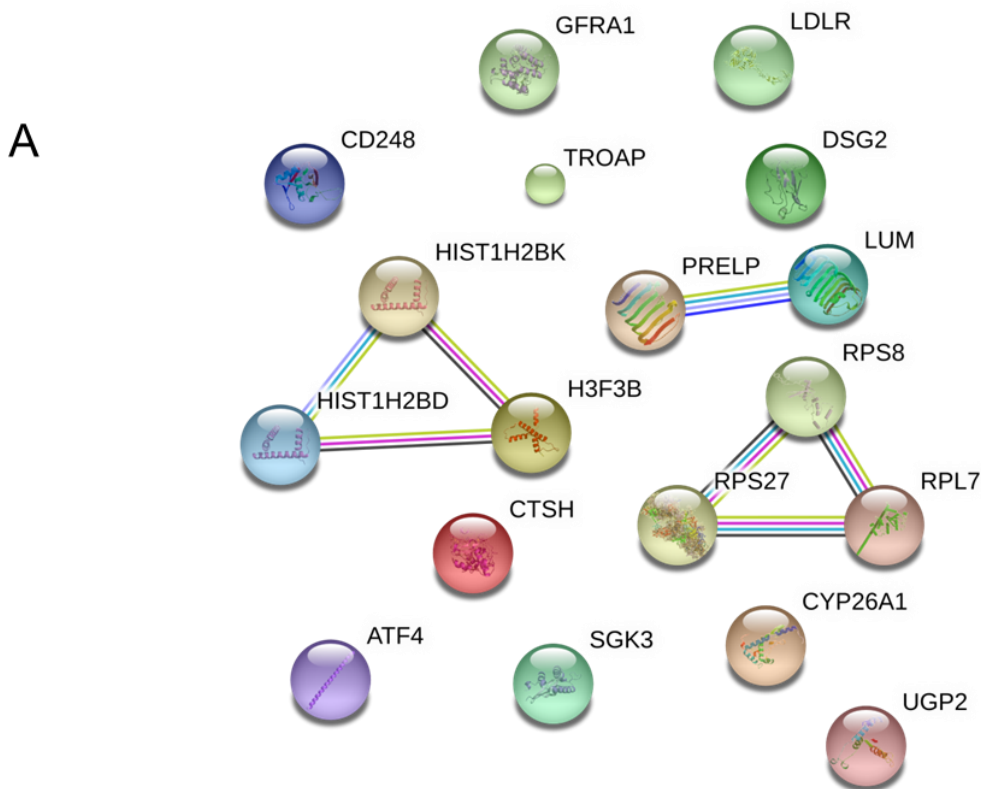


Figure 6.10. The heatmap shows the significant differentially expressed genes identified as a result of treatment of chondrocytes with 11mM glucose for 14 days (FDR-corrected p-value < 0.05, \log_2 fold change > 0.5). As can be seen, the data group according to treatment protocol.

6.3.3.2 Functional association

The estimated protein interactions for each of the differentially expressed genes were predicted by STRING (Figure 6.11A). The ribosomal proteins previously discussed are closely grouped. There are also a group of histone molecules, HIST1H2BK, HIST1H2BD, and H3F3B, the grouping of which is also supported.

Interestingly, the gene ontology terms (biological processes) significantly enriched by this gene set are “macromolecule catabolic process” (GO:0009057, $q = 0.037$) and “organic substance catabolic process” (GO:1901575, $q = 0.0417$) as can be seen from the table in Figure 6.11B. Additional gene ontology terms (cellular components) significantly enriched by this differentially expressed gene set include those relating to protein turnover, such as “cytosolic ribosome” (GO:0022626, $q = 0.0073$), “ribosomal subunit” (GO:0044391, $q =$



B

pathway ID	Pathway Description	Gene Count	FDR
GO:0009057	macromolecule catabolic process	7	0.037
GO:1901575	organic substance catabolic process	8	0.0417

C

pathway ID	Pathway Description	Gene Count	FDR
GO:0000788	nuclear nucleosome	3	0.00119
GO:0044421	extracellular region part	12	0.00119
GO:0005576	extracellular region	12	0.0019
GO:0031988	membrane-bounded vesicle	11	0.0019
GO:0070062	extracellular exosome	10	0.0019
GO:0022626	cytosolic ribosome	3	0.0073
GO:0044391	ribosomal subunit	3	0.0192
GO:0022627	cytosolic small ribosomal subunit	2	0.0367
GO:0005764	lysosome	4	0.0451

D

pathway ID	Pathway Description	count in gene set	false discovery rate
PF00125	Core histone H2A/H2B/H3/H4	3	0.0406

Figure 6.11. Expected protein interactions were identified for the list of significant differentially expressed genes using STRING (A). As was the case with the 14 day 30mM glucose treatment, it would appear that there is a highly enriched interaction network associated with ribosomal proteins (A). There was an interesting grouped interaction between histone proteins, and PRELP-LUM (A). Significantly enriched gene ontology terms associated with the gene set were also investigated (B, C and D).

0.0192), “cytosolic small ribosomal subunit” (GO:0022627, $q = 0.0367$), “extracellular exosome” (GO:0070062, $q = 0.0019$) and “lysosome” (GO:0005764, $q = 0.0451$).

6.3.3.3 Targeted replication of whole transcriptome data

As was the case with chondrocytes exposed to 30mM glucose for 14 days, the chondrocytes exposed to 11mM glucose for 14 days were also assessed for differential gene expression using targeted replication qPCR experiments.

Neither of *CTSH*, *PRELP* or *LUM* were significantly differentially expressed after 11mM glucose exposure for 14 days using targeted qPCR as can be seen from Figure 6.12A, B and D respectively.

6.4 Similarities in expression changes between chondrocytes and synoviocytes

In Chapter 5 it became apparent that the methylation status of cp07634179 and cp12071536 were significantly reduced in synoviocytes. Both of these CpG loci were associated with the promoter region of *HOXC9* transcripts. In chondrocytes, methylation of cg23470128 was significantly reduced. This CpG locus was associated with the promoter region of a *HOXB13* transcript. Due to the inter individual variability expected between the human chondrocytes used, it was suspected that this may have the effect of dampening significance of effects of DNA methylation determined from the DNA methylation microarray experiments, as evidenced by the identification of only one CpG locus that was differentially methylated as a result of high glucose treatment. Since one of the homeobox genes was identified as significantly differentially methylated in chondrocytes, it was decided to test the gene expression of the additional homeobox gene identified as significantly differentially methylated in synoviocytes. As such, gene expression of *HOXC9* was also assessed in chondrocytes. As can be seen from Figure 6.13B, there was no significant difference in *HOXC9* expression observed in chondrocytes. Inter-individual variation was indeed high as expected.

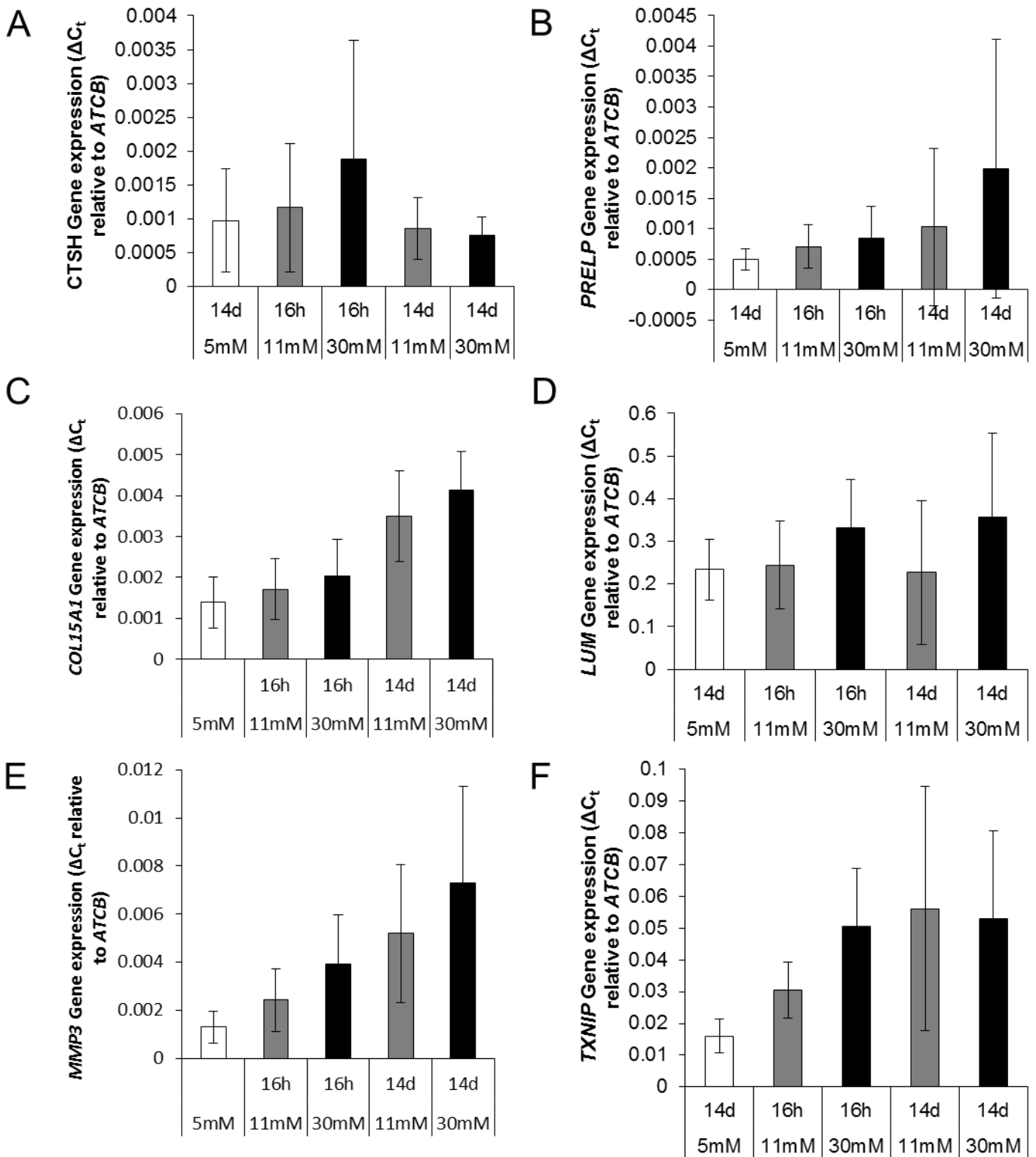


Figure 6.12. Targeted replication gene expression experiments were carried out using qPCR (A-E). There was no significant differential expression identified in the replication experiments, in contrast to the data obtained from the gene expression microarrays. Data ($n = 3$) is shown as mean \pm SD.

As with *CTSH*, another of the differentially expressed genes identified as a result of high glucose in synoviocytes was *FOS*. Due to the implications of expression of this gene being

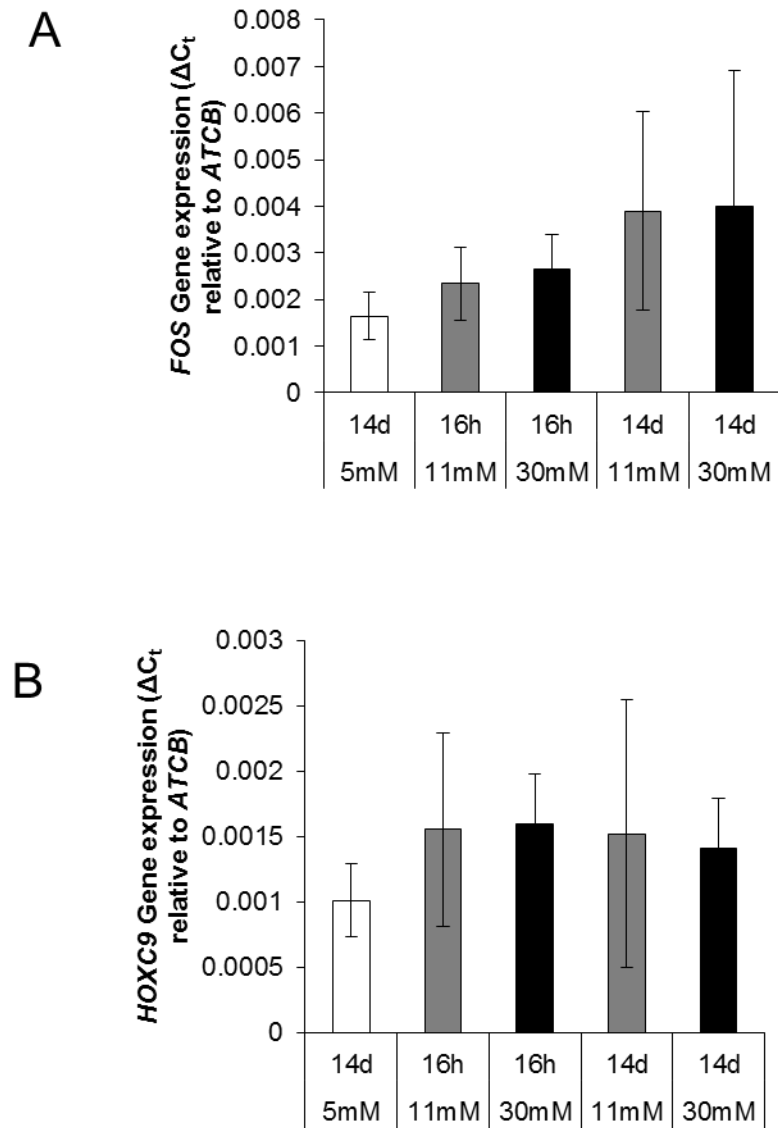


Figure 6.13. A crossover of effects of high glucose on gene expression between different cell types was assessed using targeted qPCR experiments. Both *FOS* and *HOXC9* were identified as significantly differentially expressed in the synoviocyte gene expression microarray data. There was no significant differential expression of these two genes, *FOS* (A) and *HOXC9* (B) identified in chondrocytes as a result of high glucose treatment. Data (n = 3) is shown as mean \pm SD.

affected, it was decided to also test the expression of this gene in chondrocytes in order to suggest a homologous effect between the two cell types. While there was no significant differential *FOS* expression identified in chondrocytes as a result of high glucose treatment (Figure 6.13A), the trend in the data might suggest a treatment and time dependent increase in the expression of this gene. It should be said that after the long term treatments, inter-individual variability in the expression of *FOS* greatly increased and as such little can be securely concluded from this data.

As such it would appear that there is little that can be concluded regarding a homologous effect of high glucose treatments across the two cell types except for the effect of long term (14 days) exposure of chondrocytes to 30mM glucose in increasing the expression of the gene encoding for collagen type XV, alpha 1 (*COL15A1*).

6.5 Cell adhesion

Throughout the study, successive experiments on the chondrocytes highlighted a repeatable anecdotal finding in that cells were more susceptible to trypsin upon treatment with high glucose over the 14 day treatment. In synoviocytes, as was discussed in Chapter 5, cell adhesion was highlighted as a potentially enriched GO term as a result of high glucose treatments. It was therefore decided to assess the effect of trypsin on the ability of these cells to re-adhere to cell culture plastic, as an attempt to highlight a long term effect of high glucose on the expression of cell adhesion proteins.

As can be seen from Figure 6.14A, the fluorescence of picoGreen was a strong indicator of cell number. There was no significant effect of high glucose treatments on the ability of chondrocytes to re-adhere to cell culture plastic following exposure to high glucose treatments ($p = 0.236$). However, as can be seen from Figure 6.14B, there may be a larger effect of the 30mM treatments than the 11mM treatments. There was, however, no detected difference between the ability of cells to re-adhere to cell culture plastic following a short term 16 hour and a long term 14 day treatment.

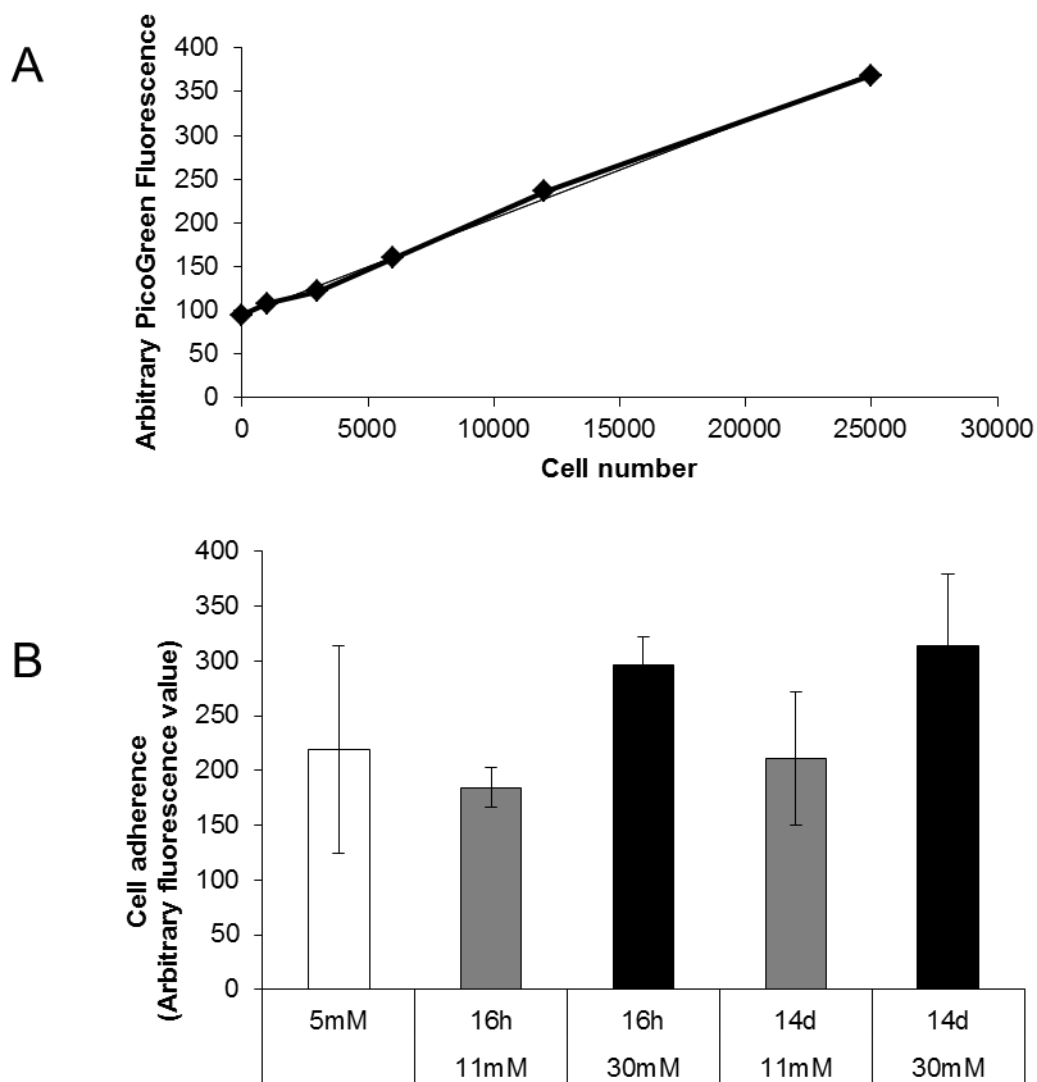


Figure 6.14. The effects of high glucose exposure on cell adhesion in chondrocytes. This was driven by an early identification of differential expression of cell adhesion associated genes in synoviocytes, along with anecdotal observations that cells exposed to long-term high glucose were more susceptible to the effects of trypsin. In contrast to early observations, a cell adhesion assay found no significant effect of high glucose on cell adhesion in chondrocytes (B, $p = 0.236$). PicoGreen was a strong indicator of cell number (A). B represents the number of cells remaining adhered after overnight re-adhesion following trypsinisation after exposure to high glucose. Data ($n = 3$) is shown as mean \pm SD.

Integrins are key molecules associated with cell adhesion and matrix adhesion. Preliminary differential gene expression microarray analysis highlighted the integrins *ITGA5* and *ITGB2* as being affected by the high glucose treatments. An additional gene identified as potentially affected by high glucose treatments was that coding for integrin binding sialoprotein, *IBSP*.

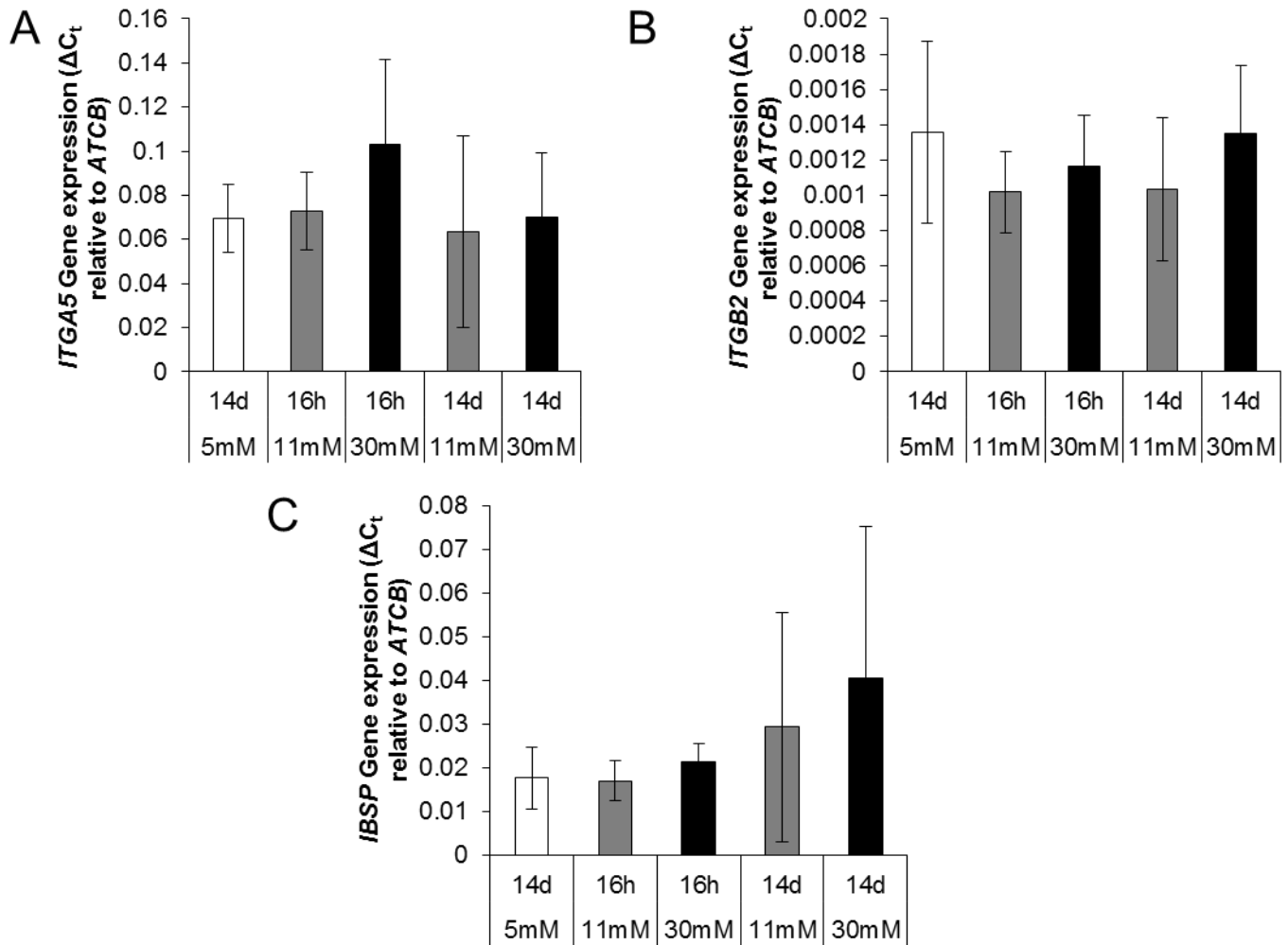


Figure 6.15. As a follow-up to the assessment of the effects of high glucose exposure on cell adhesion in chondrocytes, gene expression of some key genes involved in cell adhesion were assessed through targeted gene expression assessment using qPCR. No significant differential expression was observed in *ITGA5* (A), *ITGB2* (B) or *IBSP* (C) following exposure to high glucose. Data (n = 3) is shown as mean \pm SD.

After assessing the expression of these genes in chondrocytes following the high glucose treatments, it was apparent that these effects are not supported by qPCR data, as can be seen from Figure 6.15A-C.

6.6 Discussion

Based upon the findings of this study, it would appear that the effects of high glucose exposure on the DNA methylation of chondrocytes are relatively modest. The microarray data was unable to highlight more than one differentially methylated CpG locus within the chondrocyte genome across the three chondrocyte cell samples used. The only CpG locus affected was one associated with the HOXB13 gene, but as was identified from replication qPCR experiments, the downstream gene expression of this gene was not affected by the differential methylation. This is supported by the lack of identification of this gene as significantly differentially expressed from the gene expression microarray data. An attempt to unify an effect on homeobox genes through assessment of HOXC9 expression found that this gene was also unaffected by the high glucose treatments. From this data it is apparent that the effects of the high glucose treatments on DNA methylation were too modest or variable to be observed from a sample group of this size ($n = 3$).

The robustness of the chondrocyte methylome to the effects of high glucose exposure may correlate with an earlier identification of an apparent ability of chondrocytes to block uptake of glucose following long term exposure (30mM, 14 days, Figure 3.01). The environment in which chondrocytes exist, within the joint space and relatively isolated from a direct mode of glucose delivery (vasculature within the synovial lining and subchondral bone), may present an image of *in vivo* chondrocytes as relatively high-glucose naïve cells. Naivety to high-glucose exposure may have resulted in a lack of established response to high-glucose effects, and thus any resultant epigenetic effects may in fact be subverted as, for example, has been seen in the present study (Table 6.01).

More significant results were identified when assessing the whole transcriptome of chondrocytes after exposure to the different high glucose treatments. There were interesting findings from the whole transcriptome microarray data. Particularly, as can be seen from both the PCA plot of Figure 6.04A and the dendrogram of Figure 6.04B, cells from one of the samples would appear to be relatively phenotypically distinct from the cells of the other two samples. While this sample may have been omitted from the analysis had the sample size been larger, the decision was taken to retain this sample in the analysis in order to maintain statistical power. It is however likely that the inclusion of this sample in the analysis could affect the statistical significance of individual differentially expressed transcript data in the final results.

TXNIP has previously been associated with high glucose exposure of hepatocytes (257). The mechanism of action of *TXNIP* in hepatocytes has been shown to be to increase apoptosis, oxidative stress, *TXNIP* was linked to the secondary effects of hyperglycaemia experienced in diabetes, being shown to play a key role in enhanced oxidative stress and DNA damage in retinal pericytes as a result of high glucose exposure (161). *TXNIP* overexpression in diabetes has also been implicated in high-glucose mediated deterioration of the retina, through oxidative damage to retinal pericytes and neuroglia (258). The identification of a glucose-mediated upregulation of *TXNIP* in chondrocytes could suggest that similar effects would be expected to be observed in cartilage as a result of the secondary effects of diabetes. Further research would be required in order to clarify this potential link.

The high-glucose mediated involvement of catabolic processes as can be construed from Figure 6.11B is an interesting result of the gene ontology analysis of the significantly differentially expressed gene set returned from the long term 11mM glucose treated chondrocytes. There is a highly evidenced role of catabolic processes in ageing (259). On the topic of potential effects of catabolic processes in age-related musculoskeletal diseases,

an increase in MMP3 was found in conjunction with osteoarthritic progression in rabbits (260).

Any effect of high glucose exposure on enhancing or dampening these processes could hint at an effect of life-long high blood glucose events on ageing. High glucose has already been implicated in having a role in the modulation of anabolic and catabolic gene expression in osteoarthritic cartilage chondrocytes by Rosa et al (134).

It is interesting that the gene encoding for prolargin (*PRELP*) was upregulated in both long-term high glucose treatments. Prolargin has been shown to be responsible for connective tissue matrix assembly, particularly in the assembling of collagen type II within cartilage. In each of these treatments, the upregulation of *PRELP* was accompanied by the upregulation of genes relating to a different connective tissue matrix protein. In the case of chondrocytes treated with 30mM glucose for 14 days, the upregulation of *PRELP* was accompanied by the upregulation of the gene for collagen type XV, alpha 1 (*COL15A1*). In the case of the chondrocytes treated with 11mM glucose for 14 days, the upregulation of *PRELP* was accompanied by the upregulation of the gene for lumican (*LUM*). Collagen type XV, alpha 1 encodes for the alpha chain of collagen type XV, which is widely expressed within connective tissues, with particular localisation within basement membranes. While little is known of a role for *COL15A1* in the musculoskeletal system, a *COL15A1* deficiency has been associated with muscle and microvessel deterioration (261). Lumican has a more prominent and well defined role within the musculoskeletal system (262), and is a proteoglycan found in cartilage. Kafienah *et al* have, however suggested that disproportionate lumican within the extracellular matrix can inhibit deposition and incorporation of collagen within the matrix, thus reducing the biomechanical integrity of the tissue (263). An interesting route for further study could include an assessment of high-glucose mediated upregulation of *PRELP*, and whether high-glucose exposure plays a dose-dependent role in selecting matrix assembly proteins within connective tissue. From the results of the gene expression microarray experiments in this study, it would appear that

after long-term 11mM glucose exposure, a *PRELP-LUM* extracellular matrix assembly axis may potentially be indicated. Contrastingly, after long-term 30mM glucose exposure, a *PRELP-COL15A1* matrix assembly axis may potentially be indicated. The lack of association of *COL15A1* to the musculoskeletal system by comparison to *LUM* could potentially suggest a more profound departure from the typical articular cartilage composition with increasing dose of glucose exposure to chondrocytes, although for this to be the case may require genes for a greater number of extracellular matrix molecules to be affected.

A high-glucose mediated effect on matrix-associated processes is further supported by the detection of, after long term 30mM treatment, a significant upregulation of *MMP3*. *MMP3* is the gene coding for matrix metalloproteinase 3, a pre-enzyme responsible for matrix catabolism. An increase in expression of this gene because of high glucose could suggest an increase in matrix catabolism. A simultaneous increase in a *PRELP-COL15A1* could potentially suggest a reactionary increase in matrix assembly, although with the primary component of articular cartilage being collagen type II, the post-high-glucose matrix assembly could suffer impaired biomechanical functionality. Such a reaction could, in extreme cases, result in the cartilaginous extracellular matrix being unsuitable for purpose. Karlsson et al identified *COL15A1* as a potential new candidate gene for consideration in the aetiology and progression of osteoarthritis (264). *PRELP* has long been described as a protein associated with the extracellular matrix of articular cartilage (265), and following destabilization of the medial meniscus in mice, *Prelp* gene expression was among those that was increased (266). These could provide support for a potential role of a *COL15A1-PRELP* axis in dysregulation of articular cartilage matrix, although in both cases further targeted experimentation would be required before any link can be corroborated.

It should be said that while this is an interpretation of the gene expression microarray data, these findings were not supported by the replication experiments using qPCR. While the gene expression microarray uses probes for many transcripts to identify expression of each gene, the data can be highly affected by preprocessing methods and highly influenced by

the presence of outliers. In qPCR, only a single primer pair targeted against a single transcript was used for each gene throughout this study, and thus expression data was inferred from the detection of different amounts of a single transcript for each gene relative to that of a housekeeping gene (*ACTB*). There are potential drawbacks to each method, and thus further study is likely required to determine the correct result.

The data available from the principal component analysis in Figure 6.04A suggests that, in the case of the chondrocytes treated with 11mM glucose for 14 days, the treatment appears to be the primary driver of variability in two out of the three samples. This treatment is relatively modest by comparison to the more commonly used, and less physiologically relevant, 30mM treatment. That the variability in the gene expression of these cells is such that the treatment group is more of a driver on variability than donor is interesting. This could suggest that more physiological high glucose levels are sufficient to cause a shift in the transcriptomic profile of chondrocytes after long term exposure.

The gene for cathepsin H (*CTSH*) was reduced after both treatment with 11mM and 30mM glucose for 14 days. Interestingly, as discussed in Chapter 5, *CTSH* was also affected in synoviocytes after exposure to high glucose and this reproducibility across different cells from the musculoskeletal system is interesting. Cathepsins are proteins that are involved in lysosomal proteolysis and expression of cathepsin H is widely distributed through the body. Cathepsins have already been investigated in relation to diabetic high glucose, and advanced glycation end product exposure within the kidney (267). A role for cathepsins and lysosomal protein degradation has also been suggested in the ageing of the central nervous system (268). Protein turnover is a key topic in the field of musculoskeletal biology, and the combined effect of high glucose on cathepsin H synthesis and ribosomal proteins as shown in Figure 6.07 and Figure 6.11 could suggest an important role for glucose in mediating protein synthesis and turnover in a system wherein the composition of the proteinaceous extracellular matrix is paramount to the correct biomechanical functioning of the tissue.

As was the case in synoviocytes as discussed in Chapter 5, there would appear to be a variable effect of high glucose exposure on the expression of histone proteins. This is perhaps an additional reproducible effect of high glucose on cells within the musculoskeletal system and would present an additional potential mechanism for glucose-mediated epigenetic changes within these cells. Further experimentation would be interesting in the area of high-glucose mediated histone modifications.

While the low sample size used in this study has limited the conclusions that can be drawn about the exact effects and the mechanisms potentially affected in chondrocytes after high glucose exposure, this data should act as a suitable primer for further research into the effects of long term high glucose exposure on chondrocytes.

7. General Discussion

7.1 Glucose uptake is affected following long-term high glucose exposure of human chondrocytes and human synoviocytes

A significant reduction in glucose uptake was observed in both chondrocytes and synoviocytes following long term high glucose treatment (Figure 3.01 and Figure 3.08). While a potential mechanism remains to be elucidated, the reduced glucose uptake was not caused by a glucose-mediated reduction in cellularity (Figure 3.06 and Figure 3.13), whether through oxidative DNA damage-mediated (Figure 4.09 and Figure 4.11), or metabolic/acidosis-mediated apoptosis and necrosis (Figures 3.07, 3.14 and 3.15) or loss of cell adhesion properties (Figure 5.18 and Figure 6.14). A targeted glucose transporter gene expression assessment also failed to identify a direct link between the reduction in glucose uptake and a reduction in glucose transporter expression (Figures 3.03, 3.04, 3.05, 3.10, 3.11 and 3.12).

Since a corresponding increase in intracellular glucose was not identified by nuclear magnetic resonance spectroscopy (Figure 3.02B and Figure 3.09B), it would appear that the reduction in glucose uptake was not caused by an intracellular saturation of glucose. The exact period over which glucose was transported across the cell membrane, and the time after which glucose uptake was reduced, was not assessed during this study. Since there was no observable increase in intracellular glucose after 16 hours of high glucose exposure (Figure 3.02B and Figure 3.09B), even after a tenable increase in glucose uptake during this time period (Figure 3.01A and Figure 3.08A), it would appear that any surplus intracellular glucose was metabolised prior to assessment. Metabolism of this intracellular glucose appeared to affect the level of ATP in these cells differently depending upon the glucose dose and time period of exposure (Figures 3.07 and Figure 3.14). A significant increase in ATP in both cells after 30mM glucose for 14 days could suggest a metabolic shift in these cells to carry out more glucose metabolism. The increased glucose metabolism may have occurred via the less-efficient route of enhanced glycolysis, due to an enhanced availability of glucose over the treatment period (14 days). The reduction in glucose uptake, could

however, suggest a reduced intracellular glucose exposure during at least the final 16 hour portion of this treatment period (the beginning of which the final cell culture media was changed and after which the level of glucose uptake was measured and compared to that of the other treatment groups). This may have caused the chondrocytes and synoviocytes in the 30mM 14 days treatment to favour a more efficient form of glucose metabolism, via oxidative phosphorylation, than is carried out in the cells of the other treatment groups, and may explain the increase in ATP observed. A higher rate of oxidative phosphorylation may, however, cause the cells to produce a greater number of reactive oxygen species, as the result of the electron transport chain reaction used to produce ATP. This higher rate of oxidative phosphorylation may, therefore place the cells at a greater risk of the effects of oxidative stress.

Intracellular glucose was not significantly different in any of the treatment groups, suggesting that a consequent normalisation of intracellular glucose to a baseline is performed quickly in both cell types (maximally within the 16 hour window between the final change of cell culture media and the extraction of cell lysate). An observed increase in glucose uptake in the cells exposed to high glucose for 16 hours would suggest that enhanced glucose metabolism occurs in these treatment groups, placing the cells at risk of the acidosis effects of enhanced glycolysis, or the plethora of secondary effects associated with alternate glucose metabolism pathways discussed in the Introduction. This is not explained by the increase of ATP observed after 16 hour exposure of synoviocytes to 11mM high glucose.

There would appear to be a cellprotective reduction in glucose uptake following the exposure of chondrocytes and synoviocytes to 30mM glucose. In the normal physiology of the body, cells and tissues are exposed to high levels of blood glucose for only a short time period following a glucose load. A reactionary reduction of glucose uptake shown in this study could indicate the toxic potential of glucose, and the danger of transient spikes in glucose exposure. Such transient dietary spikes, as observed in normal physiological

systems following a high glucose load, could have a cumulative effect over the period of a lifetime.

The cells and tissues of those suffering from diabetes have an increased likelihood of longer exposure times to high blood glucose, and as such may experience what appear to be celluloprotective reactions observed in the cells of this study. Over time, such celluloprotective reactions may result in secondary adverse effects, such as increased oxidative stress as described. Oxidative stress is known to be increased in specific cell types of diabetes sufferers, and has been attributed to an increased exposure to glucose. The results of this study could suggest that at least a portion of this increased oxidative stress may be attributed to a metabolic shift in glucose metabolism following a celluloprotective reduction in glucose uptake.

It should be said that an increase in oxidative stress was not observed in these cells with the methods used in this study. The use of 2-Dichlorofluorescein diacetate as a lone measure of oxidative stress does have its limitations, since as a measure of reactive oxygen species, the contribution of said reactive oxygen species in causing oxidative stress are not observed and solid conclusions on which cannot be drawn.

Future work may look to develop upon the results of this study by further investigating the metabolic shift in cells exposed to long term high glucose indicated, and whether there are effects of this observed metabolic shift on the levels of oxidative stress in these cells. A contribution of oxidative stress to the secondary effects observed in the cells of diabetes sufferers could help to provide a fuller picture of secondary pathologies associated with this disease.

7.2 Transient high glucose may cause DNA damage and affect the cell cycle in human chondrocytes and human synoviocytes

After an initial indication from gene expression microarray data implicating DNA damage following transient high glucose exposure (30mM, 48 hours) of synoviocytes (Figures 4.06

and 4.07), follow-up functional assays failed to identify any such effects (Figure 4.09) and qPCR showed no significant difference in the gene expression of DNA damage markers (Figure 4.08).

The results of this study do however provide support for a role of high glucose affecting the cell cycle of chondrocytes and synoviocytes, with gene expression data from both cell types identifying numerous genes involved in various cell cycle processes (Table 4.02A and Figure 4.13). This was supported by an affect in synoviocytes of high glucose exposure (15mM and 25mM) on the rate of proliferation (Figure 4.12) with a near-significant equivalent effect being found in chondrocytes (15mM, Figure 4.14).

The implication of high glucose in causing oxidative DNA damage is highly supported in the literature (152, 161, 162, 168, 194). Persistent high blood glucose-mediated DNA damage, as an effect of type-II diabetes mellitus, has been implicated in a number of secondary pathologies including microangiopathies causing, for example, nephropathy(44, 81, 99) and retinopathy (81, 161, 168, 269). The vascular nature of microangiopathies indicates a relevance of immediate contact with blood glucose. The avascular environment in which chondrocytes naturally reside means that, while studies have indicated a concurrent increase in synovial fluid glucose concentration following hyperglycaemia, there is no published data known at this time describing synovial fluid glucose concentrations following a high glucose load in humans, which may be indicative of the unfeasibility of such a study. As such, while the highly vascularised synovium may be susceptible to similar DNA-damage induced microvascular complications following repeated high glucose exposure, the lack of supporting evidence of synovial fluid glucose concentrations in humans makes it difficult to suggest whether articular cartilage might face a similar risk *in vivo*.

An observed effect of high glucose exposure on the cell cycle, including an indication that high glucose caused enhanced proliferation in synoviocytes (and also potentially in chondrocytes), might provide a link between high glucose exposure and musculoskeletal

pathologies *in vivo* which could be considered a candidate for further study. Enhanced proliferation over time may accelerate the onset of replicative senescence and as such accelerate the rate at which cells reach their natural proliferative end point. Whether there is a potential role of replicative senescence in ageing has been the subject of several prior studies (82, 259, 270-272).

In both the synovium and in cartilage, premature senescence of synoviocytes and chondrocytes respectively could potentially have deleterious effects on the maintenance of such tissues which carry functions critical to the healthy functioning of articulating joints. A loss of function of the synovium brought about by premature replicative senescence of synoviocytes could potentially affect the filtration of substances entering the synovial fluid, thus altering the constituents of the primary source of nutrients for chondrocytes within articular cartilage. Senescence-induced loss of the ability of chondrocytes to maintain their extracellular matrix composition could cause a reduced biomechanical integrity of a vital buffering tissue acting to support the subchondral bone against wear. In either case, a high-glucose induced premature replicative senescence, which is time- and therefore potentially age-related, could provide a link between high glucose exposure of musculoskeletal tissues and accelerated ageing, together with premature loss of function and the onset and progression of age-related musculoskeletal pathologies.

Further study into the effects of high glucose exposure on chondrocyte and synoviocyte senescence, using for example functional assays and markers for senescence, may be able to build upon the data provided in the present study.

7.3 Transient moderate high glucose has the potential to affect the methylome of human synoviocytes

A significant effect of moderate high glucose (11mM) was observed on the DNA methylation age of synoviocytes following both short term (16 hour) and long term (14 day) exposure (Figure 5.01). This was an interesting contrast to the higher glucose dosage (30mM), which

showed less of an effect. More interestingly, it was the short term moderate high glucose exposure which was observed to have the largest effect on methylation of CpG sites in synoviocytes (Table 5.01).

As previously described, the standard high glucose concentration used throughout the literature appears to be 30mM, which carries less clinical relevance than a more physiological high glucose concentration, like 11mM. This preference for a higher dose may be driven by a greater severity of effects observed, compared to lower, more physiological doses. The results of this study indicate that, while providing results more readily transferrable to a clinical setting, the use of a lower high glucose concentration may provide a distinct, and sometimes more profound, effects profile.

The interesting effects observed following exposure of synoviocytes to 11mM glucose could indicate a heightened sensitivity of cells to concentrations within a physiological range. This could provide a window of hypersensitivity permitting a greater profundity of effects inside this realistic range of expected high glucose concentrations. Such hypersensitivity could be linked to an evolutionary adaptation to a regular exposure to glucose concentrations within said window, and may relate to the highly sensitive glycaemic control mechanisms in place to regulate blood glucose levels within a particular range. Synovium, being a highly vascularised tissue, could be sensitive to such small deviations from a normal range due to these glycaemic control measures.

Future study might look to assess the effects of high glucose concentrations which carry even further transferability to the clinic, such as for example, concentrations around 7mM which are sufficient to elucidate an insulinaemic response and as such might be considered to be within a range wherein large effects may be observed.

7.4 The chondrocyte methylome is robust to the effects of high glucose, but long term exposure could affect the chondrocyte transcriptome

It would appear from the results of this study that the chondrocyte methylome is robust to the effects of high glucose exposure (Table 6.01). Long term high glucose does, however, appear to have an effect on the transcriptomic profile of these cells (Table 6.01), which may include effects on functional proteins associated with the musculoskeletal system, and may also include histone proteins.

There have been a number of previous studies reporting on the effects of high glucose on gene expression within chondrocytes (108, 128-130, 134, 155, 273), although a study publishing a transcriptomic profiling of chondrocytes following both long term and short term high glucose exposure times has yet to be identified. As such, the length of high glucose exposure used in the present study may act to identify effects that occur outside the boundaries of experimental feasibility for other studies.

As discussed in 7.3 above, many of the currently known mechanisms indicating an adaptive sensitivity to high glucose relate to the vascular system which faces primary exposure to glucose increases following a high glucose load. The avascular nature of chondrocytes, and a potential naivety of chondrocytes to such high glucose concentrations, may cause chondrocytes to lack the hypersensitivity to high glucose exposure observed elsewhere in the body. This lack of immediate sensitivity may be a causal factor in the effects on gene expression observed after both of the long-term high glucose treatments in these cells.

Future study might look to investigate the likelihood of exposure of chondrocytes to high levels of glucose from the synovial fluid in humans. This may indicate the propensity for high glucose to have an effect on these cells *in vivo*.

7.5 Conclusions

The implications of high glucose exposure in causing deleterious effects within the musculoskeletal system presents an interesting topic for discussion, supported by the results

of the present study, which was able to investigate the effects of both transitory and protracted high glucose exposure times.

While a greater sample size would add to the confidence of the conclusions drawn from the results of the present study, there would appear to be interesting effects of both transient high glucose exposure and long term high glucose exposure on both chondrocytes and synoviocytes. An indication that both a very large high glucose exposure and a more physiologically plausible high glucose exposure can have observable effects on the methylome and transcriptome of these cells also provides a finding that might support more prominent use of physiological high glucose concentrations in future studies.

7.6 Limitations

7.6.1 Sample size

The results of this study primarily show that the effects of the chosen doses of high glucose on human chondrocytes and human synoviocytes are relatively modest. The study itself looked to investigate the effects of a relatively small departure from the physiological norm for these cells, in raising the concentration of a molecule to which the cells are very well adapted to. Small effects may, however act to accumulate over time which, when extended over a lifetime, may provide a cause for concern. Any small effects may therefore possess great biological significance, but in the present study, small sample number may have hindered the identification of the most key biologically significant modest effects.

A key limitation of the present study was sample number, which in many of the experiments, may not have been sufficiently numerous to identify a statistical significant result in support of a hypothesis. Most of the experiments of the present study used a sample size of “n = 3”. In the case of microarray data, the vast number of probes being simultaneously assessed for significant pairwise differences required a stringent false discovery rate correction (Benjamini-Hochberg) of p-values. While the number of unnecessary probes was kept to a minimum during microarray data analysis, the large number of remaining probes being

assessed caused a particularly harsh effect of multiplicity correction on the significance of the results. This was likely exacerbated by a low sample number. An example power calculation was performed as discussed in 5.5.7, which identified an optimum estimated sample size of 10, to achieve a satisfactory statistical power. While addition of further samples in the future might be useful in obtaining the required sample size, microarray experiments are highly sensitive to batch effect, and thus any attempt to achieve an optimal statistical power in the future would preferably be performed on at least 10 samples and carried out at the same time, as was the case for the sample group of the present study.

7.6.2 Transcriptomic analysis

Throughout this study, validating microarray data using more targeted approaches proved difficult. Microarray data analysis typically uses luminescence values detected within an image file of a microarray chip to assess the relative quantities of hundreds of thousands of transcripts. The use of such data carries limitations inherent in the technology, wherein during processing, large areas of a microarray chip (relatively speaking) can be appear “dimmer” than the remainder of the array. Any such spacial artefacts naturally hinder the measurement of countless probes located within and surrounding such spacial anomalies. There are a number of highly robust analysis techniques available to pre-process and normalise this raw data prior to analysis, such as the smoothing of such anomalies using neighbourhood matrices and within-chip and between-chip averaging to flatten defects in the data distributions. Accounting for such technical anomalies can inherently dampen other, perhaps more “real” effects. Larger sample sizes than that used for the present study may be more robust to such limitations. Microarray data does, however, carry a number of advantages, including the invariably large representation of genomic or transcriptomic loci within an array compared to more targeted approaches. A transcriptomic array could provide the assessment of a number of transcripts for a single gene, whereas more targeted approaches such as qPCR may only consider a single portion of a transcript. The “systems” perspective provided by microarray data also acts to mitigate the described effects on what

may be a small number of probes relatively to the full representation of genomic and transcriptomic loci on an array.

7.6.3 Cell models

The present study used primary cells and as such a number of considerations, including altered phenotype with advanced passaging and potential replicative senescence, meant that cell passage number were kept to a minimum throughout the study. This presented a limited number of cells from which to obtain results compared to studies using more readily available cells such as cell lines.

The present study used exclusively human cells in order to maximise the potential clinical relevance of any conclusions drawn from the data. This imparted a limitation common to the use of human samples, namely inter-individual variability. While the cell samples were mostly matched according to donor race, age, and gender as can be seen from Table 2.1, the natural variability between samples, particularly relating to genome and transcriptome, likely had a profound effect on the between-sample variation observed within treatment groups. The inter-individual variability between the different cell samples likely compounded the effects of low sample number on the level of statistical significance observed.

While the present study used exclusively human cells to maximise clinical relevance, the use of cell cultures comprising a single cell type as a model for complex systems carries obvious limitations. There would, however, be strict regulatory procedure and clear ethical concerns regarding the use of a high-glucose load to study the effects on transcriptome and methylome relating to ageing in humans. A possible solution could be the use of animal models as has been used extensively in previous studies, but carries a reduced relevance to a human musculoskeletal ageing. Current models of the human musculoskeletal system use animal models such as those in, *inter alia*, sheep, pigs and horses. The difference in the diet of these species compared to that of humans would need to be considered in any assessment of the effects of high glucose. Cells such as these may be high glucose naïve,

relative to corresponding cells from the human musculoskeletal system, and as such a response to a high glucose load may not be directly relatable to that expected to occur in humans cells. Conversely, an observed effect of glucose may be lower in humans due to prior exposure to large quantities of dietary glucose.

7.6.4 High glucose treatments

The high glucose treatments used in the present study have been used extensively in previous similar studies assessing the effects of high glucose (108, 130, 150-154, 157, 159, 168, 169, 274). The use of 30mM glucose is the most widely used concentration in the literature, although this does have the least clinical relevance based on the normal physiological high blood glucose levels that would typically be experienced in a healthy individual. 11mM glucose has been used in some studies (152, 153) aiming for physiological relevance, since this concentration provides an upper limit of blood glucose concentration experienced in an individual immediately following a high glucose load. It could be said that each of these concentrations exceed that experienced by most individuals and that a most physiologically normal concentration of high glucose would be approximately 7mM. This study does, however, act as a primer for further research and as such used the high glucose concentrations of 11mM and 30mM in an attempted to assess the potential for high glucose to have a measureable effect in human chondrocytes and synoviocytes.

The normal glucose control of 5.5mM is also a literature standard (150, 152, 154-157, 159-166, 274) and does represent a normal physiological level of blood glucose in a healthy individual. This study did not attempt to assess the effects of a reduced glucose concentration compared to a normal glucose control.

7.6.5 Treatment periods

The treatment periods used in the present study ranged from 1 hour to 14 days and were used to assess the potential effects of transient, short-term and long-term exposure to high glucose in chondrocyte and synoviocytes. While a diverse spectrum of time periods for

treatment was explored, a number of the experiments may have benefitted from additional measurements at alternate time points. As an example, an investigation into the effects of high glucose on glucose uptake in chondrocytes and synoviocytes was unable to provide clarity on when the majority of glucose was taken up into cells following exposure to high glucose. Additional time points during specific experiments such as these may have provided additional insight into this.

7.6.6 Functional assays

The nature of the long term high glucose treatment, and the uncertainty surrounding the likelihood that this treatment may affect cell proliferation, provided a limitation on many of the functional assays performed since, following said high glucose treatments, cell number could not accurately be accounted for and subsequently controlled or normalised. As such, many of the functional assays required a trypsinisation step to permit the controlled seeding of experimental plates prior to performing the assays. This provided the limitation that, while the functional assays attempted to assess the effects of high glucose, the effects of trypsin may have acted to compound the results. This was controlled as much as was feasible by applying the same trypsinisation protocol throughout, including an equal exposure to trypsin.

7.6.6.1 Cell adhesion assay

The cell adhesion assay used aimed to test the ability of cells to re-adhere to cell culture plastic following trypsinisation after high glucose exposure. While this assessed the ability of the cells to produce proteins associated with cell-matrix adhesion following high glucose exposure, this assay may not have assessed the ability of cells to produce cell-matrix adhesion proteins during glucose treatment.

7.6.6.2 DNA damage assay

DNA damage was assessed using single cell gel electrophoresis. The protocol for this assay included a large number of steps at which there was the potential to induce technical variation in the samples. This was due to the delicate nature of DNA once isolated within an

agarose gel. A lengthy optimisation process enabled the minimisation of technically-induced variation in the results observed using this assay.

7.6.6.3 ATP assay

ATP was assessed using luminescence. The assessment of ATP was useful in identifying the metabolic state of a controlled quantity of cells following high glucose treatments. It was, however, difficult to speculate the cause of the significant differences in ATP concentration observed following the different high glucose treatments. A further assessment of markers of glycolysis or oxidative phosphorylation may have acted to clarify this.

7.7 Further work

This study may provide the basis for subsequent research into the effects of high glucose on human musculoskeletal cells, with a particular emphasis on the epigenetic and transcriptomic effects of high glucose exposure. While the present study was not able to clearly confirm that high glucose does affect the methylome of these cells, methylation microarray results indicate an interesting subject for further validation in that it appears that short term exposure to 11mM glucose has a large, transitory effect on the methylome of human synoviocytes.

Another epigenetic modification which may be found to be affected by high glucose exposure may be the glycation of histone proteins, particularly via O-glycosylation. This could have more tangible mechanisms than a high-glucose-mediated effect on DNA methylation, since enhanced glycation has been directly linked to surplus glucose exposure (47).

Additional concentrations of high-glucose, particularly around 7mM glucose, may indicate a more physiologically relevant effect of high glucose on the epigenome and transcriptome of chondrocytes and synoviocytes.

Further samples may be needed to improve upon the sample size of the current study, potentially providing an improved statistical significance of particular results.

The use of cell models in the current study could act as an early-stage primer for more relevant experiments to human musculoskeletal ageing in the future, such as those including human tissue or even clinical intervention studies.

8. Appendices

8.1 Appendices

The following data was obtained during an MRes project (Tregilgas, L. *Investigating the effects of transient high glucose exposure on musculoskeletal cells*) prior to commencement of the present study.

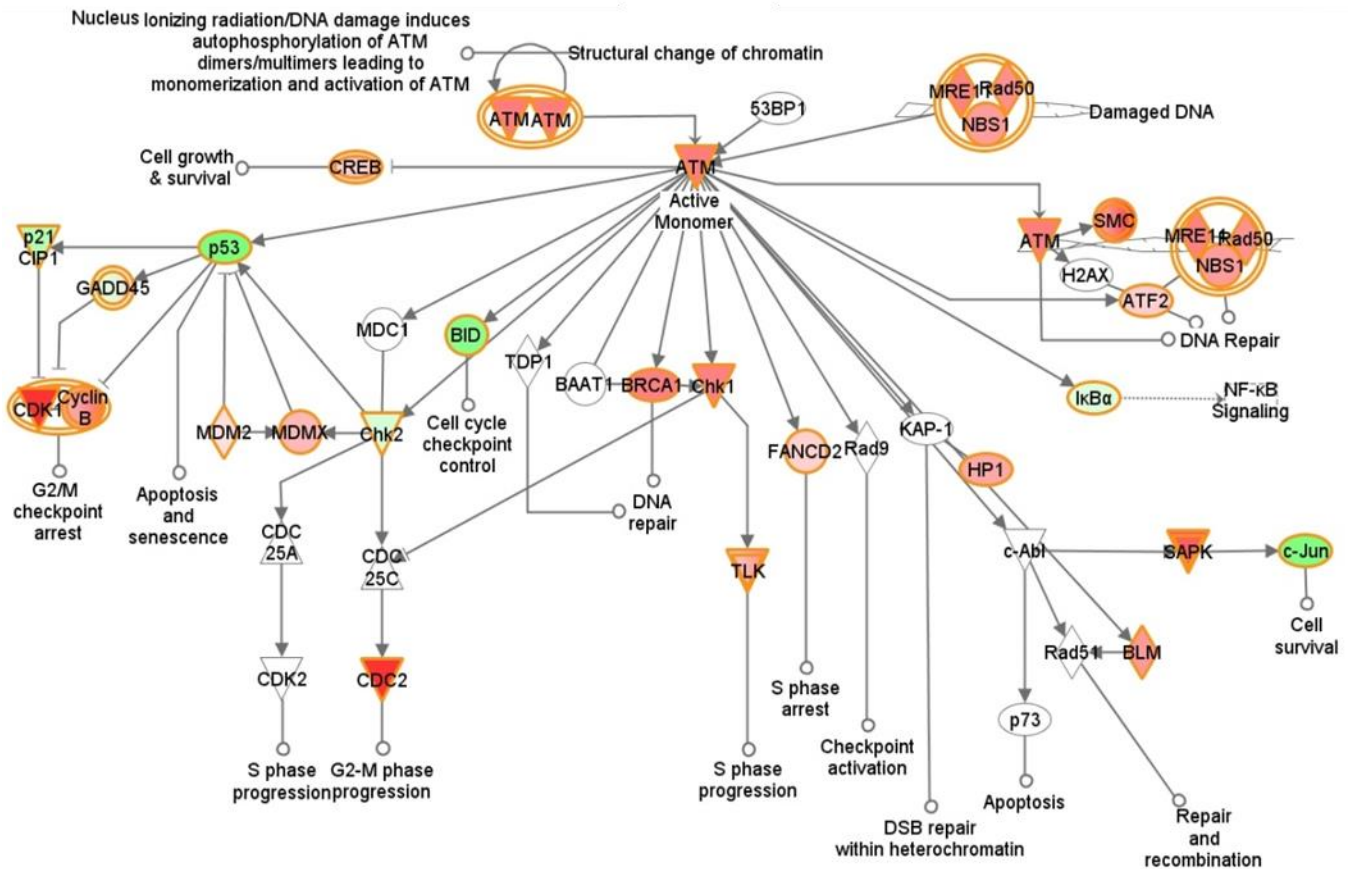


Figure. 8.01. Preliminary microarray analysis showed that one of the most significantly affected pathways in synoviocytes was the ATM signalling pathway shown (IPA, Ingenuity, p-value = 1.18E-05), where red signifies increased expression, and green signifies decreased expression in response to high glucose. DNA damage response indicators ATR and ATM were up-regulated in response to high glucose, along with DNA repair markers such as BRCA1. The protective cell-cycle arrest mechanism normally occurring via p53/p21 appears to be inhibited, with increased expression of cyclin B/CDK1 complex.

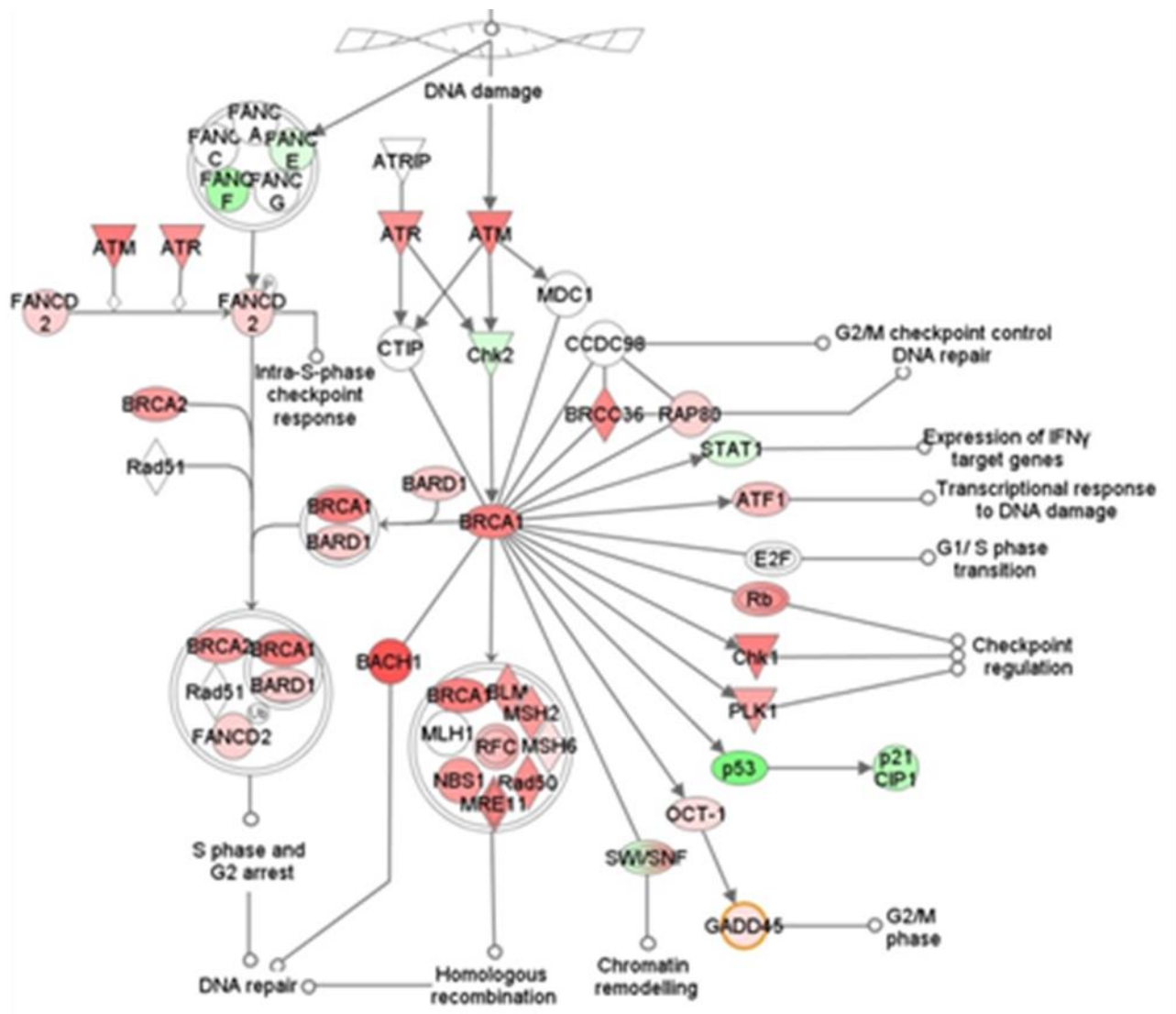


Figure. 8.02. From Figure. 8.01 it can be seen that BRCA1 is upregulated, which could potentially be due to an activation of DNA damage markers such as ATR and ATM. The above pathway in synoviocytes (IPA, Ingenuity) supports the concept that a high-glucose mediated increase in DNA damage is followed by a consequential increase in expression of DNA repair markers. Interestingly it appears that cell cycle arrest-associated genes such as p53, and p21/CIP1 are contrastingly downregulated.

9. Bibliography

9.1 References

- (1) Durrani, H. (2016) Healthcare and healthcare systems: inspiring progress and future prospects. *mHealth*. **2**, 3
- (2) Collaborators, G.B.D.C.M. (2016) Global, regional, national, and selected subnational levels of stillbirths, neonatal, infant, and under-5 mortality, 1980-2015: a systematic analysis for the Global Burden of Disease Study 2015. *Lancet*. **388**, 1725-1774
- (3) Mortality, G.B.D., and Causes of Death, C. (2016) Global, regional, and national life expectancy, all-cause mortality, and cause-specific mortality for 249 causes of death, 1980-2015: a systematic analysis for the Global Burden of Disease Study 2015. *Lancet*. **388**, 1459-1544
- (4) Bloom, D.E., Cafiero, E.T., Jané-Llopis, E., Abrahams-Gessel, S., Bloom, L.R., Fathima, S., Feigl, G., T., Mowafi, M., Pandya, A., Prettner, K., Rosenberg, L., Seligman, B., Stein, A.Z., & Weinstein, C. (2011) The Global Economic Burden of Non-Communicable Diseases. Geneva: World Economic Forum.
- (5) Anandacoomarasamy, A., Caterson, I., Sambrook, P., Fransen, M., and March, L. (2008) The impact of obesity on the musculoskeletal system. *International journal of obesity*. **32**, 211-222
- (6) de Magalhaes, J.P., Wuttke, D., Wood, S.H., Plank, M., and Vora, C. (2012) Genome-environment interactions that modulate aging: powerful targets for drug discovery. *Pharmacological reviews*. **64**, 88-101
- (7) Bifulco, M., and Caruso, M.G. (2007) From the gastronomic revolution to the new globesity epidemic. *Journal of the American Dietetic Association*. **107**, 2058-2060
- (8) Bray, G.A., Nielsen, S.J., and Popkin, B.M. (2004) Consumption of high-fructose corn syrup in beverages may play a role in the epidemic of obesity. *The American journal of clinical nutrition*. **79**, 537-543

- (9) Gaby, A.R. (2005) Adverse effects of dietary fructose. *Alternative medicine review : a journal of clinical therapeutic*. **10**, 294-306
- (10) Johnson, R.J., Segal, M.S., Sautin, Y., Nakagawa, T., Feig, D.I., Kang, D.H., Gersch, M.S., Benner, S., and Sanchez-Lozada, L.G. (2007) Potential role of sugar (fructose) in the epidemic of hypertension, obesity and the metabolic syndrome, diabetes, kidney disease, and cardiovascular disease. *The American journal of clinical nutrition*. **86**, 899-906
- (11) Keys, A., Menotti, A., Aravanis, C., Blackburn, H., Djordevic, B.S., Buzina, R., Dontas, A.S., Fidanza, F., Karvonen, M.J., Kimura, N., and et al. (1984) The seven countries study: 2,289 deaths in 15 years. *Preventive medicine*. **13**, 141-154
- (12) Keys, A. (1971) Sucrose in the diet and coronary heart disease. *Atherosclerosis*. **14**, 193-202
- (13) United States. Congress. Senate. Committee on Appropriations. Subcommittee on Agriculture Rural Development and Related Agencies. (1980) *Dietary guidelines for Americans : hearing before a subcommittee of the Committee on Appropriations, United States Senate, Ninety-sixth Congress, second session : special hearing, Department of Agriculture, Department of Health and Human Services, nondepartmental witnesses*, Washington: U.S. Govt. Print. Off. : for sale by the Supt. of Docs., U.S. Govt. Print. Off.
- (14) Khosrova, E. *Butter : a rich history*,
- (15) Keys, A. (1973) Letter: Sucrose in the diet and coronary heart disease. *Atherosclerosis*. **18**, 352
- (16) Yudkin, J. *Pure, white, and deadly : how sugar is killing us and what we can do to stop it*,
- (17) Stanhope, K.L. (2016) Sugar consumption, metabolic disease and obesity: The state of the controversy. *Critical reviews in clinical laboratory sciences*. **53**, 52-67

- (18) Tedstone, A., Targett, V., and Allen, R. (2015) Sugar Reduction: The evidence for action (Public Health England)ed^eds, *Obesity and healthy eating*.
- (19) Lustig, R.H. *Fat chance : beating the odds against sugar, processed food, obesity, and disease*,
- (20) Lustig, R.H., Schmidt, L.A., and Brindis, C.D. (2012) Public health: The toxic truth about sugar. *Nature*. **482**, 27-29
- (21) Caton, P.W., Nayuni, N.K., Khan, N.Q., Wood, E.G., and Corder, R. (2011) Fructose induces gluconeogenesis and lipogenesis through a SIRT1-dependent mechanism. *The Journal of endocrinology*. **208**, 273-283
- (22) UK, N.H.S. (2016) <https://www.nhs.uk/change4life-beta/sugar#TXmt8DYiBfk5m1xW.97>. In: Change4Life, ed^eds, *Sugar* Accessed: 25 Feb 2017.
- (23) Triggle, N. (2017) <http://www.bbc.co.uk/news/health-35824071>ed^eds, *Health*: BBC.
- (24) Farandos, N.M., Yetisen, A.K., Monteiro, M.J., Lowe, C.R., and Yun, S.H. (2015) Contact lens sensors in ocular diagnostics. *Advanced healthcare materials*. **4**, 792-810
- (25) Rippe, J.M., and Angelopoulos, T.J. (2013) Sucrose, high-fructose corn syrup, and fructose, their metabolism and potential health effects: what do we really know? *Advances in nutrition*. **4**, 236-245
- (26) Tounian, P., Schneiter, P., Henry, S., Jequier, E., and Tappy, L. (1994) Effects of infused fructose on endogenous glucose production, gluconeogenesis, and glycogen metabolism. *The American journal of physiology*. **267**, E710-717
- (27) Bjorkman, O., Crump, M., and Phillips, R.W. (1984) Intestinal metabolism of orally administered glucose and fructose in Yucatan miniature swine. *The Journal of nutrition*. **114**, 1413-1420

- (28) Tounian, P., Schneider, P., Henry, S., Delarue, J., and Tappy, L. (1997) Effects of dexamethasone on hepatic glucose production and fructose metabolism in healthy humans. *The American journal of physiology.* **273**, E315-320
- (29) Sun, S.Z., and Empie, M.W. (2012) Fructose metabolism in humans - what isotopic tracer studies tell us. *Nutrition & metabolism.* **9**, 89
- (30) Johnson, A.O., Lampson, M.A., and McGraw, T.E. (2001) A di-leucine sequence and a cluster of acidic amino acids are required for dynamic retention in the endosomal recycling compartment of fibroblasts. *Molecular biology of the cell.* **12**, 367-381
- (31) Huang, S., and Czech, M.P. (2007) The GLUT4 glucose transporter. *Cell metabolism.* **5**, 237-252
- (32) Schmidt, U., Briese, S., Leicht, K., Schurmann, A., Joost, H.G., and Al-Hasani, H. (2006) Endocytosis of the glucose transporter GLUT8 is mediated by interaction of a dileucine motif with the beta2-adaptin subunit of the AP-2 adaptor complex. *Journal of cell science.* **119**, 2321-2331
- (33) Erecinska, M., Deas, J., and Silver, I.A. (1995) The effect of pH on glycolysis and phosphofructokinase activity in cultured cells and synaptosomes. *Journal of neurochemistry.* **65**, 2765-2772
- (34) Wilson, D.K., Bohren, K.M., Gabbay, K.H., and Quiocho, F.A. (1992) An unlikely sugar substrate site in the 1.65 Å structure of the human aldose reductase holoenzyme implicated in diabetic complications. *Science.* **257**, 81-84
- (35) Brownlee, M. (2001) Biochemistry and molecular cell biology of diabetic complications. *Nature.* **414**, 813-820

- (36) Schleicher, E.D., Wagner, E., and Nerlich, A.G. (1997) Increased accumulation of the glycoxidation product N(epsilon)-(carboxymethyl)lysine in human tissues in diabetes and aging. *The Journal of clinical investigation*. **99**, 457-468
- (37) Charonis, A.S., Skubitz, A.P., Koliakos, G.G., Reger, L.A., Dege, J., Vogel, A.M., Wohlhueter, R., and Furcht, L.T. (1988) A novel synthetic peptide from the B1 chain of laminin with heparin-binding and cell adhesion-promoting activities. *The Journal of cell biology*. **107**, 1253-1260
- (38) Haitoglou, C.S., Tsilibary, E.C., Brownlee, M., and Charonis, A.S. (1992) Altered cellular interactions between endothelial cells and nonenzymatically glycosylated laminin/type IV collagen. *The Journal of biological chemistry*. **267**, 12404-12407
- (39) Paul, R.G., and Bailey, A.J. (1999) The effect of advanced glycation end-product formation upon cell-matrix interactions. *The international journal of biochemistry & cell biology*. **31**, 653-660
- (40) Abate, M., Schiavone, C., Pelotti, P., and Salini, V. (2011) Limited joint mobility (LJM) in elderly subjects with type II diabetes mellitus. *Archives of gerontology and geriatrics*. **53**, 135-140
- (41) Cagliero, E. (2003) Rheumatic manifestations of diabetes mellitus. *Current rheumatology reports*. **5**, 189-194
- (42) Chen, A.C., Temple, M.M., Ng, D.M., Verzijl, N., DeGroot, J., TeKoppele, J.M., and Sah, R.L. (2002) Induction of advanced glycation end products and alterations of the tensile properties of articular cartilage. *Arthritis and rheumatism*. **46**, 3212-3217
- (43) Berrou, J., Tostivint, I., Verrecchia, F., Berthier, C., Boulanger, E., Mauviel, A., Marti, H.P., Wautier, M.P., Wautier, J.L., Rondeau, E., and Hertig, A. (2009) Advanced glycation end products regulate extracellular matrix protein and protease expression by human glomerular mesangial cells. *International journal of molecular medicine*. **23**, 513-520

- (44) Das Evcimen, N., and King, G.L. (2007) The role of protein kinase C activation and the vascular complications of diabetes. *Pharmacological research*. **55**, 498-510
- (45) Ishii, H., Koya, D., and King, G.L. (1998) Protein kinase C activation and its role in the development of vascular complications in diabetes mellitus. *Journal of molecular medicine*. **76**, 21-31
- (46) Giaccari, A., Morviducci, L., Zorretta, D., Sbraccia, P., Leonetti, F., Caiola, S., Buongiorno, A., Bonadonna, R.C., and Tamburrano, G. (1995) In vivo effects of glucosamine on insulin secretion and insulin sensitivity in the rat: possible relevance to the maladaptive responses to chronic hyperglycaemia. *Diabetologia*. **38**, 518-524
- (47) Cortes, P., and Mogensen, C.E. (2006) *The diabetic kidney*, Totowa, N.J.: Humana Press
- (48) Giaccari, A., Sorice, G., and Muscogiuri, G. (2009) Glucose toxicity: the leading actor in the pathogenesis and clinical history of type 2 diabetes - mechanisms and potentials for treatment. *Nutrition, metabolism, and cardiovascular diseases : NMCD*. **19**, 365-377
- (49) Marshall, S., Bacote, V., and Traxinger, R.R. (1991) Discovery of a metabolic pathway mediating glucose-induced desensitization of the glucose transport system. Role of hexosamine biosynthesis in the induction of insulin resistance. *The Journal of biological chemistry*. **266**, 4706-4712
- (50) Hart, G.W. (2014) Three Decades of Research on O-GlcNAcylation - A Major Nutrient Sensor That Regulates Signaling, Transcription and Cellular Metabolism. *Frontiers in endocrinology*. **5**, 183
- (51) Zhang, S., Roche, K., Nasheuer, H.P., and Lowndes, N.F. (2011) Modification of histones by sugar beta-N-acetylglucosamine (GlcNAc) occurs on multiple residues, including histone H3 serine 10, and is cell cycle-regulated. *The Journal of biological chemistry*. **286**, 37483-37495

- (52) Dehennaut, V., Leprince, D., and Lefebvre, T. (2014) O-GlcNAcylation, an Epigenetic Mark. Focus on the Histone Code, TET Family Proteins, and Polycomb Group Proteins. *Frontiers in endocrinology*. **5**, 155
- (53) Lewis, B.A., and Hanover, J.A. (2014) O-GlcNAc and the epigenetic regulation of gene expression. *The Journal of biological chemistry*. **289**, 34440-34448
- (54) Carayannopoulos, M.O., Chi, M.M., Cui, Y., Pingsterhaus, J.M., McKnight, R.A., Mueckler, M., Devaskar, S.U., and Moley, K.H. (2000) GLUT8 is a glucose transporter responsible for insulin-stimulated glucose uptake in the blastocyst. *Proc Natl Acad Sci U S A*. **97**, 7313-7318
- (55) Gray, G.M., and Ingelfinger, F.J. (1966) Intestinal absorption of sucrose in man: interrelation of hydrolysis and monosaccharide product absorption. *The Journal of clinical investigation*. **45**, 388-398
- (56) Decombaz, J., Jentjens, R., Ith, M., Scheurer, E., Buehler, T., Jeukendrup, A., and Boesch, C. (2011) Fructose and galactose enhance postexercise human liver glycogen synthesis. *Medicine and science in sports and exercise*. **43**, 1964-1971
- (57) Chiavaroli, L., Ha, V., de Souza, R.J., Kendall, C.W., and Sievenpiper, J.L. (2014) Fructose in obesity and cognitive decline: is it the fructose or the excess energy? *Nutrition journal*. **13**, 27
- (58) Gugliucci, A. (2017) Formation of Fructose-Mediated Advanced Glycation End Products and Their Roles in Metabolic and Inflammatory Diseases. *Advances in nutrition*. **8**, 54-62
- (59) Kawasaki, T., Ogata, N., Akanuma, H., Sakai, T., Watanabe, H., Ichiyanagi, K., and Yamanouchi, T. (2004) Postprandial plasma fructose level is associated with retinopathy in patients with type 2 diabetes. *Metabolism: clinical and experimental*. **53**, 583-588

- (60) Kim, H.S., Paik, H.Y., Lee, K.U., Lee, H.K., and Min, H.K. (1988) Effects of several simple sugars on serum glucose and serum fructose levels in normal and diabetic subjects. *Diabetes research and clinical practice*. **4**, 281-287
- (61) Bray, G.A. (2007) How bad is fructose? *The American journal of clinical nutrition*. **86**, 895-896
- (62) Schalkwijk, C.G., Stehouwer, C.D., and van Hinsbergh, V.W. (2004) Fructose-mediated non-enzymatic glycation: sweet coupling or bad modification. *Diabetes/metabolism research and reviews*. **20**, 369-382
- (63) Anderson, G.H. (2007) Much ado about high-fructose corn syrup in beverages: the meat of the matter. *The American journal of clinical nutrition*. **86**, 1577-1578
- (64) Lakhan, S.E., and Kirchgessner, A. (2013) The emerging role of dietary fructose in obesity and cognitive decline. *Nutrition journal*. **12**, 114
- (65) Lecoultre, V., Egli, L., Carrel, G., Theytaz, F., Kreis, R., Schneiter, P., Boss, A., Zwygart, K., Le, K.A., Bortolotti, M., Boesch, C., and Tappy, L. (2013) Effects of fructose and glucose overfeeding on hepatic insulin sensitivity and intrahepatic lipids in healthy humans. *Obesity*. **21**, 782-785
- (66) Tappy, L., Egli, L., Lecoultre, V., and Schneider, P. (2013) Effects of fructose-containing caloric sweeteners on resting energy expenditure and energy efficiency: a review of human trials. *Nutrition & metabolism*. **10**, 54
- (67) Tappy, L., and Le, K.A. (2010) Metabolic effects of fructose and the worldwide increase in obesity. *Physiological reviews*. **90**, 23-46
- (68) Tappy, L., Le, K.A., Tran, C., and Paquot, N. (2010) Fructose and metabolic diseases: new findings, new questions. *Nutrition*. **26**, 1044-1049

- (69) Basciano, H., Federico, L., and Adeli, K. (2005) Fructose, insulin resistance, and metabolic dyslipidemia. *Nutrition & metabolism*. **2**, 5
- (70) Huang, D., Dhawan, T., Young, S., Yong, W.H., Boros, L.G., and Heaney, A.P. (2011) Fructose impairs glucose-induced hepatic triglyceride synthesis. *Lipids in health and disease*. **10**, 20
- (71) Basaranoglu, M., Basaranoglu, G., Sabuncu, T., and Senturk, H. (2013) Fructose as a key player in the development of fatty liver disease. *World journal of gastroenterology*. **19**, 1166-1172
- (72) Hallfrisch, J. (1990) Metabolic effects of dietary fructose. *Faseb J*. **4**, 2652-2660
- (73) Mayes, P.A. (1993) Intermediary metabolism of fructose. *The American journal of clinical nutrition*. **58**, 754S-765S
- (74) Tetri, L.H., Basaranoglu, M., Brunt, E.M., Yerian, L.M., and Neuschwander-Tetri, B.A. (2008) Severe NAFLD with hepatic necroinflammatory changes in mice fed trans fats and a high-fructose corn syrup equivalent. *American journal of physiology. Gastrointestinal and liver physiology*. **295**, G987-995
- (75) Rutledge, A.C., and Adeli, K. (2007) Fructose and the metabolic syndrome: pathophysiology and molecular mechanisms. *Nutrition reviews*. **65**, S13-23
- (76) Tappy, L., and Rosset, R. (2017) Fructose Metabolism from a Functional Perspective: Implications for Athletes. *Sports medicine*. **47**, 23-32
- (77) Sucha, R., Ulcova-Gallova, Z., Pavelkova-Seifertova, P., Krizanovska, K., Bouse, V., Svabek, L., Rokyta, P., Balvin, M., Pecen, L., and Rokyta, Z. (2002) [Fructose and glucose in follicular fluid and serum of women undergoing stimulation in an in vitro fertilization program]. *Ceska gynekologie*. **67**, 144-148

- (78) Levi, B., and Werman, M.J. (1998) Long-term fructose consumption accelerates glycation and several age-related variables in male rats. *The Journal of nutrition*. **128**, 1442-1449
- (79) Hers, H.G. (1952) [Liver fructokinase]. *Biochimica et biophysica acta*. **8**, 416-423
- (80) Paul, R.G., Avery, N.C., Slatter, D.A., Sims, T.J., and Bailey, A.J. (1998) Isolation and characterization of advanced glycation end products derived from the in vitro reaction of ribose and collagen. *The Biochemical journal*. **330 (Pt 3)**, 1241-1248
- (81) Klein, R. (1995) Hyperglycemia and microvascular and macrovascular disease in diabetes. *Diabetes care*. **18**, 258-268
- (82) Sell, D.R., and Monnier, V.M. (1989) Structure elucidation of a senescence cross-link from human extracellular matrix. Implication of pentoses in the aging process. *The Journal of biological chemistry*. **264**, 21597-21602
- (83) Reiser, K.M. (1998) Nonenzymatic glycation of collagen in aging and diabetes. *Proceedings of the Society for Experimental Biology and Medicine. Society for Experimental Biology and Medicine*. **218**, 23-37
- (84) Semba, R.D., Nicklett, E.J., and Ferrucci, L. (2010) Does accumulation of advanced glycation end products contribute to the aging phenotype? *The journals of gerontology. Series A, Biological sciences and medical sciences*. **65**, 963-975
- (85) DeGroot, J., Verzijl, N., Wenting-Van Wijk, M.J., Bank, R.A., Lafeber, F.P., Bijlsma, J.W., and TeKoppele, J.M. (2001) Age-related decrease in susceptibility of human articular cartilage to matrix metalloproteinase-mediated degradation: the role of advanced glycation end products. *Arthritis and rheumatism*. **44**, 2562-2571
- (86) Verzijl, N., DeGroot, J., Ben, Z.C., Brau-Benjamin, O., Maroudas, A., Bank, R.A., Mizrahi, J., Schalkwijk, C.G., Thorpe, S.R., Baynes, J.W., Bijlsma, J.W., Lafeber, F.P., and

TeKoppele, J.M. (2002) Crosslinking by advanced glycation end products increases the stiffness of the collagen network in human articular cartilage: a possible mechanism through which age is a risk factor for osteoarthritis. *Arthritis and rheumatism*. **46**, 114-123

(87) Takeuchi, M., Iwaki, M., Takino, J., Shirai, H., Kawakami, M., Bucala, R., and Yamagishi, S. (2010) Immunological detection of fructose-derived advanced glycation end-products. *Laboratory investigation; a journal of technical methods and pathology*. **90**, 1117-1127

(88) McPherson, J.D., Shilton, B.H., and Walton, D.J. (1988) Role of fructose in glycation and cross-linking of proteins. *Biochemistry*. **27**, 1901-1907

(89) Gabbay, K.H. (1975) Hyperglycemia, polyol metabolism, and complications of diabetes mellitus. *Annual review of medicine*. **26**, 521-536

(90) Gabbay, K.H. (1973) Role of sorbitol pathway in neuropathy. *Advances in metabolic disorders*. **2**, Suppl 2:417-432

(91) Jedziniak, J.A., Chylack, L.T., Jr., Cheng, H.M., Gillis, M.K., Kalustian, A.A., and Tung, W.H. (1981) The sorbitol pathway in the human lens: aldose reductase and polyol dehydrogenase. *Investigative ophthalmology & visual science*. **20**, 314-326

(92) Hamada, Y., Odagaki, Y., Sakakibara, F., Naruse, K., Koh, N., and Hotta, N. (1995) Effects of an aldose reductase inhibitor on erythrocyte fructose 3-phosphate and sorbitol 3-phosphate levels in diabetic patients. *Life sciences*. **57**, 23-29

(93) Ido, Y., Kilo, C., and Williamson, J.R. (1996) Interactions between the sorbitol pathway, non-enzymatic glycation, and diabetic vascular dysfunction. *Nephrology, dialysis, transplantation : official publication of the European Dialysis and Transplant Association - European Renal Association*. **11 Suppl 5**, 72-75

- (94) Verzijl, N., Bank, R.A., TeKoppele, J.M., and DeGroot, J. (2003) AGEing and osteoarthritis: a different perspective. *Current opinion in rheumatology*. **15**, 616-622
- (95) Schmidt, A.M., Hasu, M., Popov, D., Zhang, J.H., Chen, J., Yan, S.D., Brett, J., Cao, R., Kuwabara, K., Costache, G., and et al. (1994) Receptor for advanced glycation end products (AGEs) has a central role in vessel wall interactions and gene activation in response to circulating AGE proteins. *Proc Natl Acad Sci U S A*. **91**, 8807-8811
- (96) Maroudas, A., Bayliss, M.T., and Venn, M.F. (1980) Further studies on the composition of human femoral head cartilage. *Annals of the rheumatic diseases*. **39**, 514-523
- (97) Maroudas, A., Palla, G., and Gilav, E. (1992) Racemization of aspartic acid in human articular cartilage. *Connective tissue research*. **28**, 161-169
- (98) Monnier, V.M., Sell, D.R., Nagaraj, R.H., Miyata, S., Grandhee, S., Odetti, P., and Ibrahim, S.A. (1992) Maillard reaction-mediated molecular damage to extracellular matrix and other tissue proteins in diabetes, aging, and uremia. *Diabetes*. **41 Suppl 2**, 36-41
- (99) Beisswenger, P.J., Moore, L.L., Brinck-Johnsen, T., and Curphey, T.J. (1993) Increased collagen-linked pentosidine levels and advanced glycosylation end products in early diabetic nephropathy. *The Journal of clinical investigation*. **92**, 212-217
- (100) Pokharna, H.K., Monnier, V., Boja, B., and Moskowitz, R.W. (1995) Lysyl oxidase and Maillard reaction-mediated crosslinks in aging and osteoarthritic rabbit cartilage. *Journal of orthopaedic research : official publication of the Orthopaedic Research Society*. **13**, 13-21
- (101) Freeman, M.A. (1975) The fatigue of cartilage in the pathogenesis of osteoarthrosis. *Acta orthopaedica Scandinavica*. **46**, 323-328
- (102) Weightman, B. (1976) Tensile fatigue of human articular cartilage. *Journal of biomechanics*. **9**, 193-200

- (103) Eymard, F., Parsons, C., Edwards, M.H., Petit-Dop, F., Reginster, J.Y., Bruyere, O., Richette, P., Cooper, C., and Chevalier, X. (2015) Diabetes is a risk factor for knee osteoarthritis progression. *Osteoarthritis and cartilage / OARS, Osteoarthritis Research Society*. **23**, 851-859
- (104) Schett, G., Kleyer, A., Perricone, C., Sahinbegovic, E., Iagnocco, A., Zwerina, J., Lorenzini, R., Aschenbrenner, F., Berenbaum, F., D'Agostino, M.A., Willeit, J., and Kiechl, S. (2013) Diabetes is an independent predictor for severe osteoarthritis: results from a longitudinal cohort study. *Diabetes care*. **36**, 403-409
- (105) Sturmer, T., Brenner, H., Brenner, R.E., and Gunther, K.P. (2001) Non-insulin dependent diabetes mellitus (NIDDM) and patterns of osteoarthritis. The Ulm osteoarthritis study. *Scandinavian journal of rheumatology*. **30**, 169-171
- (106) Del Rosso, A., Cerinic, M.M., De Giorgio, F., Minari, C., Rotella, C.M., and Seghieri, G. (2006) Rheumatological manifestations in diabetes mellitus. *Current diabetes reviews*. **2**, 455-466
- (107) Waime, H., Nevinny, D., Rosenthal, J., and Joffe, I.B. (1961) Association of osteoarthritis and diabetes mellitus. *Tufts folia medica*. **7**, 13-19
- (108) Chen, Y.J., Chan, D.C., Lan, K.C., Wang, C.C., Chen, C.M., Chao, S.C., Tsai, K.S., Yang, R.S., and Liu, S.H. (2015) PPARgamma is involved in the hyperglycemia-induced inflammatory responses and collagen degradation in human chondrocytes and diabetic mouse cartilages. *Journal of orthopaedic research : official publication of the Orthopaedic Research Society*. **33**, 373-381
- (109) Courties, A., Gualillo, O., Berenbaum, F., and Sellam, J. (2015) Metabolic stress-induced joint inflammation and osteoarthritis. *Osteoarthritis and cartilage / OARS, Osteoarthritis Research Society*. **23**, 1955-1965

- (110) Tomasek, J.J., Meyers, S.W., Basinger, J.B., Green, D.T., and Shew, R.L. (1994) Diabetic and age-related enhancement of collagen-linked fluorescence in cortical bones of rats. *Life sciences*. **55**, 855-861
- (111) Monnier, V.M., Kohn, R.R., and Cerami, A. (1984) Accelerated age-related browning of human collagen in diabetes mellitus. *Proc Natl Acad Sci U S A*. **81**, 583-587
- (112) Handl, M., Filova, E., Kubala, M., Lansky, Z., Kolacna, L., Vorlicek, J., Trc, T., Pach, M., and Amler, E. (2007) Fluorescent advanced glycation end products in the detection of factual stages of cartilage degeneration. *Physiological research*. **56**, 235-242
- (113) Huber, M., Trattinig, S., and Lintner, F. (2000) Anatomy, biochemistry, and physiology of articular cartilage. *Investigative radiology*. **35**, 573-580
- (114) Heinemeier, K.M., Schjerling, P., Heinemeier, J., Moller, M.B., Krogsgaard, M.R., Grum-Schwensen, T., Petersen, M.M., and Kjaer, M. (2016) Radiocarbon dating reveals minimal collagen turnover in both healthy and osteoarthritic human cartilage. *Science translational medicine*. **8**, 346ra390
- (115) Speer, D.P., and Dahners, L. (1979) The collagenous architecture of articular cartilage. Correlation of scanning electron microscopy and polarized light microscopy observations. *Clinical orthopaedics and related research*. 267-275
- (116) Bayliss, M.T., Venn, M., Maroudas, A., and Ali, S.Y. (1983) Structure of proteoglycans from different layers of human articular cartilage. *The Biochemical journal*. **209**, 387-400
- (117) Morrison, E.H., Ferguson, M.W., Bayliss, M.T., and Archer, C.W. (1996) The development of articular cartilage: I. The spatial and temporal patterns of collagen types. *Journal of anatomy*. **189 (Pt 1)**, 9-22

- (118) Archer, C.W., Morrison, E.H., Bayliss, M.T., and Ferguson, M.W. (1996) The development of articular cartilage: II. The spatial and temporal patterns of glycosaminoglycans and small leucine-rich proteoglycans. *Journal of anatomy*. **189 (Pt 1)**, 23-35
- (119) Zanetti, M., Ratcliffe, A., and Watt, F.M. (1985) Two subpopulations of differentiated chondrocytes identified with a monoclonal antibody to keratan sulfate. *The Journal of cell biology*. **101**, 53-59
- (120) Stockwell, R.A. (1991) Morphometry of cytoplasmic components of mammalian articular chondrocytes and corneal keratocytes: species and zonal variations of mitochondria in relation to nutrition. *Journal of anatomy*. **175**, 251-261
- (121) Stockwell, R.A. (1971) The interrelationship of cell density and cartilage thickness in mammalian articular cartilage. *Journal of anatomy*. **109**, 411-421
- (122) Mitrovic, D., Quintero, M., Stankovic, A., and Ryckewaert, A. (1983) Cell density of adult human femoral condylar articular cartilage. Joints with normal and fibrillated surfaces. *Laboratory investigation; a journal of technical methods and pathology*. **49**, 309-316
- (123) Aydelotte, M.B., Greenhill, R.R., and Kuettner, K.E. (1988) Differences between subpopulations of cultured bovine articular chondrocytes. II. Proteoglycan metabolism. *Connective tissue research*. **18**, 223-234
- (124) Aydelotte, M.B., and Kuettner, K.E. (1988) Differences between subpopulations of cultured bovine articular chondrocytes. I. Morphology and cartilage matrix production. *Connective tissue research*. **18**, 205-222
- (125) Egli, P.S., Hunziker, E.B., and Schenk, R.K. (1988) Quantitation of structural features characterizing weight- and less-weight-bearing regions in articular cartilage: a stereological analysis of medial femoral condyles in young adult rabbits. *The Anatomical record*. **222**, 217-227

- (126) Archer, C.W., McDowell, J., Bayliss, M.T., Stephens, M.D., and Bentley, G. (1990) Phenotypic modulation in sub-populations of human articular chondrocytes in vitro. *Journal of cell science*. **97 (Pt 2)**, 361-371
- (127) Lee, D.A., Noguchi, T., Knight, M.M., O'Donnell, L., Bentley, G., and Bader, D.L. (1998) Response of chondrocyte subpopulations cultured within unloaded and loaded agarose. *Journal of orthopaedic research : official publication of the Orthopaedic Research Society*. **16**, 726-733
- (128) Mobasher, A., Vannucci, S.J., Bondy, C.A., Carter, S.D., Innes, J.F., Arteaga, M.F., Trujillo, E., Ferraz, I., Shakibaei, M., and Martin-Vasallo, P. (2002) Glucose transport and metabolism in chondrocytes: a key to understanding chondrogenesis, skeletal development and cartilage degradation in osteoarthritis. *Histology and histopathology*. **17**, 1239-1267
- (129) Mobasher, A., Bondy, C.A., Moley, K., Mendes, A.F., Rosa, S.C., Richardson, S.M., Hoyland, J.A., Barrett-Jolley, R., and Shakibaei, M. (2008) Facilitative glucose transporters in articular chondrocytes. Expression, distribution and functional regulation of GLUT isoforms by hypoxia, hypoxia mimetics, growth factors and pro-inflammatory cytokines. *Advances in anatomy, embryology, and cell biology*. **200**, 1 p following vi, 1-84
- (130) Rosa, S.C., Goncalves, J., Judas, F., Mobasher, A., Lopes, C., and Mendes, A.F. (2009) Impaired glucose transporter-1 degradation and increased glucose transport and oxidative stress in response to high glucose in chondrocytes from osteoarthritic versus normal human cartilage. *Arthritis research & therapy*. **11**, R80
- (131) Rufino, A.T., Rosa, S.C., Judas, F., Mobasher, A., Lopes, M.C., and Mendes, A.F. (2013) Expression and function of K(ATP) channels in normal and osteoarthritic human chondrocytes: possible role in glucose sensing. *Journal of cellular biochemistry*. **114**, 1879-1889

- (132) Goldring, M.B. (2006) Update on the biology of the chondrocyte and new approaches to treating cartilage diseases. *Best practice & research. Clinical rheumatology*. **20**, 1003-1025
- (133) Heywood, H.K., Knight, M.M., and Lee, D.A. (2010) Both superficial and deep zone articular chondrocyte subpopulations exhibit the Crabtree effect but have different basal oxygen consumption rates. *Journal of cellular physiology*. **223**, 630-639
- (134) Rosa, S.C., Rufino, A.T., Judas, F.M., Tenreiro, C.M., Lopes, M.C., and Mendes, A.F. (2011) Role of glucose as a modulator of anabolic and catabolic gene expression in normal and osteoarthritic human chondrocytes. *Journal of cellular biochemistry*. **112**, 2813-2824
- (135) Otte, P. (1991) Basic cell metabolism of articular cartilage. Manometric studies. *Zeitschrift fur Rheumatologie*. **50**, 304-312
- (136) Hodge, J.A., and McKibbin, B. (1969) The nutrition of mature and immature cartilage in rabbits. An autoradiographic study. *The Journal of bone and joint surgery. British volume*. **51**, 140-147
- (137) Maroudas, A., Bullough, P., Swanson, S.A., and Freeman, M.A. (1968) The permeability of articular cartilage. *The Journal of bone and joint surgery. British volume*. **50**, 166-177
- (138) Ropes, M.W., Muller, A.F., and Bauer, W. (1960) The entrance of glucose and other sugars into joints. *Arthritis and rheumatism*. **3**, 496-514
- (139) Cryer, P.E., Davis, S.N., and Shamon, H. (2003) Hypoglycemia in diabetes. *Diabetes care*. **26**, 1902-1912

- (140) Huh, Y.H., Ryu, J.H., and Chun, J.S. (2007) Regulation of type II collagen expression by histone deacetylase in articular chondrocytes. *The Journal of biological chemistry*. **282**, 17123-17131
- (141) Dvir-Ginzberg, M., Gagarina, V., Lee, E.J., and Hall, D.J. (2008) Regulation of cartilage-specific gene expression in human chondrocytes by SirT1 and nicotinamide phosphoribosyltransferase. *The Journal of biological chemistry*. **283**, 36300-36310
- (142) Poschl, E., Fidler, A., Schmidt, B., Kallipolitou, A., Schmid, E., and Aigner, T. (2005) DNA methylation is not likely to be responsible for aggrecan down regulation in aged or osteoarthritic cartilage. *Annals of the rheumatic diseases*. **64**, 477-480
- (143) Chabane, N., Zayed, N., Afif, H., Mfuna-Endam, L., Benderdour, M., Boileau, C., Martel-Pelletier, J., Pelletier, J.P., Duval, N., and Fahmi, H. (2008) Histone deacetylase inhibitors suppress interleukin-1beta-induced nitric oxide and prostaglandin E2 production in human chondrocytes. *Osteoarthritis and cartilage / OARS, Osteoarthritis Research Society*. **16**, 1267-1274
- (144) Hong, S., Derfoul, A., Pereira-Mouries, L., and Hall, D.J. (2009) A novel domain in histone deacetylase 1 and 2 mediates repression of cartilage-specific genes in human chondrocytes. *Faseb J*. **23**, 3539-3552
- (145) da Silva, M.A., Yamada, N., Clarke, N.M., and Roach, H.I. (2009) Cellular and epigenetic features of a young healthy and a young osteoarthritic cartilage compared with aged control and OA cartilage. *Journal of orthopaedic research : official publication of the Orthopaedic Research Society*. **27**, 593-601
- (146) Miyaki, S., Sato, T., Inoue, A., Otsuki, S., Ito, Y., Yokoyama, S., Kato, Y., Takemoto, F., Nakasa, T., Yamashita, S., Takada, S., Lotz, M.K., Ueno-Kudo, H., and Asahara, H. (2010) MicroRNA-140 plays dual roles in both cartilage development and homeostasis. *Genes & development*. **24**, 1173-1185

- (147) Chittka, A., and Chittka, L. (2010) Epigenetics of royalty. *PLoS biology*. **8**, e1000532
- (148) Darwin, C. (1859) *On the origin of species by means of natural selection*, London,: J. Murray
- (149) Mao, W., Schuler, M.A., and Berenbaum, M.R. (2015) A dietary phytochemical alters caste-associated gene expression in honey bees. *Science advances*. **1**, e1500795
- (150) El-Osta, A., Brasacchio, D., Yao, D., Poci, A., Jones, P.L., Roeder, R.G., Cooper, M.E., and Brownlee, M. (2008) Transient high glucose causes persistent epigenetic changes and altered gene expression during subsequent normoglycemia. *The Journal of experimental medicine*. **205**, 2409-2417
- (151) Kolm-Litty, V., Sauer, U., Nerlich, A., Lehmann, R., and Schleicher, E.D. (1998) High glucose-induced transforming growth factor beta1 production is mediated by the hexosamine pathway in porcine glomerular mesangial cells. *The Journal of clinical investigation*. **101**, 160-169
- (152) Hrudá, J., Sramek, V., and Lerve, X. (2010) High glucose increases susceptibility to oxidative-stress-induced apoptosis and DNA damage in K-562 cells. *Biomedical papers of the Medical Faculty of the University Palacky, Olomouc, Czechoslovakia*. **154**, 315-320
- (153) Heywood, H.K., Nalesso, G., Lee, D.A., and Dell'accio, F. (2014) Culture expansion in low-glucose conditions preserves chondrocyte differentiation and enhances their subsequent capacity to form cartilage tissue in three-dimensional culture. *BioResearch open access*. **3**, 9-18
- (154) McClain, D.A., Paterson, A.J., Roos, M.D., Wei, X., and Kudlow, J.E. (1992) Glucose and glucosamine regulate growth factor gene expression in vascular smooth muscle cells. *Proc Natl Acad Sci U S A*. **89**, 8150-8154

- (155) Laiguillon, M.C., Courties, A., Houard, X., Auclair, M., Sautet, A., Capeau, J., Feve, B., Berenbaum, F., and Sellam, J. (2015) Characterization of diabetic osteoarthritic cartilage and role of high glucose environment on chondrocyte activation: toward pathophysiological delineation of diabetes mellitus-related osteoarthritis. *Osteoarthritis and cartilage / OARS, Osteoarthritis Research Society*. **23**, 1513-1522
- (156) Ylarinne, J.H., Qu, C., and Lammi, M.J. (2014) Hypertonic conditions enhance cartilage formation in scaffold-free primary chondrocyte cultures. *Cell and tissue research*. **358**, 541-550
- (157) Tang, R., Gao, M., Wu, M., Liu, H., Zhang, X., and Liu, B. (2012) High glucose mediates endothelial-to-chondrocyte transition in human aortic endothelial cells. *Cardiovascular diabetology*. **11**, 113
- (158) Wu, C., Lei, R., Tiainen, M., Wu, S., Zhang, Q., Pei, F., and Guo, X. (2014) Disordered glycometabolism involved in pathogenesis of Kashin-Beck disease, an endemic osteoarthritis in China. *Experimental cell research*. **326**, 240-250
- (159) Gao, Q., Guan, L., Hu, S., Yao, Y., Ren, X., Zhang, Z., Cheng, C., Liu, Y., Zhang, C., Huang, J., Su, D., and Ma, X. (2015) Study on the mechanism of HIF1a-SOX9 in glucose-induced cardiomyocyte hypertrophy. *Biomedicine & pharmacotherapy = Biomedecine & pharmacotherapie*. **74**, 57-62
- (160) Takeda, M., Babazono, T., Nitta, K., and Iwamoto, Y. (2001) High glucose stimulates hyaluronan production by renal interstitial fibroblasts through the protein kinase C and transforming growth factor-beta cascade. *Metabolism: clinical and experimental*. **50**, 789-794
- (161) Devi, T.S., Hosoya, K., Terasaki, T., and Singh, L.P. (2013) Critical role of TXNIP in oxidative stress, DNA damage and retinal pericyte apoptosis under high glucose: implications for diabetic retinopathy. *Experimental cell research*. **319**, 1001-1012

- (162) Li, M., Absher, P.M., Liang, P., Russell, J.C., Sobel, B.E., and Fukagawa, N.K. (2001) High glucose concentrations induce oxidative damage to mitochondrial DNA in explanted vascular smooth muscle cells. *Experimental biology and medicine*. **226**, 450-457
- (163) Kim, Y.H., Heo, J.S., and Han, H.J. (2006) High glucose increase cell cycle regulatory proteins level of mouse embryonic stem cells via PI3-K/Akt and MAPKs signal pathways. *Journal of cellular physiology*. **209**, 94-102
- (164) Death, A.K., Fisher, E.J., McGrath, K.C., and Yue, D.K. (2003) High glucose alters matrix metalloproteinase expression in two key vascular cells: potential impact on atherosclerosis in diabetes. *Atherosclerosis*. **168**, 263-269
- (165) Gao, W., Ferguson, G., Connell, P., Walshe, T., Murphy, R., Birney, Y.A., O'Brien, C., and Cahill, P.A. (2007) High glucose concentrations alter hypoxia-induced control of vascular smooth muscle cell growth via a HIF-1alpha-dependent pathway. *Journal of molecular and cellular cardiology*. **42**, 609-619
- (166) Fisher, E., McLennan, S.V., Tada, H., Heffernan, S., Yue, D.K., and Turtle, J.R. (1991) Interaction of ascorbic acid and glucose on production of collagen and proteoglycan by fibroblasts. *Diabetes*. **40**, 371-376
- (167) Yu, X.Y., Geng, Y.J., Liang, J.L., Lin, Q.X., Lin, S.G., Zhang, S., and Li, Y. (2010) High levels of glucose induce apoptosis in cardiomyocyte via epigenetic regulation of the insulin-like growth factor receptor. *Experimental cell research*. **316**, 2903-2909
- (168) Xie, L., Zhu, X., Hu, Y., Li, T., Gao, Y., Shi, Y., and Tang, S. (2008) Mitochondrial DNA oxidative damage triggering mitochondrial dysfunction and apoptosis in high glucose-induced HRECs. *Investigative ophthalmology & visual science*. **49**, 4203-4209
- (169) Tsai, C.H., Chiang, Y.C., Chen, H.T., Huang, P.H., Hsu, H.C., and Tang, C.H. (2013) High glucose induces vascular endothelial growth factor production in human synovial

fibroblasts through reactive oxygen species generation. *Biochimica et biophysica acta*. **1830**, 2649-2658

(170) Franke, S., Sommer, M., Ruster, C., Bondeva, T., Marticke, J., Hofmann, G., Hein, G., and Wolf, G. (2009) Advanced glycation end products induce cell cycle arrest and proinflammatory changes in osteoarthritic fibroblast-like synovial cells. *Arthritis research & therapy*. **11**, R136

(171) Rasheed, Z., and Haqqi, T.M. (2012) Endoplasmic reticulum stress induces the expression of COX-2 through activation of eIF2alpha, p38-MAPK and NF-kappaB in advanced glycation end products stimulated human chondrocytes. *Biochimica et biophysica acta*. **1823**, 2179-2189

(172) Wondrak, G.T., Jacobson, E.L., and Jacobson, M.K. (2002) Photosensitization of DNA damage by glycated proteins. *Photochemical & photobiological sciences : Official journal of the European Photochemistry Association and the European Society for Photobiology*. **1**, 355-363

(173) Ott, C., Jacobs, K., Haucke, E., Navarrete Santos, A., Grune, T., and Simm, A. (2014) Role of advanced glycation end products in cellular signaling. *Redox biology*. **2**, 411-429

(174) Vandesompele, J., De Preter, K., Pattyn, F., Poppe, B., Van Roy, N., De Paepe, A., and Speleman, F. (2002) Accurate normalization of real-time quantitative RT-PCR data by geometric averaging of multiple internal control genes. *Genome biology*. **3**, RESEARCH0034

(175) Perkins, J.R., Dawes, J.M., McMahon, S.B., Bennett, D.L., Orengo, C., and Kohl, M. (2012) ReadqPCR and NormqPCR: R packages for the reading, quality checking and normalisation of RT-qPCR quantification cycle (Cq) data. *BMC genomics*. **13**, 296

(176) Livak, K.J., and Schmittgen, T.D. (2001) Analysis of relative gene expression data using real-time quantitative PCR and the 2(-Delta Delta C(T)) Method. *Methods*. **25**, 402-408

- (177) Pfaffl, M.W. (2001) A new mathematical model for relative quantification in real-time RT-PCR. *Nucleic acids research*. **29**, e45
- (178) Spandidos, A., Wang, X., Wang, H., Dragnev, S., Thurber, T., and Seed, B. (2008) A comprehensive collection of experimentally validated primers for Polymerase Chain Reaction quantitation of murine transcript abundance. *BMC genomics*. **9**, 633
- (179) Spandidos, A., Wang, X., Wang, H., and Seed, B. (2010) PrimerBank: a resource of human and mouse PCR primer pairs for gene expression detection and quantification. *Nucleic acids research*. **38**, D792-799
- (180) Wang, X., and Seed, B. (2003) A PCR primer bank for quantitative gene expression analysis. *Nucleic acids research*. **31**, e154
- (181) Ye, J., Coulouris, G., Zaretskaya, I., Cutcutache, I., Rozen, S., and Madden, T.L. (2012) Primer-BLAST: a tool to design target-specific primers for polymerase chain reaction. *BMC bioinformatics*. **13**, 134
- (182) Carvalho, B.S., and Irizarry, R.A. (2010) A framework for oligonucleotide microarray preprocessing. *Bioinformatics*. **26**, 2363-2367
- (183) Ritchie, M.E., Phipson, B., Wu, D., Hu, Y., Law, C.W., Shi, W., and Smyth, G.K. (2015) limma powers differential expression analyses for RNA-sequencing and microarray studies. *Nucleic acids research*. **43**, e47
- (184) Mootha, V.K., Lindgren, C.M., Eriksson, K.F., Subramanian, A., Sihag, S., Lehar, J., Puigserver, P., Carlsson, E., Ridderstrale, M., Laurila, E., Houstis, N., Daly, M.J., Patterson, N., Mesirov, J.P., Golub, T.R., Tamayo, P., Spiegelman, B., Lander, E.S., Hirschhorn, J.N., Altshuler, D., and Groop, L.C. (2003) PGC-1 alpha-responsive genes involved in oxidative phosphorylation are coordinately downregulated in human diabetes. *Nature genetics*. **34**, 267-273

- (185) Subramanian, A., Tamayo, P., Mootha, V.K., Mukherjee, S., Ebert, B.L., Gillette, M.A., Paulovich, A., Pomeroy, S.L., Golub, T.R., Lander, E.S., and Mesirov, J.P. (2005) Gene set enrichment analysis: A knowledge-based approach for interpreting genome-wide expression profiles. *P Natl Acad Sci USA*. **102**, 15545-15550
- (186) Huber, W., Carey, V.J., Gentleman, R., Anders, S., Carlson, M., Carvalho, B.S., Bravo, H.C., Davis, S., Gatto, L., Girke, T., Gottardo, R., Hahne, F., Hansen, K.D., Irizarry, R.A., Lawrence, M., Love, M.I., MacDonald, J., Obenchain, V., Oles, A.K., Pages, H., Reyes, A., Shannon, P., Smyth, G.K., Tenenbaum, D., Waldron, L., and Morgan, M. (2015) Orchestrating high-throughput genomic analysis with Bioconductor. *Nature methods*. **12**, 115-121
- (187) Dunning, M.J., Smith, M.L., Ritchie, M.E., and Tavare, S. (2007) beadarray: R classes and methods for Illumina bead-based data. *Bioinformatics*. **23**, 2183-2184
- (188) Aryee, M.J., Jaffe, A.E., Corrada-Bravo, H., Ladd-Acosta, C., Feinberg, A.P., Hansen, K.D., and Irizarry, R.A. (2014) Minfi: a flexible and comprehensive Bioconductor package for the analysis of Infinium DNA methylation microarrays. *Bioinformatics*. **30**, 1363-1369
- (189) Maksimovic, J., Gordon, L., and Oshlack, A. (2012) SWAN: Subset-quantile within array normalization for illumina infinium HumanMethylation450 BeadChips. *Genome biology*. **13**, R44
- (190) Peters, T.J., Buckley, M.J., Statham, A.L., Pidsley, R., Samaras, K., R, V.L., Clark, S.J., and Molloy, P.L. (2015) De novo identification of differentially methylated regions in the human genome. *Epigenetics & chromatin*. **8**, 6
- (191) Inc, A.B. (Access Date: 24 May 2017) Tm Calculator (<http://www6.appliedbiosystems.com/support/techtools/calc/ed^eds>, <http://www6.appliedbiosystems.com/support/techtools/calc/>: Applied Biosystems.

- (192) Olive, P.L., and Banath, J.P. (2006) The comet assay: a method to measure DNA damage in individual cells. *Nature protocols*. **1**, 23-29
- (193) Konca, K., Lankoff, A., Banasik, A., Lisowska, H., Kuszewski, T., Gozdz, S., Koza, Z., and Wojcik, A. (2003) A cross-platform public domain PC image-analysis program for the comet assay. *Mutation research*. **534**, 15-20
- (194) Ghiraldini, F.G., Crispim, A.C., and Mello, M.L. (2013) Effects of hyperglycemia and aging on nuclear sirtuins and DNA damage of mouse hepatocytes. *Molecular biology of the cell*. **24**, 2467-2476
- (195) Caron, M.M., Emans, P.J., Coolsen, M.M., Voss, L., Surtel, D.A., Cremers, A., van Rhijn, L.W., and Welting, T.J. (2012) Redifferentiation of dedifferentiated human articular chondrocytes: comparison of 2D and 3D cultures. *Osteoarthritis and cartilage / OARS, Osteoarthritis Research Society*. **20**, 1170-1178
- (196) Berlanga-Acosta, J., Schultz, G.S., Lopez-Mola, E., Guillen-Nieto, G., Garcia-Siverio, M., and Herrera-Martinez, L. (2013) Glucose toxic effects on granulation tissue productive cells: the diabetics' impaired healing. *BioMed research international*. **2013**, 256043
- (197) Garcia-Carbonell, R., Divakaruni, A.S., Lodi, A., Vicente-Suarez, I., Saha, A., Cheroutre, H., Boss, G.R., Tiziani, S., Murphy, A.N., and Guma, M. (2016) Critical Role of Glucose Metabolism in Rheumatoid Arthritis Fibroblast-like Synoviocytes. *Arthritis & rheumatology*. **68**, 1614-1626
- (198) Zhang, X.Q., Dong, J.J., Cai, T., Shen, X., Zhou, X.J., and Liao, L. (2017) High glucose induces apoptosis via upregulation of Bim expression in proximal tubule epithelial cells. *Oncotarget*. **8**, 24119-24129
- (199) Levigne, D., Tobalem, M., Modarressi, A., and Pittet-Cuenod, B. (2013) Hyperglycemia increases susceptibility to ischemic necrosis. *BioMed research international*. **2013**, 490964

- (200) Harwood, S.M., Allen, D.A., Raftery, M.J., and Yaqoob, M.M. (2007) High glucose initiates calpain-induced necrosis before apoptosis in LLC-PK1 cells. *Kidney international*. **71**, 655-663
- (201) Dyhdalo, K., Macnamara, S., Brainard, J., Underwood, D., Tubbs, R., and Yang, B. (2014) Assessment of cellularity, genomic DNA yields, and technical platforms for BRAF mutational testing in thyroid fine-needle aspirate samples. *Cancer cytopathology*. **122**, 114-122
- (202) Leto, D., and Saltiel, A.R. (2012) Regulation of glucose transport by insulin: traffic control of GLUT4. *Nature reviews. Molecular cell biology*. **13**, 383-396
- (203) Olson, A.L. (2012) Regulation of GLUT4 and Insulin-Dependent Glucose Flux. *ISRN molecular biology*. **2012**, 856987
- (204) Kobayashi, H., Mitsui, T., Nomura, S., Ohno, Y., Kadomatsu, K., Muramatsu, T., Nagasaka, T., and Mizutani, S. (2004) Expression of glucose transporter 4 in the human pancreatic islet of Langerhans. *Biochemical and biophysical research communications*. **314**, 1121-1125
- (205) Cheeseman, C. (2008) GLUT7: a new intestinal facilitated hexose transporter. *American journal of physiology. Endocrinology and metabolism*. **295**, E238-241
- (206) Fiorentino, T.V., Prioletta, A., Zuo, P., and Folli, F. (2013) Hyperglycemia-induced Oxidative stress and its Role in Diabetes Mellitus related Cardiovascular Diseases. *Current pharmaceutical design*.
- (207) Mueller, A.J., Tew, S.R., Vasieva, O., Clegg, P.D., and Canty-Laird, E.G. (2016) A systems biology approach to defining regulatory mechanisms for cartilage and tendon cell phenotypes. *Scientific reports*. **6**, 33956

- (208) Kim, R.P. (2002) The musculoskeletal complications of diabetes. *Current diabetes reports*. **2**, 49-52
- (209) Berenbaum, F. (2011) Diabetes-induced osteoarthritis: from a new paradigm to a new phenotype. *Annals of the rheumatic diseases*. **70**, 1354-1356
- (210) Crisp, A.J., and Heathcote, J.G. (1984) Connective tissue abnormalities in diabetes mellitus. *Journal of the Royal College of Physicians of London*. **18**, 132-141
- (211) Maier, T., Guell, M., and Serrano, L. (2009) Correlation of mRNA and protein in complex biological samples. *FEBS letters*. **583**, 3966-3973
- (212) Lorenzi, M., Montisano, D.F., Toledo, S., and Barrieux, A. (1986) High glucose induces DNA damage in cultured human endothelial cells. *The Journal of clinical investigation*. **77**, 322-325
- (213) Tregilgas, L. (2013) Does a transient increase in blood-glucose alter the gene expression profiles of musculoskeletal cells? ed^eds, Unpublished: University of Liverpool.
- (214) Irelan, J.T., Gutierrez Del Arroyo, A., Gutierrez, A., Peters, G., Quon, K.C., Miraglia, L., and Chanda, S.K. (2009) A functional screen for regulators of CKDN2A reveals MEOX2 as a transcriptional activator of INK4a. *PloS one*. **4**, e5067
- (215) Valcourt, U., Thuault, S., Pardali, K., Heldin, C.H., and Moustakas, A. (2007) Functional role of Meox2 during the epithelial cytotstatic response to TGF-beta. *Molecular oncology*. **1**, 55-71
- (216) Douville, J.M., Cheung, D.Y., Herbert, K.L., Moffatt, T., and Wigle, J.T. (2011) Mechanisms of MEOX1 and MEOX2 regulation of the cyclin dependent kinase inhibitors p21 and p16 in vascular endothelial cells. *PloS one*. **6**, e29099

- (217) Zhang, D., Lu, H., Chen, Z., Wang, Y., Lin, J., Xu, S., Zhang, C., Wang, B., Yuan, Z., Feng, X., Jiang, X., and Pan, J. (2017) High glucose induces the aging of mesenchymal stem cells via Akt/mTOR signaling. *Molecular medicine reports*. **16**, 1685-1690
- (218) Szklarczyk, D., Franceschini, A., Wyder, S., Forslund, K., Heller, D., Huerta-Cepas, J., Simonovic, M., Roth, A., Santos, A., Tsafou, K.P., Kuhn, M., Bork, P., Jensen, L.J., and von Mering, C. (2015) STRING v10: protein-protein interaction networks, integrated over the tree of life. *Nucleic acids research*. **43**, D447-452
- (219) Bugger, H., and Abel, E.D. (2014) Molecular mechanisms of diabetic cardiomyopathy. *Diabetologia*. **57**, 660-671
- (220) Vousden, K.H., and Ryan, K.M. (2009) p53 and metabolism. *Nature reviews. Cancer*. **9**, 691-700
- (221) Lee, J.Y., and Spicer, A.P. (2000) Hyaluronan: a multifunctional, megaDalton, stealth molecule. *Current opinion in cell biology*. **12**, 581-586
- (222) Golshani, R., Lopez, L., Estrella, V., Kramer, M., Iida, N., and Lokeshwar, V.B. (2008) Hyaluronic acid synthase-1 expression regulates bladder cancer growth, invasion, and angiogenesis through CD44. *Cancer research*. **68**, 483-491
- (223) Joukov, V., Groen, A.C., Prokhorova, T., Gerson, R., White, E., Rodriguez, A., Walter, J.C., and Livingston, D.M. (2006) The BRCA1/BARD1 heterodimer modulates ran-dependent mitotic spindle assembly. *Cell*. **127**, 539-552
- (224) Sohr, S., and Engeland, K. (2008) RHAMM is differentially expressed in the cell cycle and downregulated by the tumor suppressor p53. *Cell cycle*. **7**, 3448-3460
- (225) Steinbusch, M.M., Fang, Y., Milner, P.I., Clegg, P.D., Young, D.A., Welting, T.J., and Peffer, M.J. (2017) Serum snoRNAs as biomarkers for joint ageing and post traumatic osteoarthritis. *Scientific reports*. **7**, 43558

- (226) Horvath, S. (2013) DNA methylation age of human tissues and cell types. *Genome biology*. **14**, R115
- (227) Hannum, G., Guinney, J., Zhao, L., Zhang, L., Hughes, G., Sada, S., Klotzle, B., Bibikova, M., Fan, J.B., Gao, Y., Deconde, R., Chen, M., Rajapakse, I., Friend, S., Ideker, T., and Zhang, K. (2013) Genome-wide methylation profiles reveal quantitative views of human aging rates. *Molecular cell*. **49**, 359-367
- (228) Day, K., Waite, L.L., Thalacker-Mercer, A., West, A., Bamman, M.M., Brooks, J.D., Myers, R.M., and Absher, D. (2013) Differential DNA methylation with age displays both common and dynamic features across human tissues that are influenced by CpG landscape. *Genome biology*. **14**, R102
- (229) Hernandez, D.G., Nalls, M.A., Gibbs, J.R., Arepalli, S., van der Brug, M., Chong, S., Moore, M., Longo, D.L., Cookson, M.R., Traynor, B.J., and Singleton, A.B. (2011) Distinct DNA methylation changes highly correlated with chronological age in the human brain. *Human molecular genetics*. **20**, 1164-1172
- (230) Horvath, S., Langfelder, P., Kwak, S., Aaronson, J., Rosinski, J., Vogt, T.F., Eszes, M., Faull, R.L., Curtis, M.A., Waldvogel, H.J., Choi, O.W., Tung, S., Vinters, H.V., Coppola, G., and Yang, X.W. (2016) Huntington's disease accelerates epigenetic aging of human brain and disrupts DNA methylation levels. *Aging*. **8**, 1485-1512
- (231) Levine, A.J., Quach, A., Moore, D.J., Achim, C.L., Soontornniyomkij, V., Masliah, E., Singer, E.J., Gelman, B., Nemanic, N., and Horvath, S. (2016) Accelerated epigenetic aging in brain is associated with pre-mortem HIV-associated neurocognitive disorders. *Journal of neurovirology*. **22**, 366-375
- (232) Lowe, D., Horvath, S., and Raj, K. (2016) Epigenetic clock analyses of cellular senescence and ageing. *Oncotarget*. **7**, 8524-8531

- (233) Lu, A.T., Hannon, E., Levine, M.E., Hao, K., Crimmins, E.M., Lunnon, K., Kozlenkov, A., Mill, J., Dracheva, S., and Horvath, S. (2016) Genetic variants near MLST8 and DHX57 affect the epigenetic age of the cerebellum. *Nature communications*. **7**, 10561
- (234) Vidal-Bralo, L., Lopez-Golan, Y., Mera-Varela, A., Rego-Perez, I., Horvath, S., Zhang, Y., Del Real, A., Zhai, G., Blanco, F.J., Riancho, J.A., Gomez-Reino, J.J., and Gonzalez, A. (2016) Specific premature epigenetic aging of cartilage in osteoarthritis. *Aging*. **8**, 2222-2231
- (235) Huang da, W., Sherman, B.T., and Lempicki, R.A. (2009) Systematic and integrative analysis of large gene lists using DAVID bioinformatics resources. *Nature protocols*. **4**, 44-57
- (236) Huang da, W., Sherman, B.T., Zheng, X., Yang, J., Imamichi, T., Stephens, R., and Lempicki, R.A. (2009) Extracting biological meaning from large gene lists with DAVID. *Current protocols in bioinformatics*. **Chapter 13**, Unit 13 11
- (237) Johnson, A.A., Akman, K., Calimport, S.R., Wuttke, D., Stolzing, A., and de Magalhaes, J.P. (2012) The role of DNA methylation in aging, rejuvenation, and age-related disease. *Rejuvenation research*. **15**, 483-494
- (238) Stessman, J., Maaravi, Y., Hammerman-Rozenberg, R., Cohen, A., Nemanov, L., Gritsenko, I., Gruberman, N., and Ebstein, R.P. (2005) Candidate genes associated with ageing and life expectancy in the Jerusalem longitudinal study. *Mechanisms of ageing and development*. **126**, 333-339
- (239) Zampieri, M., Ciccarone, F., Calabrese, R., Franceschi, C., Burkle, A., and Caiafa, P. (2015) Reconfiguration of DNA methylation in aging. *Mechanisms of ageing and development*. **151**, 60-70
- (240) Wareham, K.A., Lyon, M.F., Glenister, P.H., and Williams, E.D. (1987) Age related reactivation of an X-linked gene. *Nature*. **327**, 725-727

- (241) Chaigne, R., and Heard, E. (2014) X-chromosome inactivation in development and cancer. *FEBS letters*. **588**, 2514-2522
- (242) Ratajczak, M.Z., Kucia, M., Liu, R., Shin, D.M., Bryndza, E., Masternak, M.M., Tarnowski, M., Ratajczak, J., and Bartke, A. (2011) RasGrf1: genomic imprinting, VSELs, and aging. *Aging*. **3**, 692-697
- (243) Kim, J., Bergmann, A., Lucas, S., Stone, R., and Stubbs, L. (2004) Lineage-specific imprinting and evolution of the zinc-finger gene ZIM2. *Genomics*. **84**, 47-58
- (244) Schragar, M.A., Roth, S.M., Ferrell, R.E., Metter, E.J., Russek-Cohen, E., Lynch, N.A., Lindle, R.S., and Hurley, B.F. (2004) Insulin-like growth factor-2 genotype, fat-free mass, and muscle performance across the adult life span. *Journal of applied physiology*. **97**, 2176-2183
- (245) Cui, H., Cruz-Correa, M., Giardiello, F.M., Hutcheon, D.F., Kafonek, D.R., Brandenburg, S., Wu, Y., He, X., Powe, N.R., and Feinberg, A.P. (2003) Loss of IGF2 imprinting: a potential marker of colorectal cancer risk. *Science*. **299**, 1753-1755
- (246) Bak, M., Boonen, S.E., Dahl, C., Hahnemann, J.M., Mackay, D.J., Tumer, Z., Gronskov, K., Temple, I.K., Guldborg, P., and Tommerup, N. (2016) Genome-wide DNA methylation analysis of transient neonatal diabetes type 1 patients with mutations in ZFP57. *BMC medical genetics*. **17**, 29
- (247) Tajika, Y., Moue, T., Ishikawa, S., Asano, K., Okumo, T., Takagi, H., and Hisamitsu, T. (2017) Influence of Periostin on Synoviocytes in Knee Osteoarthritis. *In vivo*. **31**, 69-77
- (248) Onat, D., Brillon, D., Colombo, P.C., and Schmidt, A.M. (2011) Human vascular endothelial cells: a model system for studying vascular inflammation in diabetes and atherosclerosis. *Current diabetes reports*. **11**, 193-202

- (249) Grafodatskaya, D., Choufani, S., Ferreira, J.C., Butcher, D.T., Lou, Y., Zhao, C., Scherer, S.W., and Weksberg, R. (2010) EBV transformation and cell culturing destabilizes DNA methylation in human lymphoblastoid cell lines. *Genomics*. **95**, 73-83
- (250) Chen, Y.A., Lemire, M., Choufani, S., Butcher, D.T., Grafodatskaya, D., Zanke, B.W., Gallinger, S., Hudson, T.J., and Weksberg, R. (2013) Discovery of cross-reactive probes and polymorphic CpGs in the Illumina Infinium HumanMethylation450 microarray. *Epigenetics*. **8**, 203-209
- (251) Armstrong, C.G., and Mow, V.C. (1982) Variations in the intrinsic mechanical properties of human articular cartilage with age, degeneration, and water content. *The Journal of bone and joint surgery. American volume*. **64**, 88-94
- (252) Brandt, K.D., Dieppe, P., and Radin, E.L. (2008) Etiopathogenesis of osteoarthritis. *Rheumatic diseases clinics of North America*. **34**, 531-559
- (253) Berenbaum, F. (2013) Osteoarthritis as an inflammatory disease (osteoarthritis is not osteoarthrosis!). *Osteoarthritis and cartilage / OARS, Osteoarthritis Research Society*. **21**, 16-21
- (254) Goldring, M.B. (2012) Chondrogenesis, chondrocyte differentiation, and articular cartilage metabolism in health and osteoarthritis. *Therapeutic advances in musculoskeletal disease*. **4**, 269-285
- (255) Goldring, M.B., and Goldring, S.R. (2010) Articular cartilage and subchondral bone in the pathogenesis of osteoarthritis. *Annals of the New York Academy of Sciences*. **1192**, 230-237
- (256) Dennis, G., Jr., Sherman, B.T., Hosack, D.A., Yang, J., Gao, W., Lane, H.C., and Lempicki, R.A. (2003) DAVID: Database for Annotation, Visualization, and Integrated Discovery. *Genome biology*. **4**, P3

- (257) Chutkow, W.A., Patwari, P., Yoshioka, J., and Lee, R.T. (2008) Thioredoxin-interacting protein (Txnip) is a critical regulator of hepatic glucose production. *The Journal of biological chemistry*. **283**, 2397-2406
- (258) Singh, L.P. (2013) Thioredoxin Interacting Protein (TXNIP) and Pathogenesis of Diabetic Retinopathy. *Journal of clinical & experimental ophthalmology*. **4**,
- (259) Loeser, R.F., Collins, J.A., and Diekman, B.O. (2016) Ageing and the pathogenesis of osteoarthritis. *Nature reviews. Rheumatology*. **12**, 412-420
- (260) Shi, J., Zhang, C., Yi, Z., and Lan, C. (2016) Explore the variation of MMP3, JNK, p38 MAPKs, and autophagy at the early stage of osteoarthritis. *IUBMB life*. **68**, 293-302
- (261) Eklund, L., Piihola, J., Komulainen, J., Sormunen, R., Ongvarrasopone, C., Fassler, R., Muona, A., Ilves, M., Ruskoaho, H., Takala, T.E., and Pihlajaniemi, T. (2001) Lack of type XV collagen causes a skeletal myopathy and cardiovascular defects in mice. *Proc Natl Acad Sci U S A*. **98**, 1194-1199
- (262) Matheson, S., Larjava, H., and Hakkinen, L. (2005) Distinctive localization and function for lumican, fibromodulin and decorin to regulate collagen fibril organization in periodontal tissues. *Journal of periodontal research*. **40**, 312-324
- (263) Kafienah, W., Cheung, F.L., Sims, T., Martin, I., Miot, S., Von Ruhland, C., Roughley, P.J., and Hollander, A.P. (2008) Lumican inhibits collagen deposition in tissue engineered cartilage. *Matrix biology : journal of the International Society for Matrix Biology*. **27**, 526-534
- (264) Karlsson, C., Dehne, T., Lindahl, A., Brittberg, M., Pruss, A., Sittinger, M., and Ringe, J. (2010) Genome-wide expression profiling reveals new candidate genes associated with osteoarthritis. *Osteoarthritis and cartilage / OARS, Osteoarthritis Research Society*. **18**, 581-592

- (265) Grover, J., Chen, X.N., Korenberg, J.R., Recklies, A.D., and Roughley, P.J. (1996) The gene organization, chromosome location, and expression of a 55-kDa matrix protein (PRELP) of human articular cartilage. *Genomics*. **38**, 109-117
- (266) Loeser, R.F., Olex, A.L., McNulty, M.A., Carlson, C.S., Callahan, M., Ferguson, C., and Fetrow, J.S. (2013) Disease progression and phasic changes in gene expression in a mouse model of osteoarthritis. *PloS one*. **8**, e54633
- (267) Peres, G.B., Schor, N., and Michelacci, Y.M. (2017) Impact of high glucose and AGEs on cultured kidney-derived cells. Effects on cell viability, lysosomal enzymes and effectors of cell signaling pathways. *Biochimie*. **135**, 137-148
- (268) Stoka, V., Turk, V., and Turk, B. (2016) Lysosomal cathepsins and their regulation in aging and neurodegeneration. *Ageing research reviews*. **32**, 22-37
- (269) Tien, T., Zhang, J., Muto, T., Kim, D., Sarthy, V.P., and Roy, S. (2017) High Glucose Induces Mitochondrial Dysfunction in Retinal Muller Cells: Implications for Diabetic Retinopathy. *Investigative ophthalmology & visual science*. **58**, 2915-2921
- (270) Carroll, J.E., Irwin, M.R., Levine, M., Seeman, T.E., Absher, D., Assimes, T., and Horvath, S. (2017) Epigenetic Aging and Immune Senescence in Women With Insomnia Symptoms: Findings From the Women's Health Initiative Study. *Biological psychiatry*. **81**, 136-144
- (271) Martin, J.A., and Buckwalter, J.A. (2001) Roles of articular cartilage aging and chondrocyte senescence in the pathogenesis of osteoarthritis. *The Iowa orthopaedic journal*. **21**, 1-7
- (272) Martin, J.A., and Buckwalter, J.A. (2001) Telomere erosion and senescence in human articular cartilage chondrocytes. *J Gerontol a-Biol*. **56**, B172-B179

(273) Kelley, K.M., Johnson, T.R., Ilan, J., and Moskowitz, R.W. (1999) Glucose regulation of the IGF response system in chondrocytes: induction of an IGF-I-resistant state. *The American journal of physiology.* **276**, R1164-1171

(274) Wu, S., Shi, Y., Pan, Y., Li, J., Jia, Q., Zhang, N., Zhao, X., Liu, G., Wang, Y., Wang, Y., and Wang, C. (2014) Glycated hemoglobin independently or in combination with fasting plasma glucose versus oral glucose tolerance test to detect abnormal glycometabolism in acute ischemic stroke: a Chinese cross-sectional study. *BMC neurology.* **14**, 177